UNIVERSITE DE MONTREAL

A SIMPLIFIED PROCEDURE FOR THE DESIGN OF BOLTED GASKETED FLANGES

par

ALVARO MESTRE ALVAREZ
DEPARTEMENT DE GENIE MECANIQUE
ECOLE POLYTECHNIQUE DE MONTREAL

MEMOIRE PRESENTE EN VUE DE L'OBTENTION
DU GRADE DE MAITRE EN SCIENCES APPLIQUEES (M.Sc.A.)
OCTOBRE 1990

©ALVARO MESTRE ALVAREZ 1990

National Library of Canada
Bibliothèque nationale du Canada

Canadian Theses Service
Service des thèses canadiennes

Ottawa, Canada
K1A 0N4

The author has granted an irrevocable non-exclusive licence allowing the National Library of Canada to reproduce, loan, distribute or sell copies of his/her thesis by any means and in any form or format, making this thesis available to interested persons.

L'auteur a accordé une licence irrévocable et non exclusive permettant à la Bibliothèque nationale du Canada de reproduire, prêter, distribuer ou vendre des copies de sa thèse de quelque manière et sous quelque forme que ce soit pour mettre des exemplaires de cette thèse à la disposition des personnes intéressées.

The author retains ownership of the copyright in his/her thesis. Neither the thesis nor substantial extracts from it may be printed or otherwise reproduced without his/her permission.

L'auteur conserve la propriété du droit d'auteur qui protège sa thèse. Ni la thèse ni des extraits substantiels de celle-ci ne doivent être imprimés ou autrement reproduits sans son autorisation.

ISBN 0-315-69583-8

Canada

UNIVERSITE DE MONTREAL

ECOLE POLYTECHNIQUE

Ce mémoire intitulé:

A SIMPLIFIED PROCEDURE FOR THE DESIGN OF BOLTED GASKETED FLANGES.

présenté par: ALVARO MESTRE ALVAREZ.

en vue de l'obtention du grade de: M.Sc.A.

a été dûment accepté par le jury d'examen constitué de:

M.	A. Chaaban,	Ph.D., Président
M.	A. Bazergui,	Ph.D.
M.	R. Baldur,	M.Sc.A.

SOMMAIRE

Le but de ce projet était d'étudier le comportement des brides boulonnées avec joints d'étanchéité. Deux approches étaient suivies:

1. Analyses linéaires et Élasto-plastiques par la méthode d'éléments finis (EF), pour étudier la distribution des contraintes sur les joints d'étanchéité des brides boulonnées, sous des conditions d'ajustage et d'opération. Différentes brides de géométries standards (ANSI B16), matériels de joints d'étanchéité et pressions d'opération étaient considérés.

2. Le développement d'un nouvel algorithme d'optimisation pour la conception de brides boulonnées avec joints d'étanchéité, dérivé de nouvelles équations de base pour joints d'étanchéité (1-4). Un programme interactif pour PC qui implante cette procédure était développé. Une copie de ce programme est incluse sur une disquette PC.

   Une comparaison des résultats obtenus avec les différentes méthodes est présentée:

   a. Analyse d'EF linéaire vs non-linéaire

   b. Analyse d'EF linéaire vs procédure d'optimisation analytique

   c. Nouvelle procédure d'optimisation proposée vs procédure en code ASME

Basé sur ces résultats, la nouvelle procédure constitue une amélioration par rapport à la méthode avec le code ASME car elle produit des conceptions de joints plus efficace et plus économique.

ABSTRACT

The purpose of this project was to study the behavior of gasketed bolted flanges. Two approaches were followed:

1- Linear and Elasto-plastic Finite Element (FE) analyses to study the stress distribution across gaskets on standard (ANSI B16.5) bolted flanges under seating and operating conditions. Various standard flange geometries, gasket materials and operating pressures were considered.

2- Development of a new tightness based optimizing algorithm for the design of gasketed bolted flanges, derived from new basic gasket equations [1-4]. An interactive PC program was developed which implements the new procedure. A copy of the program is included on a PC diskette.

A comparison of results obtained with the different methods is presented:

a) Linear FE vs. Non-linear FE

b) Linear FE vs. Analytical optimizing procedure

c) New proposed optimizing procedure vs. procedure in ASME code

Based on the results, the new procedure constitutes an improvement over the ASME code method as it yields more efficient and economical joint designs.

ACKNOWLEDGEMENTS

I would like to thank Professor Andre Bazergui for his invaluable help in this project, but above all for his patience, understanding and generosity all along.

I would also like to thank professor Ahmad Chaaban for his cooperation and assistance.

I want to express my gratitude to NSERC and FCAR for providing financial support to students like myself which made possible for me to acomplish this endeavor.

Finally thanks to all in the Section of Applied Mechanics in the Mechanical Engineering Department who in one way or another helped in this project.

Table of Contents

SOMMAIRE iv

ABSTRACT v

ACKNOWLEDGEMENTS vi

TABLE OF CONTENTS vii

TABLE OF FIGURES xii

TABLE OF TABLES xvii

NOMENCLATURE xix

1 CHAPTER 1 INTRODUCTION 1

1.1 GENERAL DESCRIPTION OF THE PROJECT 2

1.2 OBJECTIVES 3

1.3 ORGANIZATION OF THE REPORT. 5

2 CHAPTER 2 THEORETICAL & EXPERIMENTAL FOUNDATIONS 7

2.1 EXPERIMENTAL TESTS 8

2.1.1 MECHANICAL TESTS 9

2.1.2 LEAKAGE TESTS 9

2.2 STRESS-DEFLECTION & STRESS-TIGHTNESS DATA 11

2.2.1 **STRESS-DEFLECTION PLOTS** 11

2.2.2 **STRESS-TIGHTNESS PLOTS** 12

2.3 NEW GASKET CONSTANTS AND EQUATIONS 14

2.3.1 NEW GASKET CONSTANTS 14

2.3.2 GASKET EQUATIONS FROM IDEALIZED STRESS-TIGHTNESS PLOTS 16
2.3.2.1 Minimum Tightness Parameter T_{pmin}. 16
2.3.2.2 Gasket Stresses Sa and Sg. 19
3 CHAPTER 3 METHODOLOGY 22
3.1 FINITE ELEMENT STRESS ANALYSIS 24
3.1.1 THE PROGRAMS: ABAQUS vs GIFTS 24
3.1.2 MODELING OF THE GASKET MATERIAL 25
3.1.2.1 Nonlinear Modeling. 28
3.1.2.2 Linear Modeling. 31
3.1.3 MODELING OF THE BOLTS 35
3.1.4 THE ANALYSIS 37
3.1.4.1 The Mesh. 37
3.1.4.2 Boundary Conditions. 41
3.1.4.3 Loading. 42
3.1.4.4 Design Criteria. 43
3.2 NEW OPTIMIZING DESIGN PROCEDURE 45
3.2.1 CORRECTION FACTORS *"e"* and *"F"*: 46
3.2.2 DESIGN CRITERIA 48
3.2.3 OPTIMIZING ALGORITHM 55
3.2.4 ADDITIONAL REMARKS 60

3.2.5 IMPLEMENTATION OF THE NEW DESIGN PROCEDURE 62
3.2.5.1 Applications. 63
3.2.5.2 Models and Templates. 64
3.2.5.3 Input Screens. 64
3.2.5.4 Complete and Flexible Output. 65
4 CHAPTER 4 RESULTS FROM THE FE STRESS ANALYSES 67
4.1 RESULTS FROM THE FE PROGRAM ABAQUS 70
4.1.1 Gasket stress distribution 70
4.1.2 Average Bolt ring stresses 75
4.1.3 Average Gasket Stresses 77
4.2 RESULTS FROM THE FE PROGRAM GIFTS 80
4.2.1 Gasket Stress distribution for several gaskets 80
4.2.2 Average Bolt Ring Stresses 85
4.2.3 Average Gasket Stresses 90
4.2.4 Effect of the design pressure on the gasket stress distribution 95
4.2.5 Effect of the bolt load on the gasket stress distribution 96
4.2.6 Effect of the material properties on the gasket stress distribution 98
4.3 ABAQUS vs. GIFTS, LINEAR vs NONLINEAR APPROACH 100
4.4 CLOSING REMARKS 103

5 CHAPTER 5 RESULTS FROM THE NEW DESIGN PROCEDURE .. 105
5.1 EFFECT OF PRESSURE 105
5.2 EFFECT OF TC ON OPTIMUM 107
5.3 EFFECT OF B, d, AND S* ON THE NEW DESIGN PROCEDURE. 108
5.3.1 Effect of Gasket Factor B 109
5.3.2 Effect of Gasket Factor d 110
5.3.3 Effect of Gasket Factor S* 111
5.4 EFFECT OF *e* AND *F* ON THE NEW DESIGN PROCEDURE. 112
5.4.1 Effect of the bolt efficiency *e* 112
5.4.2 Effect of the experience factor *F* 113
5.5 OPTIMAL T_{pr} 114
5.6 ***TurboFlange*** VS. CURRENT ASME CODE 116
5.7 CLOSING REMARKS 125
6 CHAPTER 6 FE vs ***TurboFlange***: VALIDITY OF THE NEW PROCEDURE 127
7 CHAPTER 7 CONCLUSIONS 133
8 GRAPHS & FIGURES 135
9 REFFERENCES 233
10 APPENDIX A 237
10.1 STRESS-DEFLECTION CURVE GASKET: UCARB GHS 237
10.2 STRESS-DEFLECTION CURVE GASKET: DJ MICA FILLED 238

10.3 STRESS-DEFLECTION CURVE GASKET: DJ ASBESTOS FILLED 239
10.4 STRESS-DEFLECTION CURVE GASKET: SELCO 240
11 APPENDIX B 241
11.1 INPUT DATA FOR PROGRAM ABAQUS 241
11.2 INPUT DATA FOR PROGRAM GIFTS 249
12 APPENDIX C 251
12.1 CASE I : RESULTS FROM ***ASME CODE (Ref. [9])***. 251
12.2 CASE II : RESULTS FROM ***ASME CODE (Ref. [9])***. 252
12.3 CASE I : RESULTS FROM ***TurboFlange***. 253
12.4 CASE II : RESULTS FROM ***TurboFlange***. 258

Table of Figures

13 FIGURE 1. Schematic of Experimental Tests Procedures. 136

14 FIGURE 2. Gasket Stress vs Tightness, Parts A & B 137

15 FIGURE 3. Typical Stress-Tightness Plot 138

16 Figure 4. Idealized Stress-Tightness Plot. 139

17 FIGURE 5. Typical Gasket Materials Stress-Strain plots. 140

18 FIGURE 6. Example of a Plastic Stress-Strain curve in ABAQUS 141

19 FIGURE 7. Sample ABAQUS's Gasket Stress-Strain plot. 142

20 FIGURE 8. Simulation of bolt load on Bolt Ring. 143

21 FIGURE 9. Stress distribution on the bolts. 144

22 FIGURE 10. Loads and Boundary conditions. 145

23 FIGURE 11. Design Bolt Loads Wm1 & Wm2 vs ASME like Factor M 146

24 FIGURE 12. Plot of Wr1 and Wr2 vs M. 147

25 FIGURE 13. Flow Diagram of the Optimizing Algorithm. 148

26 FIGURE 14: Idealized Stress-Tightness Plot 149

27 FIGURE 15. Wm1 & Wm2 vs M: Optimal at Wm1=Wm2. 150

28 FIGURE 16. Wm1 & Wm2 vs M: Optimal at M=2. 151

29 FIGURE 17. Wm1 & Wm2 vs M: Optimal at Tpr=1. 152

30 FIGURE 18. Effect of Tpmin on an impossible solution. 153

31 FIGURE 19. TurboFlange Model & Template Input Screens. 154

32 FIGURE 20. TurboFlange Result Screens. 155

33 FIGURE 21. Wm1 & Wm2 vs M & Tpr from TurboFlange. 156
34 FIGURE 22. Wr1 & Wr2 vs M & Tpr from TurboFlange. 157
35 FIGURE 23. Sya & Sm vs M & Tpr from TurboFlange. 158
36 FIGURE 24: Stress distribution for gasket UCARB GHS (ABAQUS) .. 159
37 FIGURE 25: Stress distribution for gasket DJ MICA (ABAQUS) 160
38 FIGURE 26: Stress distribution for gasket DJ ASBESTOS (ABAQU .. 161
39 FIGURE 27: Stress distribution for gasket SELCO (ABAQUS) 162
40 FIGURE 28:Stress distribution for gasket DJ ASBESTOS (GIFTS) 163
41 FIGURE 29: Stress distribution for gasket GHS (GIFTS) 164
42 FIGURE 30: Stress distribution for gasket DJ MICA (GIFTS) 165
43 FIGURE 31: Stress distribution for gasket SELCO (GIFTS) 166
44 FIGURE 32: Stress distribution for gasket DJ ASBESTOS(GIFTS) 167
45 FIGURE 33: Stress distribution for gasket GHS (GIFTS) 168
46 FIGURE 34: Stress distribution for gasket DJ MICA (GIFTS) 169
47 FIGURE 35: Stress distribution for gasket SELCO (GIFTS) 170
48 FIGURE 36: Stress distribution for gasket DJ ASBESTOS(GIFTS) 171
49 FIGURE 37: Stress distribution for gasket GHS (GIFTS) 172
50 FIGURE 38: Stress distribution for gasket DJ MICA (GIFTS) 173
51 FIGURE 39: Stress distribution for gasket SELCO (GIFTS) 174
52 FIGURE 40: Effect of Design Pressure on the Gasket Stresses 175
53 FIGURE 41: Effect of Bolt Stress on Gasket Stresses, C1500-6 176
54 FIGURE 42: Effect of Bolt Stress on Gasket Stresses C1500-12 177

55 FIGURE 43: Effect of E on the Gasket Stresses (SEATING) 178
56 FIGURE 44: Effect of E on the Gasket Stresses (OPERATING) 179
57 FIGURE 45: Effect of E on the Gasket Stresses (OPER. & SEAT) 180
58 FIGURE 46: Effect of v on the Gasket Stresses (SEATING) 181
59 FIGURE 47: Effect of v on the Gasket Stresses (OPERATING) 182
60 FIGURE 48: Effect of v on the Gasket Stresses (SEAT. & OPER) 183
61 FIGURE 49: Stress Dist. gasket DJ ASBESTOS (ABAQUS & GIFTS) 184
62 FIGURE 50: Stress Dist. gasket GHS (ABAQUS & GIFTS) 185
63 FIGURE 51: Stress Dist. gasket DJ MICA (ABAQUS & GIFTS) 186
64 FIGURE 52: Stress Dist. gasket SELCO (ABAQUS & GIFTS) 187
65 FIGURE 53: Wm & Wm2 vs factor M, effect of Pressure. 188
66 FIGURE 54: Wm1 & Wm2 vs Tpr , Effect of Pressure. 189
67 FIGURE 55: Effect of design Pressure on Optimal Bolt load Wo 190
68 FIGURE 56: Wm1 & Wm2 vs M, effect of TC (C1500-6, ASBESTOS) 191
69 FIGURE 57: Wm1 & Wm2 vs M, Effect of TC (C1500-12, ASBESTOS) 192
70 FIGURE 58: Wm1 & Wm2 vs M, Effect of TC (C1500-6, GHS) 193
71 FIGURE 59: Wm1 & Wm2 vs M, Effect of TC (C1500-12, GHS) 194
72 FIGURE 60: Wm1 & Wm2 vs M, Effect of TC (C1500-6, DJ MICA) 195
73 FIGURE 61: Wm1 & Wm2 vs M, Effect of TC (C1500-12, DJ MICA) .. 196

74 FIGURE 62: Wm1 & Wm2 vs M, Effect of TC (C1500-6, SELCO) 197
75 FIGURE 63: Wm1 & Wm2 vs M, Effect of TC (C1500-12, SELCO) 198
76 FIGURE 64: Effect of TC on Optimal; Bolt Load Wo (C1500-6) 199
77 FIGURE 65: Effect of TC on Optimal; Bolt Load Wo (C1500-12) 200
78 FIGURE 66: Effect of factor B on the Optimal Bolt load. 201
79 FIGURE 67: Relative effect of factor B on Optimal Bolt Load. 202
80 FIGURE 68: Wm1 & Wm2 vs M, effect of B at low pressure 203
81 FIGURE 69: Wm1 & Wm2 vs M, effect of B at high pressure 204
82 FIGURE 70: Wm1 & Wm2 vs Tpr, effect of B at low pressure 205
83 FIGURE 71: Wm1 & Wm2 vs Tpr, effect of B at high pressure 206
84 FIGURE 72: Effect of factor d on the Optimal Bolt load. 207
85 FIGURE 73: Relative effect of factor d on Optimal Bolt Load. 208
86 FIGURE 74: Wm1 & Wm2 vs M, effect of d at low pressure 209
87 FIGURE 75: Wm1 & Wm2 vs M, effect of d at high pressure 210
88 FIGURE 76: Wm1 & Wm2 vs Tpr, effect of d at low pressure 211
89 FIGURE 77: Wm1 & Wm2 vs Tpr, effect of d at high pressure 212
90 FIGURE 78: Effect of factor S* on the Optimal Bolt load. 213
91 FIGURE 79: Relative effect of factor S* on Optimal Bolt Load 214
92 FIGURE 80: Wm1 & Wm2 vs M, effect of S* at low pressure 215
93 FIGURE 81: Wm1 & Wm2 vs M, effect of S* at high pressure 216
94 FIGURE 82: Wm1 & Wm2 vs Tpr, effect of S* at low pressure 217
95 FIGURE 83: Wm1 & Wm2 vs Tpr, effect of S* at high pressure 218

96 FIGURE 84: Effect of factor e on the Optimal Bolt load. 219
97 FIGURE 85: Relative effect of factor e on Optimal Bolt Load. 220
98 FIGURE 86: Wm1 & Wm2 vs M, effect of e at low pressure 221
99 FIGURE 87: Wm1 & Wm2 vs M, effect of e at high pressure 222
100 FIGURE 88: Wm1 & Wm2 vs Tpr, effect of e at low pressure 223
101 FIGURE 89: Wm1 & Wm2 vs Tpr, effect of e at high pressure 224
102 FIGURE 90: Effect of factor F on the Optimal Bolt load. 225
103 FIGURE 91: Relative effect of factor F on Optimal Bolt Load. 226
104 FIGURE 92: Wm1 & Wm2 vs M, effect of F at low pressure 227
105 FIGURE 93: Wm1 & Wm2 vs M, effect of F at high pressure 228
106 FIGURE 94: Wm1 & Wm2 vs Tpr, effect of F at low pressure 229
107 FIGURE 95: Wm1 & Wm2 vs Tpr, effect of F at high pressure 230
108 FIGURE 96: Wm1 & Wm2 vs Tpr (Approx. Soln. out of range). 231
109 FIGURE 97: Wm1 & Wm2 vs Tpr (Approx. Soln. > Opt. Soln.) 232

Table of Tables

110 TABLE 1. Standard Data to Compute Tpmin. 18

111 TABLE 2: Summary of models analyzed using ABAQUS. 38

112 TABLE 3: Summary of models analyzed using GIFTS. 39

113 TABLE 4: 2nd order polynomial fits of gasket stress distribu 73

114 TABLE 5: 1st order polynomial fits of gasket stress distribu 74

115 TABLE 6: Average bolt stresses (ABAQUS). 76

116 TABLE 7: Average Gasket Stresses (ABAQUS). 79

117 TABLE 8: Polynomial fit of gasket stress distributions (GIFT 82

118 TABLE 9: Average Bolt Stresses, Class 1500-24 (GIFTS). 87

119 TABLE 10: Average Bolt Stresses Class, 1500-12 (GIFTS). 88

120 TABLE 11: Average Bolt Stresses, Class 1500-6 (GIFTS). 89

121 TABLE 12: Average Gasket Stresses, Class 1500-24 (GIFTS). 92

122 TABLE 13: Average Gasket Stresses, Class 1500-12 (GIFTS). 93

123 TABLE 14: Average Gasket Stresses, Class 1500-6 (GIFTS). 94

124 TABLE 15: Percentage Difference in average bolt stresses, AB 102

125 TABLE 16: Percentage Difference in average gasket stresses, ... 102

126 TABLE 17: CASE I. Current Code vs TurboFlange (Bolt Loads). 117

127 TABLE 18: CASE I. Current Code vs TurboFlange (Flange Moment 118

128 TABLE 19: CASE I. Current Code vs TurboFlange (Flange Stress ... 119

129 TABLE 20: CASE II. Current Code vs TurboFlange (Bolt Loads). 121

130 TABLE 21: CASE II. Current Code vs TurboFlange (Flange Momen
..... 122
131 TABLE 22: CASE II. Current Code vs TurboFlange (Flange Stres ... 123
132 TABLE 23: FE vs TurboFlange. Equivalent Average Operating S ... 130
133 TABLE 24: FE vs TurboFlange. Equivalent Average Seating Str 131
134 TABLE 25: FE vs TurboFlange. Equivalent Average Bolt Stress 132

NOMENCLATURE

A_g	Full Gasket contact area.
A_i	Pressurized Gasket.
A_r	Ratio of Effective Gasket area and pressurized area.
B	Gasket constant B.
d	Gasket constany d.
E	Modulus of Elasticity.
e	Joint Efficiency.
F	Leakage experience factor.
M	Ratio of Gasket operating stress (Sm) over pressure (P).
P	Fluid Operating Pressure.
S^*	Point of ambient tightness on S_a, S_g vs. T_p plot.
S_a	Gasket assembly or seating stress.
S_g	Gasket operating stress.
S_b	Design Bolt Stress.
S_m	Design Gasket operating stress.
S_{ya}	Design Gasket seating stress.
TC	Tightness Class.
T_p	Tightness.
T_{pmin}	Minimum level of tightness.

T_{pn}	Tightness level for a particular level of stress.
T_{pr}	Ratio of Tpn over Tpmin.
v	Young's Modulus.
W_{m1}	Operating design bolt load.
W_{m2}	Seating design bolt load.
W_o	Optimum design bolt load.

1 CHAPTER 1

INTRODUCTION

In recent years, an effort has been under way to improve the accuracy of the design of gasketed bolted flanges. Many experimental and analytical studies have been sponsored by the Subcommittee on Bolted Flange Connections of the Pressure Vessel Research Council (PVRC) and by the Subcommittee's Task Group on Gasket Testing.

The design of Bolted flanges in North America (and many other countries) is governed by a set of rules specified in the ASME Boiler and Pressure Vessel Code (Sections III and VIII). One of the objectives of the ongoing research program is to incorporate the new findings into the ASME Code so as to improve its accuracy and reliability.

Although many critical joints operate at elevated temperature, the majority of the tests and the results obtained up to date involve joints operating at room temperature. This is a necessary simplification in order to study the basic mech-

anisms which produce leaks. In the last months, however, preliminary data for elevated temperature tests has been obtained by Bazergui and collaborators, and the elevated temperature test program is now well under way.

1.1 GENERAL DESCRIPTION OF THE PROJECT

The present study is based on the results and findings from the room temperature test program. This work was conducted in an attempt to develop a practical procedure for the design of bolted flanges, which could serve as an alternative to the current ASME Code design procedure.

The project was conducted in two phases :

- Development of an optimizing design procedure incorporating the findings from the room temperature test program.

- Finite Element (FE) Stress Analysis of standard ANSI B16.5 flanges in conjunction with several gasket materials.

These two phases of the study were conducted simultaneously. The idea behind this approach was to check the validity of the new proposed design procedure using the results from the finite element stress analysis.

1.2 OBJECTIVES

The first phase of the study pursued the following objectives:

a. To gain a better understanding of the overall behavior of the joints.

b. To incorporate the experimental results from the room temperature tests in a simple analytical design procedure for the design of bolted flanges.

c. To provide a better understanding of the stress-tightness behavior of the gasket materials, and its significance to the design of safe joints.

d. To assess the relative effect of the different design parameters on the new procedure.

e. To develop an interactive computer program implementing the new procedure.

f. To compare the results obtained from the new procedure with those obtained with the current ASME Code.

The Finite Element Stress analysis, on the other hand, pursued the following objectives:

a. To gain a better understanding of the overall behavior of the stresses on the joints, specially at the flange-gasket contact area.

b. To develop useful simplifications in the Finite Element Analysis of the joints, specially when it comes to the modeling of the gasket material.

c. To compare the difference in the results between a linear-elastic and a nonlinear-elastoplastic analysis of the joints.

c. To obtain a more realistic representation of the mechanical behavior of the assembly, and to use the results obtained to improve the new analytical method being developed.

d. To study the relative effect of the different design parameters on the behavior of the joints. Specifically, the design pressure, the material properties, the bolt load and the size of the assembly.

1.3 ORGANIZATION OF THE REPORT.

This document is divided in 7 Chapters.

Chapter 1 is the Introduction to this report.

Chapter 2 introduces the reader to the experimental tests and results that served as the basis for this study, and how new basic equations are derived from the experimental data.

Chapter 3 presents the methodology of the analysis employed in both the development of the new design procedure, and the Finite Element analysis of the joints. Relevant equations are developed and the underlying principles and assumptions are presented and discussed.

Chapters 4, 5 and 6 present and discuss the results obtained from this study.

Chapter 4 presents the results from the Finite Element stress analyses; Chapter 5 discusses the results from the new proposed design procedure; and Chapter 6 compares the FE analysis results with those obtained from the new proposed procedure.

Finally, the Conclusions and recommendations are presented in Chapter 7, followed a list of references and various appendices.

Figures referenced in the text are included in the **GRAPHS & FIGURES** section immediately after Chapter 7.

Appendix A, presents the data used in the FE stress analyses; and Appendix B outlines the data and the results obtained for two sample cases analyzed using both the current ASME code and the new design procedure.

2 CHAPTER 2

THEORETICAL & EXPERIMENTAL FOUNDATIONS

In this chapter, a review of the experimental and theoretical foundations of the study are presented.

Section 1.1 provides a brief discussion of the nature of the experimental results used in the study, and the tests from which these were obtained.

Section 1.2 introduces the relevant test data used in the study and its phisical significance.

Section 1.3 reviews the basic equations derived from the experimental results (Ref. [1-4]), which served as the basis for the new proposed procedure.

For the reader's convenience, figures are included in the **GRAPHS & FIGURES** section starting on page 135.

2.1 EXPERIMENTAL TESTS

Over recent years, extensive gasket tests have been carried out under the auspices of the Pressure Vessel Research Committee (PVRC) of the Welding Research Council (WRC) in cooperation with the American Society of Mechanical Engineers (ASME) and the American Society for Testing and Materials (ASTM). The tests, formulated by the Task Group on Gasket Testing of the Sub-Committee on Bolted Flange Connections of the PVRC, are aimed at understanding gasket behavior and at improving methods of designing gasketed joints.

In general, this testing effort has been divided in two parts: 1) room temperature gasket testing, and; 2) elevated temperature tests. In both cases two types of tests may be performed: Mechanical tests and Leakage tests.

The present study only considered results from room temperature tests since the elevated temperature results were not available at the onset. The results from leakage tests served as the basis for the development of a new more accurate design procedure, while mechanical test results were used in the finite element analysis of the joints.

2.1.1 MECHANICAL TESTS

The Mechanical Tests consist of two portions: a) The Stress vs Deflection portion; and b) The Creep portion. Each gasket style is tested typically 4 times, each at a higher maximum stress level. These 4 stress levels are selected from 5 "standard" levels identified as K1 to K5. For a detailed explanation of how these stress levels are calculated please see references [1-2].

The Stress-Deflection test consist of two parts: First, the gasket is loaded at a constant rate of 100 psi/sec, (0.69 MPa/s), until the desired level of stress is reached. Then, an unloading-reloading phase follows. At each stress level (K1 to K5) three unloading-reloading cycles are applied. The load vs. deflection diagrams are recorded on an X-Y plotter.

References [1] and [2] provide more detail concerning the testing set-up and procedure.

2.1.2 LEAKAGE TESTS

Several set-ups are used to conduct the leakage tests [1]. These can be generally classified as Hydraulic Test Rigs, and Bolted-Up Rigs. In spite of

major differences in concept, construction and capacity between the various set-ups, the results are usually quite comparable.

The Leakage Test Procedure is outlined in Figure 1. The various paths in the test sequence are referred to as either Part-A or Part-B as follows:

Part-A: This part of the test represents initial joint tightening and gasket seating. Each new gasket stress level is higher than any previously applied stress and is referred to as the gasket "assembly" stress Sa. Leakage is measured at constant predetermined assembly stress levels for three helium pressures.

Part-B: This part of the test simulates the cyclic load variations in a bolted joint. In these cycles, the test gas pressure is maintained constant and leakage is measured for different levels of gasket stress, Sa. Gasket stress is first decreased to a low initial level and then increased back to S_g. The assembly stress is then further increased, so that the test sequence reverts back to Part-A. Then a new Part-B cycle is carried out from and to a higher assembly stress level, and so on. Ussually, up to three such cycles may be performed.

2.2 STRESS-DEFLECTION & STRESS-TIGHTNESS DATA

Some of the results obtained from the mechanical and leakage tests can be summarized in two basic plots: **stress-deflection** plots from mechanical tests, and **stress-tightness** plots from leakage tests. For the purpose of this study, the stress-deflection plots were used to model the stress-strain behavior of the gasket material in the finite element analysis of the joints, while the stress-tightness plots served as the basis for the development of a new tightness based more accurate design procedure.

2.2.1 STRESS-DEFLECTION PLOTS

A typical stress-deflection curve, as obtained from the tests, is shown in Figure 1. In it we can identify two regions: a) The upper, non-linear, part of the curve, representing the seating of the gasket due to the initial tightening of the bolted joint; and b) The unloading-reloading portion of the diagram, which represents the cyclic loading on the gasket under operating conditions. The general non-linear form of part A may vary considerably from one gasket to another, on the other hand, most gaskets typically present the practically linear unloading-reloading behavior shown in Figure 1.

From the slope of the linear unloading-reloading part of the curve, a Modulus of Decompression, Eg, may be determined in the following manner [21]:

$$E_g = \frac{dS_g}{dD_g} \frac{1}{(T_i - D_{gmax})} \tag{1}$$

Where:

E_g = modulus of decompression,

dS_g/dD_g = slope,

T_i = initial gasket thickness,

D_{gmax} = maximum gasket deflection.

This factor will be further analyzed in the next chapter, when the mechanical behavior of the joint is discussed.

2.2.2 STRESS-TIGHTNESS PLOTS

According to Bazergui et al [1-4], since the probability of leakage increases with gasket diameter, it is reasonable to assume that leakage is proportional to gasket diameter. For this reason, leak rate per unit gasket

diameter is used for comparing the results for different types of gaskets and joint sizes. The authors [1-4] have also observed over the years a strong correlation between fluid pressure and leakage, as follows:

$$P = (constant)(L_{rm})^a \tag{2}$$

From which a non-dimensional tighness parameter was derived

$$T_p = \frac{P}{P^*}\left(\frac{L^*_{RM}}{L_{rm}D_t}\right)^a \tag{3}$$

Where:

P^* = reference atmospheric pressure , 0.1 Mpa (14.7 psi)

P = test pressure,

L_{RM}^* = reference mass leak rate (1 mg/s) based on a 150 mm OD gasket,

D_t = test gasket OD,

a = leakage exponent.

A value of a = 0.5 has been adopted to standardize tightness data for gases [3,4].

In order to interpret gasket sealing behavior in terms of gasket stress, a log-log plot of Gasket Stress, S_g, as a function of T_p was devised (Figures 2 & 3). This plot, called a Stress-Tightness Plot, illustrates the complete leakage test sequence in a condensed format, and constitutes the basis for the new gasket equations that will be presented in the next section.

2.3 NEW GASKET CONSTANTS AND EQUATIONS

The developments and observations given in this section are based on material presented in references [3] and [4]. They are included here for clarity and continuity.

2.3.1 NEW GASKET CONSTANTS

Three important points which serve to characterize gasket behavior can be observed from most Stress-Tightness plots. These are:

(1) The upper part of the plot, Part A, is characterized by the presence of a "knee" beyond which tightness increases more rapidly with increasing stress. This indicates improved sealing performance and is considered physical evidence of seating.

(2) The high stress portion of Part A (beyond the knee) can be adequately represented by a straight line. This line represents the gasket assembly or seating stress S_A.

(3) The unloading-reloading part of the plot, Part B, is characterized by a series of straight lines that tend to converge to a point. These converging lines represent the gasket operating stresses S_g. For most gaskets the converging point is at a gasket stress close to ambient pressure (P^*), and a tightness of 1, for this reasons it has been called the "Point of Ambient Tightness".

Based on the above considerations we can construct a simplified, "ideal", Stress-Tighness plot, as the one shown in Figure 4. This type of plot summarizes the stress tightness performance of gaskets, and allows important design simplifications.

On Figure 4 we can observe three parameters labeled B, d and S*:

- "B" is the intercept of this line with the stress axis at Tp=1, and;
- "d" is the slope of the upper, high stress, line;
- "S^*" is the point to which all unloading-reloading lines are assumed to converge, the point of Ambient Tightness.

These three constants completely define any ideal Stress-Tightness plot and, hence, the design Stress-Tightness behavior of the gasket material. They are unique for a given gasket type and allow numerical characterization of gasket materials.

2.3.2 GASKET EQUATIONS FROM IDEALIZED STRESS-TIGHTNESS PLOTS

The idealized Stress-Tightness plot, Figure 4, serves as the basis for the new equations describing the stress tightness behavior of the gasket.

2.3.2.1 Minimum Tightness Parameter T_{pmin}.

Figure 4 also introduces a new parameter, the minimum required tightness, T_{pmin}. This value sets a lower bound for the tightness level on a joint and thus determines a minimum seating stress, S_{amin}, and minimum operating stresses, S_{gmin}. Note, that while S_{amin} is unique for a given value of T_{pmin}, S_{gmin} is not. From Figure 4 we can see that there is a value of S_{gmin} for each Part B line intersecting the vertical line T_p=T_{pmin}. Thus, there are infinite values of S_{gmin} each associated to a particular value of S_a.

In order to select a value for T_{pmin}, a maximum allowable leak rate must be defined. Using Eqn. 3 we could then compute the corresponding

tightness value. In order to simplify the use of these new equations and parameters, three standard tightness classifications (T1 to T3) have been defined for design purposes.

TABLE 1: Standard tightness data to compute T_{pmin}.

Tightness classification (Tpmin)	Corresponding Mass Unit Leak Rate
Economy : T1	1/5 mg/s.mm
Standard: T2	1/500 mg/s.mm
Tight : T3	1/50000 mg/s.mm
Reference Diameter : 150 mm Tightness exponent a: 0.5	

Introducing the above data into Eqn. 3 we obtain the following general expression for T_{pmin}:

$$T_{pmin} = (1.82574)(c)\left(\frac{P}{P^{*}}\right) \tag{4}$$

Where for:

T1 c = 1/10

T2 c = 1

T3 c = 10

The value 1.82574 = $(500/150)^{0.5}$ assumes a reference test diameter, Dt, of 150 mm, which is used to normalize the standard mass unit leak rates above in mg/s.mm. These are leak rates per unit diameter. In volumetric terms a Standard class T2 leak rate is approximately 35 liters/day (75 pints/day) of nitrogen gas at standard conditions for a 10 in NPS joint [4].

2.3.2.2 Gasket Stresses Sa and Sg.

Form Figure 4 the Assembly stress, S_a, corresponding to a given tightness level of T_{pn}, is given by:

$$S_a = B(T_{pn})^d \tag{5}$$

(Obviously letting T_{pn}=T_{pmin} would yield S_{amin})

A corresponding minimum operating stress, S_{gmin}, can be determined from:

$$S_{gmin} = S^*(T_{pmin})^{kf} \tag{6}$$

Where kf is the slope of the line joining S^* and S_a.

These two equations can be rearranged so the slope kf need not be known. From the equivalent triangles on Figure 4, the linear relationships on log-log plot yield:

$$kf = \frac{\log(S_a) - \log(S^*)}{\log(T_{pn}) - \log(T_a)} = \frac{\log(S_{gmin}) - \log(S^*)}{\log(T_{pmin}) - \log(T_a)}$$

since T_a (Ambient tightness) = 1, then $\log(T_a) = 0$

Thus we can obtain the following relation:

$$\frac{S_{gmin}}{S^*} = \frac{S_a}{S^*}^{\left(\frac{1}{T_r}\right)} \qquad (7)$$

$$\text{Where}: T_r = \frac{(\log(T_{pn}))}{(\log(T_{pmin}))}$$

This equation is directly applicable to design, at least for ideal conditions. For a given gasket type (B, d, S^*) and a desired seating tightness (T_{pn}) we can obtain the required seating stress, S_a, using Eqn. 6. Then, given a Tightness Class (TC) and the design pressure (and thus T_{pmin}), a corresponding minimum operating stresses, S_{gmin}, can be calculated using

Eqn. 7.

Recall that for any S_a, at $T_p=T_{pn}$, there is a corresponding S_{gmin} at $T_p=T_{pmin}$. This is an important point since it means that we can always get a MINIMUM operating stress, given an initial assembly stress. The fact that S_g is directly minimized by these equations is of great interest in the design of joints.

In the next chapter, these ideal and basic design principles will be further developed into a practical design procedure.

3 CHAPTER 3

METHODOLOGY

This Chapter describes the methodology employed in the present study. Based on the discussion presented in Chapter 1, the principles, techniques and assumptions involved in the study will be presented and discussed.

For the reader's convenience, figures are included in the **GRAPHS & FIGURES** section starting on page 135.

The study was divided in two parts:

1 - Finite Element (FE) Stress Analysis of the Joints.

2 - Development of a new, ASME like, analytical procedure for the optimal design of bolted flanges.

These two phases of the study were conducted simultaneously. The idea behind this approach was to check the validity of the new proposed design procedure using the results from the finite element stress analysis. In addition to this, the FE study was conducted for the following reasons:

a. To gain a better understanding of the overall behavior of the joints.

b. To develop useful simplifications in the study of the joints, specially when it comes to the modeling of the gasket material.

c. To obtain a more realistic representation of the mechanical behavior of the assembly, and to use the obtained results to improve the new analytical method being developed.

As for the new proposed design procedure; it is intended as an alternative to the ASME Code procedure currently being used for the design of bolted flanges (For a complete description of the ASME procedure, see Ref. [5]). As discussed in the previous Chapters, the ASME Code may eventually be revised with the objective of taking into account more realistic gasket factors. This is exactly the aim of the procedure presented in this thesis, it is a simple and accurate method, which departs slightly from the mechanics of the current ASME Code, specifically

in the computation of the bolt loads.

3.1 FINITE ELEMENT STRESS ANALYSIS

In this part of the study, linear and nonlinear stress analyses of various standard flange geometries and gasket materials were conducted. This section will outline the approach followed for the analysis, the difficulties encountered, the assumptions and simplifications adopted and, finally, an assessment of the relative validity of the method.

3.1.1 THE PROGRAMS: ABAQUS vs GIFTS

Two Finite Element programs were used to carry out the analyses: a linear elastic code, GIFTS; and an elastoplastic code, ABAQUS.

ABAQUS is a mainframe-based program which provides the designer with multiple modeling and analysis options. It allows elastic and elastoplastic analysis, thermal analysis, linear and nonlinear modeling options, etc. This program was used to do nonlinear, elastoplastic analyses of the joints.

GIFTS is a linear/elastic analysis program which runs on an IBM PC/AT. The program includes sub-structuring, thermal analysis (steady state), and

dynamic analysis as well. It provides multiple types of elements, including second order 9-noded four sided axisymetric elements, and second order 7-noded triangular axisymetric elements.

GIFTS was used to do elastic analyses of the bolted joints, the program only permits linear material modeling, and does not offer any type of plastic analysis option. The results obtained using this program were verified with elastic results from sample runs using ABAQUS.

3.1.2 MODELING OF THE GASKET MATERIAL

Figure 5 presents two typical stress-strain plots for gasket materials. As shown in the figure the stress-strain behavior of most gasket materials presents a marked nonlinear behavior (These kind of plots are based on the stress-deflection curves discussed in Chapter 1). The Figure also shows the lines simulating the unloading-reloading cycles represented by the modulus of decompression, Eg, introduced in Chapter 1. From Figure 5 we can also observe the following:

1. The nonlinear, high-stress, portion of the plot (seating conditions) does not present the same nonlinear behavior for all gasket materials. In some

cases the degree of nonlinearity is more pronounced than others. Moreover, some gaskets present nonlinear behavior only at low stress levels, while others are quite nonlinear throughout.

2. The modulus of decompression, Eg, varies from one stress level to another, K1 to K5, sometimes quite considerably. Thus, the stress behavior under operating conditions appears to depend on the maximum seating stress level achieved.

If we analyze the loading-unloading behavior of the gasket materials, it becomes apparent that they present a definite plastic behavior. At a significant level of loading stress or initial deflection, the gasket always retains some accumulated deflection when unloaded. In this respect, (loading-unloading) it would be hard to say if the materials behaved in an elastic manner at all, maybe at very low stress levels this is true, but the available experimental data does not include such information, and for any meaningful purposes the materials present a fully plastic behavior. On the other hand the unloading-reloading behavior of the gasket is almost elastic and practically linear. This fact will be put to use in the modeling of the material. In the light of the above statements and considering that the materials also exhibit thermal and creep effects, it is evident that, in order to make use of all the experimental data for design purposes, it is necessary

to impose certain simplifications.

The goal of this research was not to develop a highly sophisticated model for gasket materials, but rather to formulate useful simplifications that would permit easier modeling of these using commercial FE codes. Several approaches have been followed involving different levels of simplification, with the objective of achieving time savings when using FE methods in the design of bolted joints. In fact, the results obtained from this research could be ideally implemented in a simple customized program to do this type of analysis.

Both linear and nonlinear material modeling was used to represent the mechanical behavior of the gaskets. On the one hand, linear-elastic behavior of the gasket was assumed and a constant modulus of elasticity was chosen for each gasket material from the unloading-reloading part of the gasket stress-deflection test plots. The limitations of this approach will be discussed later. On the other hand, nonlinear modeling was done because, as discussed above, the real behavior of the gasket is linear only under unloading-reloading conditions (operating condition). During seating or initial loading, the material presents substantial nonlinear behavior. In this respect, a varying modulus of elasticity was prescribed for the gaskets, and the analysis was performed using the nonlinear elastoplastic code (ABA-

QUS).

The results from these two methods were compared in order to asses the relative merits of each approach. These will be discussed later. We will discuss first the nonlinear modeling of the gasket and then the linear approach.

3.1.2.1 Nonlinear Modeling.

The task of modeling the behavior of the gasket material in a nonlinear fashion is not a trivial one. It is particularly difficult when using commercial FE packages, since, depending on the program, the analysis and modeling tools vary greatly.

First, there is the problem of how to assign nonlinear properties to the material. One alternative is to define a Stress-Strain function that fits the experimental stress-strain plots. This could be done using polynomial interpolation [13]. Unfortunately, this approach involves the development of external routines to be called from the FE program, and this is quite complicated and tedious.

Another consideration is the non-elastic behavior of the gasket materials as they do not follow the same path for initial loading than for unloading. Consequently, it becomes necessary to carry out an elasto-plastic analysis as well as to define a nonlinear model for the material.

These considerations and the options available in the ABAQUS FE program, determined the implemented modeling procedure which consisted in combining the nonlinear seating and linear operating behavior of the gasket, with the elastoplastic nature of the material.

In ABAQUS, it is possible to prescribe complex plastic stress-strain material behaviors by defining different key points. The program interpolates linearly between these points as shown in Figure 6. Thus, by defining several linear segments we can adequately approximate the nonlinear behavior of the gasket under initial loading. Note, however, that in order to formulate this behavior one must define a Young's modulus, E, and prescribe isotropic plastic behavior on the material. That is, when loading the material follows the segmented upper line, while unloading, however, it will follow a path parallel to the elastic portion (modulus E). This is very convenient since it resembles very closely the behavior of the gasket materials, namely: A nonlinear path while loading, and a linear cyclic path while unloading (Fig. 7).

In order to model the behavior of the gasket using this method the following steps were followed:

1- Define *E*.

2- Define the yield point, or elastic stress limit.

3- Define plastic key stress-strain points.

The yield point should be a low value (bellow K1), a value of approximately K1/10 or 300 psi (2 Mpa) was used. The stress key points can be obtained from the experimental gasket stress-strain plots, the corresponding strain levels are calculated using the following equation:

$$e_p = e - \frac{S}{E} \tag{8}$$

Where:

e_p = Plastic strain.

e = Total strain.

S = Stress level corresponding to *e*.

E = Young Modulus.

A problem remains however. The stress distribution across the gasket is not uniform. For a typical raised-face flange geometry, gasket compression is generally lower towards the inner circle and higher on the outside due to the deflection of the flange during initial bolting-up. Therefore, different points on the gasket will reach different maximum seating stresses, and will thus have different slopes on the unloading-reloading lines (Eg). Since only one value of *E* is allowed, the selected approach was to use the modulus of decompression , E_g corresponding to the average seating stress across the gasket from the appropriate Gasket Stress-Strain plot, thus determining *E*. After the analysis is performed the assumed average stress is checked against the results obtained.

3.1.2.2 Linear Modeling.

Most FE stress analysis codes only permit linear modeling of material behavior. This limitation introduces the need to attempt to linearize the behavior of the gasket materials.

As mentioned earlier, the linear modeling was performed using GIFTS, a FE program that runs on desktop computers (AT and 386 PC's).

Given the gasket behavior of Figure 5, the question arises as to what should be the value of *E* used to most accurately represent the mechanical behavior of the gasket.

Three possibilities were considered:

1. To take a linear approximation on the nonlinear seating curve, using the slope of this line as *E*.
2. To take an average of the values of Eg, for stress levels K1 to K5.
3. To take the value of the modulus of decompression, Eg, closest to the maximum seating stress level expected.

Let us discuss the relative merits of each approach:

Due to the marked nonlinear form of the seating behavior of most gaskets, it sometimes becomes very difficult and inaccurate to attempt a first order approximation. From Figure 5 we can see that sometimes this is possible, but in many cases the error involved is just too large. Fur-

thermore, this approach completely neglects the operating behavior of the gasket, which is very important in terms of the performance of the gasket. This approach (Option 1 above) is thus inappropriate.

Depending on the bolt loading and operating pressure on the joint, the gaskets may not reach stress levels as high as K5, and these levels are usually well above K1. In most cases the gasket stress distribution lies between levels K2 and K3. Thus, taking a simple average between K1 and K5 does not follow a rational approach, representing the actual conditions on the gasket. For this reason Option 2 was not selected either.

The selected alternative was to take the value of the modulus of decompression, Eg, closest to the maximum stress level expected (Option 3). This is the same criterion used in the nonlinear case. Since practically all gasket materials present a linear behavior under operating conditions, there is no need to linearize the value of Eg. It is also true that this operating, unloading-reloading, phase is more meaningful than the initial compression in terms of the flexibility analysis of the joint [4]. This is because it is under these conditions that the behavior of the joint is most relevant to the designer. Joints only leak under pressure, and the aim of the design is precisely to obtain leak-free assemblies.

By using the modulus of decompression as the Young's Modulus of the material, we are really assuming that the operating condition takes precedence over the seating condition in the general behavior of the gasket-joint assembly. It is for this reason that the actual seating behavior of the gasket and the joint is not as accurately represented in the analysis. This is a very important assumption and we will come back to it when discussing the results.

In order to determine the appropriate value of modulus of decompression to be used, one must know beforehand the approximate maximum value of the seating stress. Using an experimental stress-strain plot we can then select the unloading-reloading line closest to this value and thus a value of Eg, to be used as *E* in the analysis. As mentioned before, the stress distribution across the gasket is not uniform, and different points on the gasket will reach different maximum seating stresses. The same approach discussed under the nonlinear analysis was used to solve this problem.

Another alternative would have been to force each element or groups of elements in the gasket to follow a different modulus of elasticity corresponding to different maximum values of Sg. This is possible by introducing dummy temperatures across the gasket, thus, simulating a

variation of Eg with temperature, but this is possible with only certain FE programs, and complicates the analysis considerably. It is preferred to use one single most representative value of Eg.

Evidently, the linear approach involves simplifications and is by no means as comprehensive as the nonlinear model previously discussed. Nevertheless, the results obtained using this method will be compared with those obtained from the more realistic and accurate nonlinear approach. Of great interest is to determine the degree of discrepancy between the two models. If this method yields good approximate results, then it could be of great help to the designer since it is much simpler to implement and can be done using almost any readily available linear FE code. Furthermore, this approach is particularly suited for comparison purposes with analytical design methods such as the one given by the ASME Code, or the new proposed procedure outlined in this paper.

3.1.3 MODELING OF THE BOLTS

To truly represent the assembly, a solid model of the flange should have been constructed and beam elements used to represent the bolts. However, this is unnecessary and inconvenient because of the almost fully axisym-

metric nature of the problem (see Fig. 8).

In the present analysis, the bolts were replaced by a solid ring with an equivalent cross sectional area. This decision was made based on the experience of previous researchers [10-13] , which suggests that the elimination of the bolt holes does not significantly affect the behavior of the joint. This solid ring is physically superimposed over the flange, they are two independent bodies which share a common surface, and occupy the same space. The ring is fully connected to the flange on one end, whereas the other end is initially free, and eventually fixed to the line of horizontal symmetry (Figure 8).

When using a ring, it is assumed that the bolt load acts uniformly over the joint (Figure 9). In reality this is generally not so, because when tightening the bolts non-uniform loads are applied. Nevertheless, this is a very useful design simplification. To simulate the actual tightening of the bolts, the lower end of the ring is stretched, that is, a fixed displacement on all nodes in this line is prescribed. This induces internal tensile stresses on the bolt ring which produces a compressive reaction on the flange (Fig. 8). This method avoids specifying a constant bolt load acting on the assembly. The bolt load will adjust itself as the assembly reaches equilibrium, both under seating and operating conditions, and constitutes an accurate representation of the

actual varying nature of the bolt load.

3.1.4 THE ANALYSIS

Based on the assumption that the geometry of the joint and the applied loads are axisymmetrical, and by using the modeling techniques described earlier, the stress distribution on the gasket was studied using the two finite element programs, ABAQUS and GIFTS. The analysis was divided in two parts: Seating of the gasket, and Operating condition of the joint.

3.1.4.1 The Mesh.

Standard Flange Classes from ANSI B16.5, in conjunction with 4 different gasket materials were used in the analyses. A summary of these also included in Tables 2 and 3 bellow.

TABLE 2: Summary of models analyzed using ABAQUS.

GASKETS	FLANGE CLASS	NOMINAL SIZE	YOUNG'S MODULUS	POISSON'S RATIO
GHS	1500	24 in (600 mm)	150 ksi (1000 Mpa)	0.4
SELCO	1500	24 in (600 mm)	232 ksi (1600 Mpa)	0.4
DJ MICA FILLED	1500	24 in (600 mm)	234 ksi (1613 Mpa)	0.4
DJ ASBESTOS FILLED	1500	24 in (600 mm)	244 ksi (1682 Mpa)	0.4

NOTE: Complete stress-strain data for the ABAQUS models is included in APPENDIX A.

TABLE 3: Summary of models analyzed using GIFTS.

GASKETS	FLANGE CLASS	NOMINAL SIZE	YOUNG'S MODULUS	POISSON'S RATIO
GHS	1500	24,12,6 in (600,300, 150 mm)	150 ksi (1000 Mpa)	0.4
SELCO	1500	24,12,6 in (600,300, 150 mm)	232 ksi (1600 Mpa)	0.4
DJ MICA FILLED	1500	24,12,6 in (600,300, 150 mm)	234 ksi (1613 Mpa)	0.4
DJ ASBESTOS FILLED	1500	24,12,6 in (600,300, 150 mm)	244 ksi (1682 Mpa)	0.4

Several grids were constructed representing the different geometries studied. The grids used in both programs were geometrically equivalent. They were not completely identical because both programs do not support exactly the same types of elements.

The main objective of the analysis was to study the stress distribution across the gasket. In order to obtain accurate results, the mesh was progressively refined towards the gasket. Since the gasket is very thin in relation to its width, a large number of elements must be defined across the width, this is necessary to keep a sensible ratio between the sides of the elements.

The ABAQUS gasket grid consisted of second order 8 noded quadrilateral elements. One layer of 32 elements was used to model the gasket. Using two layers doubled the number of elements across the width which resulted in a considerable and unnecessary increase in computation time and cost which was already quite high.

In GIFTS, quadrilateral elements were also used for the gasket mesh. Several trial runs were conducted using second order elements, as these yield more accurate results. Unfortunately, in GIFTS, their use increases considerably the time of the analyses, up to 10 hours on an IBM AT. When

using a large number of first order elements, however, the results obtained from the analysis are sufficiently close to those obtained using second order elements. Moreover, using first order elements drastically reduces the time of the analysis. Average times were below an hour, except when a very large number of elements were used. Consequently, the gasket mesh used in GIFTS for the elastic-linear analyses consisted of two layers of 30, 38 and 90 linear, 4-noded quadrilateral elements. The number of elements across the width varied according to the size of the flange and the gasket.

3.1.4.2 Boundary Conditions.

Due to the symmetry of the problem, only one half of the rotationally axysymmetric assembly needs to be defined in the analysis. Two lines of symmetry were defined: The axial line at the center of the pipe, S1; and the horizontal line dividing the assembly in half, S2 (Figure 10). Notice that only one half of the gasket thickness is defined.

As shown also in Figure 10, very simple boundary conditions are applied on the models. Because of the symmetry with respect to S2, the displacement at the middle plane of the gasket is fixed in the axial direction,

and free in all other directions. The bolt ring is attached to the flange on one end, the other is stretched and fixed to the horizontal line of symmetry. The stretched end is only constrained on the axial direction.

3.1.4.3 Loading.

Different loads are applied on the joint for the two design conditions:

In the seating condition, only the bolt force resulting from the elongation of the ring is applied. The desired bolt force is obtained by iteration. As explained before, a fixed displacement is prescribed on the free end of the bolt ring and the stresses are computed. If the desired bolt load is not obtained, the cycle is repeated until the computed stresses on the ring correspond to the desired bolt load. The resulting stress distribution on the gasket is recorded as that corresponding to the seating condition.

In the operating condition the forces due to pressure are introduced, while maintaining the prescribed displacement on the lower end of the bolt ring. In this way the operating stress distribution of the gasket is obtained.

Three fixed area loads are applied on the flange. These are also shown in Figure 10.

1- The hydrostatic end pressure assumed to be acting on the end of the hub.

$$F_1 = \frac{P r_1^2}{r_2^2 - r_1^2} \tag{9}$$

Where :

r_1 = inner radius of the hub.

r_2 = outer radius of the hub.

2- The fluid pressure acting on the inner wall of the pipe.

$$F_2 = P \tag{10}$$

3- The fluid pressure acting on the inner face of the flange.

$$F_3 = P \tag{11}$$

3.1.4.4 Design Criteria.

In general, a leak in a joint is produced when some separation occurs between the gasket and the flange. Since in this analysis the flange and

the gasket are attached to each other, separation will be determined by inspecting the stresses and not the deflections in the contact zone. It will be thus assumed that, in general, the joint will tend to leak when the contact stress between the gasket and the flange is significantly reduced.

For both the seating and operating condition, a minimum gasket stress level has been defined in [4] as, $S_{min} = 2P$. When the resulting level of stress on the gasket is above this value the joint is considered to be stable, i.e., not subject to a sudden blow-out. Separation of the gasket is assumed to occur when positive (tensile) or low negative values, below S_{min}, are obtained in the stress distribution. An unacceptable design condition depends on both the relative size of the "separated" area, and the magnitude of the stresses.

All the preceding considerations have been applied to both the elastic and elastoplastic analyses. The results obtained from these will be presented and discussed later in Chapter 4.

3.2 NEW OPTIMIZING DESIGN PROCEDURE

In addition to the Finite Element analysis of the joints described in the previous section, a new ASME like optimizing procedure was also developed as part of this study. This section outlines the development of this procedure and its applications to the design of bolted flanges.

The new optimizing procedure minimizes the design bolt loads acting on pressurized gasketed flanges, this results in smaller and more efficient structures. The basic idea behind the method is to find the lowest possible value for the bolt load, that will also yield a safe and practical design. The procedure is based on the experimental data obtained from the hundreds of tests commissioned by the Pressure Vessel Research Committee. The tests and the resulting data were discussed in Chapter 1.

According to the present ASME Pressure Vessel Code, there are two bolt loads to be taken into account in the design of a flanged joint. The bolt load required for proper seating of the gasket (W_{m2}), and that required to ensure a "leak free" joint under operating, pressurized, conditions (W_{m1}). In the Code these two loads are calculated independently using current gasket constants, m and y, and equilibrium equations.

The new procedure follows a different approach: Instead of using fixed gasket design constants such as m and y, it makes use of the new gasket equations developed from the experimental tests mentioned above. These equations relate the gasket seating stress, S_m, to the operating stress, S_{ya}, by way of two tightness parameters, T_{pmin} and T_{pn}. Since W_{m1} and W_{m2} are functions of S_m and S_{ya}, then these new equations also permit to relate W_{m1} to W_{m2}.

3.2.1 CORRECTION FACTORS "e" and "F":

Before proceeding with the development of equations relating bolt loads to the new gasket equations, we need to introduce two new factors in the discussion:

e the Joint Assembly Efficiency, and

F the Operating Experience Factor.

These two factors were introduced by Payne et al. [3]. They serve as safety factors in order to adjust results computed from the ideal gasket equations into more realistic field behavior.

Factor "*e*" is introduced recognizing that S_{gmin} improves depending on the minimum value of S_a actually achieved during bolt up. For example a value of 0.75 assumes manual bolt up, while a value of 1.0 assumes almost ideal bolt up.

Experience shows that there needs to be a prudent buffer between S_{gmin} as obtained from laboratory data, and values for gasket operating stress that are appropriate for design. "*F*" is introduced as an operating leakage factor that is intended to serve as that buffer. It is intended to account for things such as the variation of gasket stress between bolts, or the rotation of flexible flanges; flange facing surface defects; field vs laboratory leakage rates, etc. Presently a value of $F = 1.0$ is being used for lack of more significant data.

These two factors affect the basic gasket equations for S_{gmin} and S_a and yield design values for these two ideal gasket stresses. We compute S_m and S_{ya} as follows:

The Design Gasket Seating Stress, S_{ya}

$$S_{ya} = \frac{S_a}{e} = \frac{B(T_{pn})^d}{e} \tag{12}$$

The Design Gasket Operating Stress, S_m

$$S_m = FS_{gmin} = FS^*\left(\frac{S_a}{S^*}\right)^{T_r} \tag{13}$$

The results from the FE stress analysis will help provide new information that will allow a better numerical evaluation for both *e* and *F*.

3.2.2 DESIGN CRITERIA

When W_{m1} and W_{m2} are plotted against the non-dimensional parameter $M = S_m/P$, Figure 11, we observe that the resulting curves cross at a point: This point of convergence determines the minimum, yet safe, (optimum) design bolt load to be used in the calculation of the stresses in the flange. By using this load value we can minimize the thickness of the flange, the number of bolts and their size, and hence produce a more economical design.

A simplified form of the plot of Figure 11 can be developed by defining two non-dimensional load parameters, Wr1 and Wr2. These two are obtained as follows:

From the ASME Code we have the Seating Design Bolt Load

$$W_{m2} = A_g S_{ya} \tag{14}$$

And the Operating Design Bolt Load

$$W_{m1} = A_g S_m + PA_i \tag{15}$$

Where P is the fluid pressure,

A_g is the full Gasket Contact area,

A_i is the Pressurized area,

S_m is the operating gasket stress,

S_{ya} is the gasket seating stress.

Dividing Equations (14) and (15) by PA_i we get:

$$W_{r1} = \frac{W_{m1}}{PA_i} = \frac{A_g S_m + PA_i}{PA_i} = A_r M + 1 \tag{16}$$

$$W_{r2} = \frac{W_{m2}}{PA_i} = \frac{A_g S_{ya}}{PA_i} = \frac{A_r S_{ya}}{P} \tag{17}$$

Where

$$A_r = \frac{A_g}{A_i} = \frac{4N}{(Go - N)} \tag{18}$$

Eqn. 17 follows the Code assumption of defining the effective gasket area in terms of half of the gasket width.

As shown in Figure 12, by plotting these parameters against M, we can readily get an optimal value for the design bolt load. However, since the "Optimal" design Bolt Load was defined as that corresponding to $W_{m1} = W_{m2}$, we can also equate these two loads and solve for the design operating and seating stresses in the gasket, S_{ya} and S_m, using the new gasket equations.

From the new gasket equations and equilibrium we have:

$$S_{ya} = \frac{B(Tpn)^d}{e} \tag{12}$$

$$S_m = FS^* \left(\frac{eS_{ya}}{S^*} \right)^{T_r} \tag{19}$$

Where:

S^*	=	Gasket Constant
B	=	Gasket Constant
d	=	Gasket Constant
e	=	Joint Efficiency
F	=	Leakage Experience Factor
P	=	Operating Pressure

and,

$$T_r = \frac{\log(T_{pmin})}{\log(T_{pn})} \tag{20}$$

So that

$$W_{m1} = S_m A_g + P A_i \tag{21}$$

$$W_{m2} = A_g S_{ya} \tag{22}$$

Combining these into $W_{m1} = W_{m2} = W_m$, we get

$$A_g S_m = A_g S_{ya} - P A_i \tag{23}$$

dividing by A_i,

$$A_r S_m = A_r S_{ya} - P \tag{24}$$

Expanding in terms of S_a,

$$A_r F S^* \left(\frac{S_a}{S^*} \right)^{T_r} = A_r \frac{S_a}{e} - P \tag{25}$$

Also since,

$$S_a = B (T_{pn})^d \tag{26}$$

We obtain

$$\log(T_{pn}) = \frac{\log\left(\frac{S_a}{B}\right)}{d} \tag{27}$$

So that,

$$T_r = \frac{\log(T_{pmin})}{\log(T_{pn})} = \frac{d\log(T_{pmin})}{\log\left(\frac{S_a}{B}\right)} \tag{28}$$

Rearranging Eqn.(28), and introducing factors *e* and *F* we get

$$\left(\frac{S_a}{S^*}\right)^{T_r} = \frac{S_a}{S^*}\frac{1}{eF} - \frac{P}{A_r F S^*} \tag{29}$$

Where:

A_r = Ratio of effective Gasket area and pressurized area.

Finally taking the log on both sides and rearranging using equation (28),

$$dlog(T_{pmin})\log\left(\frac{S_a}{S^*}\right) - \log\left(\frac{S_a}{B}\right)\log\left(\left(\frac{S_a}{S^*}\right)\left(\frac{1}{eF}\right) - \left(\frac{P}{A_r F S^*}\right)\right) = 0 \tag{30}$$

So that

$$W_{m1} = W_{m2} = W_m = f(Sa) = 0 \tag{31}$$

Equation 31, $f(S_a) = 0$, can be solved numerically (using the method of bisections for example) or graphically using a plot as the one in Figure 12. However, there are certain physical constraints on the system that sometimes make it impossible to find an acceptable design solution by just solving for $W_{m1} = W_{m2}$. These are :

1 - An unacceptable value of M (S_m/P), i.e. $M < 2$

2 - An optimum solution which, although numerically possible, is physically unsound. For example, an "optimum" seating stress may be found to be lower than the "optimum" operating stress, ($S_a/S_{gmin} < 1$). This is obviously physically impossible since, at best, the seating stress, S_a (or S_{ya}), can only be equal or greater than the operating stress, S_{gmin} (or S_m). Thus, there is a limiting ratio of $S_a/S_{gmin} = 1$.

The new optimizing design procedure aims at finding a converging value of W_{m1} and W_{m2} while still observing these limiting conditions. These two conditions have important physical significance.

The factor M serves as an indicator of the performance of the joint. If the design operating stress S_m is not sufficiently higher than the pressure, a leak will probably occur. As suggested previously, a value of $S_m = 2p$ ($M = 2$) is

accepted as safe. When solving Equation 20, we must then check that the resulting value of S_m is acceptable, if this is not the case, then the solution is unsatisfactory.

The limiting ratio of $S_a/S_{gmin} = 1$ is physically equivalent to a ratio of $T_{pn}/T_{pmin} = 1$ (see eqn. 7). Actually, the true limiting factor in the design is not the ratio T_{pn}/T_{pmin} but rather T_{pmin} in relation to M_{min} (M = 2). When using the procedure, the designer must select a tightness class, TC, high enough to satisfy the minimum desired stress on the gasket.

3.2.3 OPTIMIZING ALGORITHM

Using the equations derived above with the equilibrium equations developed in the ASME Code, a computational algorithm for the new optimizing procedure has been developed. A diagram showing this is presented in Figure 13.

Since T_{pn} and T_{pmin} are the basic parameters determining the relationship between the stresses and the loads, the ratio between them, defined as T_{pr}, is used in the procedure instead of S_a/S_{gmin}.

In the procedure, successive values of W_{m1} and W_{m2} (or Wr1 and Wr2) are calculated by varying the ratio of T_{pn}/T_{pmin} (T_{pr}), while the constraining parameters M >= 2 and T_{pr} >= 1 are not violated and/or until $W_{m1} = W_{m2}$, whichever occurs first.

Figure 14, shows the idealized stress-tightness plot which helps understand the way the algorithm works. We start at point A, $T_{pn} = T_{pmin}$ (T_{pr} = 1), we compute both S_{ya} and S_m, and with these, W_{m1} and W_{m2}. We then compute M (S_m/p) and check if this initial value is less than the predefined minimum (usually 2), if this condition occurs, then there is no real solution to the system (the solution would correspond to $T_{pn}/T_{pmin} < 1$ or $S_{ya} < S_m$ which is physically impossible). Otherwise, T_{pr} is increased progressively until one of the terminating conditions described above is reached (M <= 2 or $W_{m1} = W_{m2}$).

A sample plot of "W_{m1} & W_{m2} vs M" is included in Figure 15. Following the algorithm, the plot is generated from right to left. On the right, the graph is bounded by the computed values of W_{m1}, W_{m2}, and M corresponding to the starting condition $T_{pr} = 1$, while on the left it is bounded by the minimum acceptable value of M, in this case M = 2. Thus there is a maximum possible value of M (at $T_{pr} = 1$) as well as a minimum acceptable value (M = 2). In Figure 15, W_{m1} and W_{m2} intersect between these two constraining

conditions and a "true optimum" $W_{m1} = W_{m2}$ is found.

Figure 16 shows another case where the intersection of W_{m1} and W_{m2} does not occur because of the minimum limiting value of M. Notice that an unacceptable intersection would occur at a point where $M < 2$. However, still an "optimum" value must be chosen, which is the value of W_{m1} corresponding to $M = 2$. W_{m1} is chosen because it is higher than W_{m2}.

Figure 17 illustrates another case in which W_{m1} and W_{m2} converge as we go to the right. Since T_{pr} decreases as M increases, and the rightmost values of W_{m1} and W_{m2} correspond to $T_{pr} = 1$, then, in order for the two curves to intersect, T_{pr} must be less than 1 or $S_{ya}<S_m$, which is impossible. In this case the "optimum" value corresponds to the rightmost value of W_{m2} at $T_{pr}/T_{pmin} = 1$. In this case W_{m2} is chosen over W_{m1} because it is higher.

Note that in both Figures, 16 and 17, we have chosen as the "optimum" value, the lowest bolt load that would yield a safe design. We are also being conservative by choosing the highest of W_{m1} and W_{m2} at the optimum.

Once we have found this lowest safe value, the procedure checks if the obtained optimum seating stress S_{ya} is lower than the limiting maximum allowable gasket stress. Obviously we must check that the gasket is not

being over-compressed or, in other words, "crushed".

From this point on, the design procedure follows the rules of the present ASME Code for the calculation of the stresses in the flange and bolts. Naturally, it also imposes the appropriate limiting design values as established in the Code.

Before concluding this section let us take a closer look at the case when an impossible solution occurs, and the significance of the selection of T_{pmin} or the selected TC in the procedure.

Figure 18 illustrates the role of T_{pmin} in the design procedure. Observe that if we set $T_{pmin} = T_{pmin1}$ (Line T1) , it would be impossible to find a valid solution for S_{gmin} (or S_m). This is so because at $S_a = S_{gmin}$ (Point A) the stress level is below that of the minimum allowable operating stress, $S_m = 2p$ (Line S1). By increasing T_{pn} we get higher values of S_a but lower values of S_{gmin}, thus subsequent values of S_{gmin} will always be lower than the initial value at point A, which was too low to start with.

Graphically this would mean that S1 is above the starting point A, so that S_{gmin} and S1 never intercept. Therefore, the minimum stress condition cannot

be satisfied. On the other hand by letting $T_{pmin} = T_{pmin2}$ (Line T2), the starting stress at $S_a = S_{gmin}$ (Point B) is above S1. Hence, by increasing T_{pn}, S_{gmin} could eventually intercept S1, and an impossible condition does not occur.

Notice that all the previous discussion is due to the fact that we always compute a minimum value for the operating stress S_{gmin} which always has tightness coordinate T_{pmin}. The selected T_{pmin} must correspond to a level of S_{gmin} greater or equal to the minimum allowed operating stress. Otherwise an impossible solution occurs, and the initial tightness on the joint must be increased to satisfy the minimum stress on the gasket.

It is clear, then, that in some instances we must select a higher tightness class TC, and hence a higher T_{pmin}, in order to satisfy a prescribed minimum level of operating stress on the gasket (M_{min}).

The above discussion is only relevant to the understanding of the inner workings of the new procedure and the significance of the predetermined standard Tightness Classes, T1, T2 and T3. Obviously, in practice an increase in tightness automatically implies an increase in stress, and vice versa. However, since the operating stresses are minimized with respect to a predetermined tightness level, the algorithm must check whether the

selected minimum tightness would provide high enough stresses. The algorithm could be modified to automatically increase the minimum tightness until the desired stress levels are reached.

3.2.4 ADDITIONAL REMARKS

The new proposed procedure differs from previous approaches in several key points. Some of these are:

a) The ratio of T_{pn}/T_{pmin}, $\bar{T}_{pr}$, is introduced as a new design parameter. Together with M (S_m/P). It serves as a constraining parameter in the iterative procedure to find optimal values for the design bolt load Wm. The two factors are included in the optimization algorithm.

b) The ratio between T_{pn} and T_{pmin} is not fixed to any particular value as some other researchers have suggested. For example, a value of 1.5 is suggested in Ref. [4] as a simplification. Based on the results obtained in this study, it seems unnecessary to do so. This will be discussed further in the next Chapter.

c) The concept of tightness introduced by Payne et al. [3] is new to the designer and may not be easily understood. In the proposed procedure

this factor is included in a very simple way. Basically, the procedure offers several predefined tightness options (tightness classes, T1, T2 and T3) to be chosen by the user. Based on this choice, the procedure will automatically compute the value of T_{pmin} to be used in the calculations. These three levels T1 to T3, are by no means unchangeable. A wider range of values could be specified that would provide more gradual increments in tightness. For example two other classes can be introduced at intermediate tightness levels between T1 and T2, and T2 and T3.

Up to this point the procedure does not take into account the varying nature of the bolt force. It follows the present ASME Code assumption of a constant bolt load in the seating and operating conditions. However, it would not be hard to introduce a varying bolt load while still optimizing the design.

For example, assuming the operating bolt load increases relatively to the seating load by a certain percentage, say 10%, we could define a design ratio between W_{m1} and W_{m2}, i.e. $W_{m1} = 1.1W_{m2}$. The optimizing algorithm would then be modified to accept this as the optimal condition, and not $W_{m1}=W_{m2}$.

Since the new equations permit the expression of the bolt loads in terms of the gasket stresses, introducing a varying bolt load will not violate the basic principles behind this approach.

3.2.5 IMPLEMENTATION OF THE NEW DESIGN PROCEDURE

As part of this research, a computer program for the complete design of gasketed bolted flanges was developed. This program, called "***Turbo-Flange***", implements the new design procedure which optimizes the design bolt loads acting on the flange.

TurboFlange is an interactive, menu-driven program written in Turbo Pascal. Some of the key features of the program are:

1- Optimization of bolt loads using the new proposed design procedure.
2- Compliance with the ASME Code design criteria.
3- Implementation of a File Database of up to 5000 models.
4- Easy input of data and validation.
5- Flexible presentation of results, including Graphs.

6- Support for the 8087/80287 math co-processor.

7- Fast execution.

3.2.5.1 Applications.

TurboFlange was conceived as a design tool. It is fast and flexible, and specially suited for quick optimization. However, the program can also be used for educational or demonstration purposes. Its graphical output helps in the visualization of the behavior of the Bolt Loads and Gasket Stresses. It also makes it easy to conduct parametric studies. With the program one can change any of the design parameters and quickly observe its effect on the behavior of the joint.

In this research the program was used to examine the effectiveness of the new design procedure. Several interesting design conditions and trends were observed. These will be discussed in the next Chapter.

From the functional point of view, ***TurboFlange*** offers three important features to the user.

3.2.5.2 Models and Templates.

In ***TurboFlange,*** a Model is a complete set of data defining a bolted joint (Fig. 19). Templates are predefined subsets of a model which define either Gasket Material Data or Flange Geometry (Fig. 20).

Complete or partial Models can be created and saved for future study. Templates allow the creation of libraries of commonly used Gasket Materials and/or Flange Geometries, ready to be imported into a new or an existing model. Both Models and Templates are kept as records in a Database. The program offers standard functions such as Delete, Rename, List, New and Get to access and modify the state of any record in the Data Base.

3.2.5.3 Input Screens.

In ***TurboFlange*** the user enters and modifies the design data by way of Input Screens. There are two Input Screens, one for Gasket/Bolt information and another for Gasket Material and Size information. The screens are self-explanatory, clearly identifying the data requested by the program (Figs. 19 & 20).

To make the input fool-proof, input fields are clearly indicated on the screen. Furthermore, as the user fills an entry the program instantaneously validates the data, and provides feedback if invalid or unacceptable data is entered. Input does not need to be sequential, the user can navigate within an input screen or from one screen to the other, by pressing a key.

TurboFlange supports both SI and Imperial units, either of which can be selected with a toggle switch.

3.2.5.4 Complete and Flexible Output.

TurboFlange also provides the user with two complete Result Screens. The first screen presents to the user the resulting Bolt and Gasket stresses and loads, together with the calculated optimum values found, and Design vs. Calculated Values. It also provides diagnostics about violating conditions when appropriate (Fig. 21).

The second screen presents information about the Forces, Lever Arms and Moments acting on the flange, together with the resulting Stresses. Again, Design and Computed values are presented with relevant diagnostics if required. In addition to these Result Screens, it is possible to print Input Data, Results or both, either to an ASCII file or

to the printer. In this way the results can be included in reports or exported to other programs such as Spreadsheets, Word Processors, Graphics packages, etc.

Finally the program produces four basic types of graphs. Two of these are plots of the Bolt Loads W_{m1} and W_{m2} vs the ASME-like factor M (S_m/P) and the Ratio of T_{pr}/T_{pmin} (T_{pr}). The other two are S_{ya} and S_m vs. M, and vs. T_{pr}. (Figures 22 and 23). These graphs serve as a visual aid in the study of the behavior of the bolt loads, in order to visualize the optimal Bolt Load, and to picture the behavior of the gasket stresses in the optimization.

4 CHAPTER 4

RESULTS FROM THE FE STRESS ANALYSES

This Chapter presents the results obtained from the finite element analysis of the bolted flanges. As described in the previous chapters, the analysis was divided in two parts: Nonlinear-elastoplastic analysis, using the ABAQUS FE program; and linear-elastic analysis of the joints using the program GIFTS.

Most of the results are presented in graphs (Figures) which are referenced in the text. For the reader's convenience, figures are included in the **GRAPHS & FIGURES** section starting on page 135.

Due to the fact that it is common practice in the industry to employ Imperial Units, and that the ASME Code uses them as well, the results are presented in Imperial units with their equivalent SI values in parentheses.

In some instances a reduced notation will be used to refer to the standard flanges used in the FE analyses and in the new procedure. An example of this is a flange "Class 1500-24". This means an ANSI B16.5 standard Class 1500 flange, with a nominal diameter of 24" (600 mm). The gasket dimensions correspond to the specified flange geometry, per ANSI B16.5.

The results from ABAQUS will be discussed first, followed by the results from GIFTS, and finally a comparison between the two.

ABAQUS was used to analyze the behavior of the stress distribution across the gasket at high pressure in relatively large diameter standard flanges. A summary of the analyses performed with ABAQUS was presented in Table 2 (Chapter 2).

Because of system overhead on the mainframe, the analyses run using ABAQUS typically took one day to execute, and in some cases more. In contrast to this, the analyses performed with GIFTS, typically averaged an hour each, and less than six hours even in the longest cases. For this reason GIFTS was used to study not only the stress distribution across several gasket materials, but also the effect of other design parameters on the gasket stresses, namely: the design pressure; the bolt loads; and the material properties used in the linear analysis. A summary of all the models was presented in Table 3 (Chapter 2).

Throughout the discussion that follows one must keep in mind that the objective of the study is to compare the results between the linear and nonlinear modeling approaches, and to study the general behavior of the gaskets under design conditions. Consequently, the emphasis in the discussion will be on the qualitative aspects of the results rather than their actual numerical values. Both approaches are approximations of a very complex situation, and the results obtained will serve

to provide a better understanding of the behavior of the joints.

4.1 RESULTS FROM THE FE PROGRAM ABAQUS

4.1.1 Gasket stress distribution

Figures 24 to 27 show the gasket stress distribution obtained from the nonlinear-elastoplastic stress analyses. All these figures present the gasket seating and operating stress distributions for the different gasket materials outlined in Table 2. (All stresses are compressive).

As expected, under both seating and operating conditions, the stresses reach their maximum values near the outer periphery of the gasket. This is due to the deflection of the flange caused by the moment arm between the hub and the bolt circle, which is more pronounced on the outer edge and thus compresses the gasket more in this area.

The gasket stress distribution is clearly nonlinear, particularly towards the edge, where the stresses decrease rapidly in relation to the values at the center of the gasket. It is interesting to note that both the seating and operating conditions present the same general shape, and that there is an almost constant offset between the two. This is despite the fact that the material stress-strain plot used for the analysis prescribes quite different stress behaviors for these two conditions.

This stress offset indicates that the operating loads on the joint, produce an almost uniform effect on the contact area between the flange and the gasket. This may be due to the fact that the flange is very stiff in this area due to the added rigidity of the hub, and hence does not deflect considerably so as to affect the stresses on the gasket. In other words, the pressure produces an uniform average lifting effect on the flange which results in the almost constant offset between the seating and operating gasket stress distributions observed in the results.

In general, the gasket stress distribution presents a parabola-like shape. Tables 4 and 5 present the results from the polynomial fit of the stress distributions. From the results we can appreciate that in most cases the stress distribution can be quite accurately represented by a second order polynomial. The correlation parameter RVAL indicates how good the fit is: a value of 1 indicates a perfect fit.

For the second order fit, RVAL is always greater than 0.95, which indicates good results (Table 4). On the other hand the linear fit shows very poor results, RVAL is less than 0.5 (Table 5).

The values in Table 4 will be used to compute average stresses for both the seating and operating condition. These average values provide a mea-

sure of the net effect of the gasket stresses and the performance of the gasket. They also permit to compare the results from the FE analyses with the results obtained from analytical methods which generally provide one design value for the gasket stress.

TABLE 4: Second order fit coefficients (ABAQUS).

Flange Class: 1500

Nominal Dia.: 24 in (600 mm)

GASKET	Second Order Fit: S_{ya}	Second Order Fit: S_m
GHS	Ao= 2.361E6 A1=-3.689E5 A2= 1.431E4 RVAL=0.956	Ao= 2.167E6 A1=-3.378E5 A2= 1.310E4 RVAL=0.966
DJ MICA	Ao= 2.927E6 A1=-4.569E5 A2= 1.773E4 RVAL=0.967	Ao= 2.696E6 A1=-4.201E5 A2= 1.629E4 RVAL=0.973
DJ ASBESTOS	Ao= 1.783E6 A1=-2.760E5 A2= 1.059E4 RVAL=0.889	Ao= 1.737E6 A1=-2.676E5 A2= 1.024E4 RVAL=0.914
SELCO	Ao= 2.724E6 A1=-4.250E5 A2= 1.647E4 RVAL=0.954	Ao= 2.599E6 A1=-4.046E5 A2= 1.568E4 RVAL=0.963

TABLE 5: First order fit coefficients (ABAQUS).

Flange Class: 1500

Nominal Dia.: 24 in (600 mm)

GASKET	First Order Fit: S_{ya}	First Order Fit: S_m
GHS	Ao= 2.543E4 A1=-2892.90 RVAL=0.416	Ao= 3.034E4 A1=-2949.20 RVAL=0.458
DJ MICA	Ao= 3.372E4 A1=-3605.31 RVAL=0.423	Ao= 3.754E4 A1=-3555.71 RVAL=0.450
DJ ASBESTOS	Ao= 5.582E4 A1=-5400.42 RVAL=0.687	Ao= 6.561E4 A1=-5811.74 RVAL=0.736
SELCO	Ao= 3.455E4 A1=-3691.61 RVAL=0.446	Ao= 3.914E4 A1=-3701.12 RVAL=0.468

NOTE: The data in the tables above yields values for the stress distribution in psi given the radial coordinates of the gasket in in.

4.1.2 Average Bolt ring stresses

Table 6 presents the average bolt stresses on the bolt ring. All 4 cases studied with ABAQUS present the same flange and bolt geometries, making it possible to compare the stresses on the bolt ring directly without having to compute the equivalent bolt loads.

In Table 6 the average seating bolt stresses are compared with the operating values. From the results we can observe that in some cases the bolt stress (or load) actually decreases as the pressure is introduced. However, this occurs only in one of the four cases (SELCO). Nevertheless, we will verify this behavior when we discuss the equivalent results obtained from GIFTS.

For this particular case we can observe that the maximum variation in the bolt stresses (loads) is of the order of only 10% despite the relatively high pressure (1500 psi). This suggests that it is the gasket and the flange, and not the bolts, which compensate for the loading due to pressure. However, this is not always the case, it depends on the geometry of the joint.

As we look at the results from other analyses we will be able to comment further on the behavior of the bolt ring.

TABLE 6: Average bolt stresses (ABAQUS).

Flange Class: 1500

Pressure : 1500 psi.

Nominal Dia.: 24 in (600 mm)

GASKET	Seating Bolt Stress	Operating Bolt Stress	Relative variation
GHS	11534 psi (80 Mpa)	12514 psi (86 Mpa)	8 %
DJ MICA	12421 psi (86 Mpa)	12513 psi (86 Mpa)	1 %
DJ ASBESTOS	13232 psi (94 Mpa)	13877 psi (96 Mpa)	5 %
SELCO	11734 psi (81 Mpa)	11534 psi (80 Mpa)	-2 %

4.1.3 Average Gasket Stresses

Using the results from the polynomial fit of the gasket stress distributions, average seating and operating stresses were computed by integrating the stresses over the gasket area. This method is required to obtain a true average as opposed to a simple arithmetic mean, because as the radius increases the stresses will contribute more to the gasket reaction since the area where they act upon increases. For this reason, if the stresses on the outer area are high enough, a gasket will often seal even when separation occurs at the inner edge. Following this reasoning, and being conservative, the ASME Code assumes, in most cases, the effective width of the gasket to be only about one half of the full width.

From the results in Table 7 we can observe that the sealing performance of the analyzed joints is quite satisfactory. Both the seating, and more important, the operating stresses are well above the minimum stress value of 2P (3000 psi, 20 MPa) i.e. $M = 2$; in fact they are all greater than 5P ($M = 5$). Notice that the corresponding bolt stresses are approximately 13 ksi (90 MPa), only one half of the maximum allowable bolt stress, which is typically 25 ksi (172 MPa). This is an indication that the particular standard flanges used in the analyses provide very safe designs.

Another interesting fact is that the reduction in seating stresses appears to be consistent for similar gasket materials, approx. 30% for the two Double Jacketed (DJ) gaskets MICA and ASBESTOS, and 40% for the other two GHS and SELCO.

Notice that the seating bolt stresses in Table 6 are of the same order of magnitude as the seating gasket stresses in Table 7. However, the maximum variation in bolt stresses between seating and operating conditions., about 10%, is very low in comparison with the variation in gasket stresses, 46%. Again, this indicates, that for these particular geometries, the loads due to pressure act principally on the gasket and not on the bolts, and hence the variation in the bolt load can be considered secondary in the analysis.

TABLE 7: Average gasket stresses (ABAQUS).

Flange Class: 1500

Pressure : 1500 psi.

Nominal Dia.: 24 in (600 mm)

GASKET	Seating Stress	Operating Stress	Relative variation
GHS	-13360 psi (-92 Mpa)	-7782 psi (-54 Mpa)	-41 %
DJ MICA	-12705 psi (-88 Mpa)	-8903 psi (-61 Mpa)	-31 %
DJ ASBESTOS	-12557 psi (-87 Mpa)	-8465 psi (-58 Mpa)	-33 %
SELCO	-14098 psi (-97 Mpa)	-7577 psi (-52 Mpa)	-46 %

4.2 RESULTS FROM THE FE PROGRAM GIFTS

Several models were analyzed using the Finite Element program GIFTS. The results include the gasket stress distributions for several gasket materials and standard flanges (see Table 3); plus the effect of pressure, material properties (E and ν), and the behavior of the bolt loads.

4.2.1 Gasket Stress distribution for several gaskets

The results obtained from the linear, elastic, finite element stress analyses are presented in Figures 28 to 39. These figures show the gasket stress distributions for several gaskets and flanges, under seating and operating conditions.

The results present a rather linear behavior, except at the inner and outer gasket periphery. The stresses increase towards the outer edge of the gasket because of the deflection of the flange. The stress level at the outer edge are considerably higher than those on the inside of the gasket, this effect varies from one gasket to another and is probably caused by the modulus of elasticity, E, of the gasket material which will be discussed later.

The sudden decrease in the stress levels towards the edges is due to the fact that the gasket is more free to expand laterally, and hence will be less compressed there. This effect is affected by the Poisson's ratio of the material as will we explained in the following subsections.

In general, all cases present a safe and satisfactory behavior; the stress levels at the inner edge are generally within the limit of $M = 2$ or two times the pressure, and they are well above this value beyond the first 1/5 of the gasket width.

Table 8a, 8b and 8c present the results from the linear fit of the gasket stress distributions. As expected from the plots, the results reveal that the stress distributions can be easily and accurately approximated by straight lines. Even though the results include the behavior at the edges, we obtained reasonable correlation factors, this indicates that the edges have a limited effect on the overall behavior of the stresses.

TABLE 8a: Class 1500-24, polynomial fit coefficients (GIFTS).

Flange Class: 1500

Nominal Dia.: 24 in (600 mm)

GASKET	1st Order Fit: S_{ya}	1st Order Fit: S_m
GHS	Ao= 6.68E4 A1=-6239.5 RVAL=0.947	Ao= 8.08E4 A1=-6939.7 RVAL=0.978
DJ MICA	Ao= 1.01E5 A1=-8880.2 RVAL=0.974	Ao= 1.17E5 A1=-9692.9 RVAL=0.988
DJ ASBESTOS	Ao= 1.05E5 A1=-9220.7 RVAL=0.976	Ao= 1.21E5 A1=-1.00E4 RVAL=0.989
SELCO	Ao= 1.01E5 A1=-8880.2 RVAL=0.974	Ao= 1.17E5 A1=-9692.9 RVAL=0.988

TABLE 8b: Class 1500-12, polynomial fit coefficients (GIFTS).

Flange Class: 1500

Nominal Dia.: 12 in (300 mm)

GASKET	1st Order Fit: S_{ya}	1st Order Fit: S_m
GHS	Ao= 2.67E4 A1=-6389.9 RVAL=0.803	Ao= 3.41E4 A1=-6988.1 RVAL=0.870
DJ MICA	Ao= 5.28E4 A1=-1.04E4 RVAL=0.905	Ao= 6.13E4 A1=-1.11E4 RVAL=0.937
DJ ASBESTOS	Ao= 5.59E4 A1=-1.09E4 RVAL=0.911	Ao= 6.45E4 A1=-1.16E4 RVAL=0.942
SELCO	Ao= 5.22E4 A1=-1.03E4 RVAL=0.903	Ao= 6.07E4 A1=-1.10E4 RVAL=0.936

TABLE 8c: Class 1500-6, polynomial fit coefficients (GIFTS).

Flange Class: 1500

Nominal Dia.: 6 in (150 mm)

GASKET	1st Order Fit: S_{ya}	1st Order Fit: S_m
GHS	Ao= 4440.2 A1=-5081.2 RVAL=0.703	Ao= 8096.3 A1=-5595.4 RVAL=0.770
DJ MICA	Ao= 1.38E4 A1=-7499.6 RVAL=0.841	Ao= 1.82E4 A1=-8158.8 RVAL=0.886
DJ ASBESTOS	Ao= 1.50E4 A1=-7858.4 RVAL=0.852	Ao= 1.91E4 A1=-8528.3 RVAL=0.894
SELCO	Ao= 1.36E3 A1=-7430.7 RVAL=0.839	Ao= 1.80E4 A1=-5595.4 RVAL=0.884

NOTE: The data in the tables above yields values for the stress distribution in psi given the radial coordinates of the gasket in in.

4.2.2 Average Bolt Ring Stresses

Tables 9, 10 and 11 summarize the average bolt stresses obtained from the GIFTS's analyses. The results are presented for each geometry. From these tables we can appreciate that the behavior of the bolt loads (stresses) is affected by the flange size.

The results for the 24 in (600 mm) Dia. flanges (Tab. 9) indicate that in some cases the bolt load actually decreases when pressure is introduced which was also observed in the analyses performed with ABAQUS. Note that in three cases the stresses decrease by approximately 10%, which is not a negligible variation. As mentioned before, it is widely assumed that the bolt load should increase under operating conditions, as it takes some of the loading due to pressure. From these results we can see that this is not always the case, making the behavior of the joint more difficult to predict.

The results in Tables 10 and 11, indicate that for smaller flanges (12 and 6 in), the bolt load increases as the pressure is introduced. In all the cases studied this is true, even though the increase varies from case to case.

Based on the results presented in Tables 9 - 11, it can be concluded the bolt loads (stresses) vary from -10% to +10%, at a relatively high pressure. This upper bound is consistent with the results from ABAQUS.

When examining the variation in bolt stresses for different gasket geometries, we can observe a pattern. The relative variation in the stresses is of the same order for the last three gaskets (ASBESTOS, MICA & SELCO) and higher for the first one (GHS). This behavior seems to be caused in part by the Young's modulus of the gasket materials. The GHS gasket has the lowest value of E (150 ksi) and also the highest increase in bolt stresses (S_b). For the other materials which have similar values of E (234 ksi, 244 ksi and 232 ksi), the increase in bolt stresses is about the same, and lower than that of GHS. Even in Table 9 this is true, where the bolt stresses of the last three materials decrease while that of GHS increases slightly. Thus, the results seem to indicate that the stiffer the gasket material the lower the relative variation in the bolt stresses or load.

However, given the limited range of variation of the bolt load between the seating and operating condition, the absolute effect of the Young's modulus of the gasket material on the bolt load, is really not very significant in terms of the design of the joint.

TABLE 9: Average bolt stresses, Class 1500-24 (GIFTS).

Flange Class: 1500

Nominal Dia.: 24 in (600 mm)

GASKET	Seating Bolt Stress	Operating Bolt Stress	Relative variation
GHS	13208 psi (91 Mpa)	13271 psi (91 Mpa)	0 %
DJ MICA	13029 psi (90 Mpa)	12112 psi (84 Mpa)	-8 %
DJ ASBESTOS	13092 psi (90 Mpa)	11770 psi (81 Mpa)	-11 %
SELCO	13029 psi (90 Mpa)	12112 psi (84 Mpa)	-8 %

TABLE 10: Average bolt stresses, Class 1500-12 (GIFTS).

Flange Class: 1500

Nominal Dia.: 12 in (300 mm)

GASKET	Seating Bolt Stress	Operating Bolt Stress	Relative variation
GHS	20029 psi (138 Mpa)	20795 psi (143 Mpa)	4 %
DJ MICA	21969 psi (152 Mpa)	22395 psi (154 Mpa)	2 %
DJ ASBESTOS	22128 psi (153 Mpa)	22527 psi (155 Mpa)	2 %
SELCO	21926 psi (151 Mpa)	22368 psi (154 Mpa)	2 %

TABLE 11: Average bolt stresses, Class 1500-6 (GIFTS).

Flange Class: 1500

Nominal Dia.: 6 in (150 mm)

GASKET	Seating Bolt Stress	Operating Bolt Stress	Relative variation
GHS	23313 psi (161 Mpa)	25897 psi (179 Mpa)	10 %
DJ MICA	22960 psi (158 Mpa)	23596 psi (163 Mpa)	3 %
DJ ASBESTOS	23175 psi (160 Mpa)	23782 psi (164 Mpa)	2.5 %
SELCO	22915 psi (158 Mpa)	23557 psi (162 Mpa)	2.5 %

4.2.3 Average Gasket Stresses

Tables 12, 13 and 14 present the computed average gasket stresses for the different analyses.

The results indicate proper gasket sealing in all cases. Tables 13 and 14 show higher values of S_m than Table 12, partly because the values of the bolt stresses applied are almost doubled. As mentioned before, even for relatively low bolt loads and larger flanges, the performance of the standard ANSI B16.5 flanges studied is very good, as expected.

For the 12" and 6" flanges and bolt stresses of approximately 22 ksi (close to maximum allowable), the gasket stresses are very high, of the order of 9 times the pressure (Tables 13 & 14). This is a sign of good seal on the joint. The ratio of the gasket stress over the Pressure is denoted as M, and typically this ratio should be higher than 2. The results from Table 12 show that at about half the maximum allowable bolt stress, the resulting operating gasket stresses correspond to about 5 times the pressure.

In the linear analyses, the only input parameters that vary between analyses are the magnitude of the seating bolt load and the properties of the gasket material. Thus for the same geometry, and the same bolt load, the resulting stresses on the gasket will depend solely on the material properties

E and *v*.

In all analyses, *v* was kept constant at 0.4, while the seating bolt load varied only by about 10%. From the results we can see that from one gasket to another, the average value of stresses vary slightly. For the last three gaskets (MICA, ASBESTOS & SELCO) the results are very similar; which was expected because they all have very close values of *E*. The important point is that small differences in *E*, do not greatly affect the resulting gasket stresses. The effect of *E* and *v* on the gasket stress distribution will be discussed further in a subsequent section.

As expected the effect of pressure on the gasket stresses is more significant on flanges of larger diameter, because of the resulting increased end force, F_1 Eqn. (9). The decrease in S_{ya} is higher for larger diameter flanges. Also notice that the relative decrease in stress is almost constant for all four gasket materials, this relative offset will be described again in the next section where the effect of pressure on the gasket stress distribution will be discussed.

TABLE 12: Average gasket stresses, Class 1500-24 (GIFTS).

Flange Class: 1500

Nominal Dia.: 24 in (600 mm)

GASKET	Seating Stress	Operating Stress	Relative variation
GHS	-13190 psi (-91 Mpa)	-8144 psi (-56 Mpa)	-38 %
DJ MICA	-13015 psi (-90 Mpa)	-7630 psi (-53 Mpa)	-41 %
DJ ASBESTOS	-13078 psi (-90 Mpa)	-7808 psi (-54 Mpa)	-40 %
SELCO	-13015 (-90 Mpa)	-7630 (-53 Mpa)	-41 %

TABLE 13: Average gasket stresses, Class 1500-12 (GIFTS).

Flange Class: 1500

Nominal Dia.: 12 in (300 mm)

GASKET	Seating Stress	Operating Stress	Relative variation
GHS	-17601 psi (-121 Mpa)	-14413 psi (-99 Mpa)	-22 %
DJ MICA	-19329 psi (-133 Mpa)	-15835 psi (-109 Mpa)	-22 %
DJ ASBESTOS	-19471 psi (-134 Mpa)	-15906 psi (-110 Mpa)	-22 %
SELCO	-19255 psi (-133 Mpa)	-15781 psi (-109 Mpa)	-22 %

TABLE 14: Average Gasket Stresses, Class 1500-6 (GIFTS).

Flange Class: 1500

Nominal Dia.: 6 in (150 mm)

GASKET	Seating Stress	Operating Stress	Relative variation
GHS	-14784 psi (-102 Mpa)	-13073 psi (-90 Mpa)	-13 %
DJ MICA	-14564 psi (-100 Mpa)	-12637 psi (-87 Mpa)	-15 %
DJ ASBESTOS	-14691 psi (-101 Mpa)	-12755 psi (-88 Mpa)	-15 %
SELCO	-14533 psi (-100 Mpa)	-12612 psi (-87 Mpa)	-15 %

4.2.4 Effect of the design pressure on the gasket stress distribution

As discussed earlier, both the seating and operating gasket stress distributions present the same general form. The slope on both is almost identical, although the operating condition shows signs of increased flange deflection at the edges. This makes sense, since the rotation and bending of the flange will be increased when the pressure is introduced.

Figure 40 illustrates how the gasket stress distribution varies as the design pressure is increased. These results were obtained by varying the design pressure while keeping the seating bolt load constant. Naturally, the operating bolt load will vary as the loads due to pressure are increased.

From Figure 40 we can observe how the operating stress distribution of the gasket decreases almost uniformly as the pressure is increased. This behavior was also observed in the nonlinear analyses from ABAQUS. The results in the plot, correspond to a Class 1500-6 flange. This is a very stiff flange, so that the increase in pressure does not translate in considerable increased rotation and deflection of the flange. For this reason the stress distributions appear to be almost parallel to one another.

Based on the results presented in Figure 40 and those in Figures 28 to 39, one may note that the loads due to pressure act almost uniformly upon the gasket-flange contact zone, without considerably increasing the bending and rotation on the flange, at least across the gasket area. However, this behavior cannot be considered universal, since it will be affected by changes in the geometry. Using non-standard flanges may produce different results. This could be the subject of a further study.

4.2.5 Effect of the bolt load on the gasket stress distribution

In order to visualize the effect of the bolt load on the gasket stress distribution, two standard flanges were analyzed at a low bolt stress (12.6 ksi or 87 Mpa) and at a high bolt stress (22 ksi or 152 Mpa).

The results plotted in figures 41 and 42 show an increase in the gasket stresses as the bolt load is increased. The plots also show an increase in the outer stresses in relation to the inner ones, that is, the slope of the linear stress distribution is more pronounced for the case of higher loading. This behavior indicates increased defection of the flange with the load. This is similar to the effect of increased design pressure on flexible flanges.

Figures 41 and 42 also show that the stress levels on the gasket increase considerably for a higher size flange, under the same levels of bolt stress. Note that the stress levels at the inner edge of the gasket are similar for both plots, but for the larger diameter flange, which is more flexible, the stresses towards the outer edge become much larger than those for the smaller flange. Again this indicates increased flange defection, caused by the bolt load acting on a more flexible flange.

4.2.6 Effect of the material properties on the gasket stress distribution

When assuming linear-elastic behavior, the modeling of the gasket material (under isotropic and isothermal conditions) is reduced to the selection of two basic material properties, these are: the material's Young's modulus, E; and Poisson's ratio, v. Hence, it is of interest to know how the gasket stress distribution is affected by varying these parameters.

Figures 43, 44 and 45 show the effect of E on the gasket stress distribution, the effect on the seating and operating design conditions are illustrated. From the results we can observe that in general E affects the slope of the linear gasket stress distribution. The higher the value of the Young's modulus, the steeper the slope will be. This makes sense since, as E increases the gasket becomes stiffer, and thus offers more resistance to the flange, which will tend to bend more as it compresses the gasket. At the same time the stresses on the inner edge of the gasket are reduced, which increases the possibility of separation in this area. However, as long as excessive separation does not occur, the stiffer gasket will seal better since the mid and outer stresses will be higher producing an effective sealing area.

Figures 46, 47 and 48 portray the effect of Poisson's ratio on the gasket stress distribution. As seen on the plots, v affects the stress distribution

particularly at the edges of the gasket. The nonlinear stress pattern on the edges is accentuated as Poisson's ratio of the material is increased. This is expected since, as v increases, the material on the free edges will deflect more laterally, and thus will produce a decrease on the stresses shown in the plot. For very low values of v, the effect on the edges is not very significant, the stress distribution remains quite uniform throughout, however at $v = 0.3$ and $v = 0.4$, the end effects become quite noticeable and give rise to a reduction of the contact stresses on the gasket edges, particularly at the inner edge. Hence, if the gasket stresses are not sufficiently high, these end effects could result in insufficient contact stress in this area and therefore separation between the gasket and the flange.

The results on Fig. 47 suggest that Poisson's ratio affects not only the gasket stress distribution near the edges but also over the entire gasket width. The effect of Poisson's ratio on the gasket stresses is almost as significant as that of the Young's modulus.

4.3 ABAQUS vs. GIFTS, LINEAR vs NONLINEAR APPROACH

Figures 49 to 52 show equivalent results from both ABAQUS and GIFTS. The plots depict gasket stress distributions for four different gasket types used with ANSI B16.5, class 1500, 24 in (600 mm) nominal Dia. standard flanges.

From the plots, several important points can be observed:

1- The stresses on the inner edge of the gasket for both distributions are relatively close, with the linear stresses being slightly lower in some cases.

2- The stresses on the outer edge obtained from GIFTS are higher than those from ABAQUS. However, the stresses on the center present the opposite behavior.

3- Both methods present a nonlinear decreasing stress behavior at the ends but it is more pronounced in the elastoplastic analyses.

Since the geometry, boundary conditions, and loads due to pressure are very close for both programs, the respective results may be compared directly.

The general form of the stress distribution from the nonlinear analysis differs from that of the linear one; the former has parabolic shape while the latter is

predominantly linear. Nevertheless, the mean values are quite close for the two methods (Tables 15 and 16), indicating that equilibrium conditions are primarily satisfied in both cases.

Table 15 compares the data of Tables 6 and 9 for stresses computed using ABAQUS and GIFTS respectively. The results indicate that the applied bolt loads are very close in both cases. Similarly, Table 16 gives the percentage difference between the computed average stresses presented earlier in Tables 7 and 12.

TABLE 15: ABAQUS vs GIFTS: % Difference in bolt mean stresses.

GASKET	Seating condition.	Operat. condition.
GHS	-11 %	-8 %
DJ MICA	-5 %	3 %
ASBESTOS	1 %	10 %
SELCO	-11 %	-5 %

TABLE 16: ABAQUS vs GIFTS: % difference in gasket mean stresses.

GASKET	Seating Stress	Operat. Stress
GHS	1 %	4 %
DJ MICA	-2 %	14 %
ASBESTOS	-4 %	9 %
SELCO	8 %	0 %

4.4 CLOSING REMARKS

The stress distributions of the gasket materials as obtained from the non-linear, elastoplastic, analyses appear to be parabolic and not linear as widely assumed.

Since the nonlinear, elastoplastic, analysis allows a better more accurate representation of the gasket behavior, it is recommended over the linear approach.

The linear approach works, at least for design purposes where the overall performance of the gasket is desired as opposed to a detailed picture of the stresses on the gasket. The method yields a linear approximation of stress distribution where the end effects are not as pronounced as in the nonlinear analysis.

The fact that the linear approach has proven to be effective, and given that this model is based on the modulus of decompression, E_g, a parameter directly related to the operating behavior of the gasket, indicates that in fact the operating condition plays a prevailing role in the overall behavior of the gasket. This was one of our original assumptions.

It is very important that when using the linear approach, appropriate values of E and v be chosen, since these two parameters characterize completely the gasket materials. In this respect more information is needed on the true values of the Poisson's ratio, v, of the gasket materials. In this study a constant value of 0.4 was assumed for all materials, but the availability of actual experimental results will increase the accuracy of this type of analysis and the results. Unfortunately, gasket material are very complex non-isotropic, non-homogeneus materials, which makes very difficult to determine values for v.

Bolt stresses and thus loads do not always increase under operating conditions. Sometimes they may decrease, this seems to depend on the flange geometry, specially for large diameter flanges.

This concludes the discussion of the results from the Finite Element analyses of the joints. In the next Chapter we will discuss the results for the new design procedure obtained from ***TurboFlange***.

5 CHAPTER 5

RESULTS FROM THE NEW DESIGN PROCEDURE

In this Chapter the results obtained using the new proposed procedure will be discussed. All the results were generated using the program ***TurboFlange*** described in Chapter 2. With the aid of this program, the effect of the different design parameters used in the procedure where analyzed, namely: the design pressure; the tightness class TC; the gasket factors, B, d and S*; the bolt efficiency, *e*, and the experience factor, *F*. Each of these will be discussed individually. Finally the effect of fixing the tightness ratio T_{pr} on the optimal solution will be discussed.

5.1 EFFECT OF PRESSURE

The design pressure affects directly the behavior of the bolt loads W_{m1} and W_{m2}, and hence the optimal solution. Figure 53, shows W_{m1} and W_{m2} vs. the ASME like factor *M*, for several pressure levels. From the graph we can observe that both W_{m1} and W_{m2} are affected by a change in pressure. The effect on W_{m1} is as expected from Eqn.(15), also W_{m2} varies since tightness is affected by the

pressure and thus influences the gasket stress S_{ya} and W_{m2}. However, for different pressure levels W_{m2} follows the same general behavior, as the different W_{m2} lines are superimposed.

Figure 54 shows the design bolt loads vs. the tightness ratio, T_{pr}. From this graph we can observe the same general behavior described above. Both graphs illustrate how the optimal solution is affected by the pressure. At low pressure, W_{m2} tends to be higher than W_{m1}. When the pressure is low, the seating condition determines the value of the optimal bolt load, and hence the stresses on the joint. On the other hand, at high pressure, the operating condition becomes more important, and determines the selection of the design bolt load, W_m.

As W_{m1} increases in comparison to W_{m2}, a point is reached beyond which W_{m1} is greater than W_{m2} for all computed values of *M*. When this condition occurs, there is no intersection between the two lines, and the optimal bolt load, W_o or W_m, becomes the value of W_{m1} at the lowest specified value of *M* (usually *M*=2).

Figure 55 shows a plot of W_o vs Pressure. The results indicate that the optimal load increases with pressure as expected. The figure also depicts an almost linear relationship between the two parameters at hihg pressure where the operating bolt load W_{m1} dominates the behavior of the joint.

5.2 EFFECT OF TC ON OPTIMUM

As explained in Chapter 2, the tightness classes T1, T2 and T3, define three standard levels of tightness to be selected by the designer, which simplify the selection of a minimum tightness parameter T_{pmin}.

Figures 56 to 63 present the behavior of the design bolt loads W_{m1} & W_{m2} vs M for the gasket materials studied, at different tightness classes, T1 to T3.

If we select a high tightness class, this will result in a tighter joint, and one would expect higher stresses as well. From the results obtained we can observe that this is not always the case. That is, even though the stresses on the gasket will be higher because of the increase in tightness, the design bolt load, Wo or Wm, does not necessarily increase accordingly, and hence the stresses on the flange do not change as much.

The above is particularly true at high pressure levels when the operating condition prevails. In many cases, the optimal bolt load corresponds to $M = 2$ (at different levels of tightness). Thus, as we increase TC, the optimal S_m remains constant ($S_m = 2P$) while the corresponding value of S_{ya} increases with increasing tightness. However, if the operating condition prevails, $W_{m1} > W_{m2}$, then S_m will prevail and the optimal bolt load does not change as much.

In Figures 64 and 65 we can observe the increase in Wo (or Wm) for different tightness values (T1 to T3) and for several gaskets. Observe that there is little increase in Wo from T1 to T2, and the increase becomes relevant only at the highest tightness class (T3).

From the above discussion follows that when Wo is not affected by TC, there will not be an increase in the stresses on the flange, which are strongly dependent on this load. What this means is that one can get a tighter joint (say of tightness T3), without compromising the integrity of the joint or increasing the cost of the design.

5.3 EFFECT OF B, d, AND S* ON THE NEW DESIGN PROCEDURE.

The gasket factors B, d, and S*, are intended to completely define the stress-tightness behavior of a gasket material. The procedure outlined in this report relies heavily on these factors. Since they are obtained experimentally, scatter is naturally involved. In order to asses the sensitivity of the design equations and the proposed method to changes in these factors, a sensitivity analysis was performed using ***TurboFlange***.

The plots in Figures 66 to 97 were obtained by fixing all other design parameters, and varying each one of these gaskets constants at a time. The range of variation of the parameters was kept within reasonable limits consistent with the range of experimental values for different types of gasket. The plots illustrate both the absolute and relative effect of these parameters on the bolt loads, and the optimal design load.

5.3.1 Effect of Gasket Factor B

Figures 66 and 67 are plots of W_o vs B, the former shows absolute results and the latter the relative effect of B on W_o. Figure 67 is of special interest since it shows qualitatively the relationship between the two variables. From the figures we can observe that W_o increases as we increase B, for both low and high pressure.

At high pressure, the change appears to be almost directly proportional. However, this is only so because, as shown in Figure 69, by increasing B we increase W_{m2}, so that W_{m2} becomes greater than W_{m1} and thus determines the optimal bolt load. The fact that W_{m2} is proportional to B is evident from the equations, since W_{m2} is proportional to S_{ya}, and S_{ya} is proportional to B.

By comparing Figures 68 and 69, with Figures 70 and 71, we can observe the effect of B on W_{m1}. By varying B we offset W_{m1} with respect to T_{pr}, notice that W_{m1} seems not to be affected by B in the plots of W_{m1} vs. *M* (W_{m1} appears as a straight line in these plots). However, by plotting it against T_{pr} we see the true behavior. As we increase B, W_{m1} moves towards the right (increasing T_{pr}), a behavior which is not evident from the equations. Thus by increasing B, W_{m1} also increases in a highly nonlinear fashion.

From the preceding discussion we can appreciate the fact that the results obtained are not absolute. The behavior of the bolt loads depend on multiple parameters.

5.3.2 Effect of Gasket Factor d

Figures 72 and 73 illustrate the effect of gasket factor d on the optimal load Wo (or Wm). From the plots, we can observe that the effect of d varies considerably with pressure. At low pressure, this parameter has very little effect on the optimal load, whereas at high pressure the contrary is true. Moreover in one case the effect is quite linear (low pressure) while it is very nonlinear in the other(high pressure). From the equations, one would expect a nonlinear effect of d on the results since it acts as an exponent in the calculation of S_{ya} (Eqn. 12).

Figures 74 and 75 show the effect of d on W_{m2}. From these plots we can also understand better the results described above. At low pressure, W_{m2} prevails over W_{m1} and hence determines the optimal load. The effect of d on W_{m2} is readily apparent from Equations (12) and (14). At high pressure this effect is magnified due to the fact that we are dealing with higher values of tightness, which is proportional to pressure (Eqn. 3).

The effect of factor d on W_{m1}, can be appreciated from Figures 76 and 77 where we observe that in general, d has very little effect on W_{m1}. It is interesting to note from these plots, how the range of T_{pr} increases with increasing pressure (1 to 1.7 in Fig. 76; 1 to 4 in Fig. 77).

*5.3.3 Effect of Gasket Factor S**

The effect of gasket factor S* on the design loads is illustrated in Figures 78 and 79. From these figures it is evident that S* does not have a significant effect on the optimal bolt load. At low pressure the effect is practically negligible and even at high pressure it is also very small. Figure 79 which illustrates the relative effect of S* on Wo: consider the fact that an increase of 1000 times on S* only increases slightly the value of Wo.

Figures 80 to 83 present the effect of S^* on W_{m2} and W_{m1} respectively. At low pressure, when W_{m2} prevails, S^* does not affect W_o since the W_{m2} lines converge as *M* increases (Figures 80 and 81). At high pressure, the optimum occurs as W_{m1} intersects W_{m2} at low values of *M*, where the W_{m2} lines still do not converge. The intersecting values (W_o) are quite close, which explains the results in Figure 79. As shown in Figures 82 and 83, the effect on W_{m1} is not negligible. However, although W_{m1} varies significantly for the different cases, W_o does not. Again we appreciate the usefulness of this type of plot, since it complements the plots of "W_{m1} & W_{m2} vs *M*" in illustrating the complete behavior of the bolt loads.

5.4 EFFECT OF *e* AND *F* ON THE NEW DESIGN PROCEDURE.

5.4.1 Effect of the bolt efficiency e

Figures 84 and 85 illustrate the effect of the bolt efficiency, *e*, on the optimal bolt load W_o. At both low and high pressure, W_o decreases as *e* increases. This behavior can be explained by looking at equations (12) and (14), which show that S_{ya} is inversely proportional to *e*, which in turn determine W_{m2}.

Figures 86 to 89 show the behavior of W_{m1} and W_{m2} as *e* increases. As expected from the equations, *e* affects only the seating design bolt load, W_{m2}, which decreases with increasing *e*. The optimal load is also affected. The plots show several conditions where W_o is determined by W_{m1}, the intersection between W_{m1} and W_{m2}, and finally by W_{m2}.

5.4.2 Effect of the experience factor F

The effect of the factor *F* on the optimal bolt load W_o is presented in figures 90 and 91. As can be seem this factor has a relatively small effect on the optimal load. This is an important fact, since so far a value of $F = 1$ has been used in the procedure. From the results, we can see that this assumption does not affect significantly the effectiveness of the method. Even at high pressure doubling *F* only increases W_o by about 10%.

Figures 92 to 95 present the effect of *F* on the design bolt loads W_{m1} and W_{m2}. From the plots we can see how W_{m1} increases as *F* increases, the effect being increased by pressure. The plots of W_{m1} & W_{m2} vs *M* seem to indicate that W_{m2} is also affected by *F*, but from equations (12) and (14) we see that this is not so. The problem is the ordinate *M*, which is affected by *F* since it depends on S_m, hence it is incorrect to assume that the increase in W_{m2}

shown in the plots is due to *F*. Again we can appreciate the usefulness of plotting the bolt loads vs. the tightness ratio T_{pr} (Figs. 94 & 95). Plotting these against *M* sometimes provides a confusing picture of their behavior.

5.5 OPTIMAL T_{pr}

As mentioned in Chapter 3, it has been suggested in Ref. 4 that to simplify the computation of the optimal load, a fixed ratio of T_{pr}/T_{pmin} (T_{pr}) be taken as 1.5. As shown in Figures 96 and 97, this factor can greatly affect the value of the optimal load. The important point is that by fixing T_{pr} to a given value we are no longer optimizing the bolt loads. Depending on the design parameters, gasket constants, pressure, etc., the value of T_{pr} that correspons to the optimal condition may vary greatly.

Sometimes this parameter ranges from 1 to less than 1.5. In this particular case (Fig. 96), considering $T_{pr} = 1.5$ would correspond to $M < 2$ (remember that M decreases to the right in these plots, M=2 at W_o). In this case the approximating method would use the highest of W_{m1} and W_{m2} at $M = 2$.

However, in many cases, computing the approximate design bolt load W_m at $T_{pr} = 1.5$, yields a higher value than the optimal value (W_o) computed using the proposed design procedure (see Fig. 97). Thus, if a truly efficient design value of W_m is desired, the full procedure should be used.

5.6 *TurboFlange* VS. CURRENT ASME CODE

The results obtained with the new design procedure were compared with those calculated using the current ASME Code. For illustration purposes, two cases are presented in APPENDIX B, and a summary of these results is included in Tables 17 to 22. CASE I consists of a large diameter (42.25") flange at a high design pressure (925 psi), CASE II is also a large flange but at a low design pressure (120 psi). The complete set of data and results is included in Appendix C.

From the results in Tables 17 to 22 we observe that the new procedure gives lower design bolt loads, W_m, and consequently lower flange stresses. The design bolt load was 6% (Tab. 17) lower for the high pressure case, and 14% (Tab. 20) lower at low pressure, while the design flange stresses were 25% (Tab. 19b) and 28% (Tab. 22b) lower respectively. From these results the advantages of the new method are clear: 1) it is based on true experimental parameters, which can be verified; and 2) it yields a more efficient design with greater flexibility, since it does not constrain or fix the stresses on the gasket, but actually computes them based on the tightness requirements of the design. In addition to this, the designer can visualize the behavior of the joint not only in terms of S_m, but also in terms of tightness. This is possible by inspecting the plots of "W_{m1} & W_{m2} vs *M*" and "W_{m1} & W_{m2} vs Tpr" respectively.

TABLE 17: CASE I. Current Code vs ***TurboFlange*** (Bolt Loads).

P = 925 psi.

BOLT LOADS	CURRENT ASME CODE	***TurboFlange***	% DIFF.
W_{m1}	1560710 lb (6937 kN)	1611886 lb (7164 kN)	-3 %
W_{m2}	1304300 lb (5797 kN)	1583542 lb (7038 kN)	-18 %
W_m (W_o)	1704370 lb (7575 kN)	1611886 lb (7163 kN)	6 %

TABLE 18: CASE I. Current Code vs ***TurboFlange*** (Flange Moments).

P = 925 psi.

FLANGE MOMENTS	CURRENT ASME CODE	***TurboFlange***	% DIFF.
M_D	3809440 lb.in	3807524 lb.in	1 %
M_G	413810 lb.in	556544 lb.in	26 %
M_C	384260 lb.in	386282 lb.in	1 %
M_O	4607510 lb.in	4750351 lb.in	3 %
M_S	4793540 lb.in	4531586 lb.in	6 %

TABLE 19a: CASE I. Current Code vs ***TurboFlange*** (Flange Stresses). Seating Condition

FLANGE STRESSES (seating)	CURRENT ASME CODE	***TurboFlange***	% DIFF.
S_H	22970 psi (158 MPa)	14839 psi (102 MPa)	55 %
S_R	2880 psi (20 MPa)	2551 psi (18 MPa)	13 %
S_T	10570 psi (73 MPa)	9806 psi (68 MPa)	8 %
$.5(S_H + S_R)$ or $.5(S_H + S_T)$	16770 psi (116 MPa)	12323 psi (85 MPa)	36 %

TABLE 19b: CASE I. Current Code vs ***TurboFlange*** (Flange Stresses).

P = 925 psi.

Operating Condition

FLANGE STRESSES (operating)	CURRENT ASME CODE	***TurboFlange***	% DIFF.
S_H	22080 psi (152 MPa)	15555 psi (107 MPa)	42 %
S_R	2770 psi (19 MPa)	2674 psi (18 MPa)	4 %
S_T	10160 psi (70 MPa)	10280 psi (71 MPa)	-1 %
$.5(S_H + S_R)$ or $.5(S_H + S_T)$	16120 psi (111 MPa)	12917 psi (89 MPa)	25 %

TABLE 20: CASE II. Current Code vs ***TurboFlange*** (Bolt Loads).

P = 120 psi.

BOLT LOADS	CURRENT ASME CODE	***TurboFlange***	% DIFF.
W_{m1}	444380 lb (1975 kN)	356297 lb (1584 kN)	25 %
W_{m2}	542910 lb (2413 kN)	383973 lb (1707 kN)	41 %
W_m (W_o)	437550 lb (1945 kN)	383973 lb (1707 kN)	14 %

TABLE 21: CASE II. Current Code vs ***TurboFlange*** (Flange Moments).

P = 120 psi.

FLANGE MOMENTS	CURRENT ASME CODE	***TurboFlange***	% DIFF.
M_D	256100 lb.in	255921 lb.in	0 %
M_G	283220 lb.in	218619 lb.in	30 %
M_T	17320 lb.in	17328 lb.in	0 %
M_O	556650 lb.in	491868 lb.in	13 %
M_S	467440 lb.in	409920 lb.in	14 %

TABLE 22a: CASE II. Current Code vs ***TurboFlange*** (Flange Stresses).

Seating Condition

FLANGE STRESSES (seating)	CURRENT ASME CODE	***TurboFlange***	% DIFF.
S_H	31650 psi (218 MPa)	23767 psi (164 MPa)	33 %
S_R	3200 psi (22 MPa)	2810 psi (19 MPa)	14 %
S_T	8870 psi (61 MPa)	7757 psi (53 MPa)	14 %
$.5(S_H + S_R)$ or $.5(S_H + S_T)$	20260 psi (140 MPa)	15762 psi (109 MPa)	29 %

TABLE 22b: CASE II. Current Code vs ***TurboFlange*** (Flange Stresses).

P = 120 psi.

Operating Condition

FLANGE STRESSES (operating)	CURRENT ASME CODE	***TurboFlange***	% DIFF.
S_H	37690 psi (260 MPa)	28518 psi (197 MPa)	32 %
S_R	3810 psi (26 MPa)	3372 psi (23 MPa)	13 %
S_T	10560 psi (73 MPa)	9308 psi (64 MPa)	14 %
$.5(S_H + S_R)$ or $.5(S_H + S_T)$	24130 psi (166 MPa)	18913 psi (130 MPa)	28 %

5.7 CLOSING REMARKS

To close this chapter a summary of the most important findings of the study is provided based on the previous discussion of the results:

New Proposed Procedure :

The new proposed procedure allows increased tightness with little increase in bolt load, this improves the design performance without considerable increase in the cost.

As expected, the seating condition prevails at low pressure, whereas at high pressure the operating condition dominates the behavior of the bolt load and the gasket stresses.

From the examples considered, the factor B seems to be most critical; S* is almost insignificant; and d varies with pressure.

The bolt efficiency *e* affects directly the calculation of the design bolt load and thus the stresses. Given the results from the FE analysis, this value is more critical for large flanges where the seating stresses decrease as the pressure is applied.

The experience factor *F* has a relatively small effect on the resulting design bolt load, W_m. In this respect its effect is not very significant to the procedure. Further study is required to propose specific values for *F*.

The new procedure is better than the one available in the ASME Code in several areas. It is more efficient, providing lower loads and flange stresses for an equivalent safe design. It also has the advantage of including tightness in the design, which provides greater flexibility to the designer and a more realistic representation of the gasket materials.

6 CHAPTER 6

FE vs *TurboFlange*: VALIDITY OF THE NEW PROCEDURE

In order to compare the results from the Finite Element stress analyses with those obtained from ***TurboFlange***, the computed mean values from the linear analyses (GIFTS) were compared with the values of S_{ya}, S_m and Wm/Ab from the design program.

One very useful feature of the design program, and the new method, is that in addition to the calculated optimal value of W_m (Wo), it also provides a whole range of values of W_{m1} and W_{m2} vs *M*, and S_{ya} and S_m vs *M*. These values are provided graphically and numerically.

The mean values obtained from the finite element analyses do not necessarily correspond to the "optimal" results from ***TurboFlange***. This is so since, for the finite element analyses, no optimization criteria was imposed.

By using the plots and data described above, one can look-up the corresponding values of S_{ya} and Wm, for given values of S_m (P or *M* can be used as well). The results in Tables 23, 24 and 25 were obtained in this fashion. Using values of S_m from the FE results as our starting point, we looked-up the corresponding values of S_{ya} and Wm/Ab from the plots of "W_{m1} & W_{m2} vs *M*" and "S_{ya} and S_m vs *M*" produced by ***TurboFlange.*** Notice that $W_m/A_b = S_b$, that is, the average bolt stress. Several gasket material and flange sizes are compared in the Tables.

From the results in Table 24 we can appreciate that the new proposed procedure gives a good approximation of the average stresses on the gasket when compared with the FE results. Notice also that the new procedure tends to give higher values of S_{ya}, than those obtained from the FE analysis. The results from Table 25 indicate that the opposite is true for the bolt stresses, which tend to be as much as 26% lower.

In the calculations done using ***TurboFlange***, a value of $e = 0.75$ and $F = 1.0$ were used. Varying these parameter will affect the results (as shown previously), *F* will affect mainly the stresses and not Wm, while *e* will affect both. The important fact is that these values can serve to fine-tune the results and increase their accuracy, but even when using the default values proposed, $e = 0.75$ and $F = 1.0$, the results obtained with the new procedure compare favorably with those obtained using the finite element method.

The results from the FE analyses, correspond to high values of M, over $M = 5$ in all cases. The new procedure approaches the FE results for these cases. The question remains as to what happens at lower values of M, say between $M = 2$ and $M = 4$. In these cases the design conditions become more critical since the gasket stresses are lower, and hence the possibility of a leak increases. This question could be a part of a future study on the accuracy of the new method.

TABLE 23: FE vs ***TurboFlange***. Equivalent Mean Operating Stresses.

GASKET & CLASS	S_m FE GIFTS	S_m ***TurboFlange***	% DIFF.
GHS Class 1500-24	-8144 psi (-56 MPa)	-8103 psi (-56 MPa)	0.5 %
DJ MICA Class 1500-24	-7630 psi (-53 Mpa)	-7604 psi (-53 MPa)	0.3 %
DJ ASBESTOS Class 1500-24	-7808 psi (-54 MPa)	-7831 psi (-54 MPa)	0.3 %
SELCO Class 1500-24	-7630 psi (-53 MPa)	-7692 psi (-53 MPa)	0.8 %
DJ MICA Class 1500-12	-15835 psi (-109 MPa)	-15740 psi (-109 MPa)	0.6 %
DJ ASBESTOS Class 1500-12	-15906 psi (-110 MPa)	-15946 psi (-110 MPa)	0.3 %

TABLE 24: FE vs ***TurboFlange***. Equivalent Mean Seating Stresses.

GASKET & CLASS	S_{ya} FE GIFTS	S_{ya} ***TurboFlange***	% DIFF.
GHS Class 1500-24	-13190 psi (-91 MPa)	-15056 psi (-104 MPa)	12 %
DJ MICA Class 1500-24	-13015 psi (-90 MPa)	-13619 psi (-94 MPa)	4 %
DJ ASBESTOS Class 1500-24	-13078 psi (-90 MPa)	-13520 psi (-93 MPa)	3 %
SELCO Class 1500-24	-13015 psi (-90 MPa)	-13515 psi (-93 MPa)	4 %
DJ MICA Class 1500-12	-19329 psi (-133 MPa)	-22146 psi (-153 MPa)	12 %
DJ ASBESTOS Class 1500-12	-19471 psi (-134 MPa)	-22050 psi (-152 MPa)	11 %

TABLE 25: FE vs ***TurboFlange***. Equivalent Mean Bolt Stresses.

GASKET & CLASS	S_b FE GIFTS	S_b ***TurboFlange***	% DIFF.
GHS Class 1500-24	13 ksi (90 MPa)	14 ksi (97 MPa)	7 %
DJ MICA Class 1500-24	13 ksi (90 MPa)	9.5 ksi (66 MPa)	26 %
DJ ASBESTOS Class 1500-24	13 ksi (90 MPa)	10.4 ksi (72 MPa)	20 %
SELCO Class 1500-24	13 ksi (90 MPa)	12.7 ksi (88 MPa)	2 %
DJ MICA Class 1500-12	22 ksi (152 MPa)	17 ksi (116 MPa)	23 %
DJ ASBESTOS Class 1500-12	22 ksi (152 MPa)	18.3 ksi (126 MPa)	17 %

7 CHAPTER 7

CONCLUSIONS

- The new procedure is an improvement over the one currently used in the ASME Pressure Vessel Code in several areas. It is more efficient, providing lower bolt loads and flange stresses for an equivalent safe design. It also provides greater flexibility to the designer, and a more realistic representation of the gasket materials.

- The nonlinear-elastoplastic analysis of the joints provides an accurate representation of the gasket behavior. However, it is very costly in both time and money.

- The linear-elastic analysis of the joints proves to be a simple approximating method that can be used for design purposes where the overall performance of the gasket is desired as opposed to a detailed and highly accurate picture of the stresses on the gasket.

- It is very important that when using the linear approach, appropriate values of E and v be chosen, since these two parameters characterize completely the gasket materials. In this respect more information is needed on the actual values

of Poisson's ratio, v, of the gasket materials.

- The results obtained with the new design procedure indicate that at low pressure, the seating condition prevails, while at high pressure it is the operating condition which dominates the behavior of the load and stresses.

- Moreover, from the FE stress analysis results there is indication that, in fact, the operating condition does prevail in the behavior of the joint. This is suggested by the success of the linear approach, which is based on the modulus of decompression from the operating stress-strain curve of the gasket material.

8 GRAPHS & FIGURES

Figures start on next page.

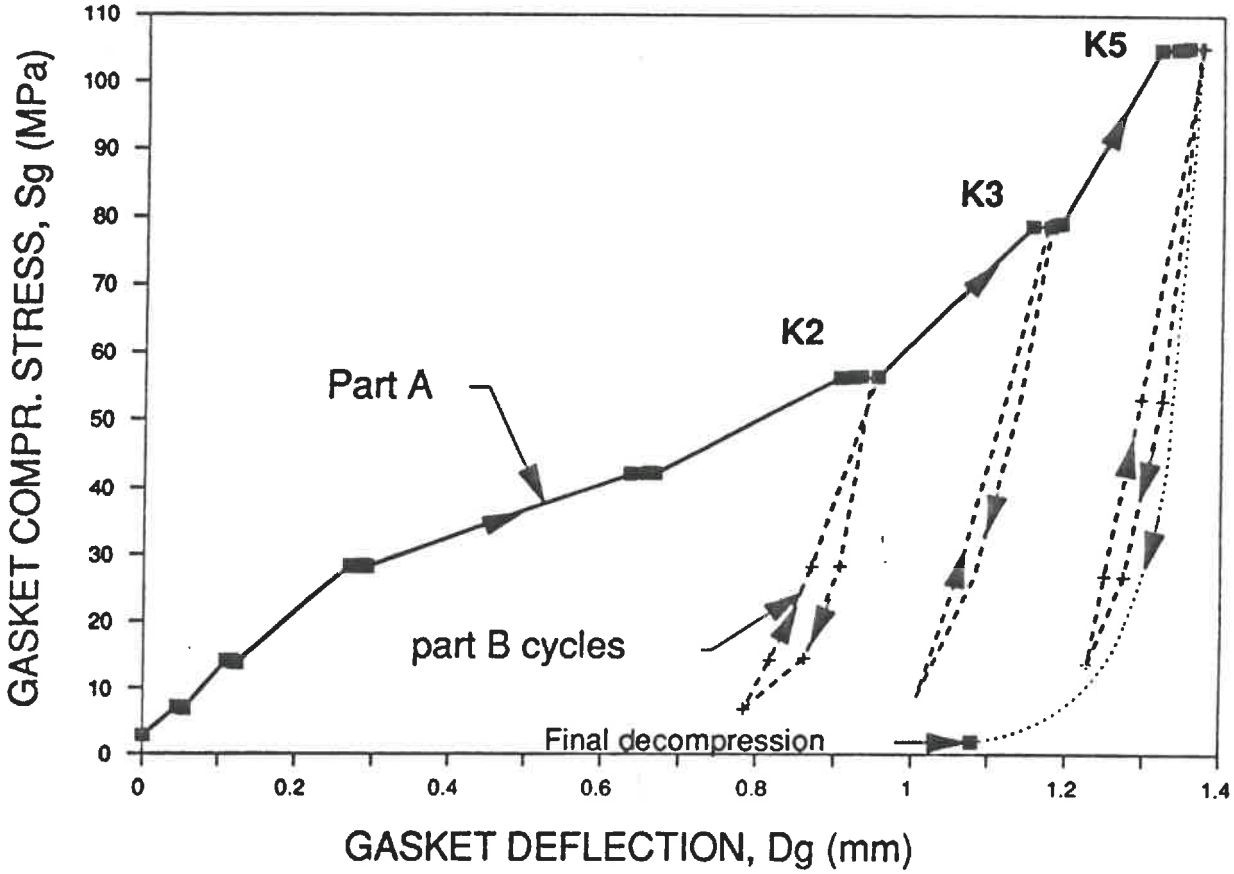

FIGURE 1 : Schematic of Experimental Test Procedures.

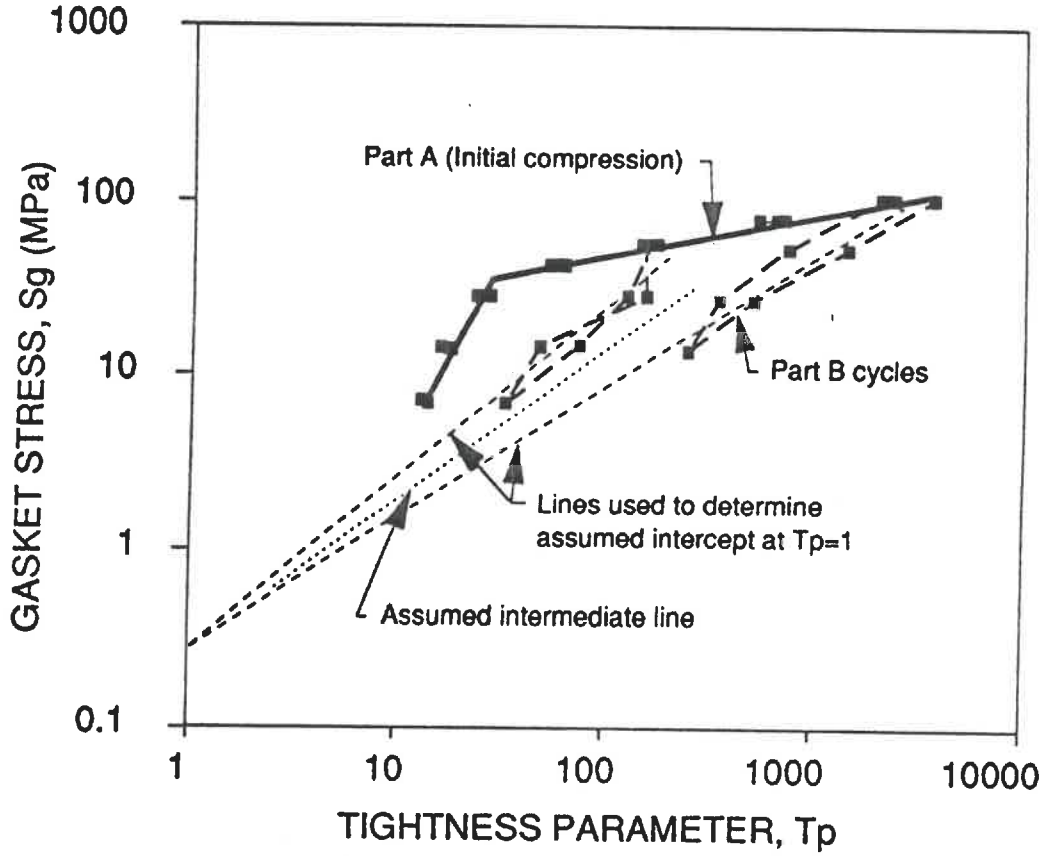

FIGURE 2 : Gasket Stress vs Tightness, Parts A & B.

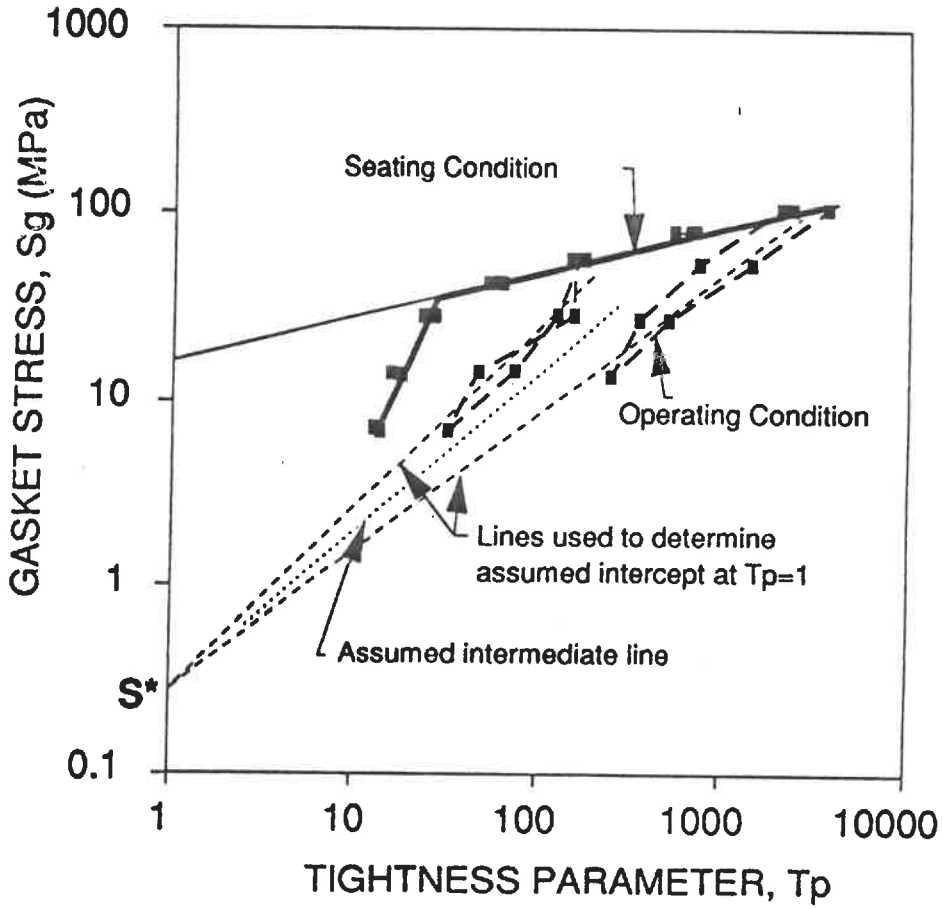

FIGURE 3 : Typical Gasket Stress-tightness plot.

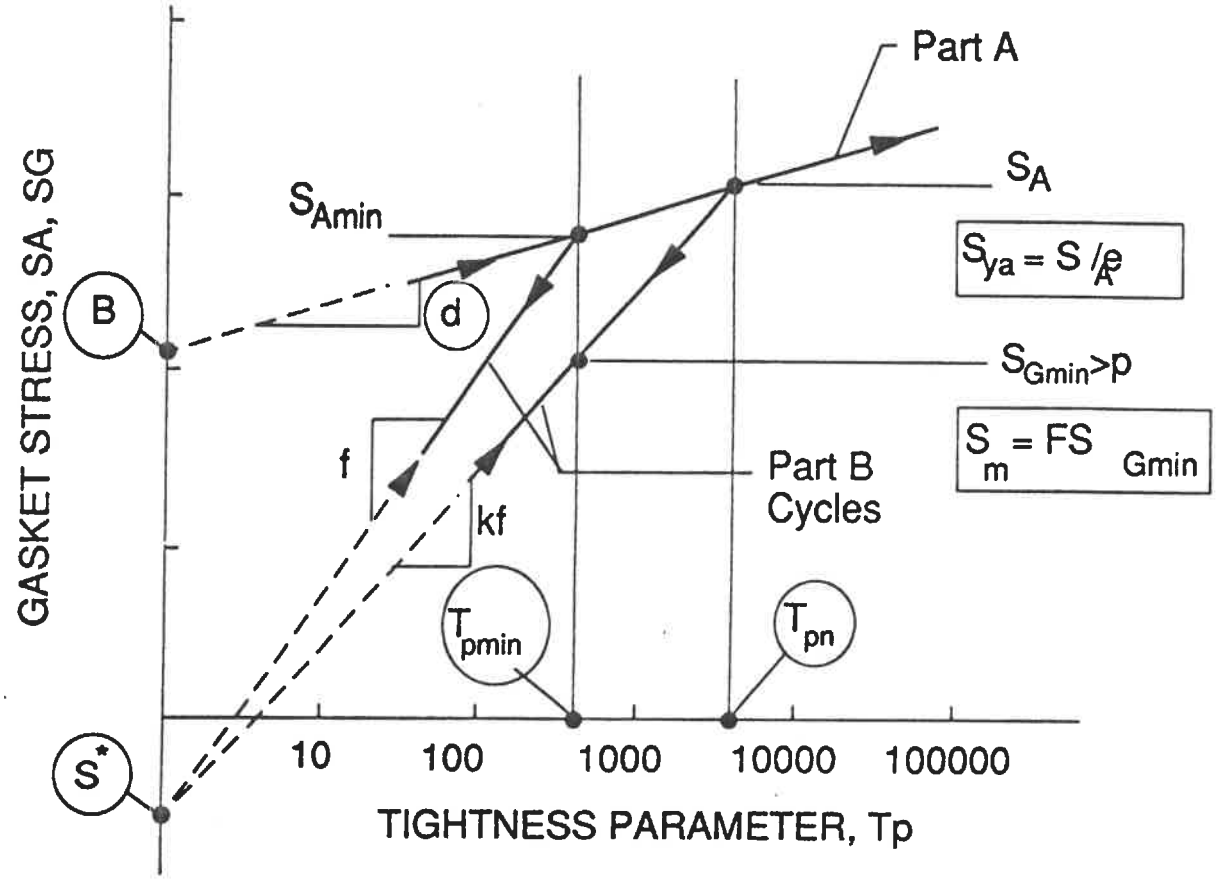

FIGURE 4 : Simplified Stress-tightness plot

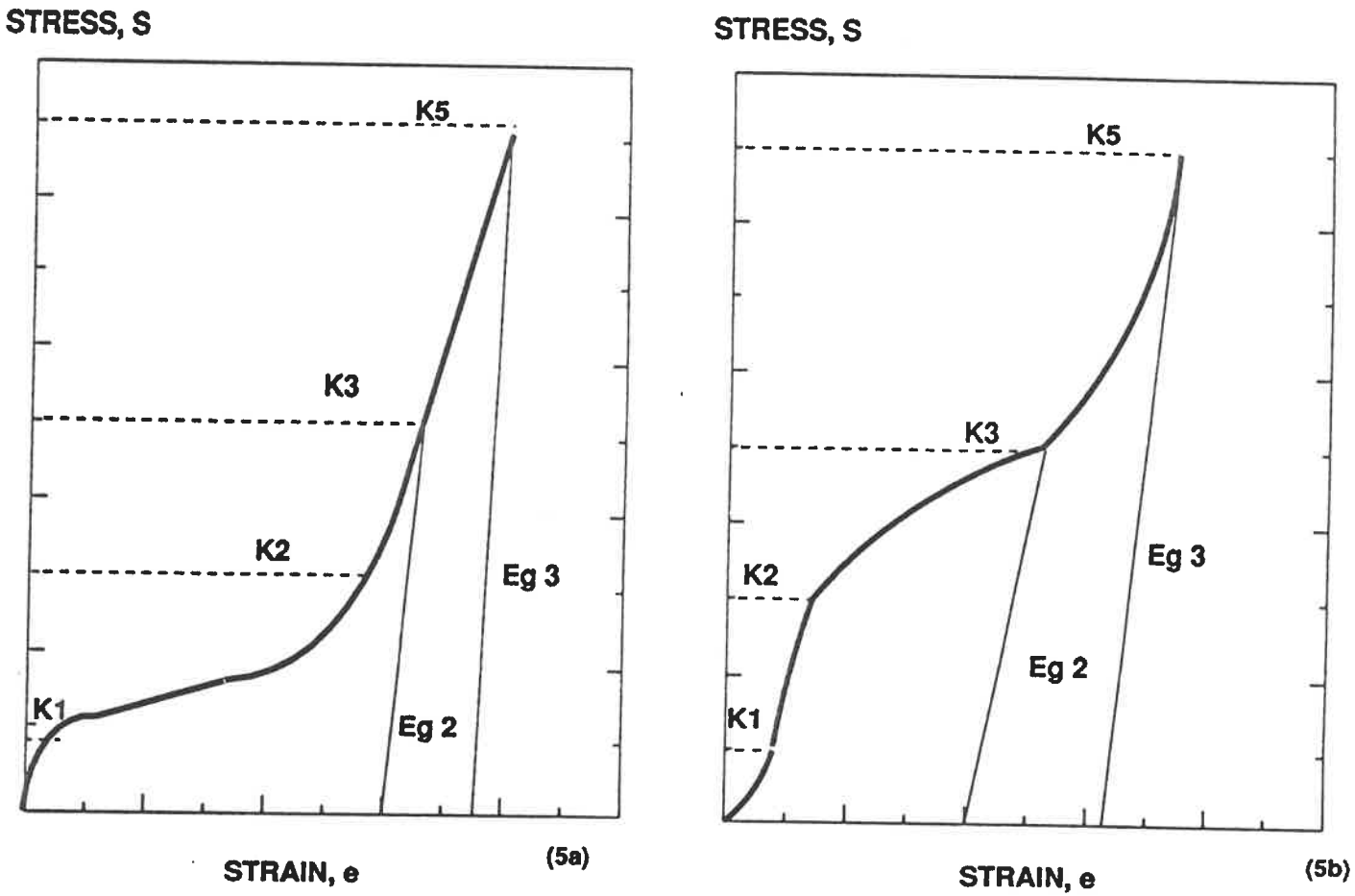

FIGURE 5 : Typical Gasket Materials Stress-strain plots.

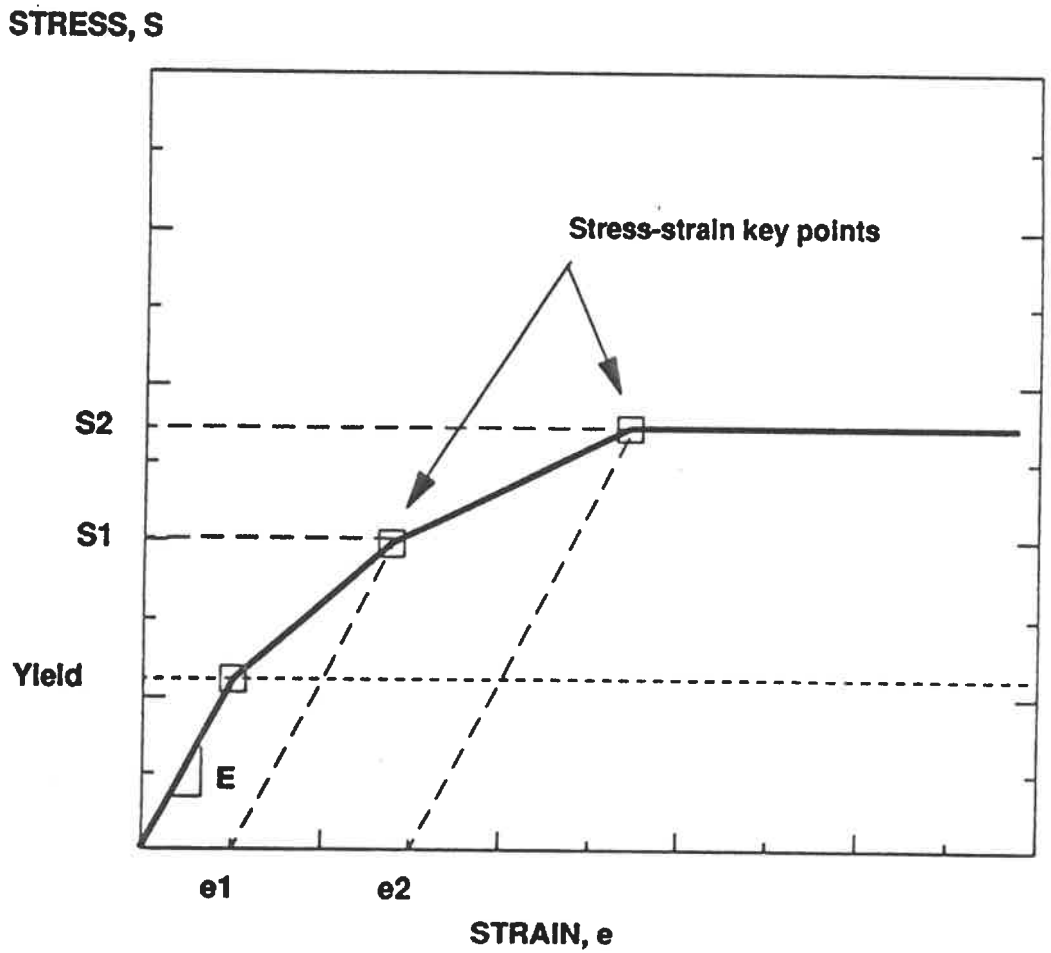

FIGURE 6 : Example of a plastic Stress-Strain material curve in ABAQUS.

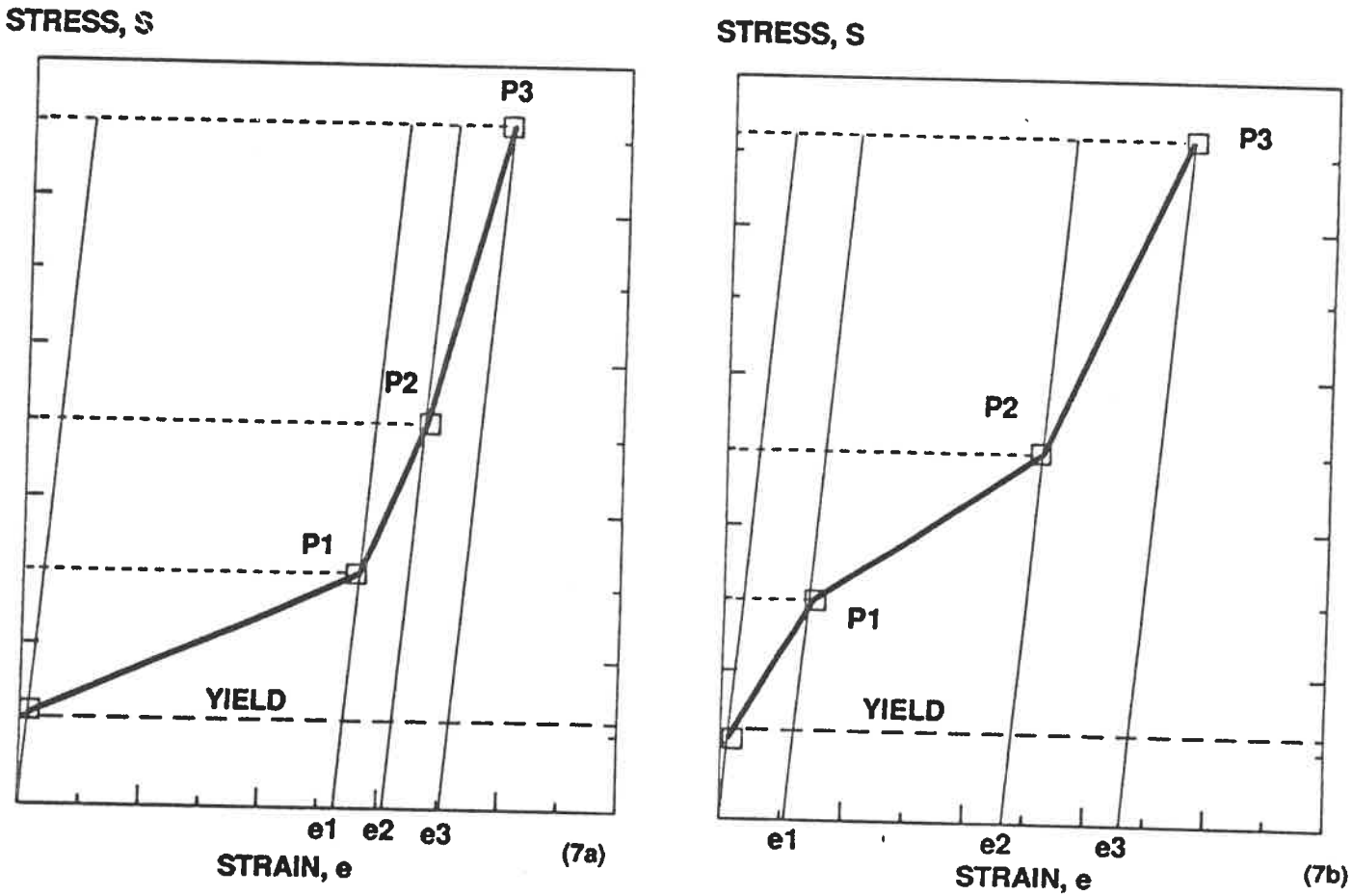

FIGURE 7 : Sample Gasket Stress-strain plots used in ABAQUS

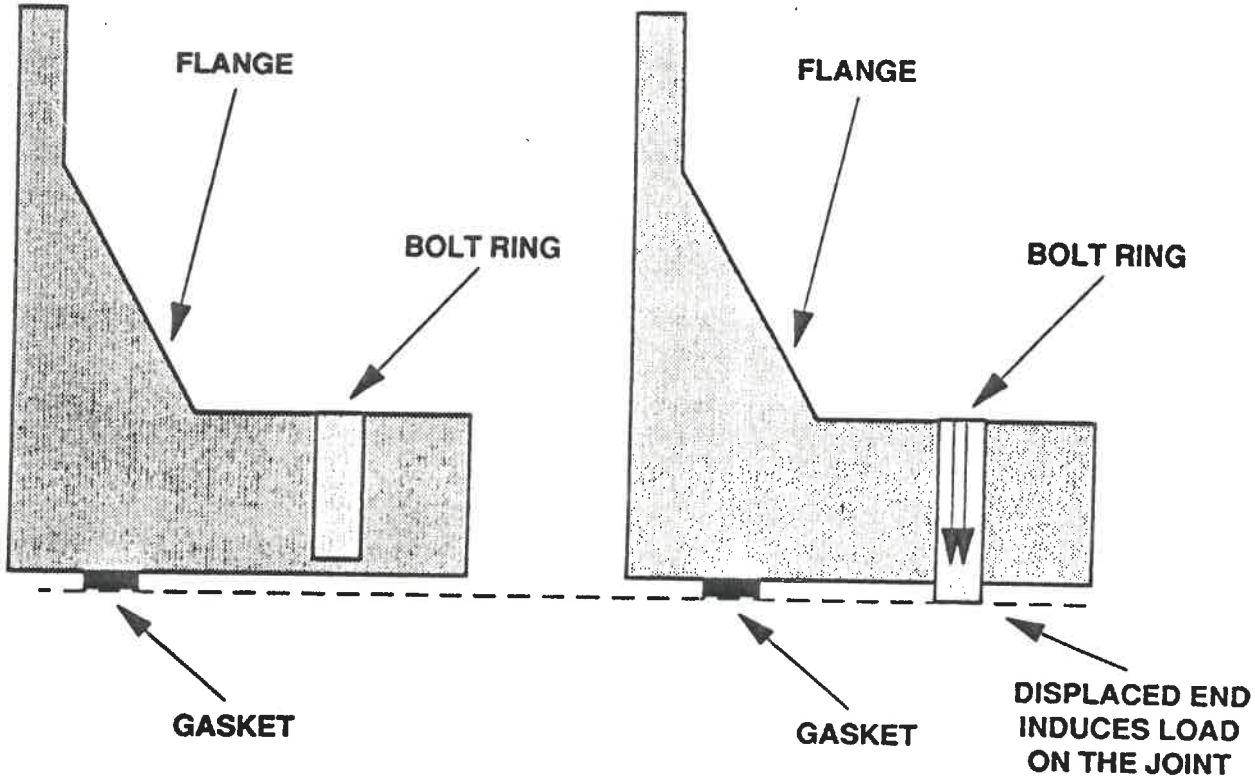

FIGURE 8 : Induced bolt load on the Bolt Ring

BOLT RING AREA = BOLT ROOT AREA x NUMBER OF BOLTS

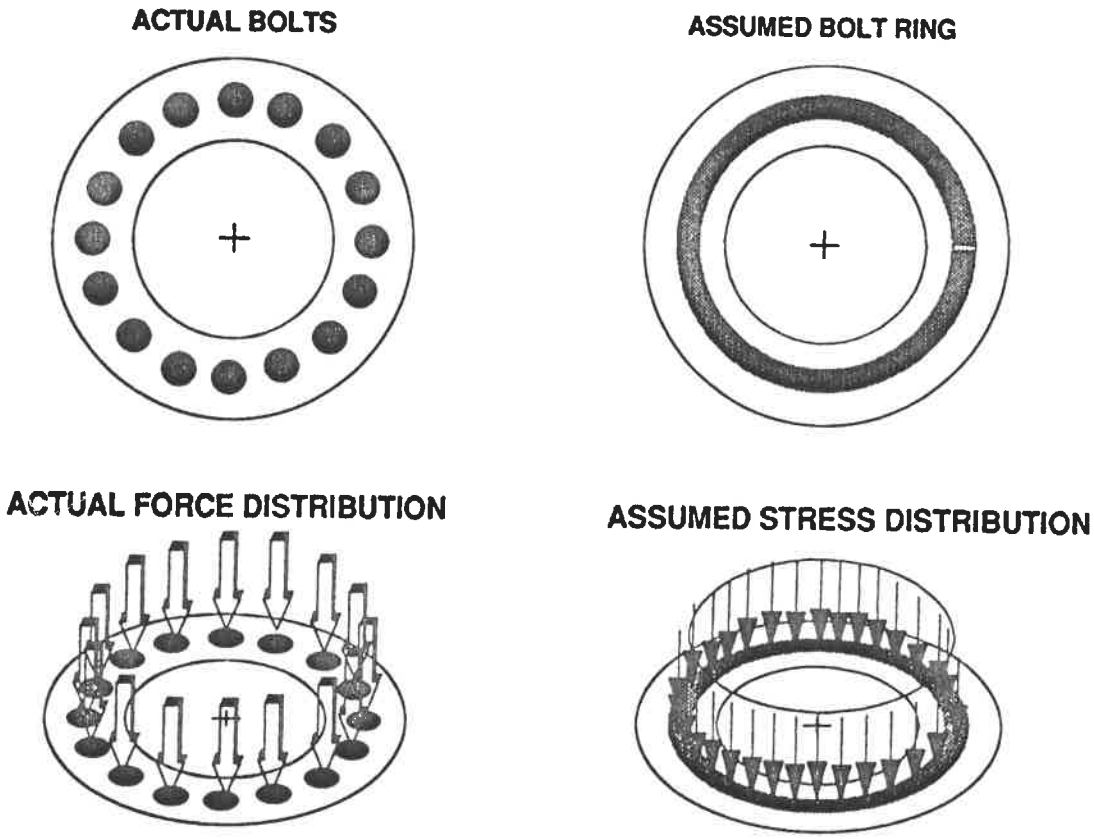

FIGURE 9 : Bolt Ring and assumed stress distribution

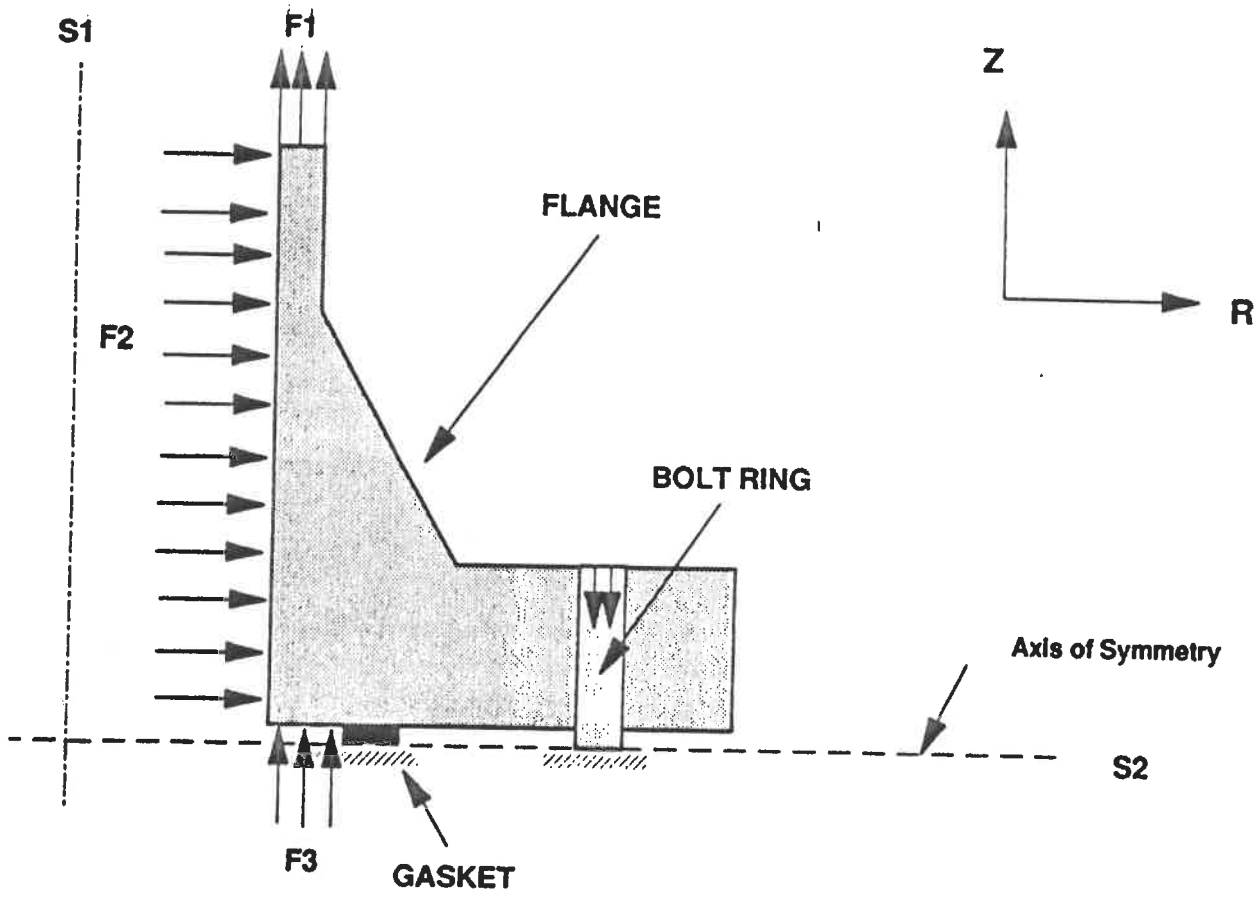

FIGURE 10 : Loads and boundary conditions on the joint

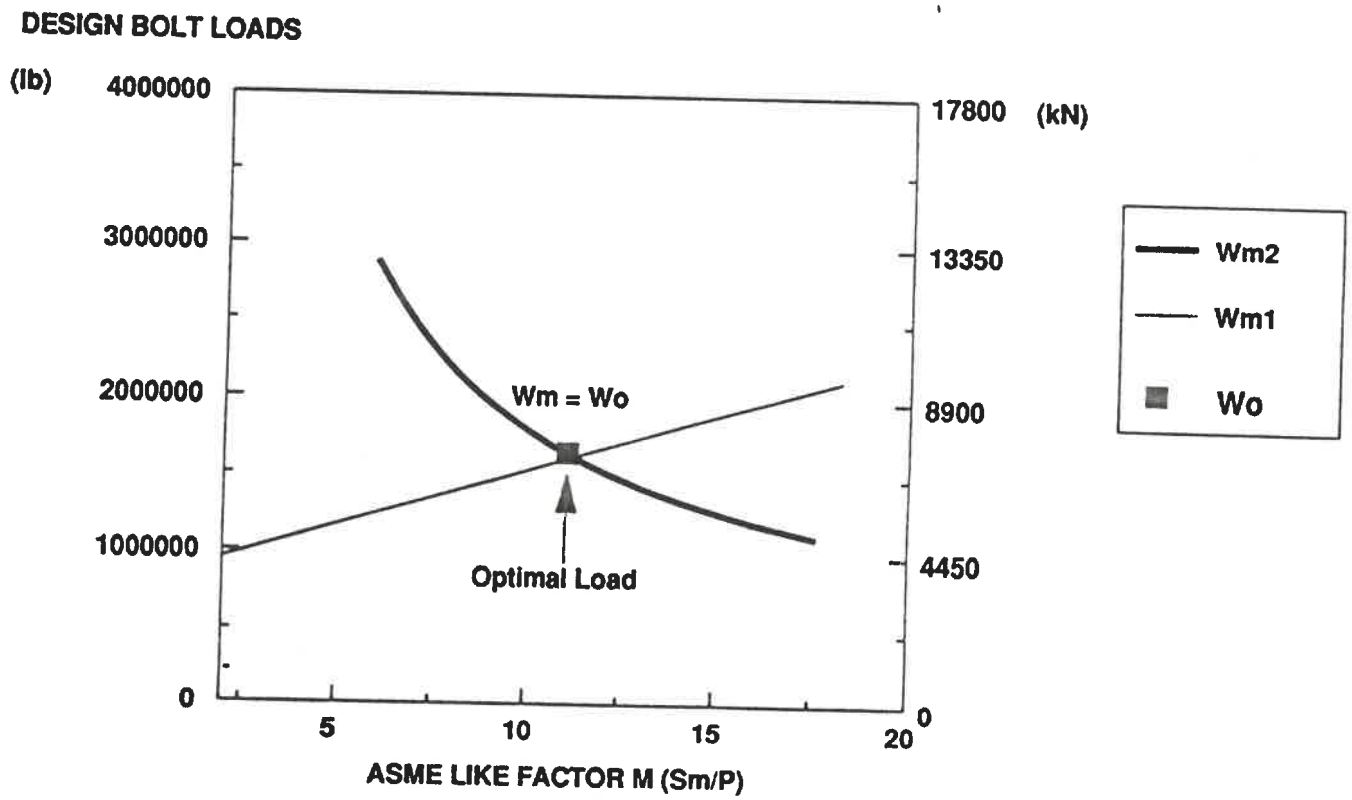

FIGURE 11 : Design Bolt loads Wm1 & Wm2 vs. factor M

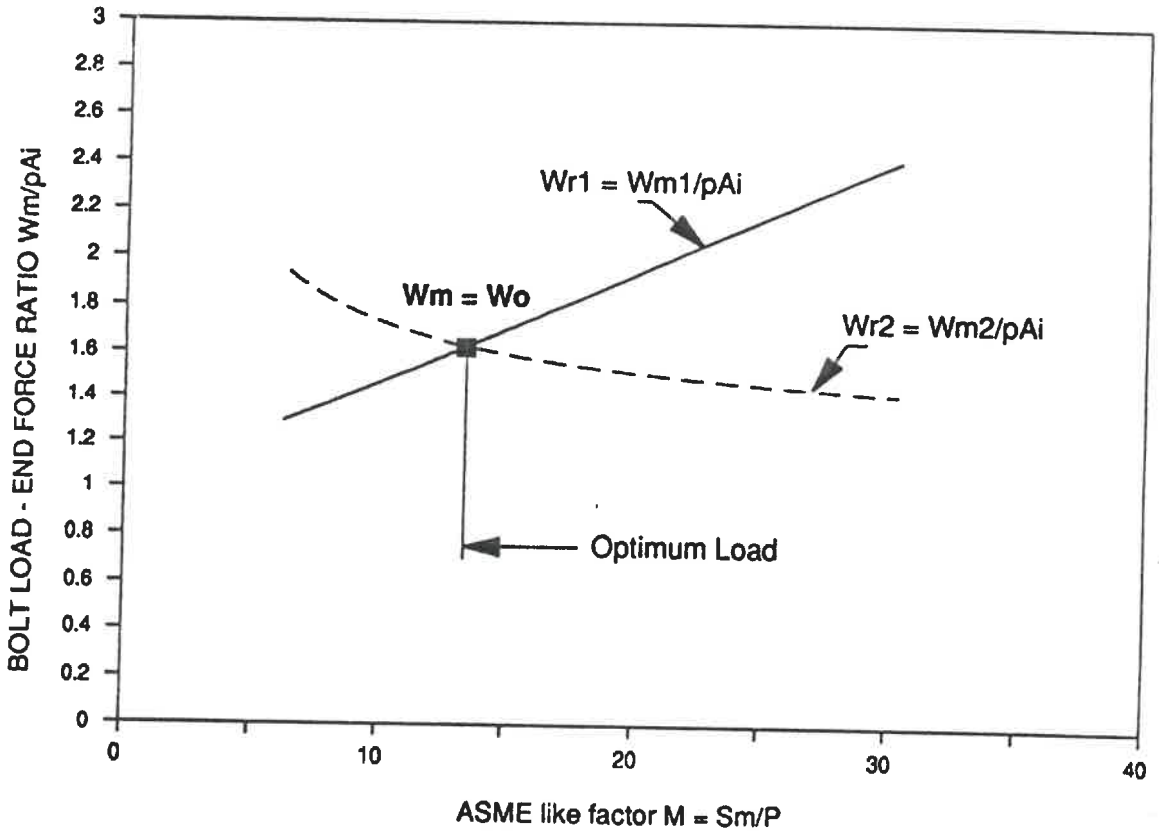

FIGURE 12 : Design bolt loads ratio, Wr1 & Wr2 vs factor M

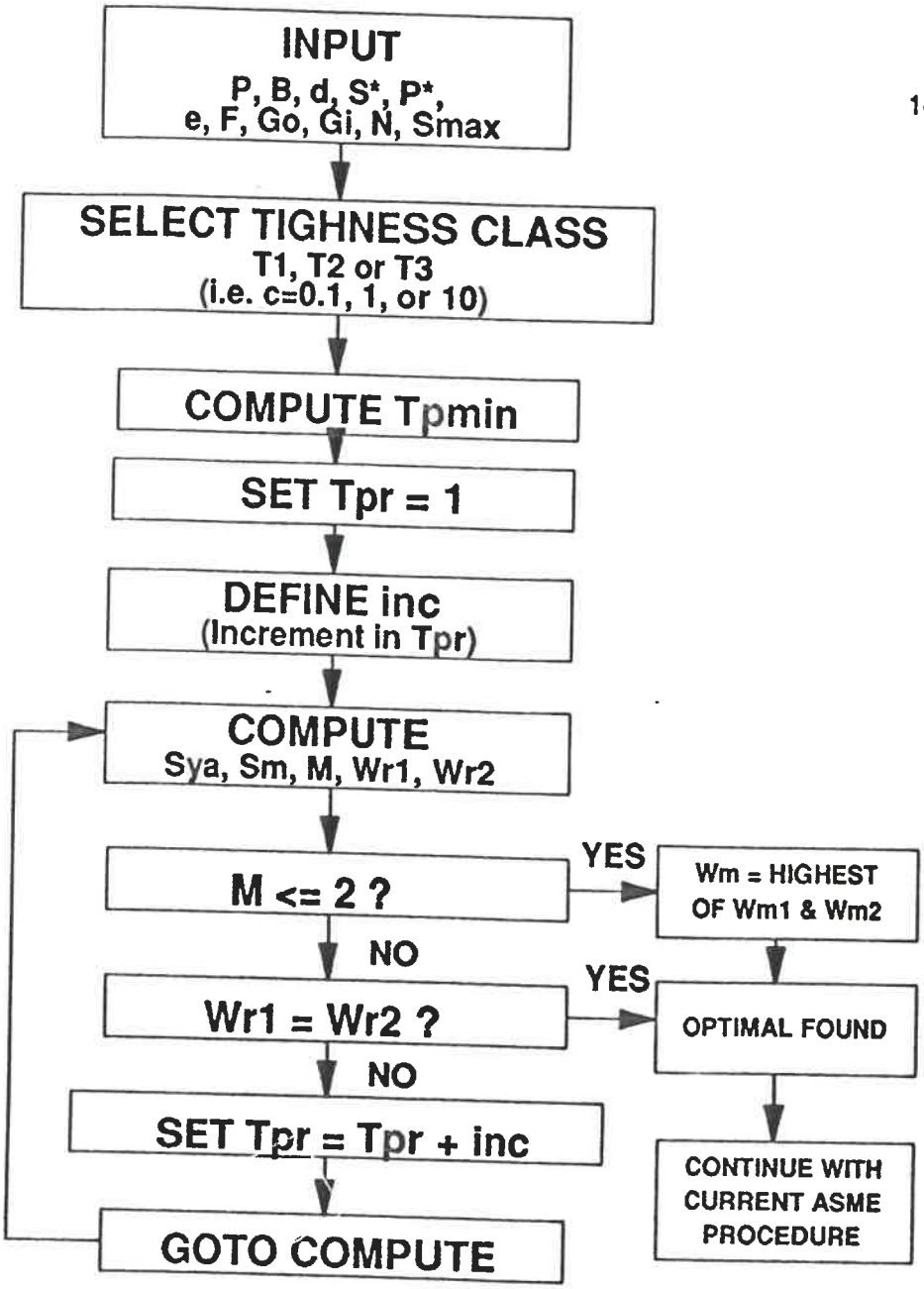

FIGURE 13 : BLOCK DIAGRAM OF OPTIMIZING ALGORITHM

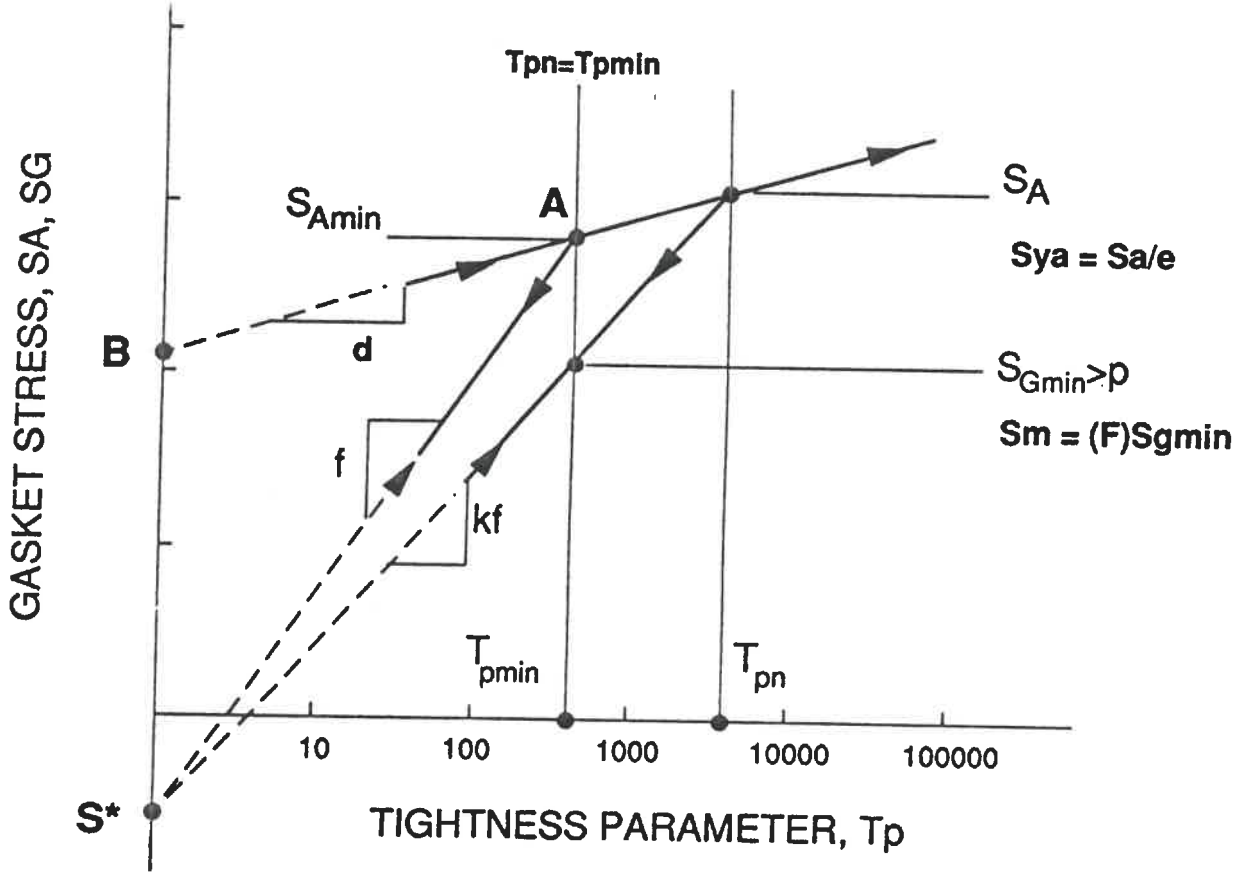

FIGURE 14 : Idealized Stress-tightness plot

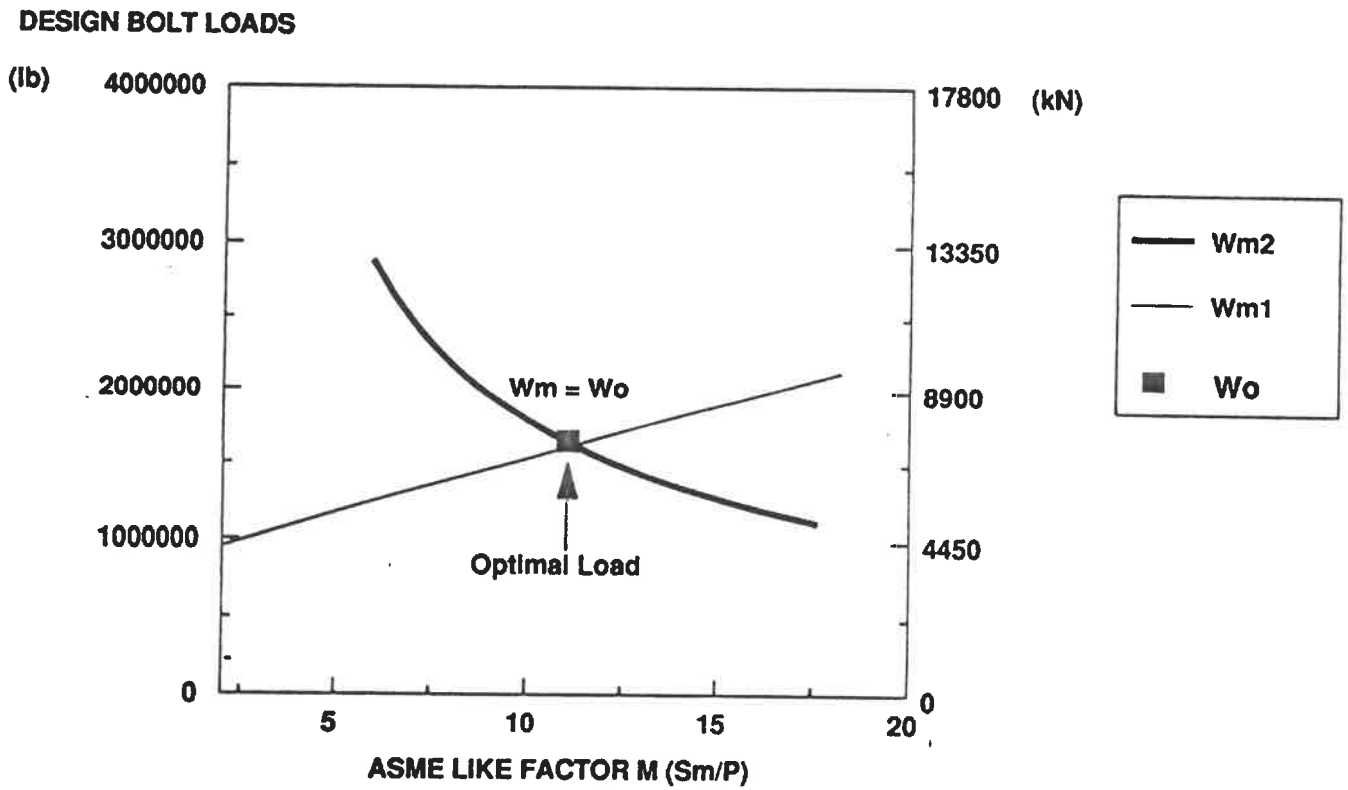

FIGURE 15 : Design Bolt loads Wm1 & Wm2 vs. factor M (Optimal at Wm1=Wm2)

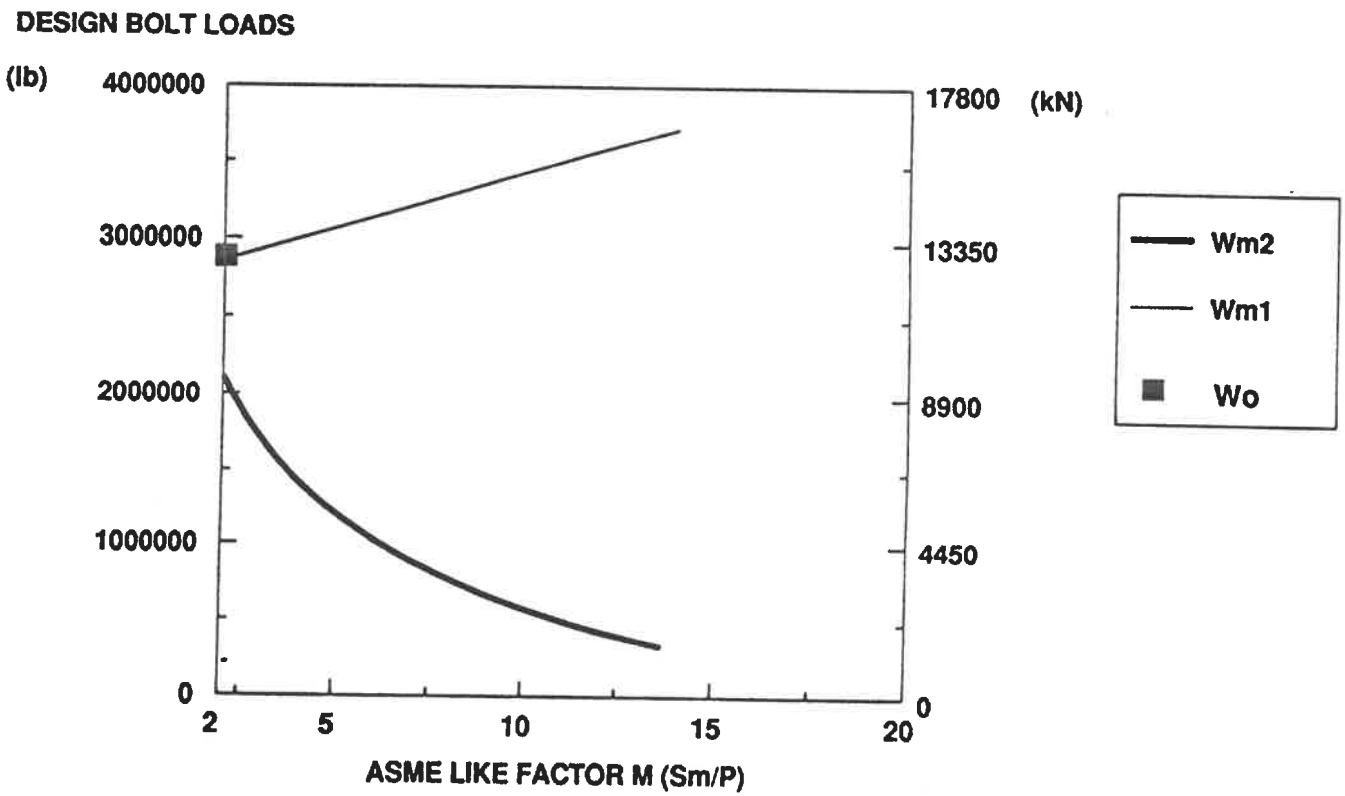

FIGURE 16 : Design Bolt loads Wm1 & Wm2 vs. factor M (Optimal at M = 2).

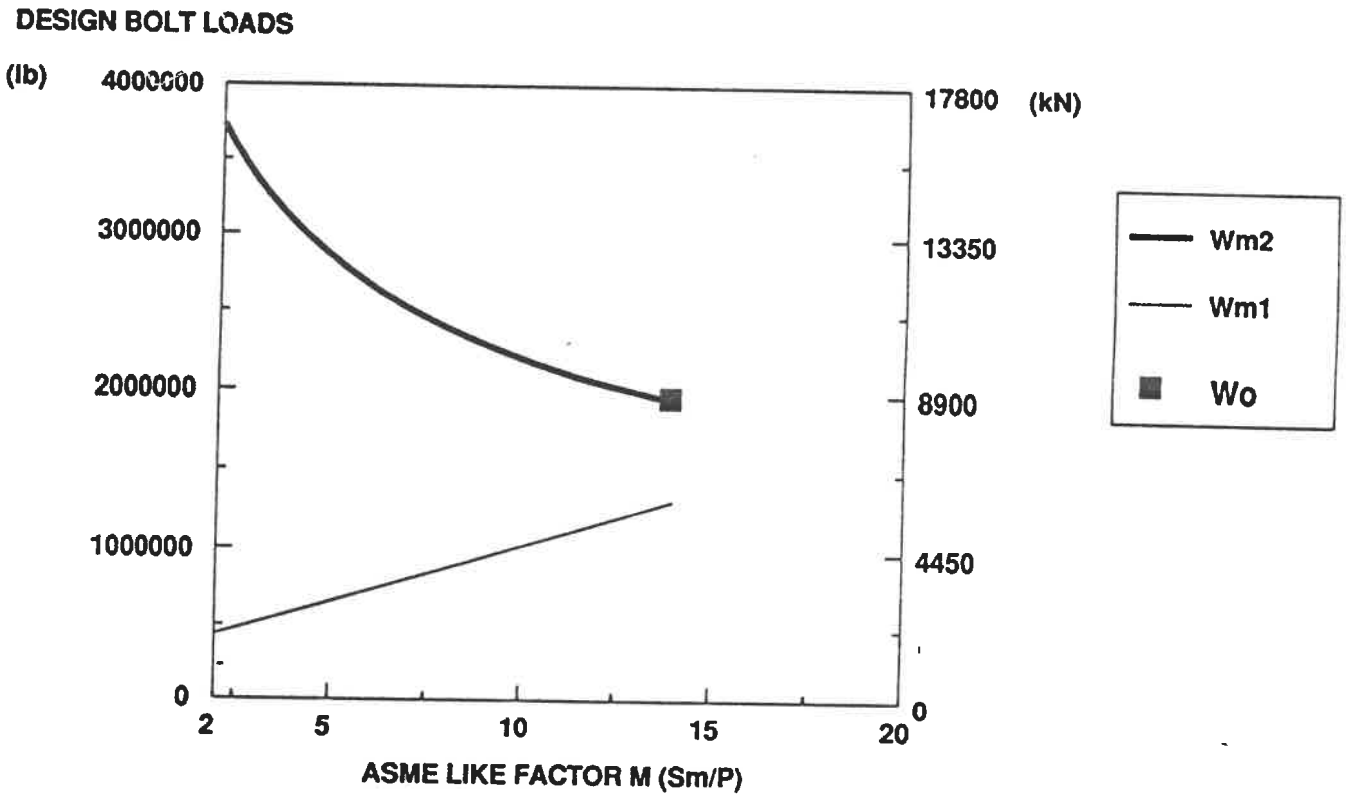

FIGURE 17 : Design Bolt loads Wm1 & Wm2 vs. factor M (Optimal at Tpr = 1).

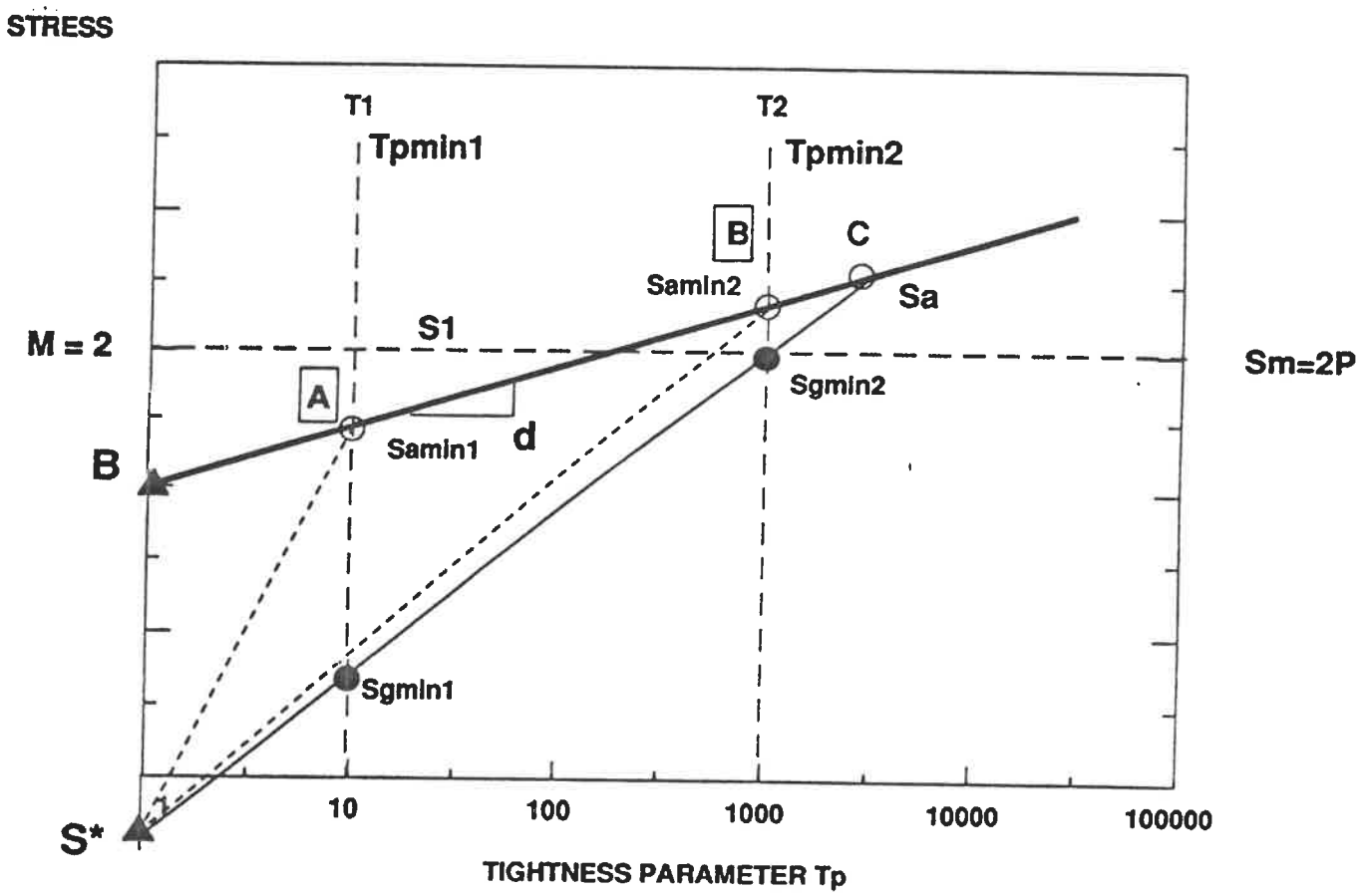

FIGURE 18 : Effect of Tpmin on the design gasket stresses

FIGURE 19: TurboFlange Model Data Screens.

```
                                TURBO-FLANGE
  MODEL      TEMPLATE      EDIT      SOLVE      RESULTS      OUTPUT      QUIT
                         FLANGE INFORMATION SHEET
MODEL DJA1506      COMMENTS ANSI C1500/6 DJ SS/ASB          UNITS IN/PSI/°F

FLANGE MAT.                BOLTING MAT.                FLANGE TYPE INTEGRAL

OP. PRESSURE  1500.000  OP. TEMPERATURE   500.000  CORROSION ALLOW.   0.125

FLANGE OUTSIDE DIA., A          15.500  FLANGE INSIDE DIA., B           6.000

SMALL HUB THICKNESS, go          0.315  LARGE HUB THICKNESS, gi         1.500

HUB LENGTH, h                    3.500  FLANGE THICKNESS, t             3.250

BOLT CIRCLE DIA., C             12.500  DIA. OF BOLTS, Bd               1.375

NUMBER OF BOLTS, NB             12.000  ROOT AREA OF BOLTS, RA          1.155

ATM. FLANGE STRESS, Sf       17500.000  DESIGN FLANGE STRESS, Sn    17500.000

ATM. BOLT STRESS, Sa         25000.000  DESIGN BOLT STRESS, Sb      25000.000

     LOADED MODEL :  DJA1506              Import     saVe      Done
```

```
                                TURBO-FLANGE
  MODEL      TEMPLATE      EDIT      SOLVE      RESULTS      OUTPUT      QUIT
                         GASKET INFORMATION SHEET
MODEL DJASB-6      COMMENTS FLAT SSDJ/ASB/MILL IIb ANSIB16  UNITS IN/PSI/°F

GASKET MATERIAL ASB/MILL      NOMINAL SIZE  6

GASKET INSIDE DIA., Gi           7.500  GASKET OUTSIDE DIA., Go         8.500

GASKET WIDTH, N                  0.500  ATM. PRESSURE, Po              14.700

GASKET CONSTANT, So             14.690  GASKET CONSTANT, d              0.230

GASKET CONSTANT, B            2900.000  MIN. ASME FACTOR M, Mmin        2.000

JOINT ASSEMBLY EFF., e           0.750  LEAKAGE FACTOR, F               1.000

MAX. ALLOW. STRESS, Sg       20000.000  TIGHTNESS CLASS, TC      ECONOMY:  T1

     LOADED MODEL :  DJA1506              Import     saVe      Done
```

FIGURE 20: TurboFlange Template Data Screens.

```
                                TURBO-FLANGE
  MODEL     TEMPLATE     EDIT     SOLVE     RESULTS     OUTPUT     QUIT
                 FLANGE TEMPLATE INFORMATION SHEET
TEMPLATE C150-12  COMMENTS                                  UNITS IN/PSI/°F


FLANGE OUTSIDE DIA., A          19.000  FLANGE INSIDE DIA., B          12.000
SMALL HUB THICKNESS, go          0.375  LARGE HUB THICKNESS, gi          1.190
HUB LENGTH, h                    4.500  FLANGE THICKNESS, t              1.250
BOLT CIRCLE DIA., C             17.000  DIA. OF BOLTS, Bd                0.875
NUMBER OF BOLTS, NB             12.000  ROOT AREA OF BOLTS, RA           0.495

     LOADED TEMPLATE :  C150-12                      saVe      Done
```

```
                                TURBO-FLANGE
  MODEL     TEMPLATE     EDIT     SOLVE     RESULTS     OUTPUT     QUIT
                 GASKET TEMPLATE INFORMATION SHEET
TEMPLATE MICA-12  COMMENTS SS/MICA DJ IIa ANSIB16.5         UNITS IN/PSI/°F

GASKET MATERIAL SS/MICA DJ   NOMINAL SIZE  12


GASKET INSIDE DIA., Gi          12.750  GASKET OUTSIDE DIA., Go        14.250
GASKET WIDTH, N                  0.750  ATM. PRESSURE, Po              14.700
GASKET CONSTANT, So             14.690  GASKET CONSTANT, d              0.230
GASKET CONSTANT, B            2900.000  MIN. ASME FACTOR M, Mmin        2.000

     LOADED TEMPLATE :  MICA-12                      saVe      Done
```

FIGURE 21: TurboFlange Results Screens.

```
                                TURBO-FLANGE
MODEL     TEMPLATE     EDIT     SOLVE     RESULTS     OUTPUT     QUIT
                          RESULTS  PAGE-1
                    -GASKET STRESS AND BOLT LOAD-

TIGHTNESS PARAMETERS        Tpmin  = 1.863E+003   Tpn    =  1.863E+003
OPERATING STRESS            Sa     = 9.874E+003   Sya    =  1.317E+004
SEATING   STRESS            Sgmin  = 9.874E+003   Sm     =  9.874E+003
GASKET AREAS                Ag     = 2.233E+001   Ai     =  4.489E+001
BOLT LOADS                  Wm1    = 2.878E+005   Wm2    =  2.939E+005
OPTIMAL  VALUES             Mo     = 6.583E+000   Wo     =  2.939E+005

                     -BOLT STRESS AND BOLT AREA-

DESIGN BOLT AREA   (Num. of Bolts * Root Area)     Ab     =  1.386E+001
DESIGN STRESSES             Sa     = 2.500E+004   Sb     =  2.500E+004
COMPUTED BOLT AREA (Greater of Wo/Sa and Wo/Sb)    Am     =  1.176E+001
COMPUTED BOLT STRESS   So = Wo/Ab  = 2.121E+004
DESIGN vs COMPUTED VALUES   Ab/Am  = 1.179E+000   Sa/So =  1.179E+000

   LOADED MODEL :  SEL1506
```

```
                                TURBO-FLANGE
MODEL     TEMPLATE     EDIT     SOLVE     RESULTS     OUTPUT     QUIT
                          RESULTS PAGE-2
                -FLANGE LOADS, LEVER ARMS, AND MOMENTS-

                 LOAD            LEVER ARM           MOMENT
                  Hd =  4.239E+004  hd =  2.500E+000  Md =  1.060E+005
OPERATING         Hg =  2.220E+005  hg =  2.343E+000  Mg =  5.201E+005
                  Ht =  2.951E+004  ht =  2.796E+000  Mt =  8.253E+004
                                                  Md+Mg+Mt =  7.086E+005
SEATING           Wo =  2.939E+005  hg =  2.343E+000  Ms =  6.886E+005
                  MAXIMUM MOMENT ACTING ON FLANGE     Mo =  7.086E+005

                     - HUB AND FLANGE STRESSES -

            LONGITUDINAL          RADIAL          TANGENTIAL
OPERATING        Sh =  -2.05E+003  Sr =  8.097E+003  St =  1.334E+004
SEATING          Sh =  -2.00E+003  Sr =  7.868E+003  St =  1.297E+004
GREATER OF (Sh+Sr)/2 AND (Sh+St)/2     =  5.644E+003
MAX. ALLOW. STRESS  =  1.750E+004  MAX. COMPUTED STRESS =  5.644E+003
ALLOWABLE vs COMPUTED STRESS         S(allow.)/S(comp.) =  3.101E+000

   LOADED MODEL :  SEL1506
```

FIGURE 22: Wm1 & Wm2 vs M & Tpr from TurboFlange.

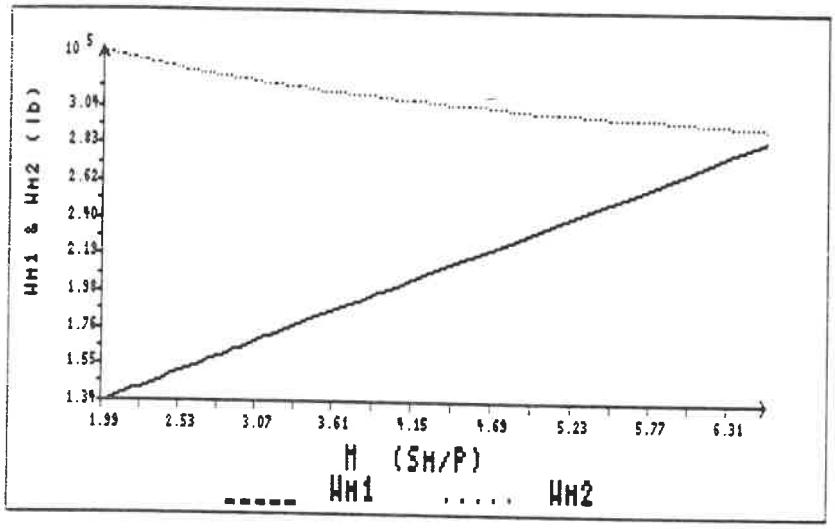

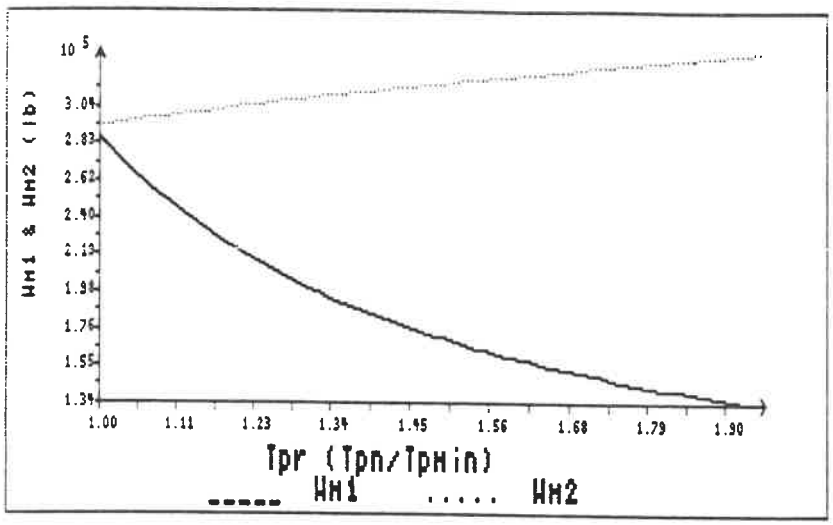

FIGURE 23: Wr1 & Wr2 vs M & Tpr from TurboFlange.

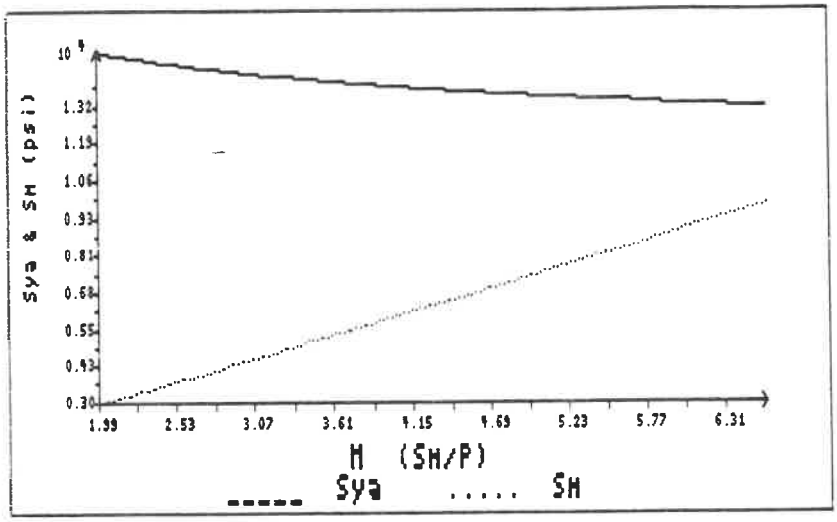

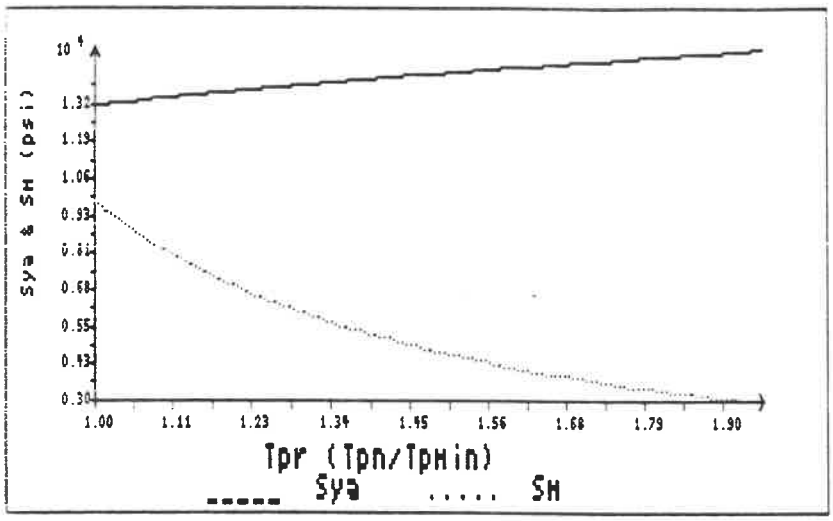

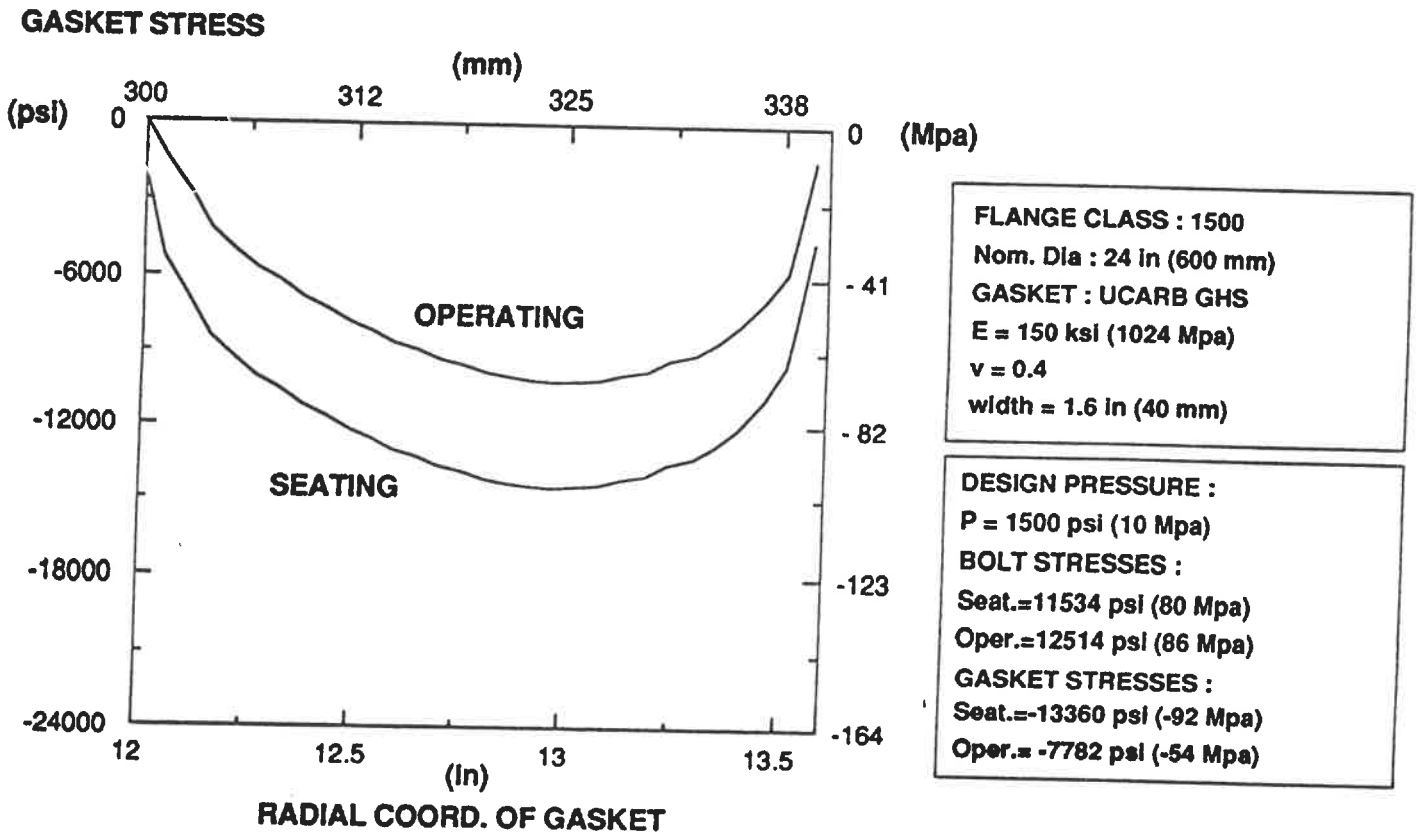

FIGURE 24 : Stress distribution for gasket GHS (ABAQUS)

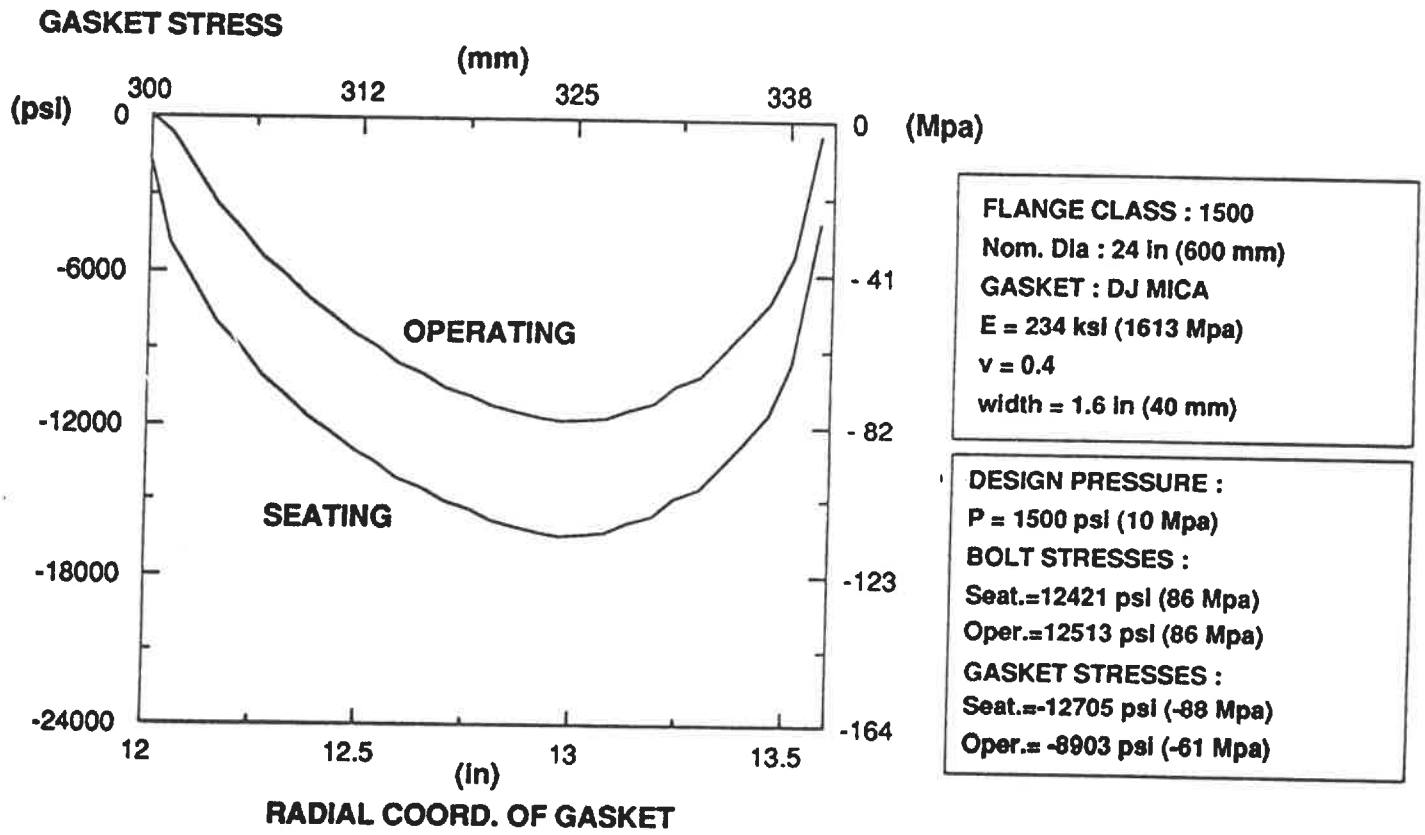

FIGURE 25 : Stress distribution for gasket DJ MICA (ABAQUS)

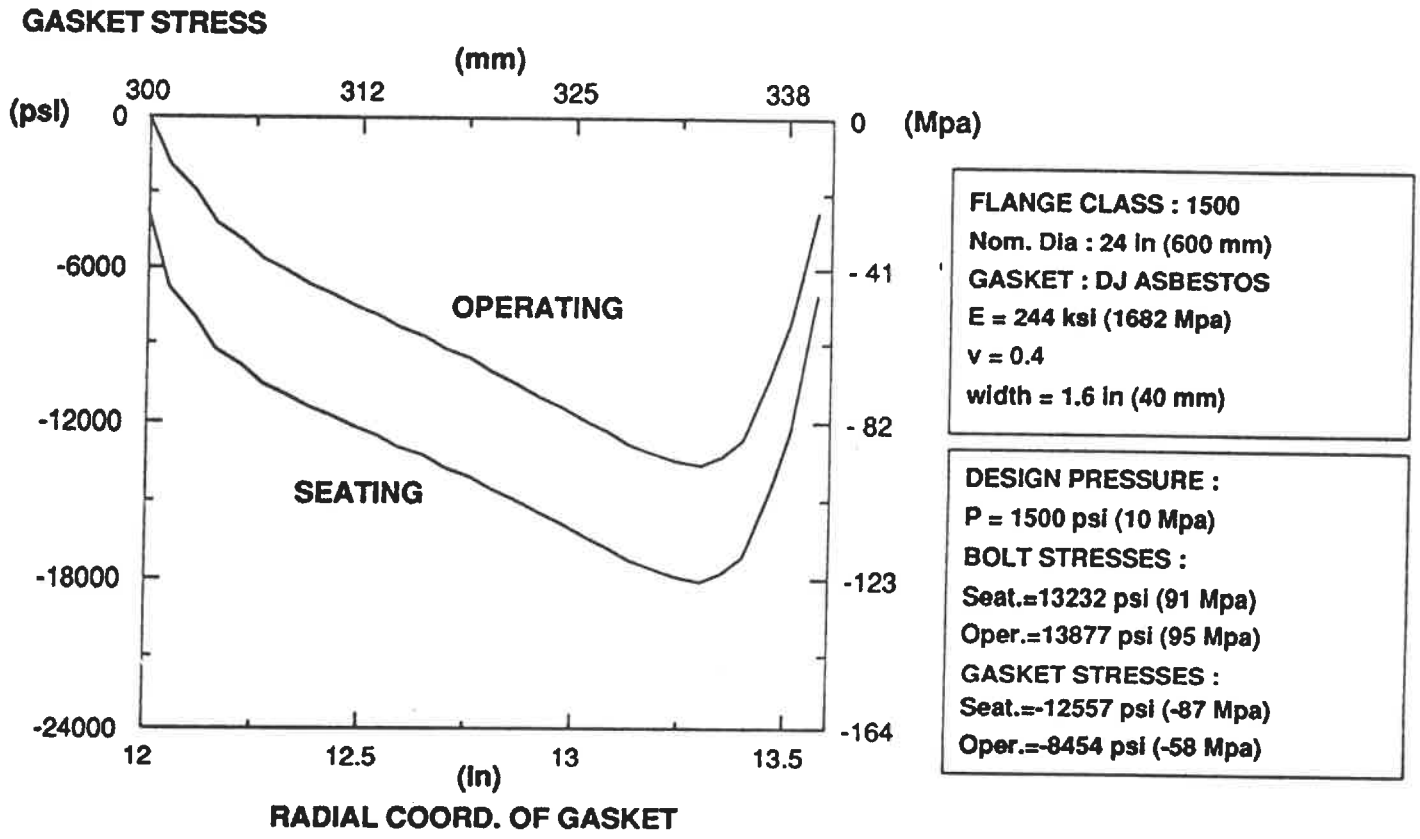

FIGURE 26 : Stress distribution for gasket DJ ASBESTOS (ABAQUS)

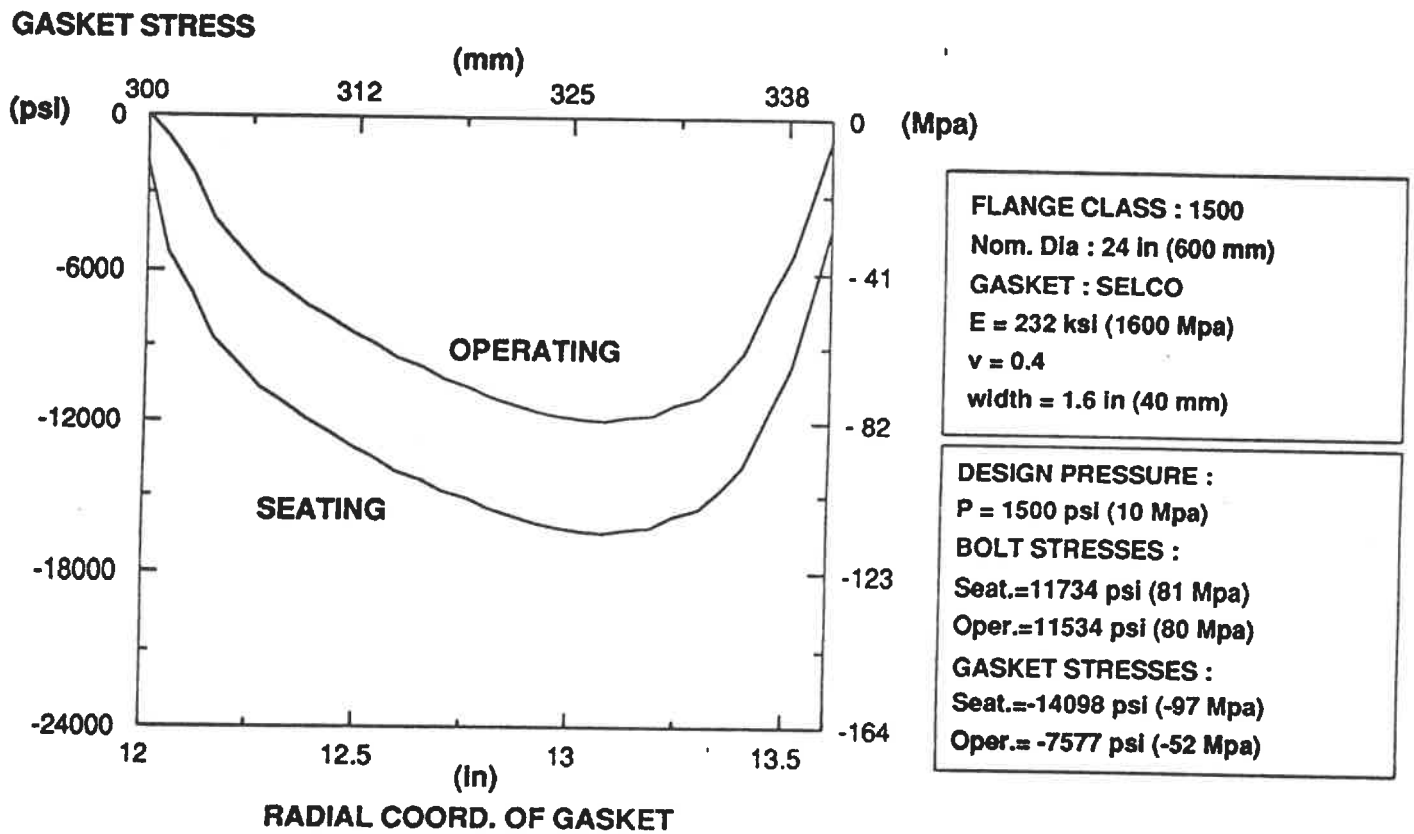

FIGURE 27 : Stress distribution for gasket SELCO (ABAQUS)

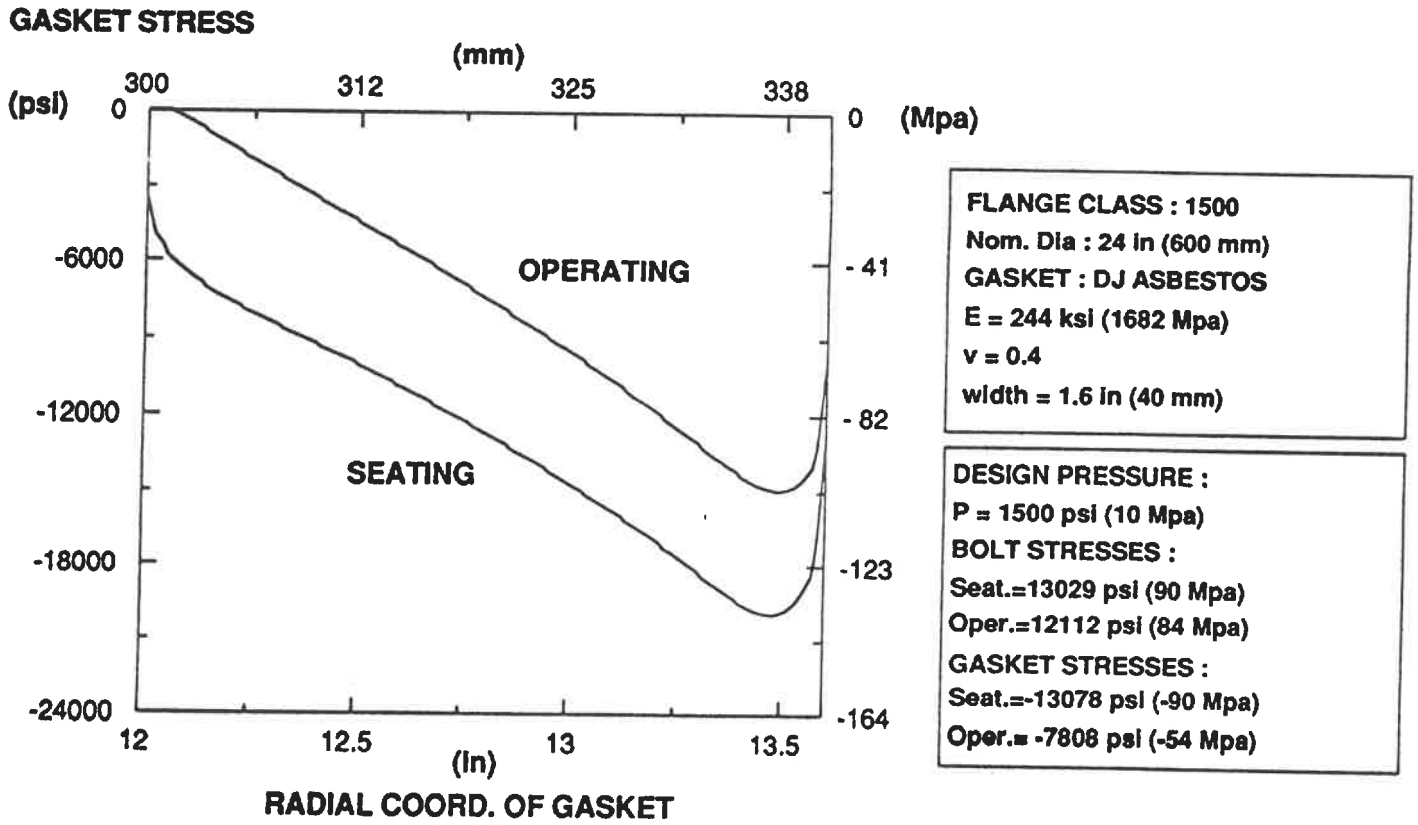

FIGURE 28 : Stress distribution for gasket DJ ASBESTOS (GIFTS)

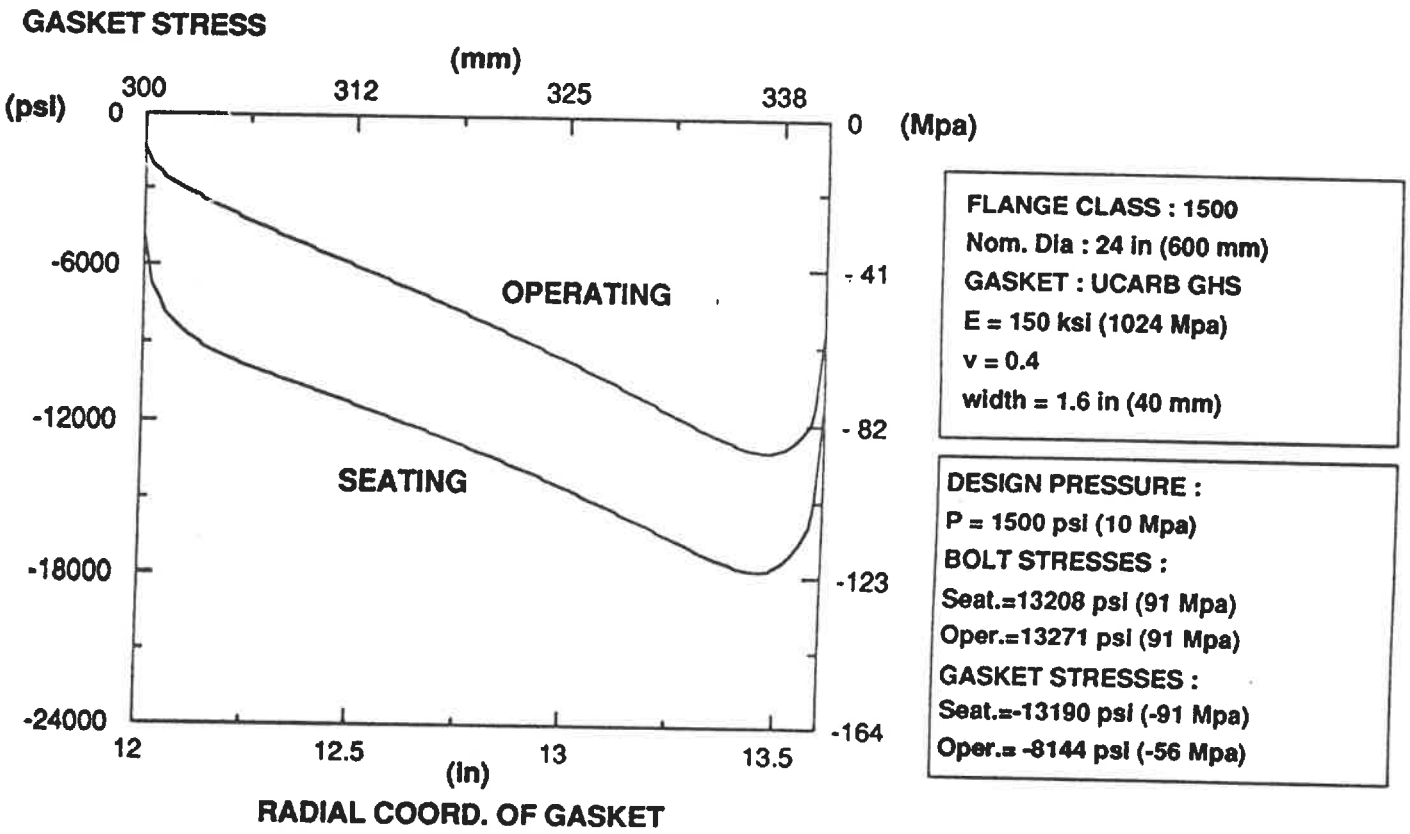

FIGURE 29 : Stress distribution for gasket GHS (GIFTS)

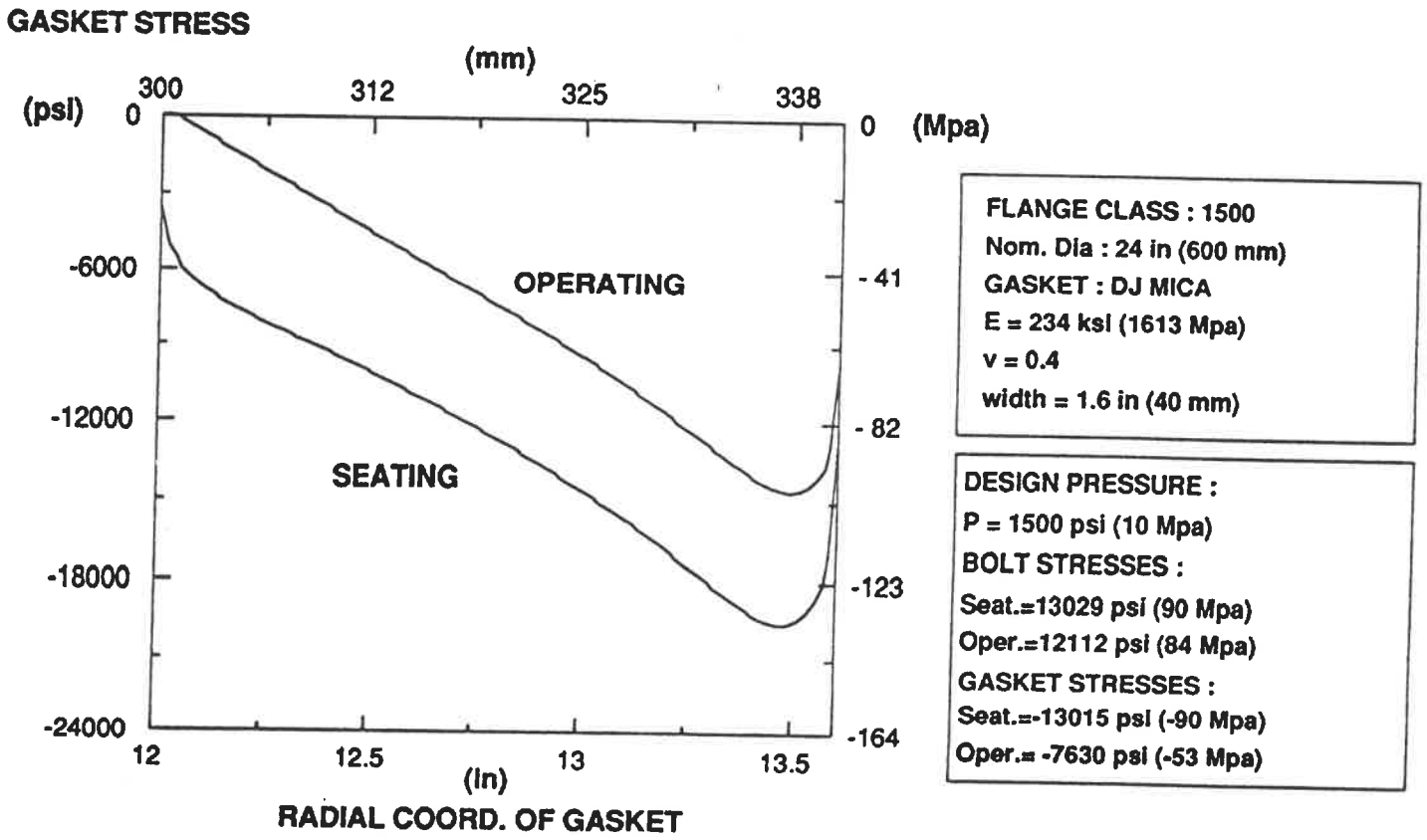

FIGURE 30 : Stress distribution for gasket DJ MICA (GIFTS)

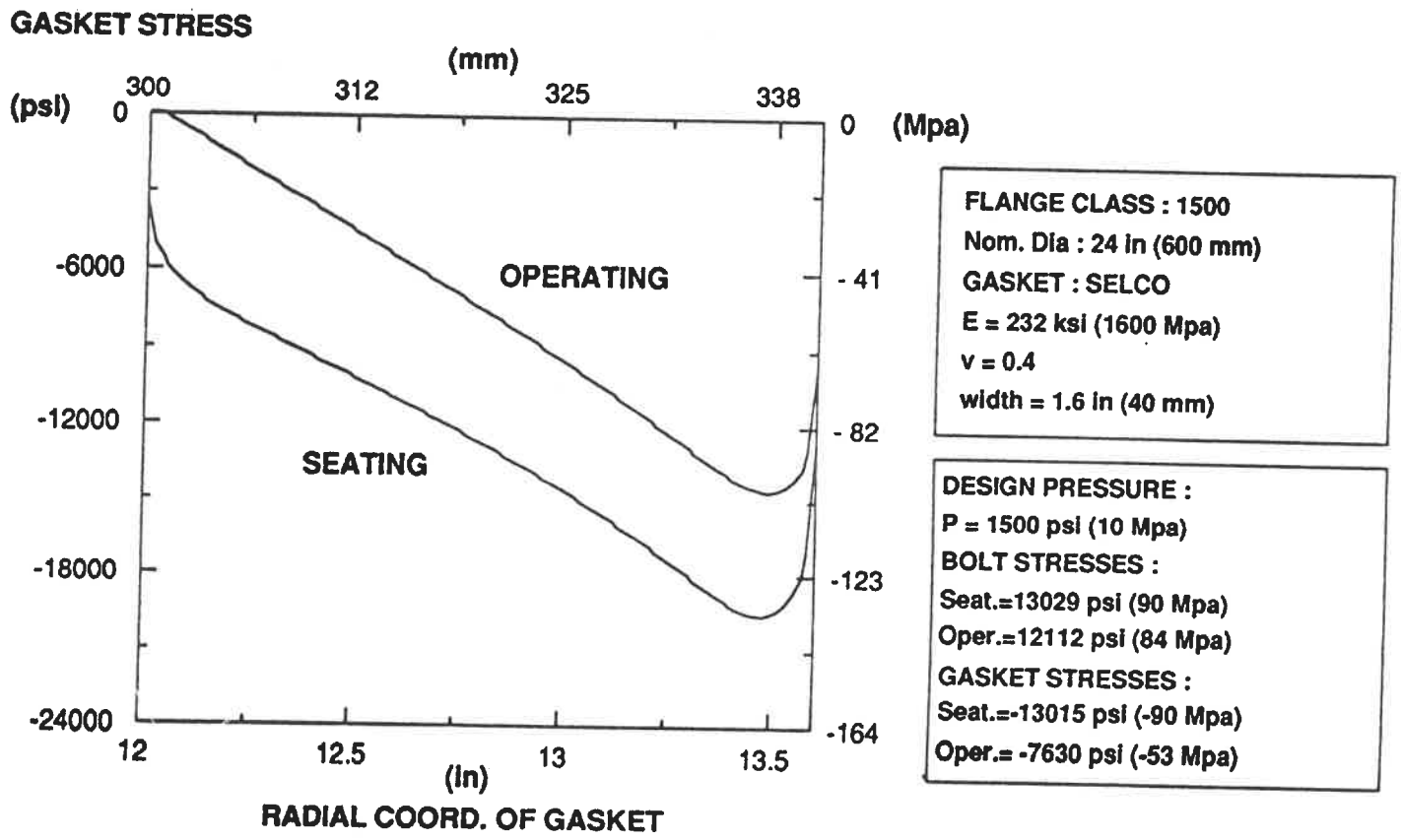

FIGURE 31 : Stress distribution for gasket SELCO (GIFTS)

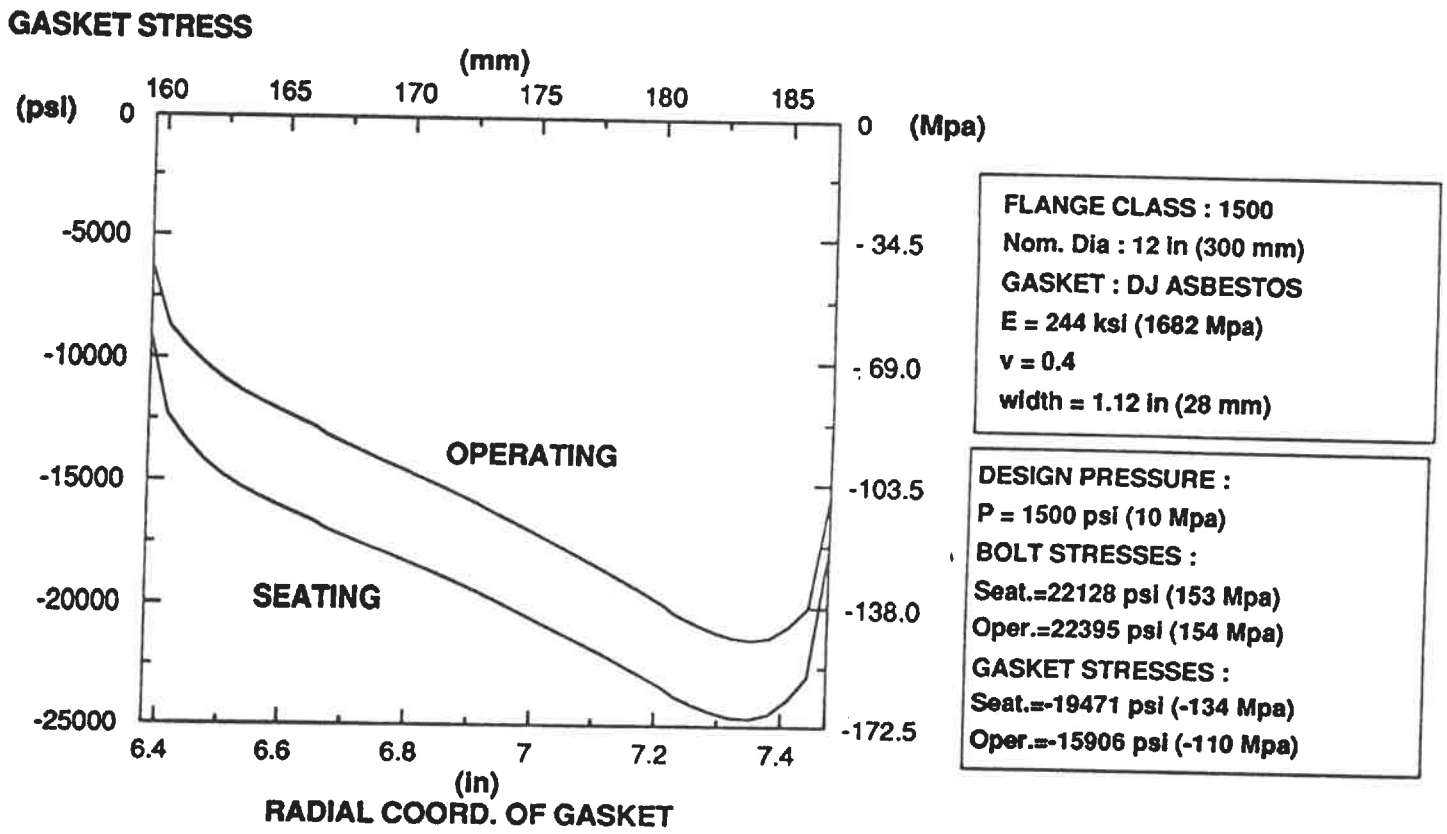

FIGURE 32 : Stress distribution for gasket DJ ASBESTOS (GIFTS)

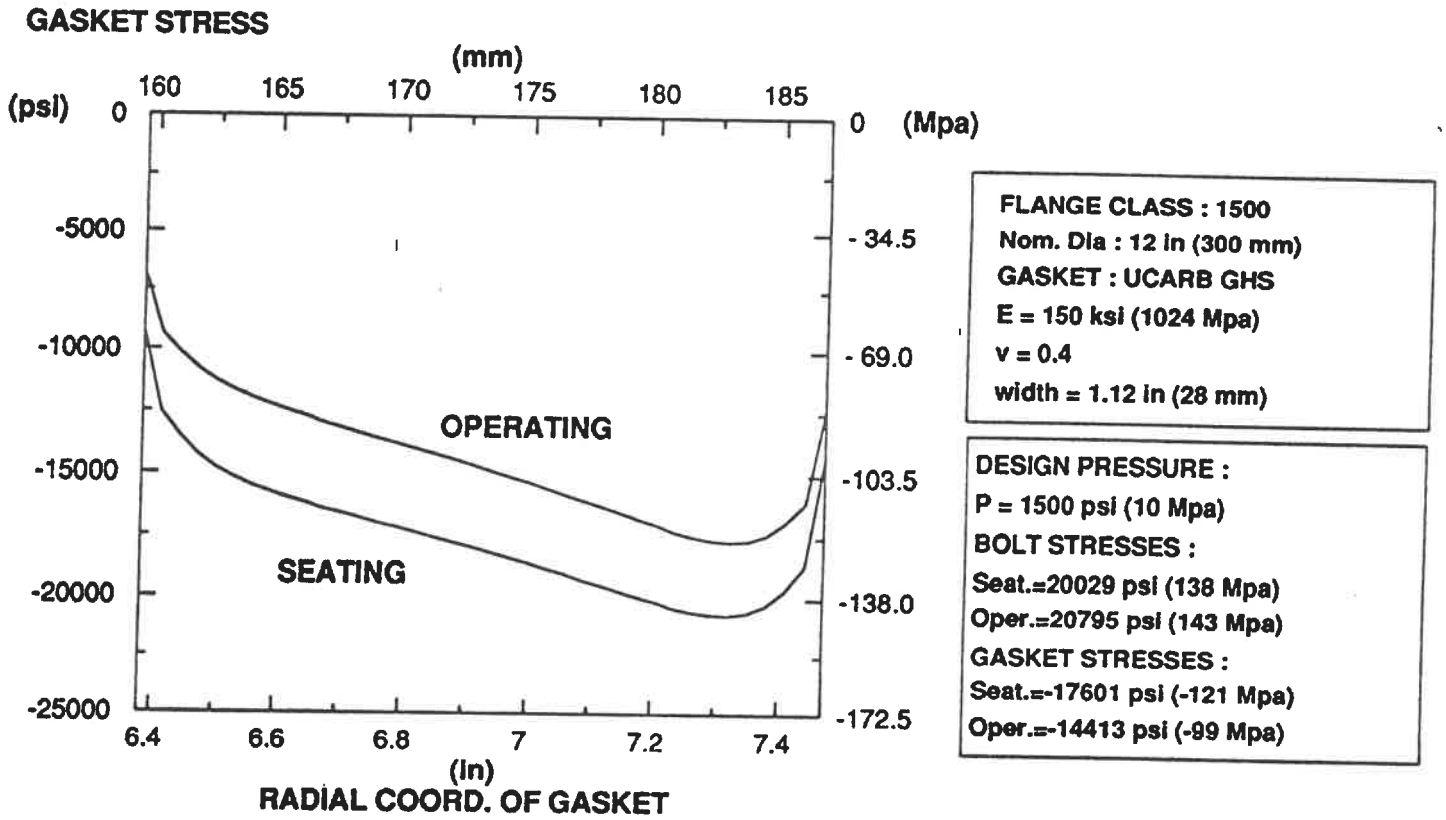

FIGURE 33 : Stress distribution for gasket GHS (GIFTS)

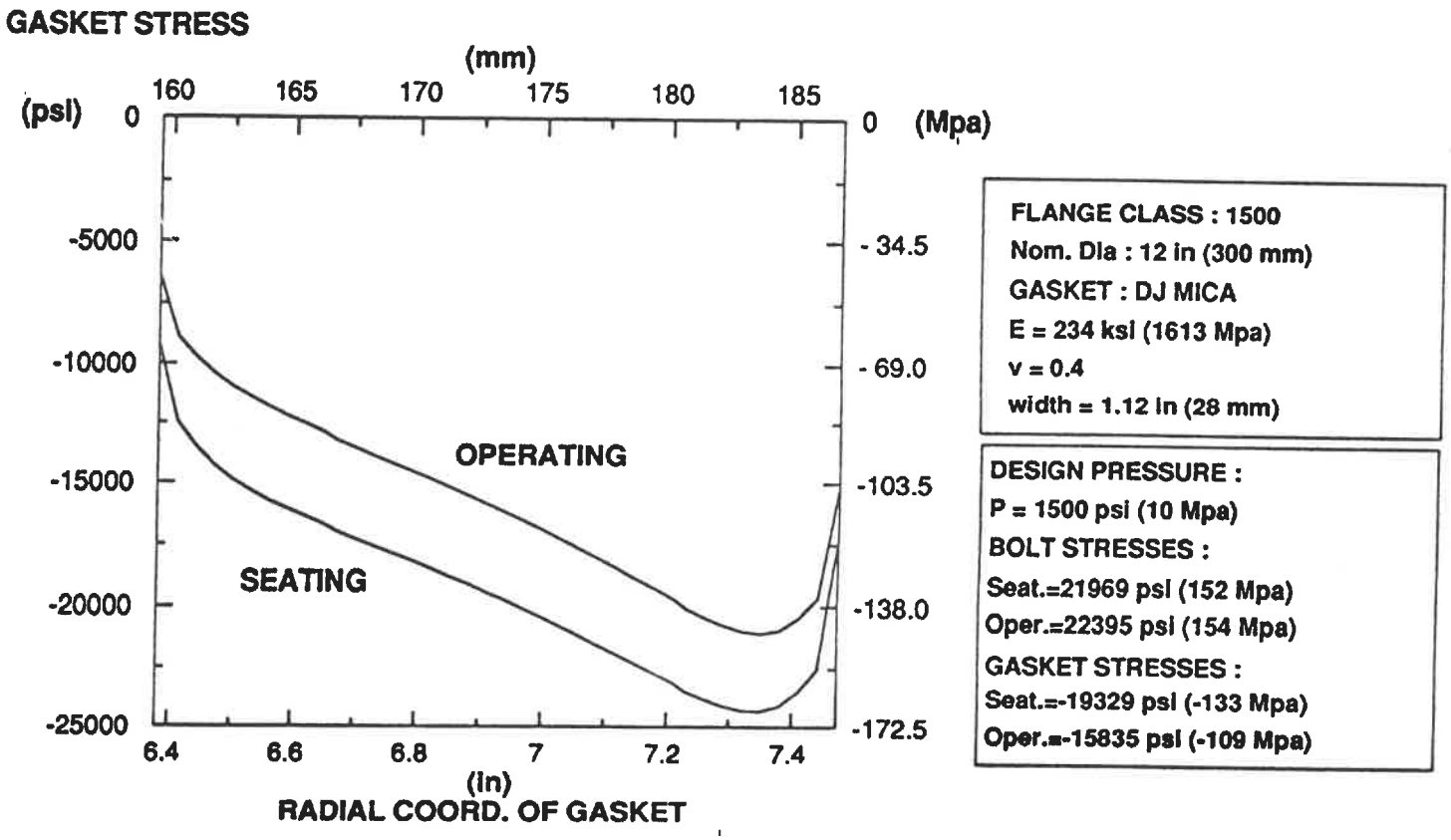

FIGURE 34 : Stress distribution for gasket DJ MICA (GIFTS)

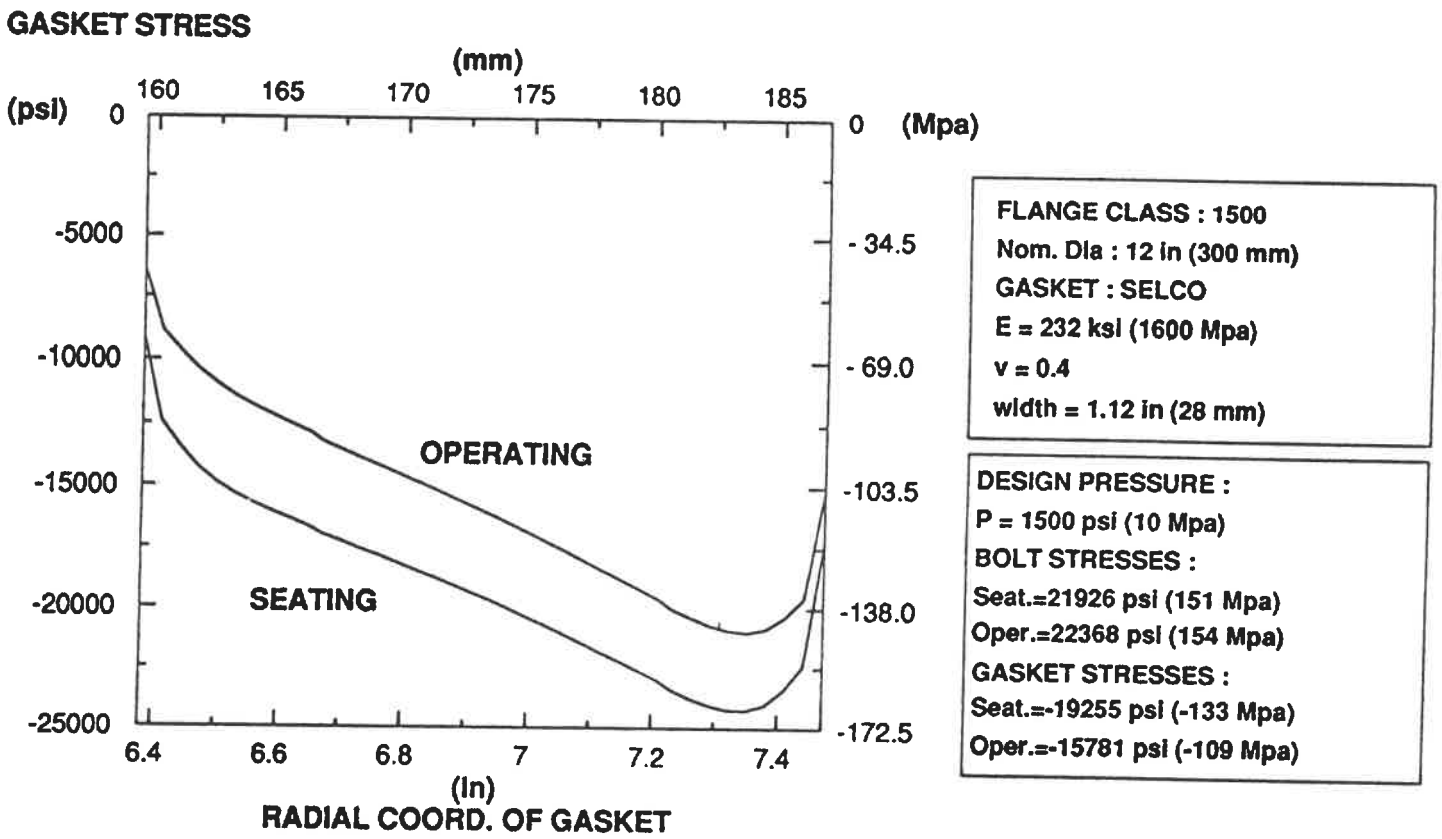

FIGURE 35 : Stress distribution for gasket SELCO (GIFTS)

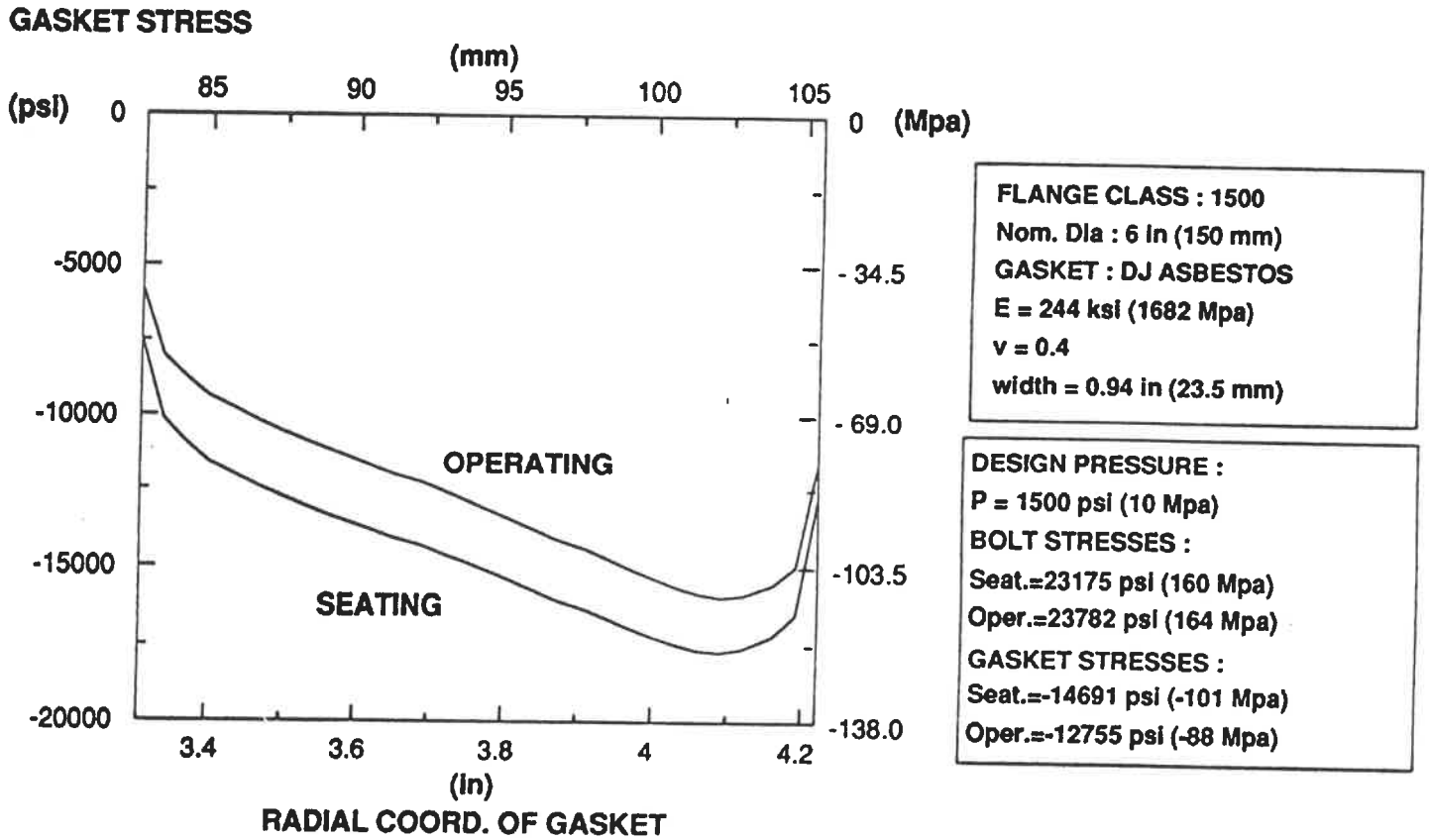

FIGURE 36 : Stress distribution for gasket DJ ASBESTOS (GIFTS)

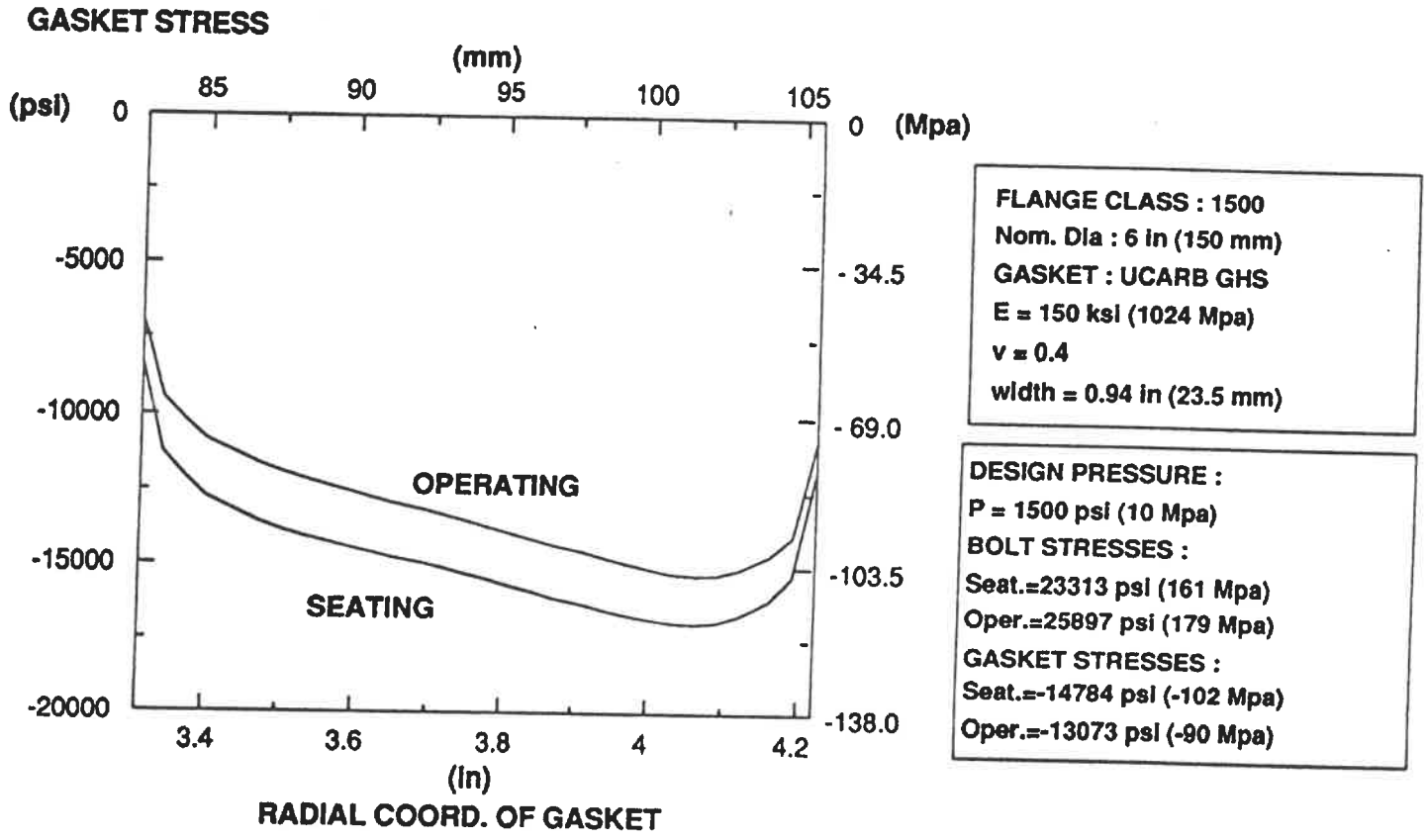

FIGURE 37 : Stress distribution for gasket GHS (GIFTS)

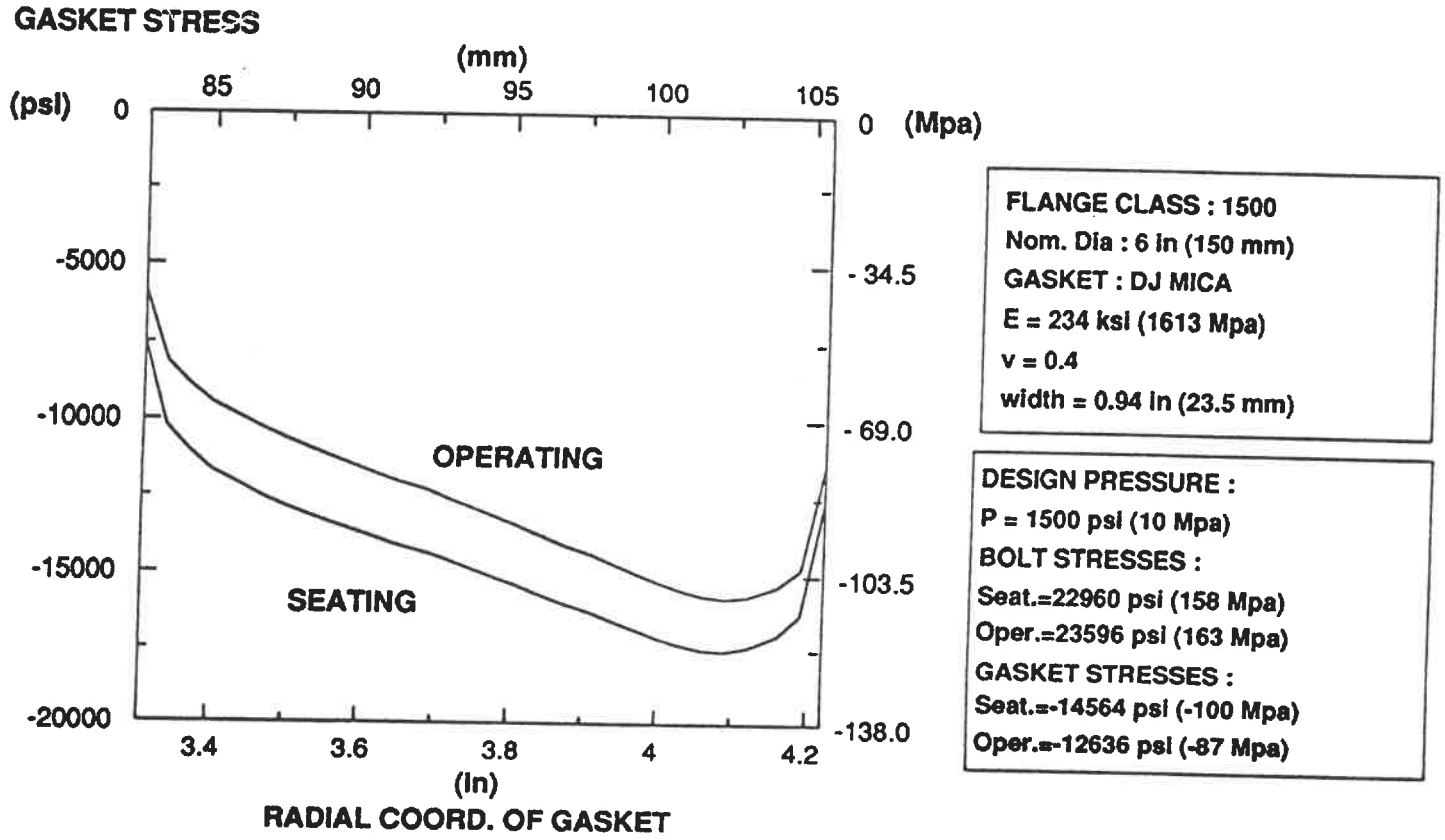

FIGURE 38 : Stress distribution for gasket DJ MICA (GIFTS)

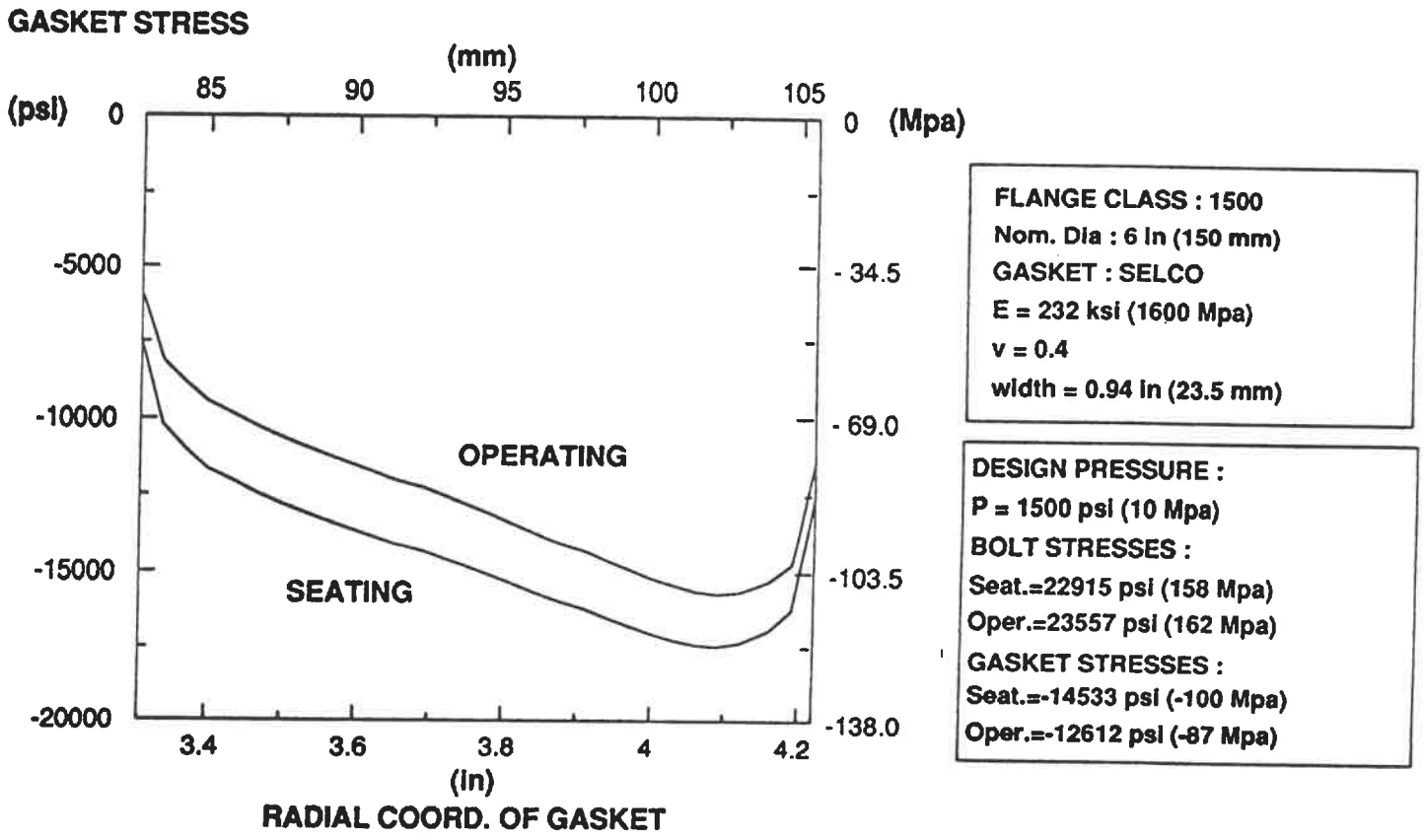

FIGURE 39 : Stress distribution for gasket SELCO (GIFTS)

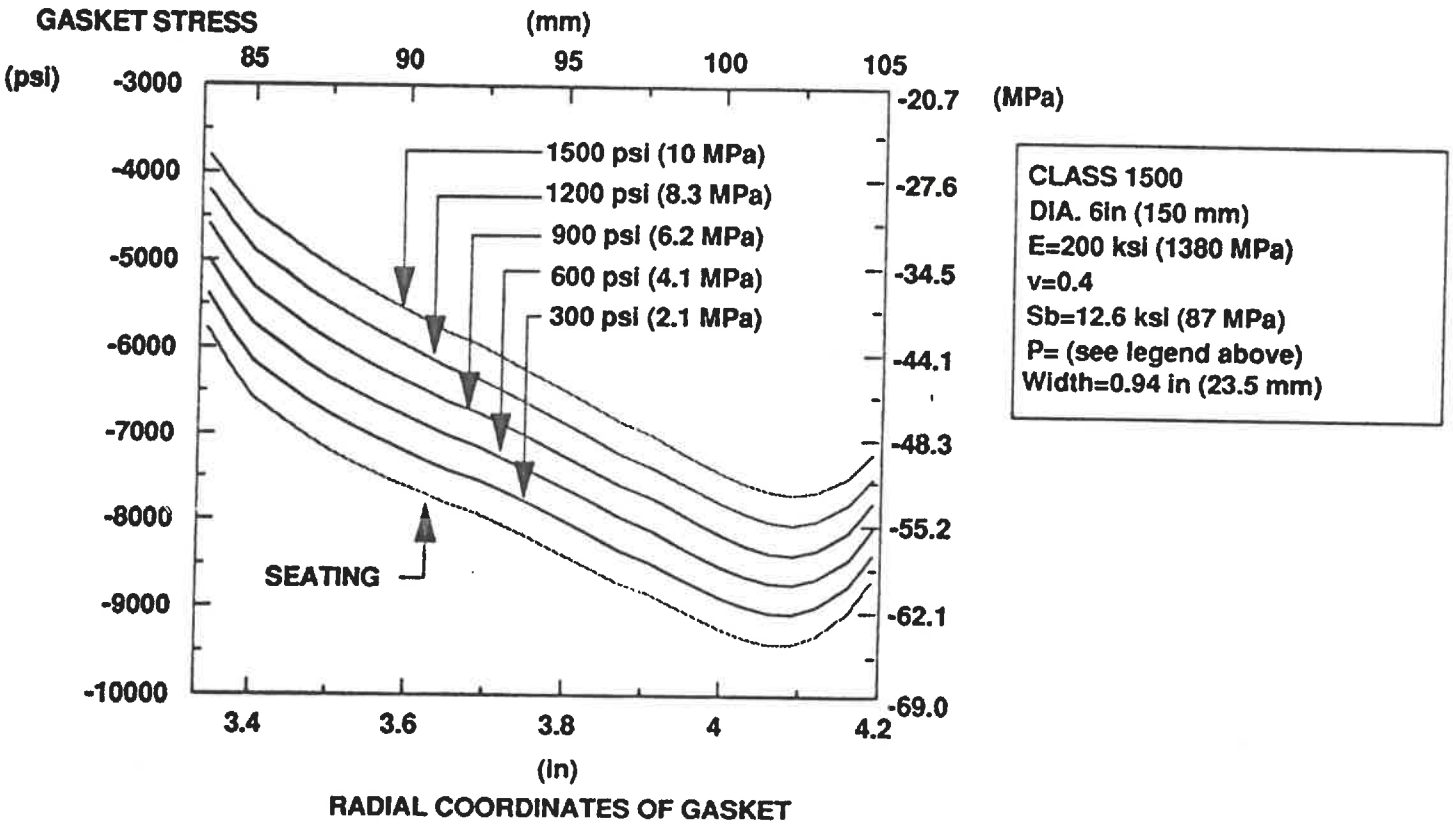

FIGURE 40 : Effect of Design Pressure on the Gasket Stress Dist.

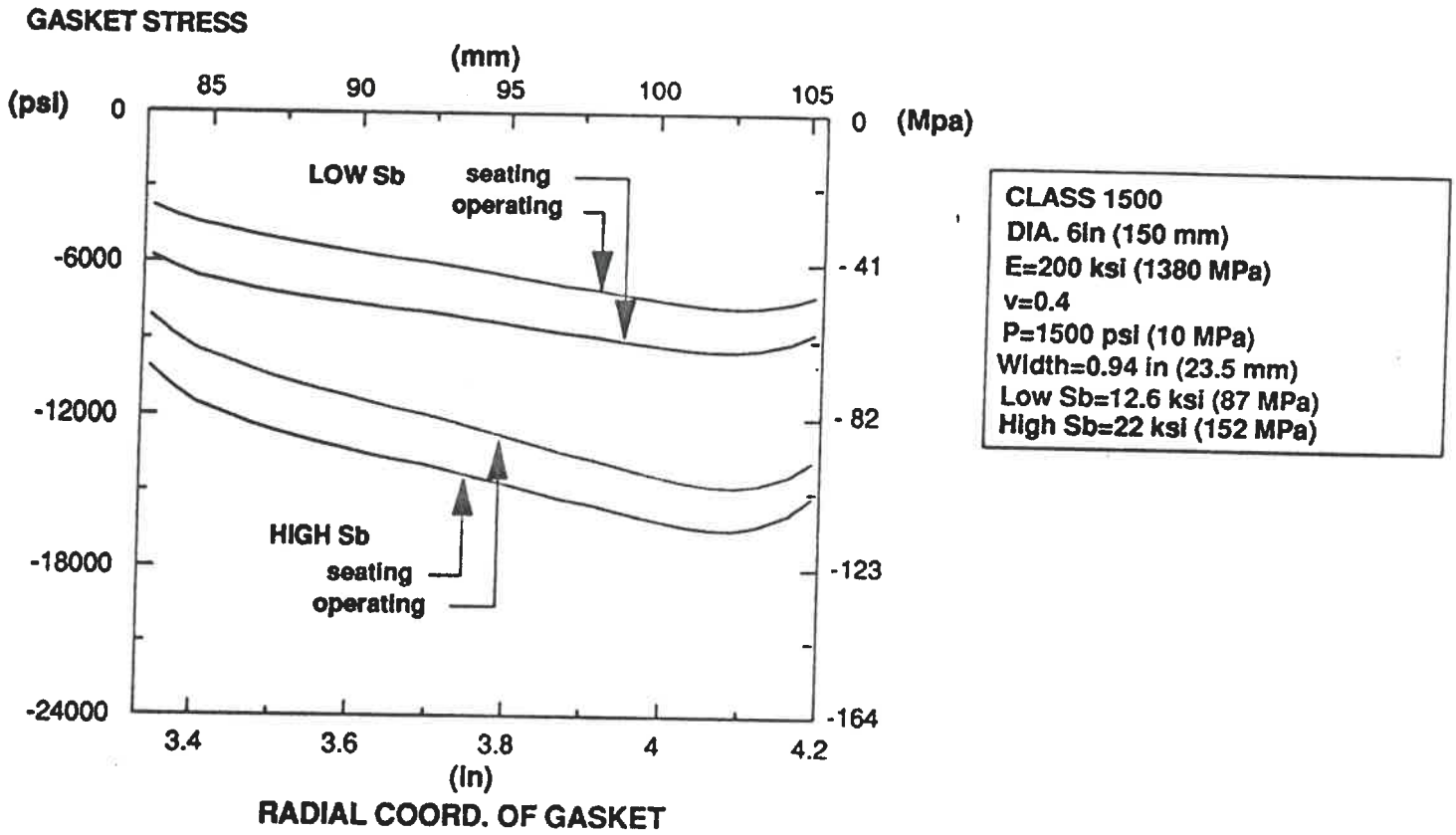

FIGURE 41 : Effect of Bolt Stress on the Gasket Stress Dist. (Class 1500-6)

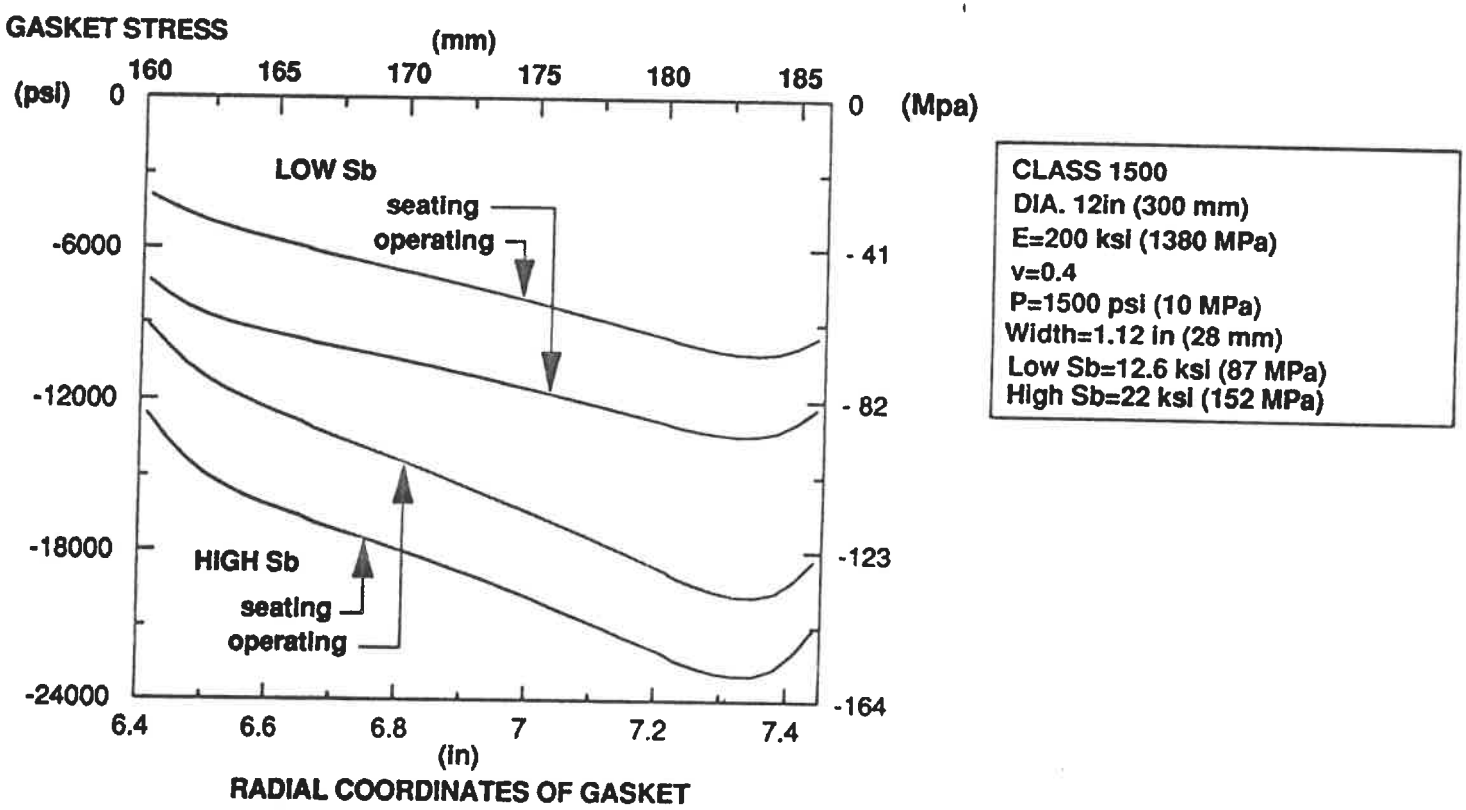

FIGURE 42 : Effect of Bolt Stress on the Gasket Stress Dist. (Class 1500-12)

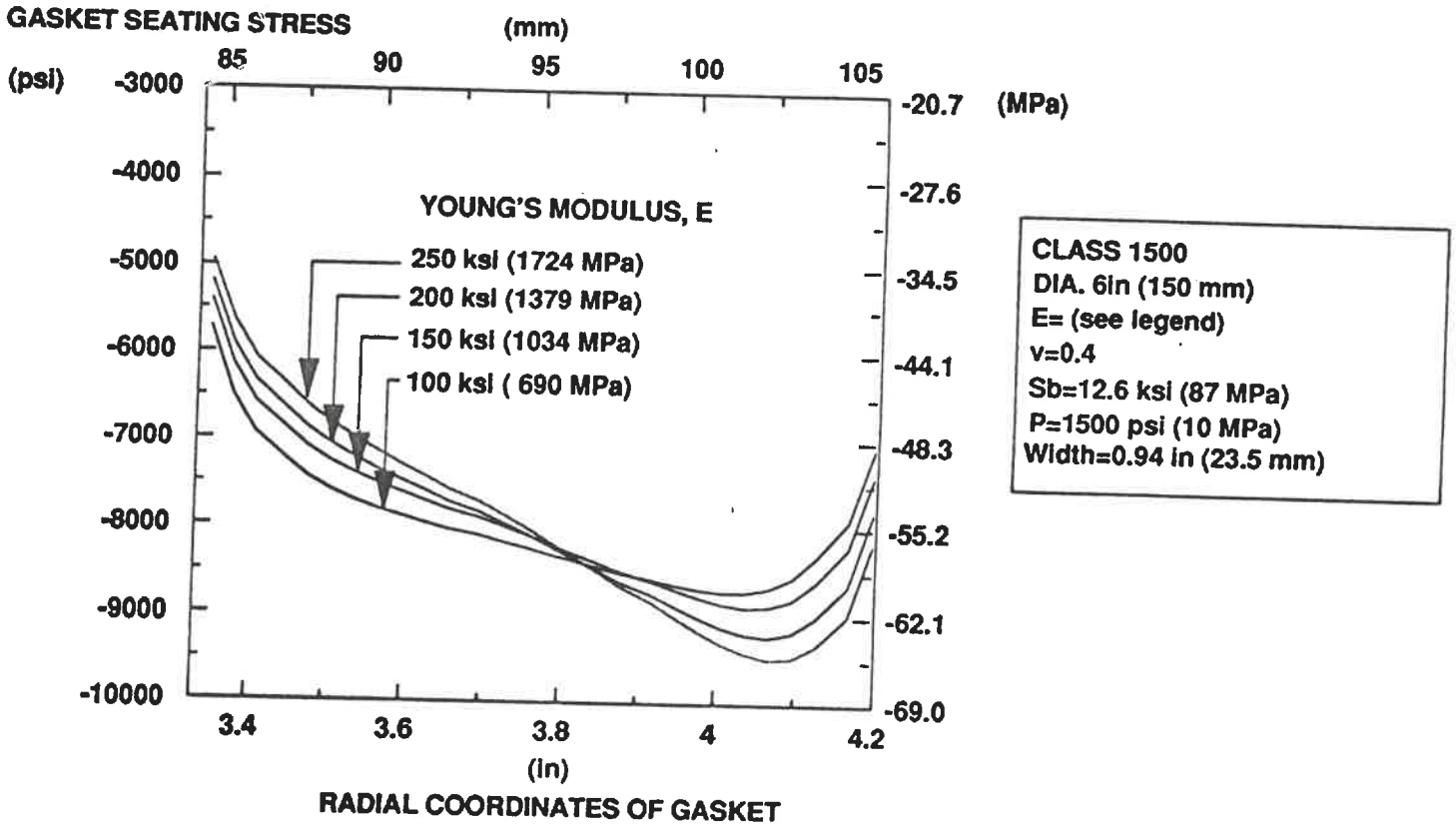

FIGURE 43 : Effect of Young's Modulus on the Gasket Stress Dist.
(SEATING CONDITION)

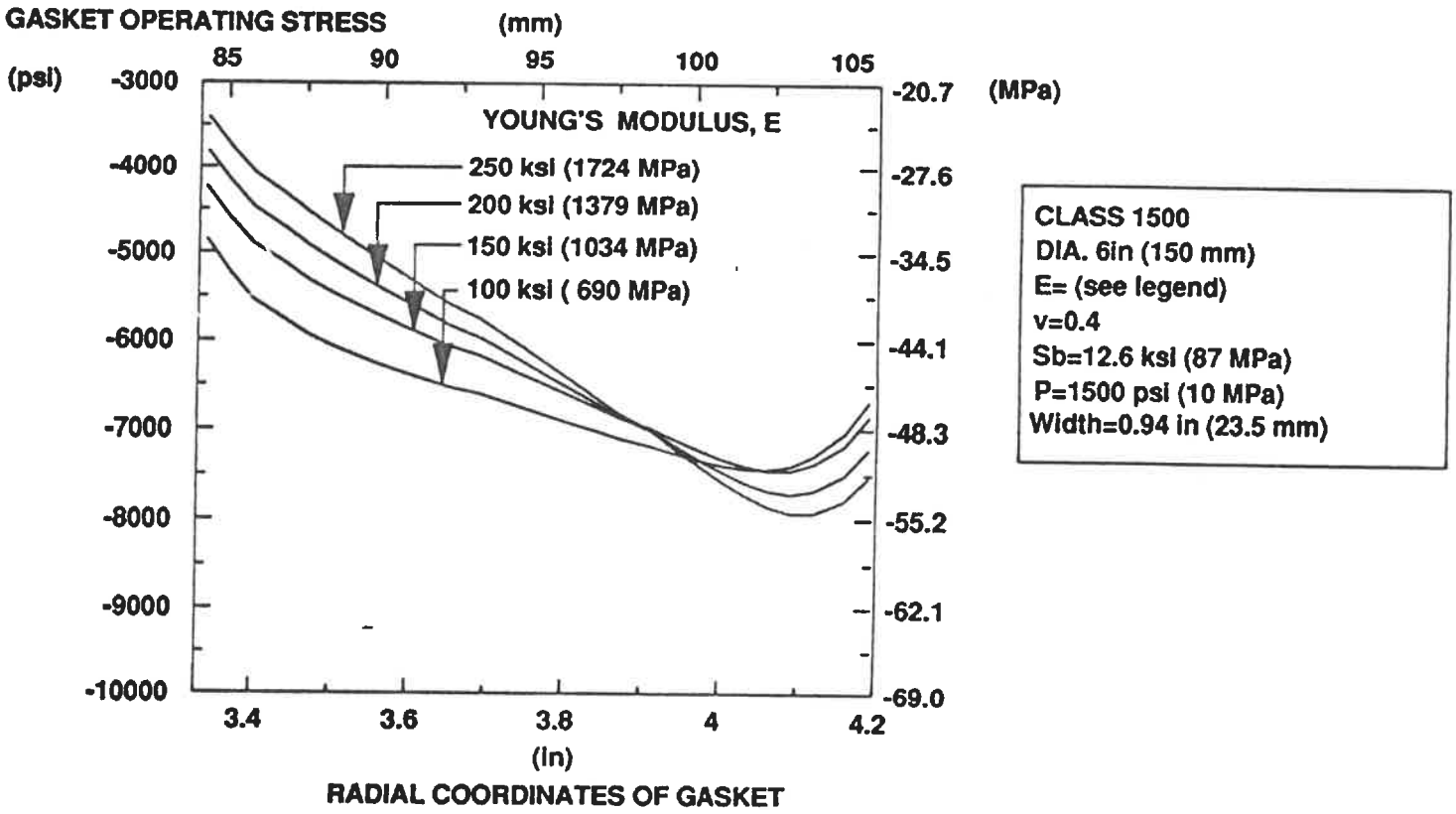

FIGURE 44 : Effect of Young's Modulus on the Gasket Stress Dist.
(OPERATING CONDITION)

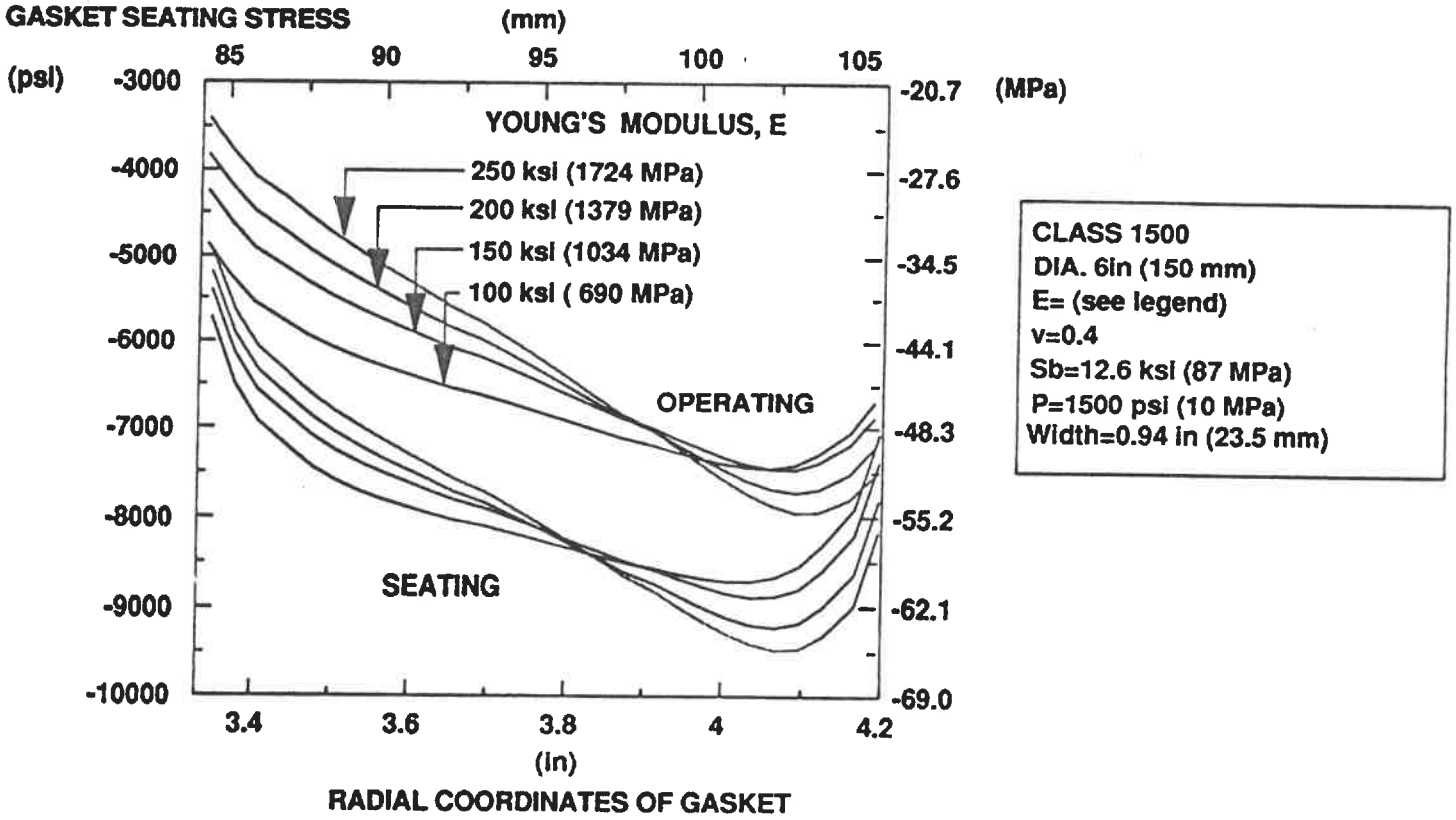

FIGURE 45 : Effect of Young's Modulus on the Gasket Stress Dist. (SEATING AND OPERATING CONDITION)

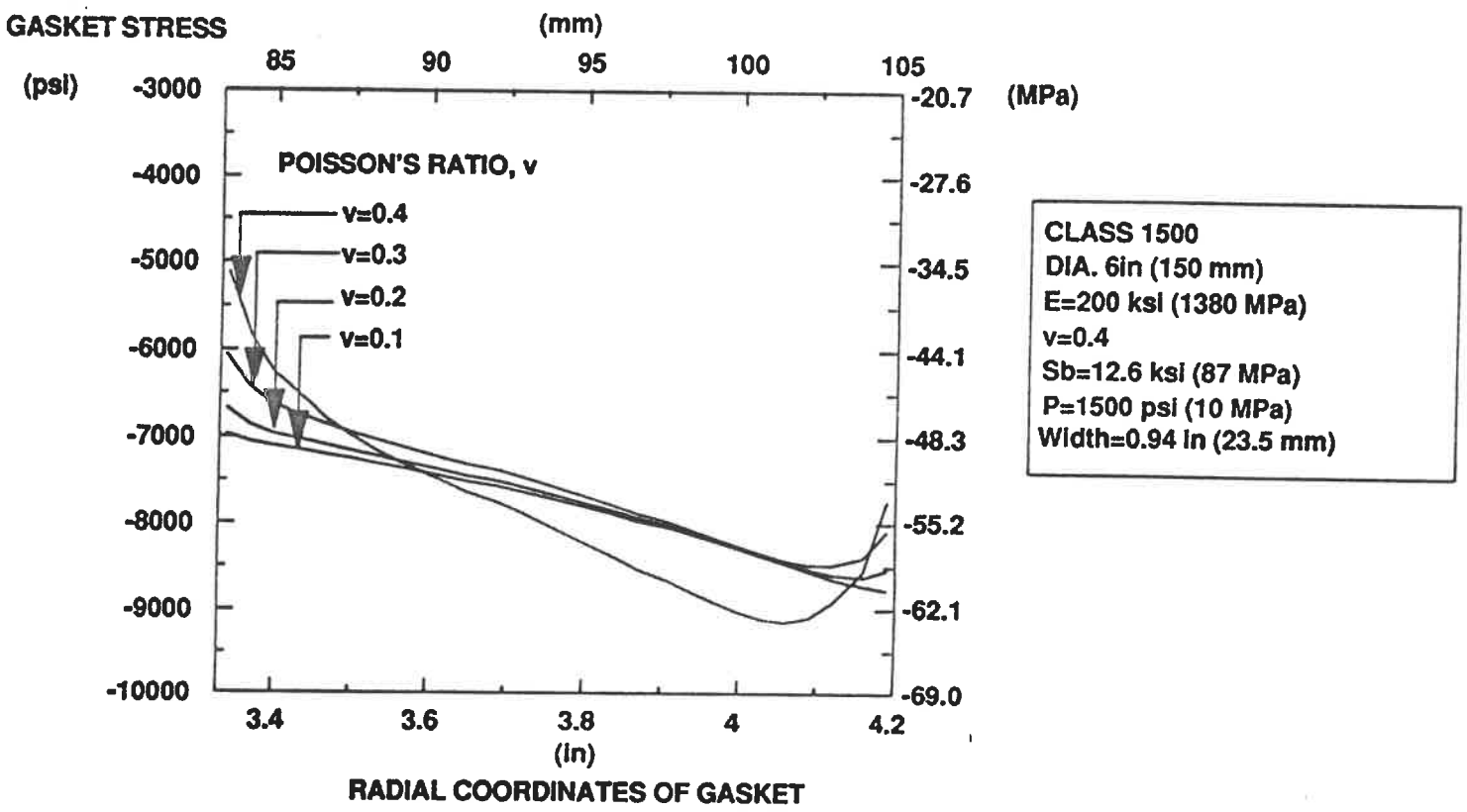

FIGURE 46 : Effect of Poisson's Ratio on the Gasket Stress Dist.
(SEATING CONDITION)

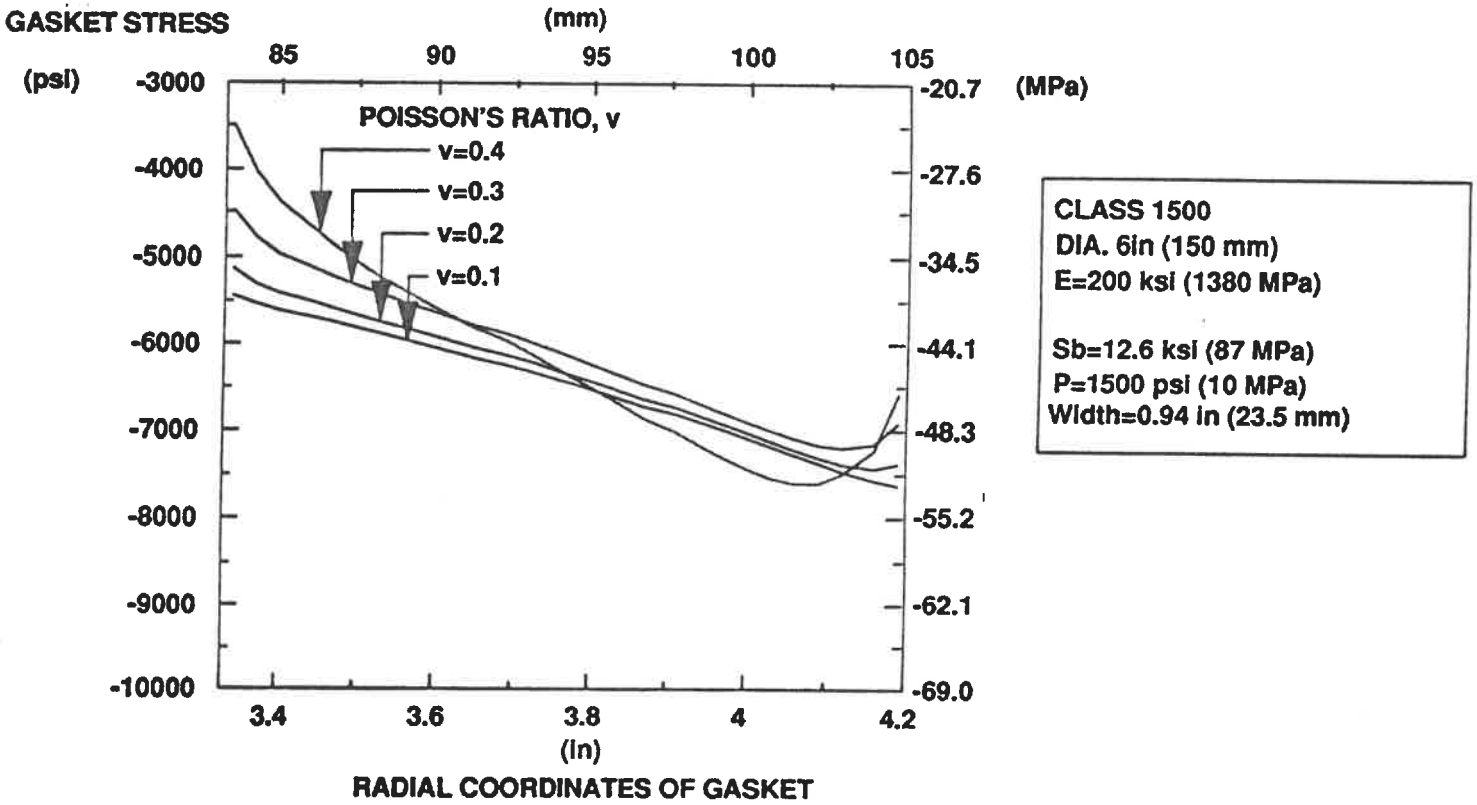

FIGURE 47 : Effect of Poisson's Ratio on the Gasket Stress Dist. (OPERATING CONDITION)

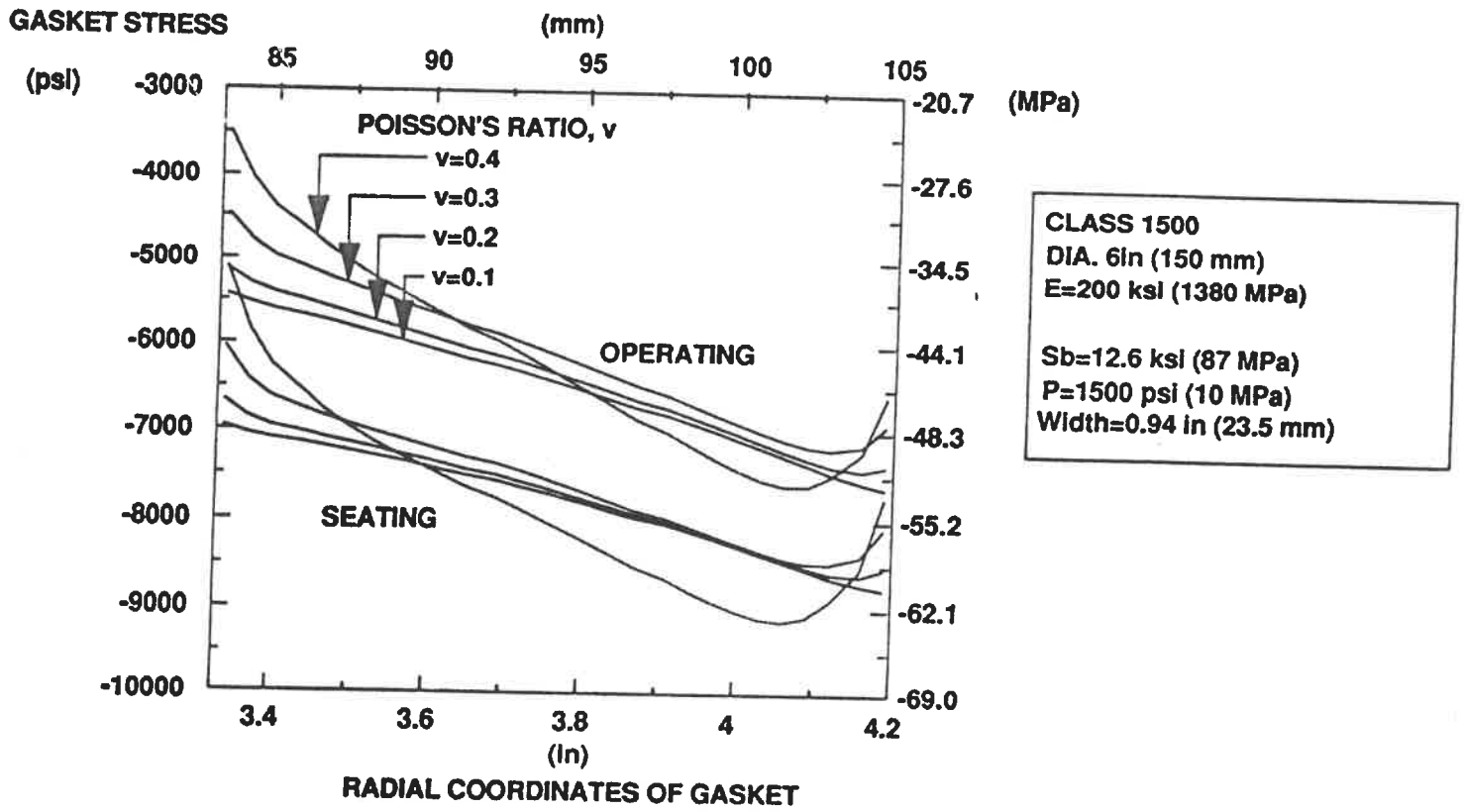

FIGURE 48 : Effect of Poisson's Ratio on the Gasket Stress Dist.
(OPERATING & SEATING CONDITION)

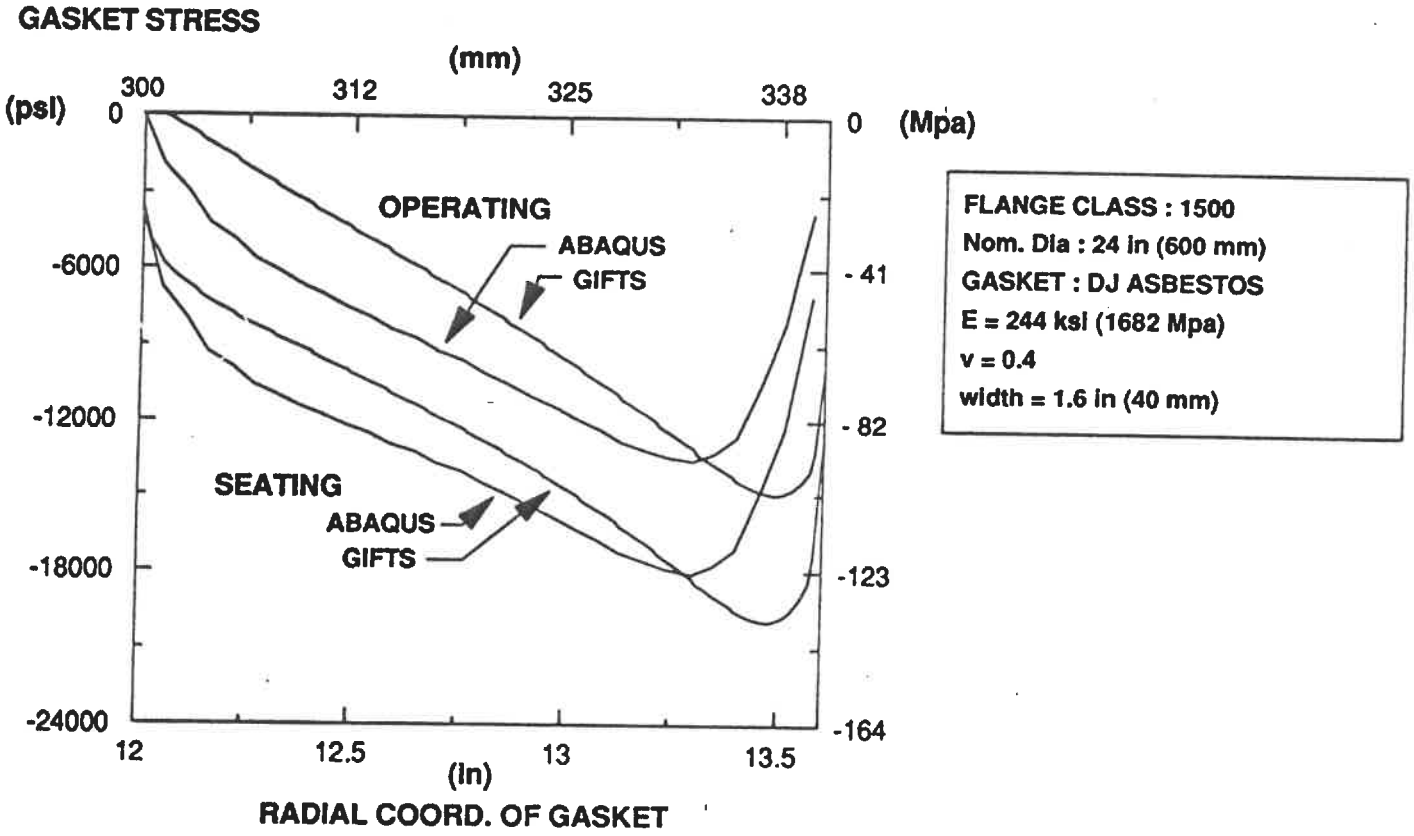

FIGURE 49 : Stress distribution for gasket DJ ASBESTOS (ABAQUS & GIFTS)

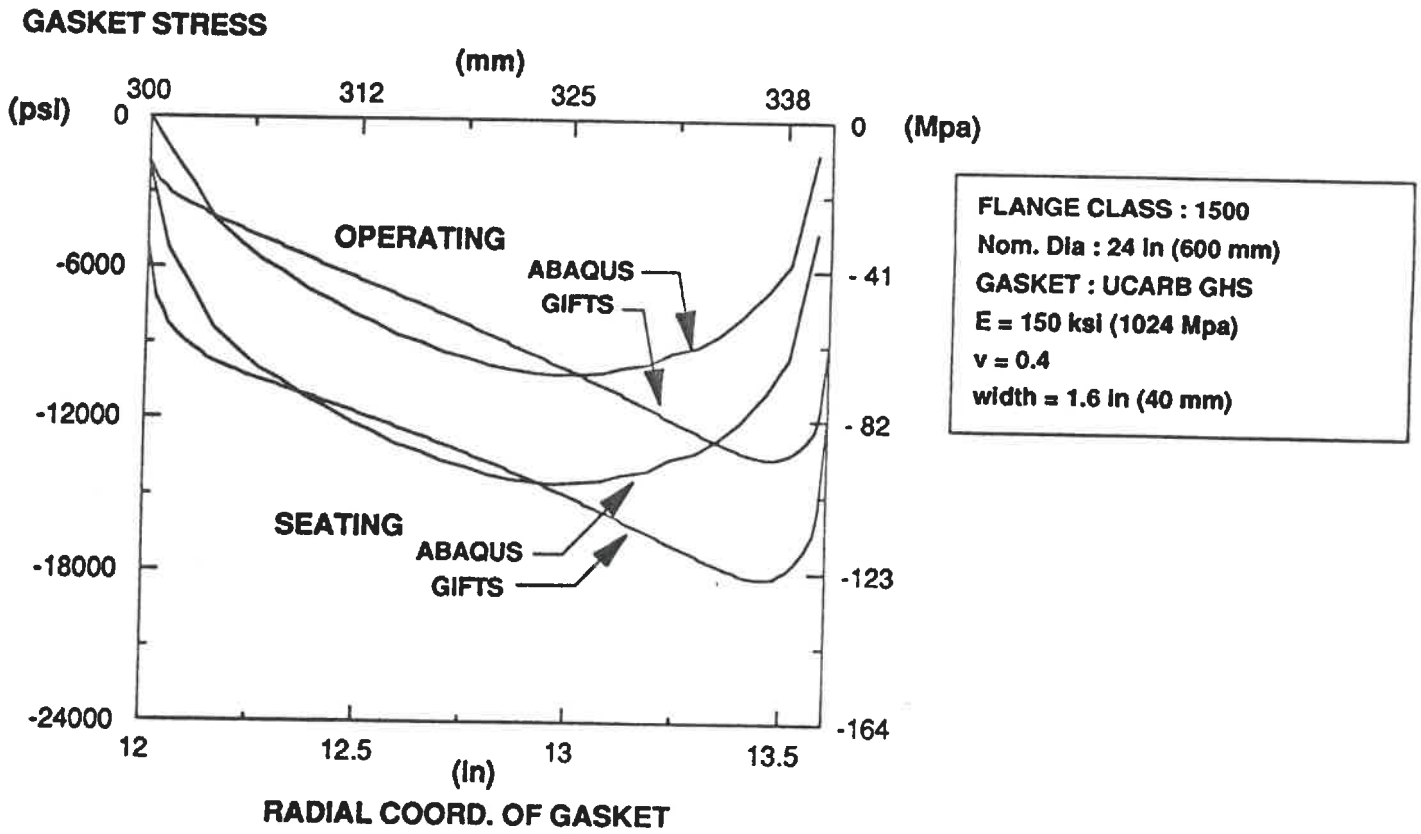

FIGURE 50 : Stress distribution for GHS gasket (ABAQUS & GIFTS)

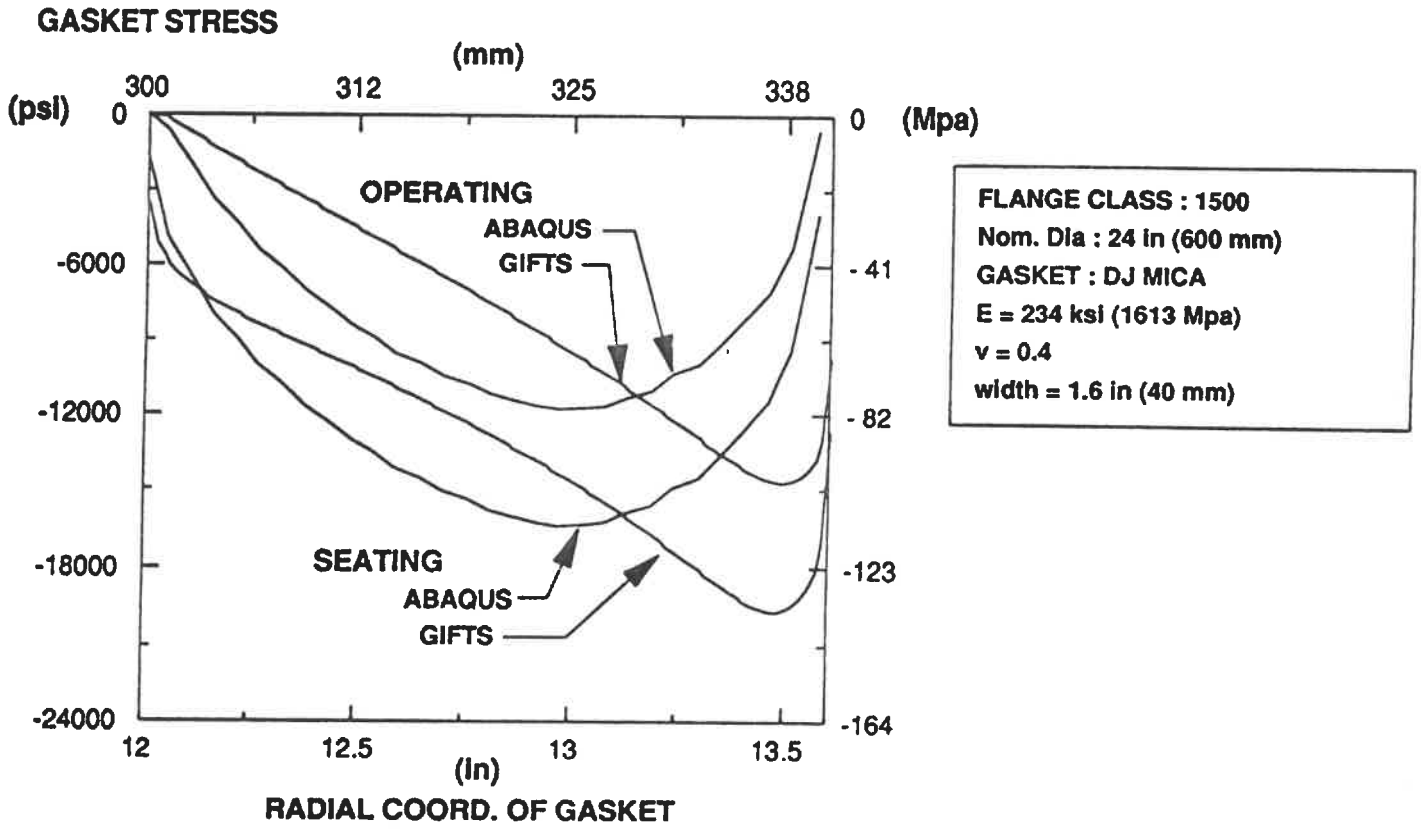

FIGURE 51 : Stress distribution for gasket DJ MICA (ABAQUS & GIFTS)

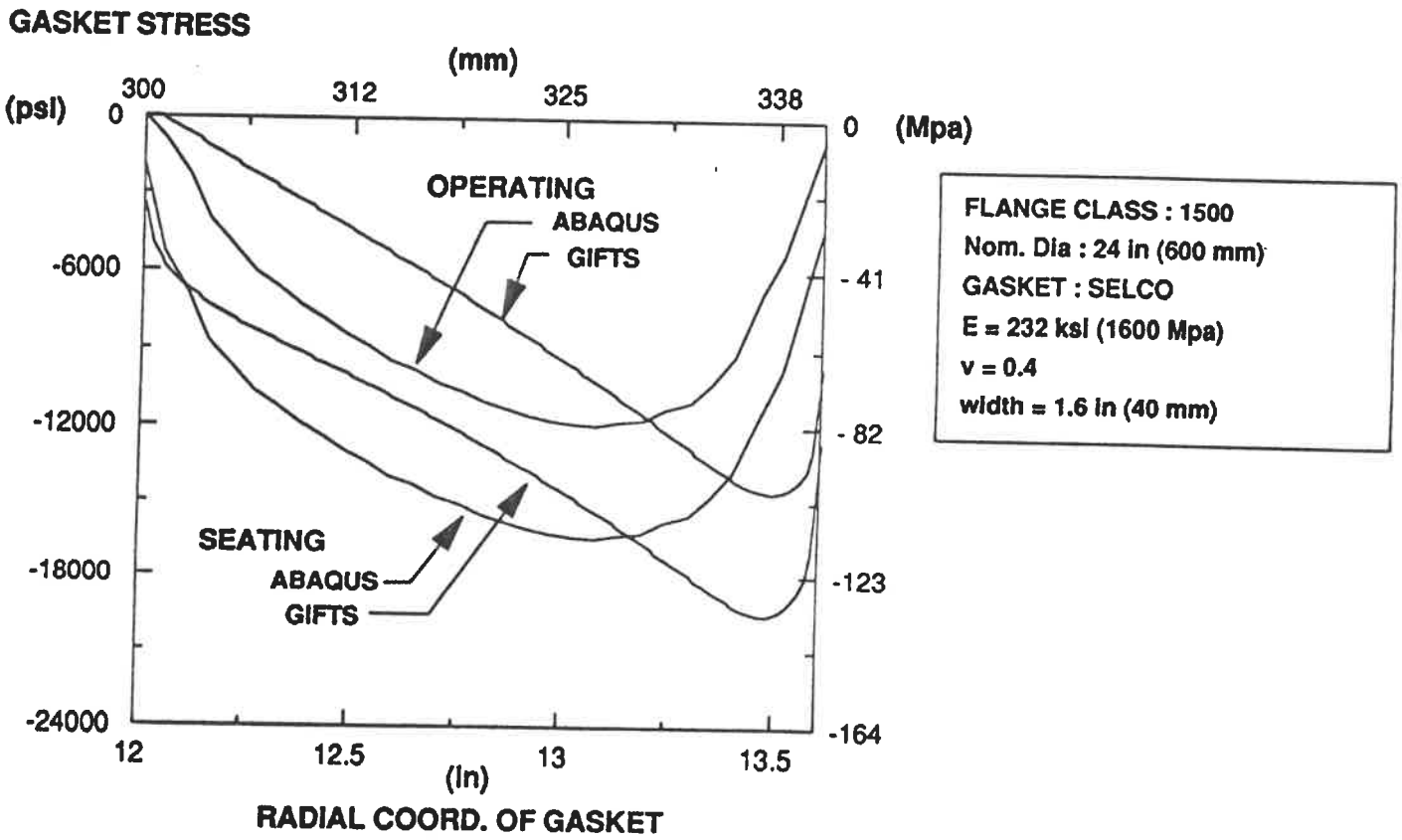

FIGURE 52 : Stress distribution for gasket SELCO (ABAQUS & GIFTS)

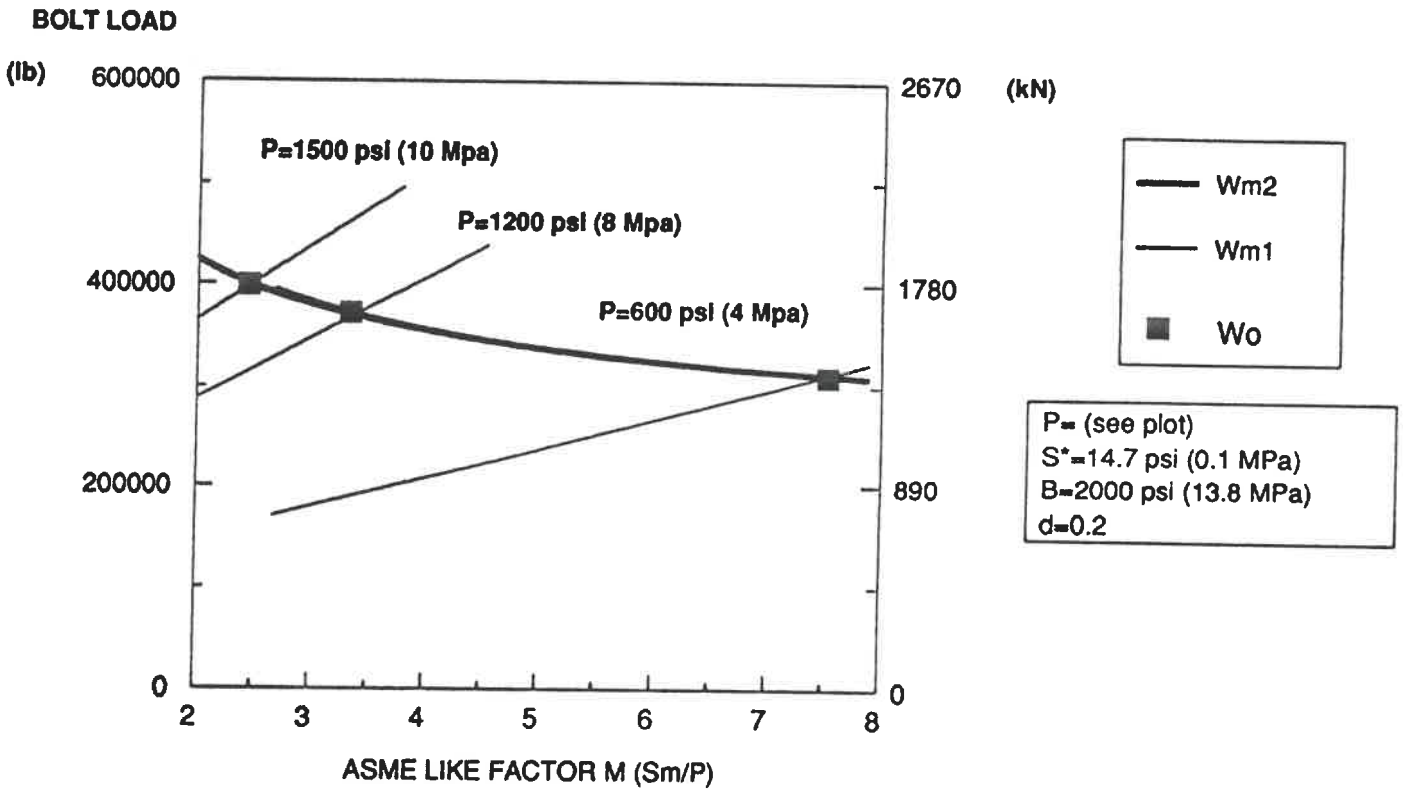

FIGURE 53 : Design bolt loads Wm1 & Wm2 vs factor M

(Effect of Pressure)

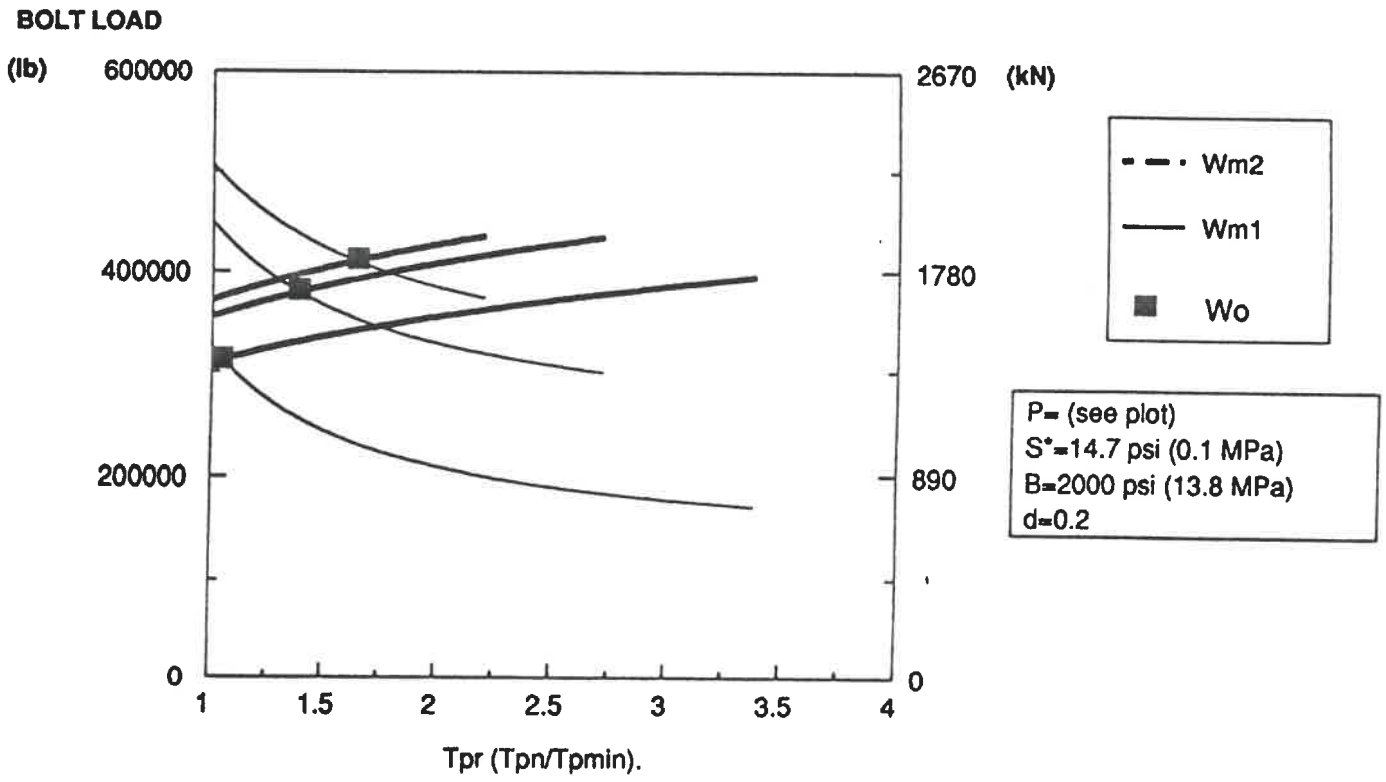

FIGURE 54 : Design bolt loads Wm1 & Wm2 vs tightness ratio Tpr
(Effect of Pressure)

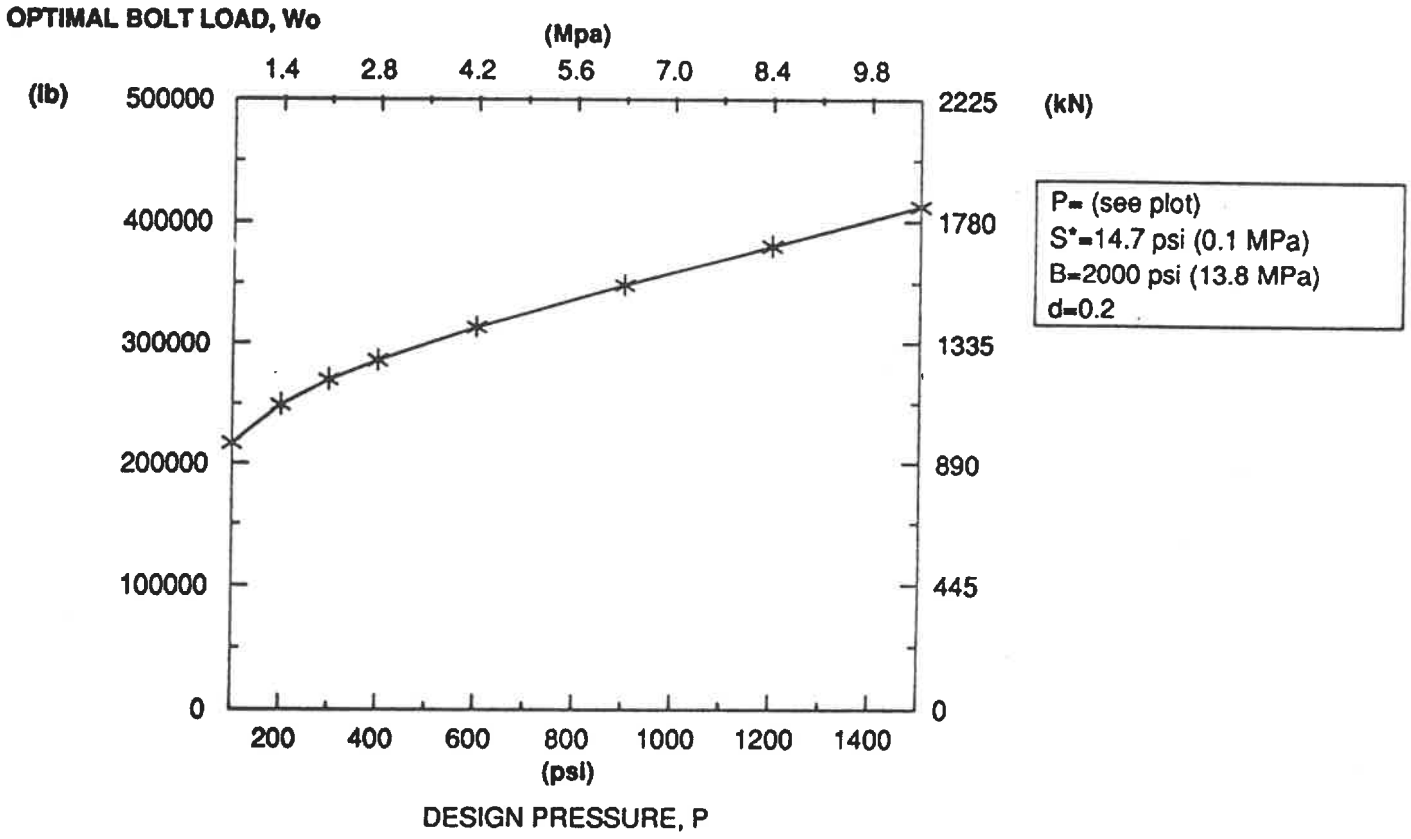

FIGURE 55 : Effect of the design pressure on the optimal bolt load.

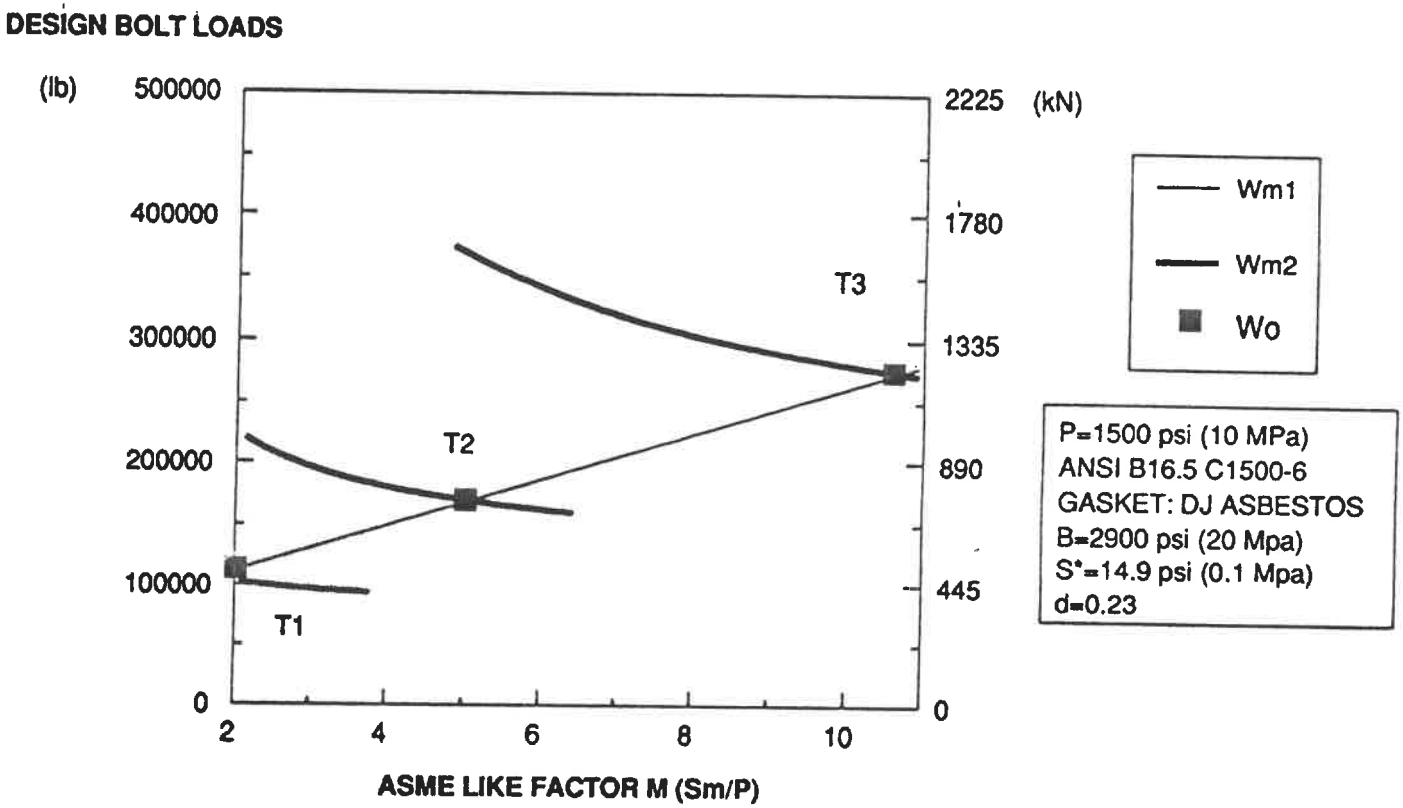

FIGURE 56 : Design Bolt loads Wm1 & Wm2 vs. factor M (DJ ASBESTOS)
Effect of Tightness Class TC

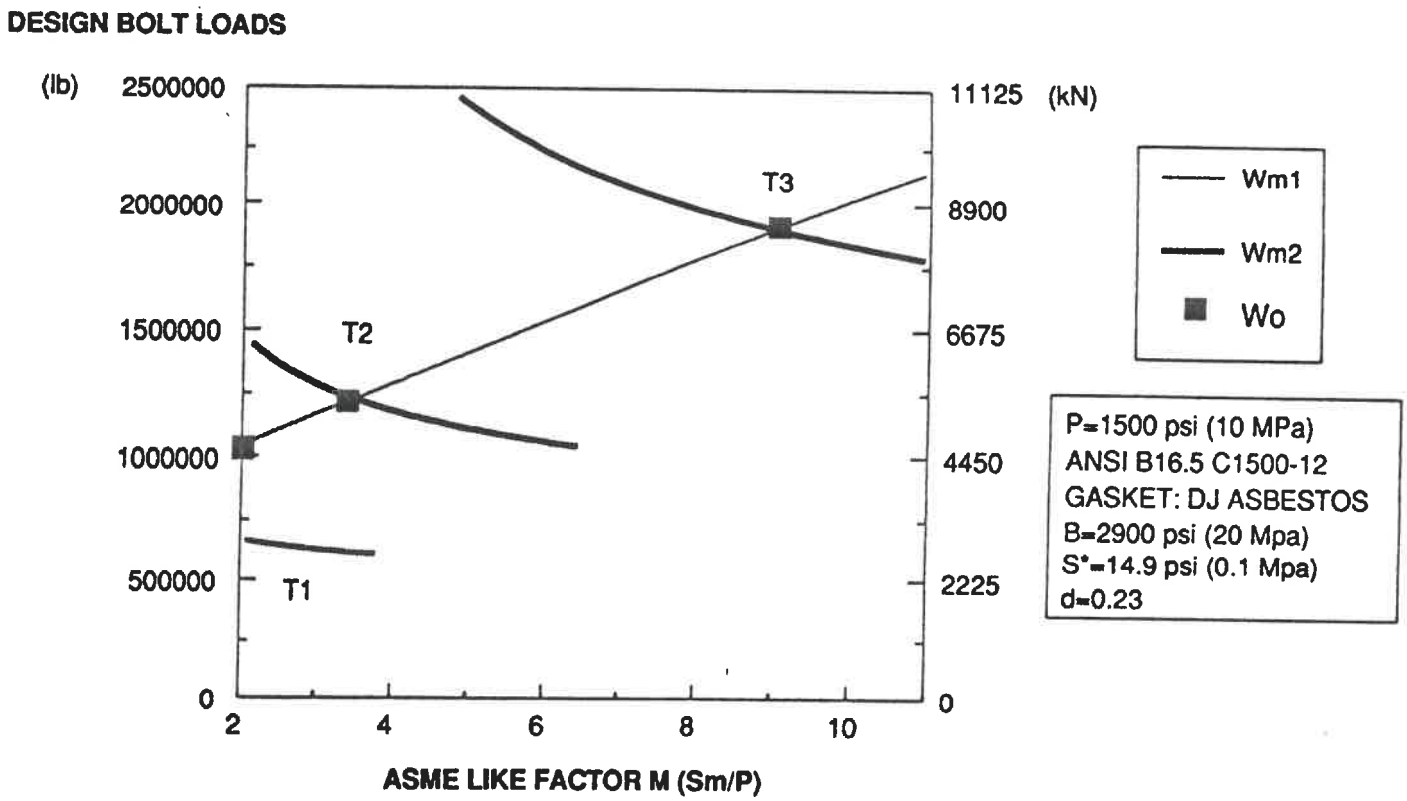

FIGURE 57 : Design Bolt loads Wm1 & Wm2 vs. factor M (DJ ASBESTOS)
Effect of Tightness Class TC

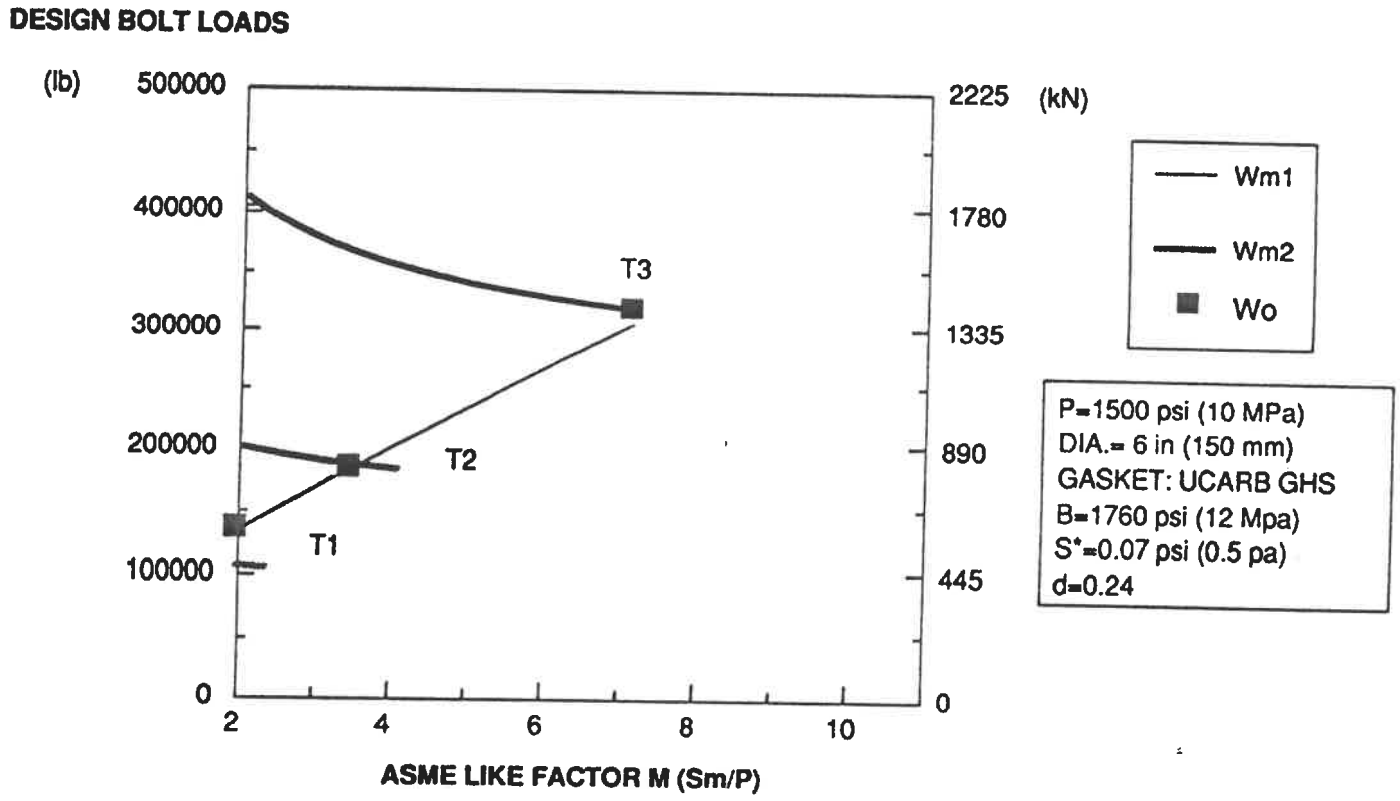

FIGURE 58 : Design Bolt loads Wm1 & Wm2 vs. factor M (UCARB GHS)
Effect of Tightness Class TC

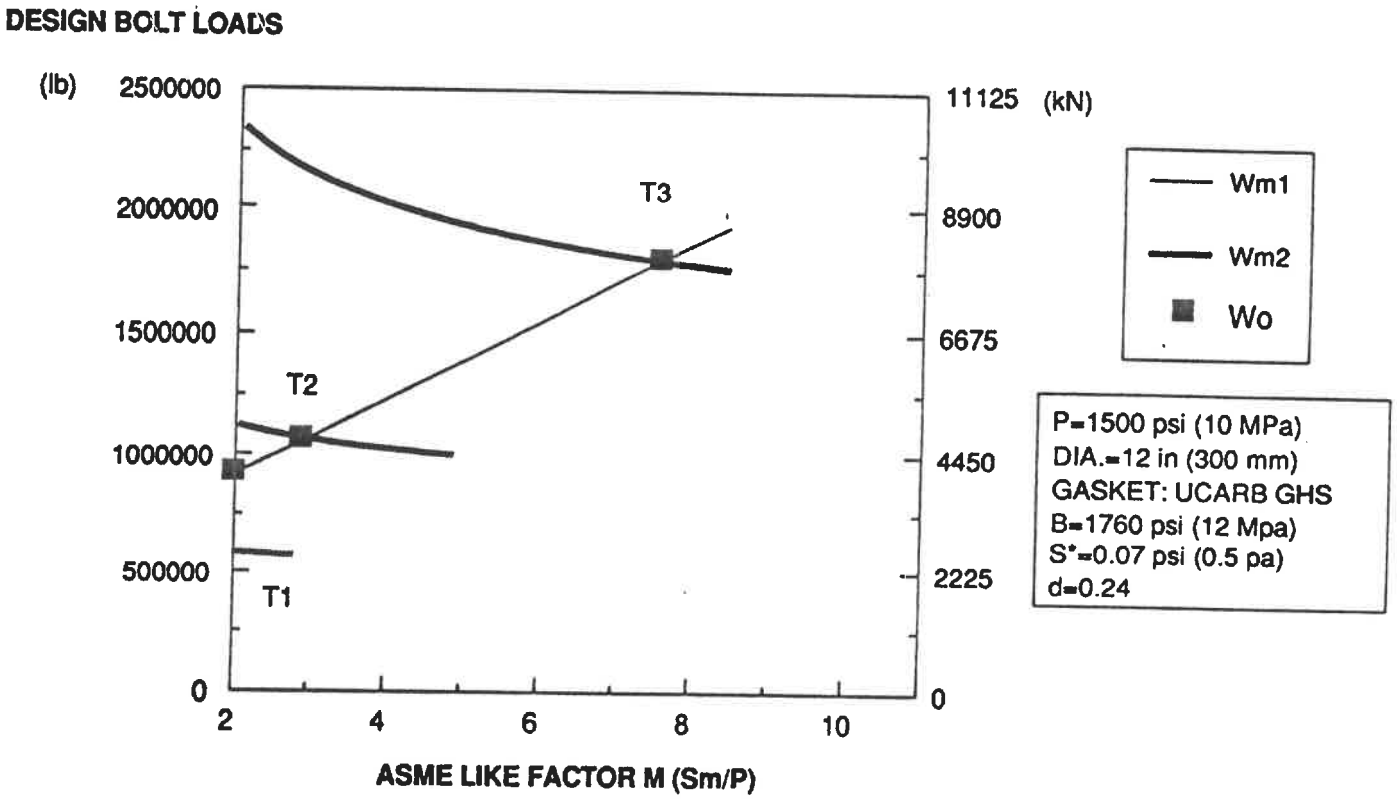

FIGURE 59 : Design Bolt loads Wm1 & Wm2 vs. factor M (UCARB GHS)
Effect of Tightness Class TC

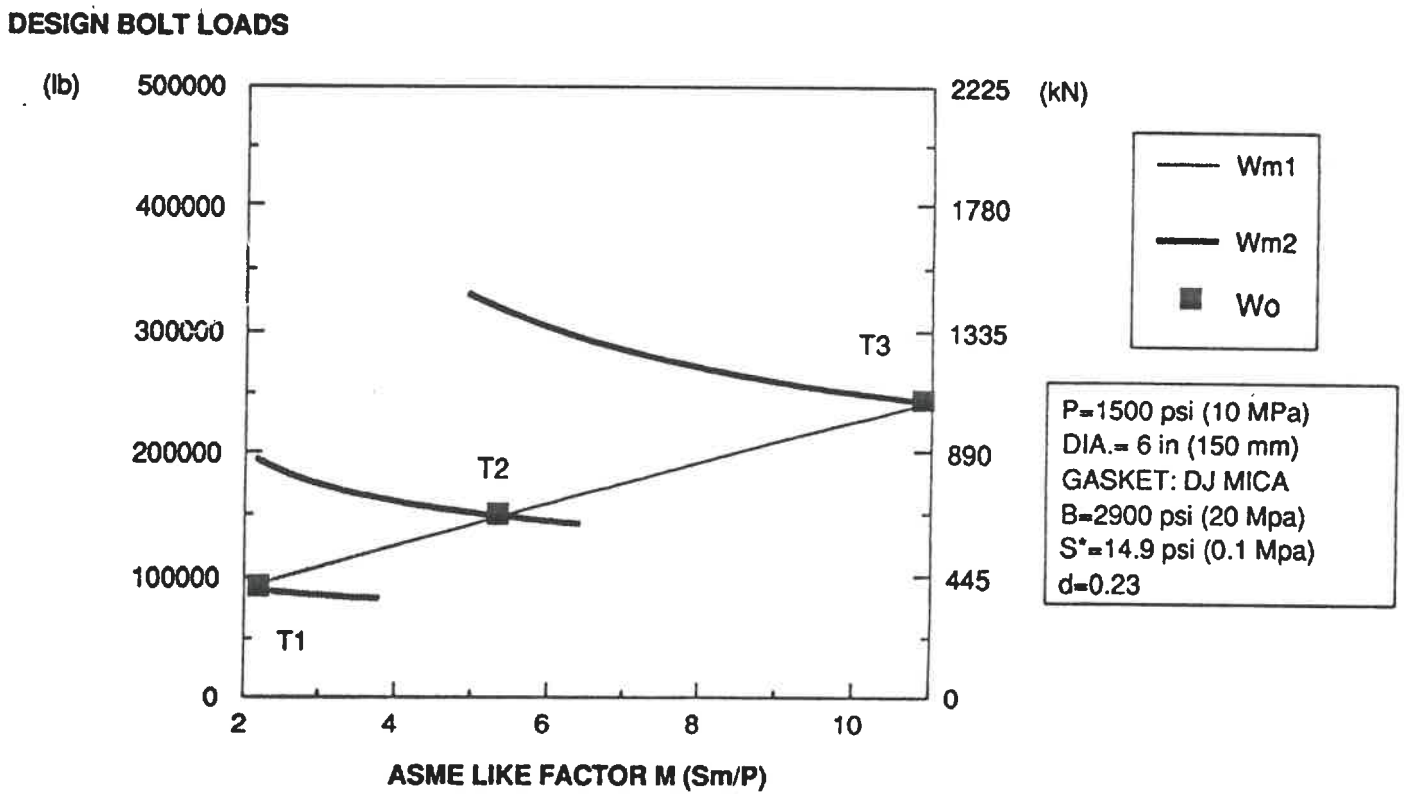

FIGURE 60 : Design Bolt loads Wm1 & Wm2 vs. factor M (DJ MICA)
Effect of Tightness Class TC

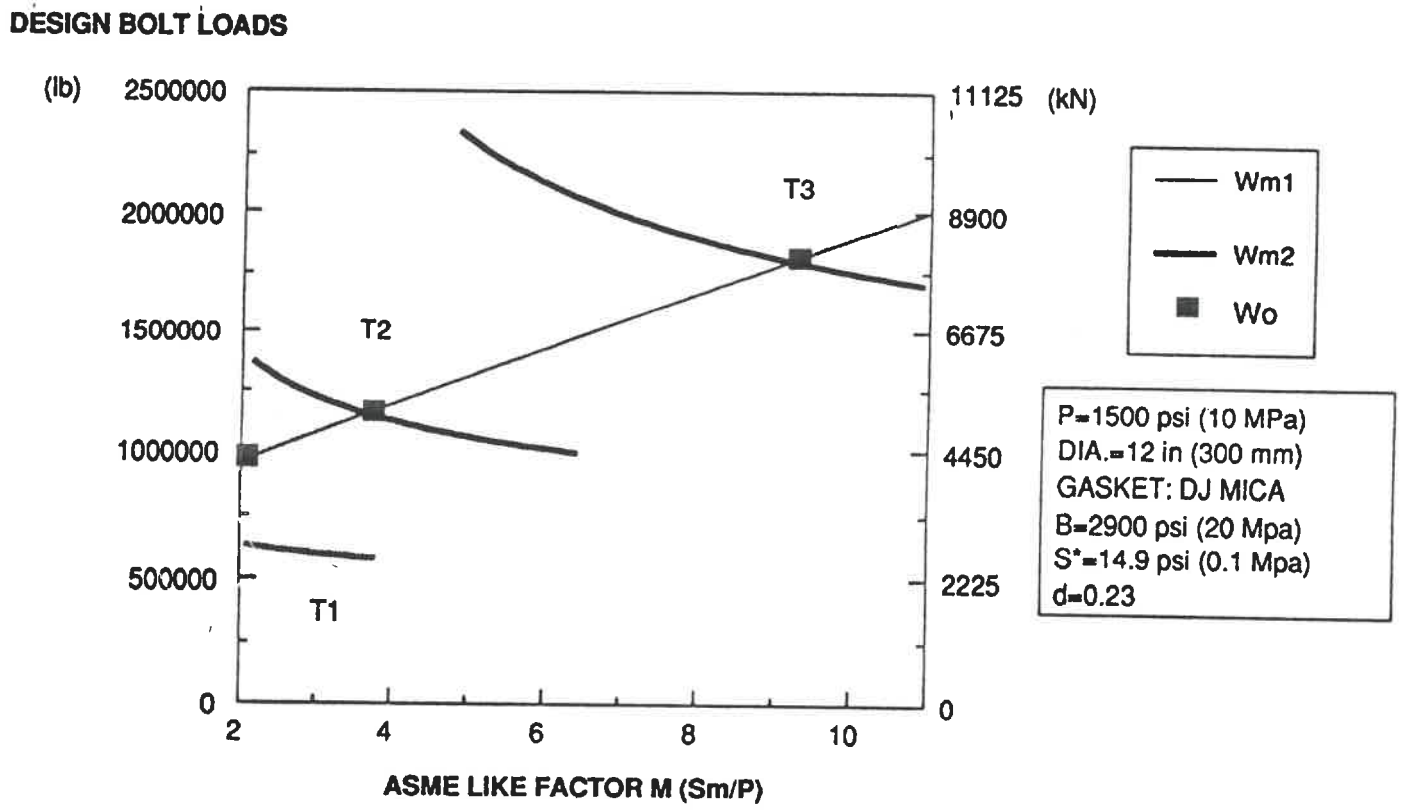

FIGURE 61 : Design Bolt loads Wm1 & Wm2 vs. factor M (DJ MICA)
Effect of Tightness Class TC

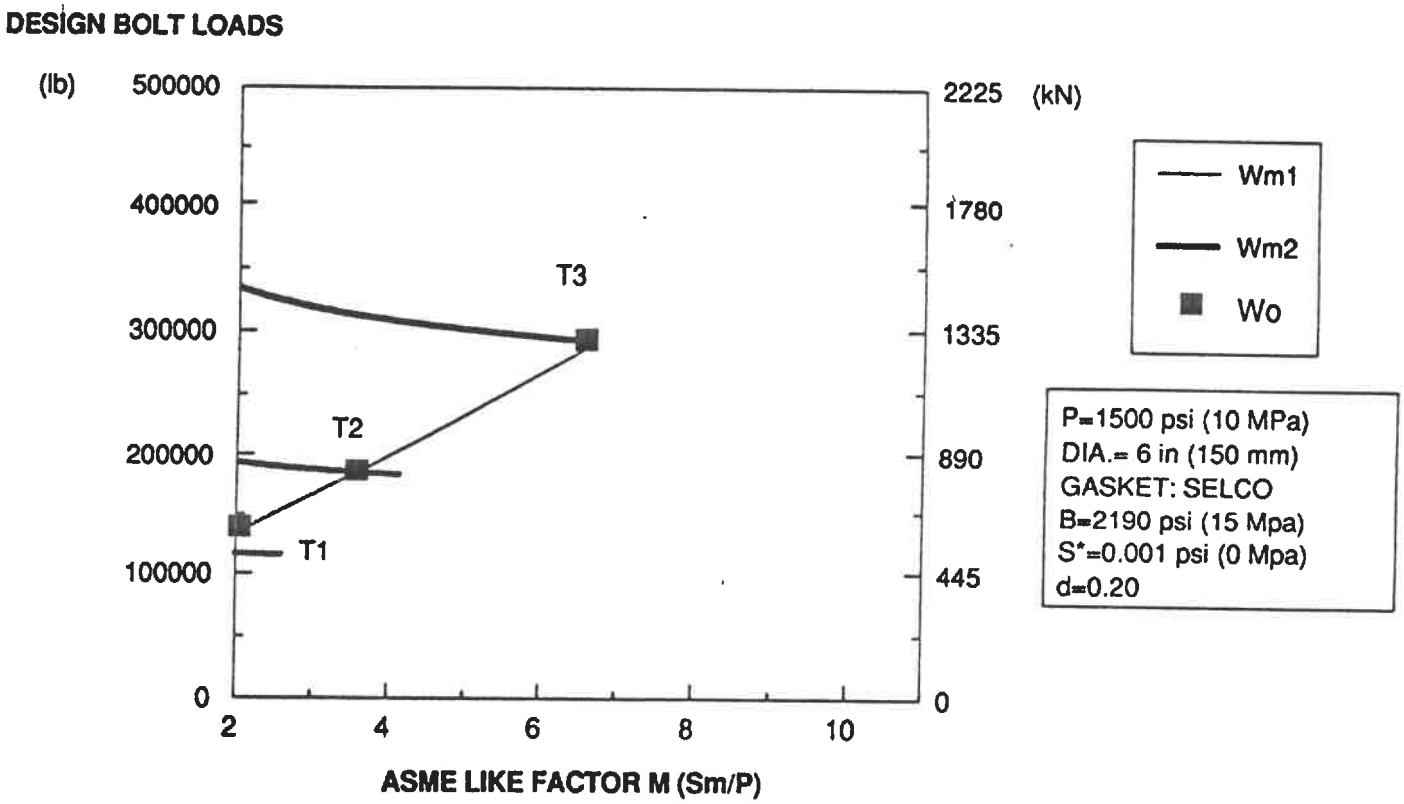

FIGURE 62 : Design Bolt loads Wm1 & Wm2 vs. factor M (SELCO)
Effect of Tightness Class TC

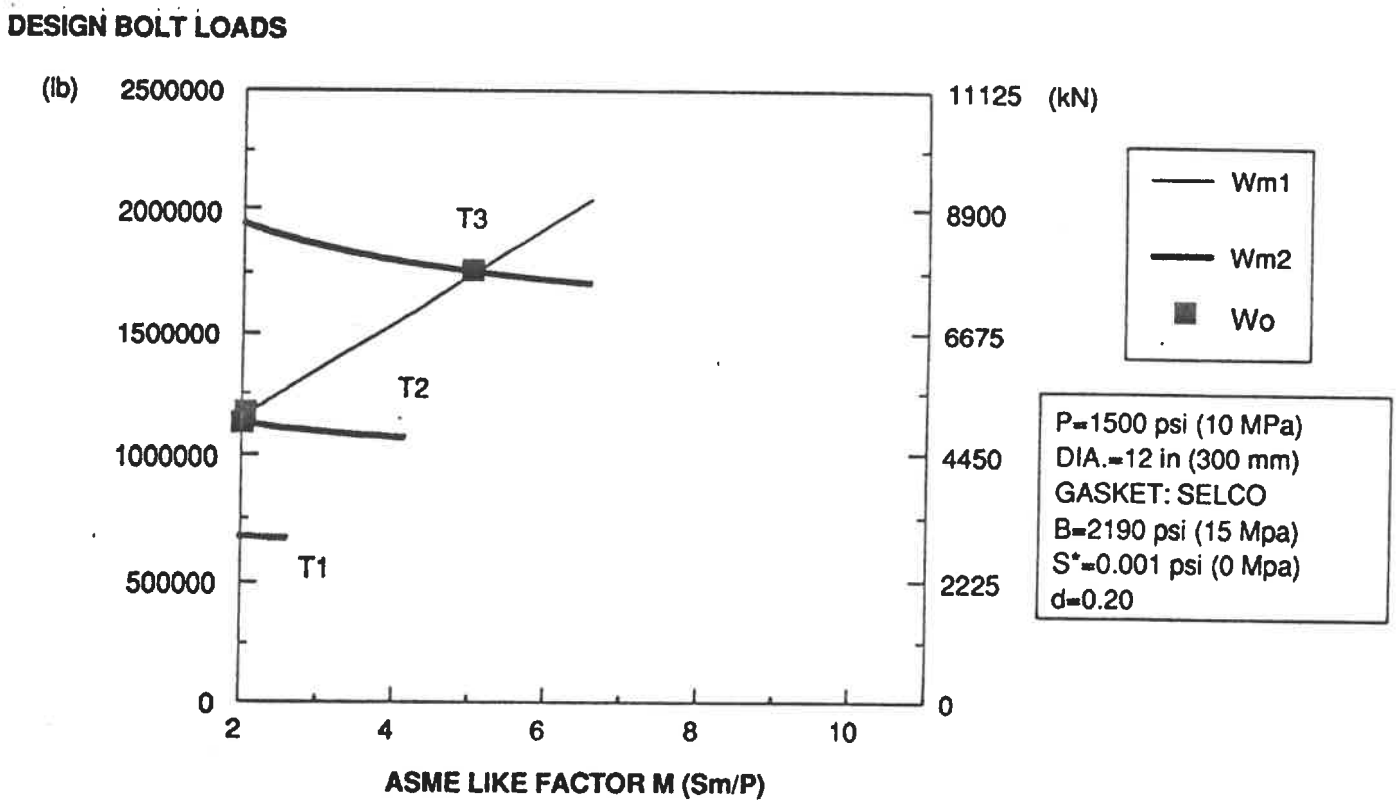

FIGURE 63 : Design Bolt loads Wm1 & Wm2 vs. factor M (SELCO)
Effect of Tightness Class TC

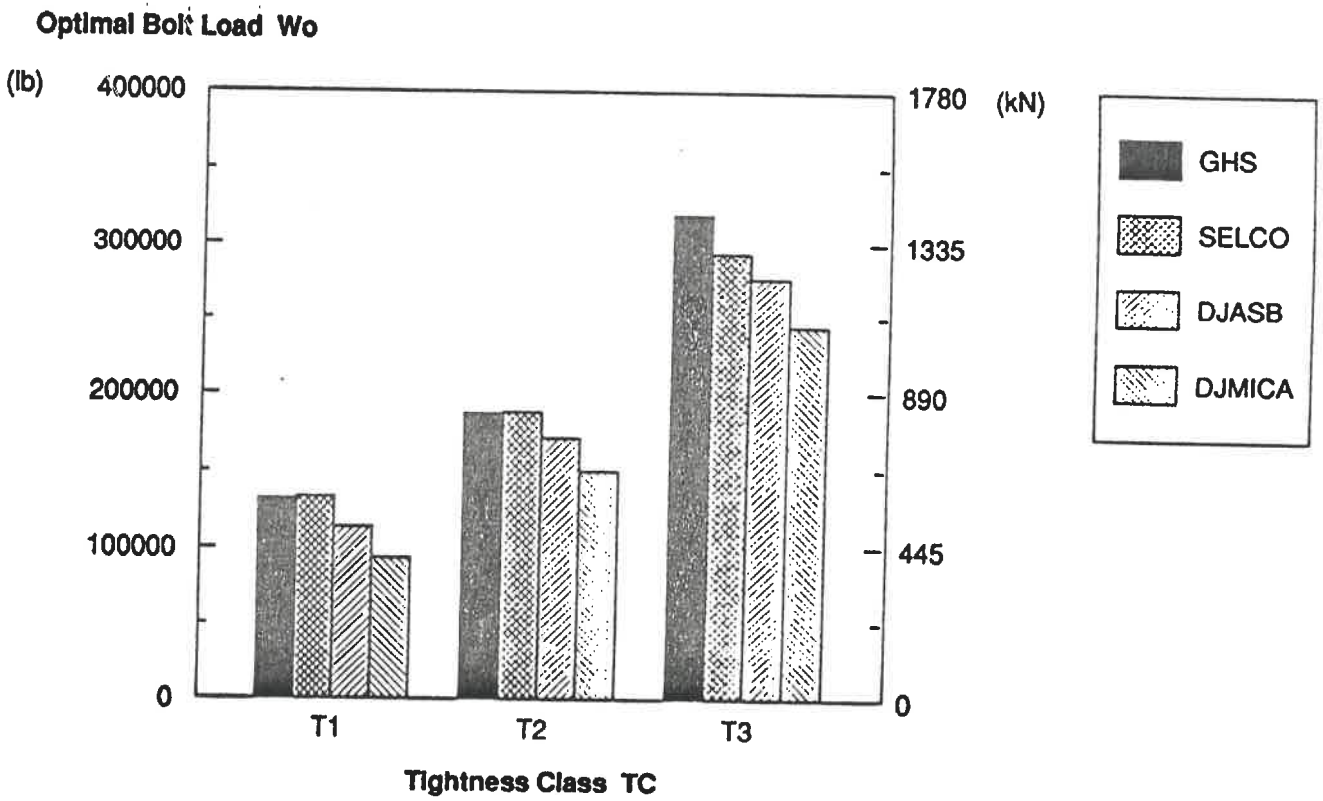

FIGURE 64 : Effect of Tightness Class on the Optimal Bolt Load ANSI B16.5 Class 1500, pipe Dia 6in.

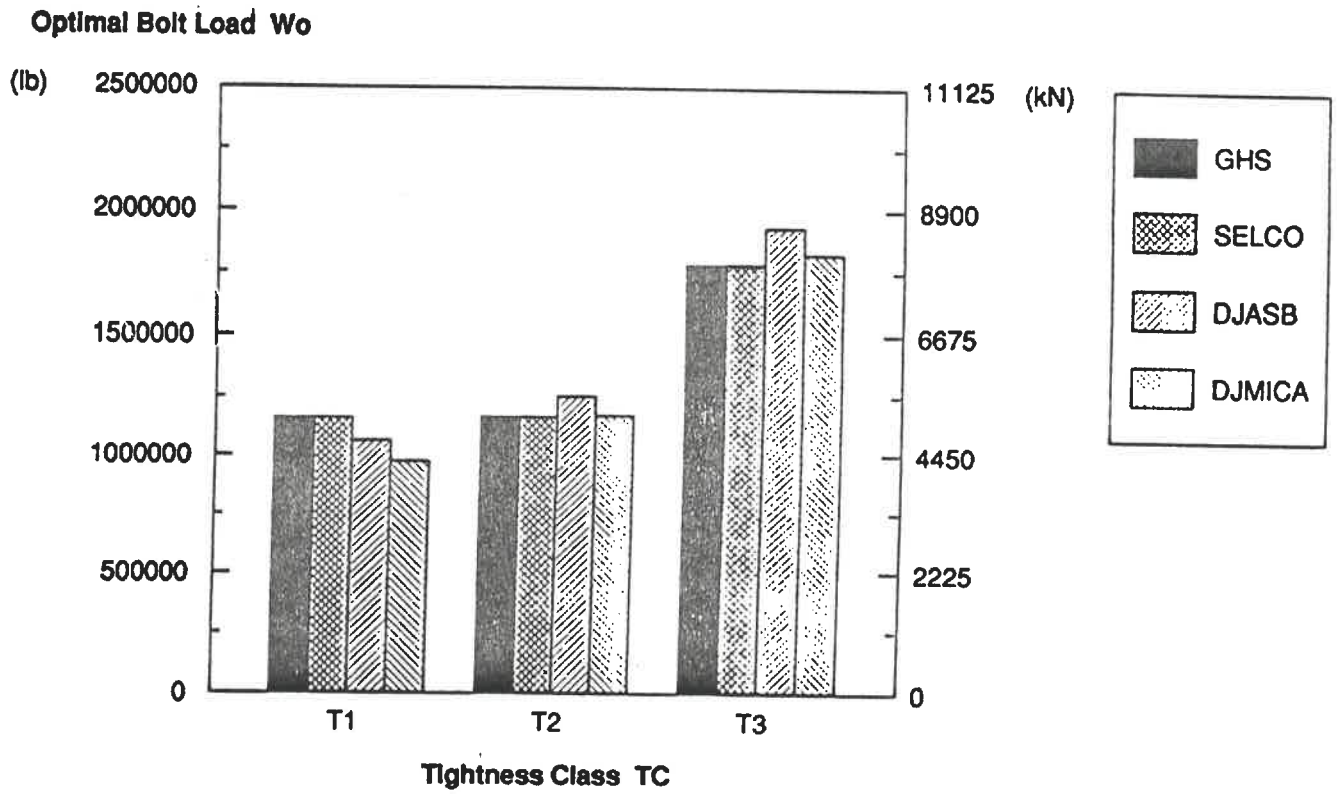

FIGURE 65 : Effect of Tightness Class on the Optimal Bolt Load
ANSI B16.5 Class 1500, pipe Dia 12in.

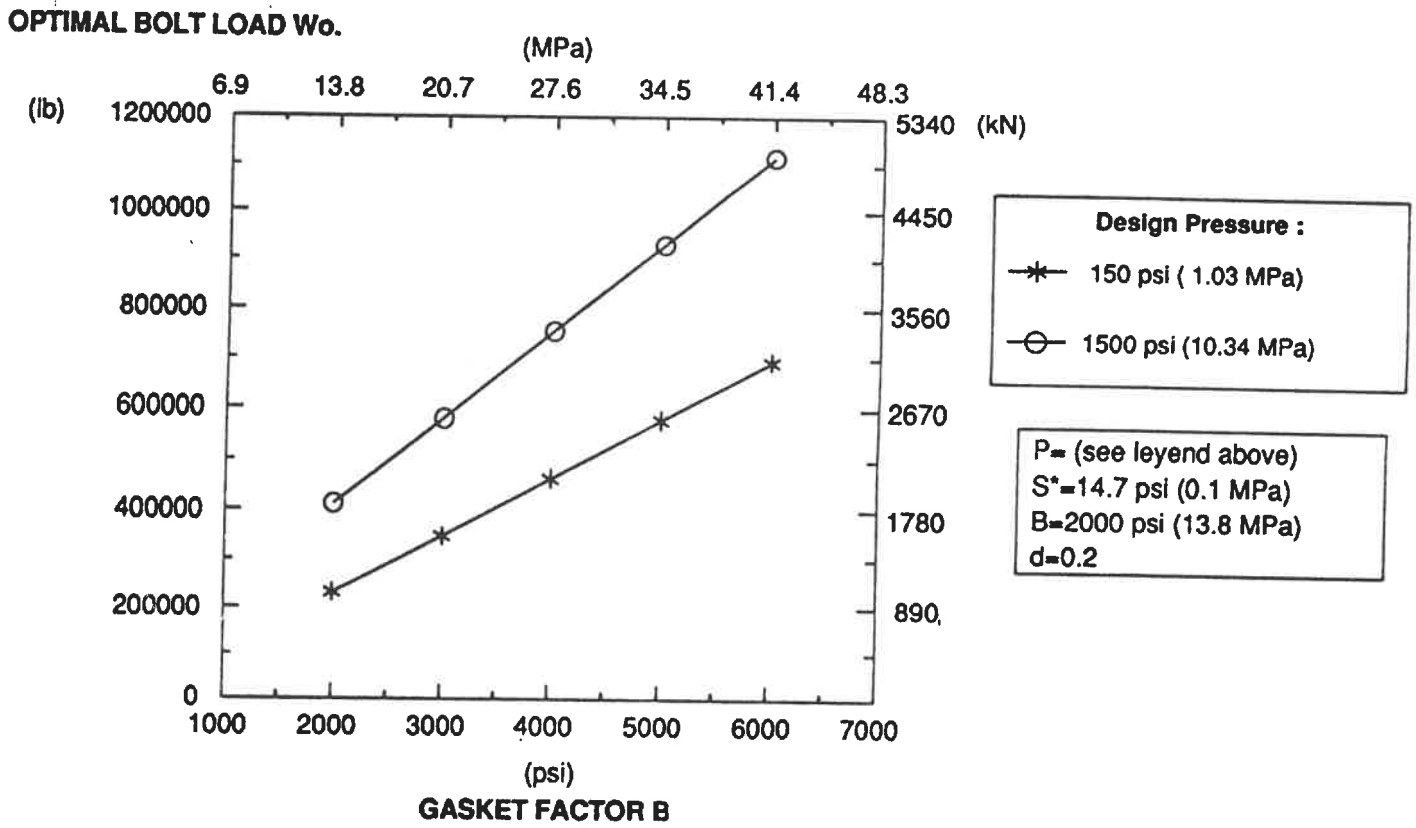

FIGURE 66 : Effect of Gasket Factor B on the optimal load Wo.
(Effect at high and low design pressure).

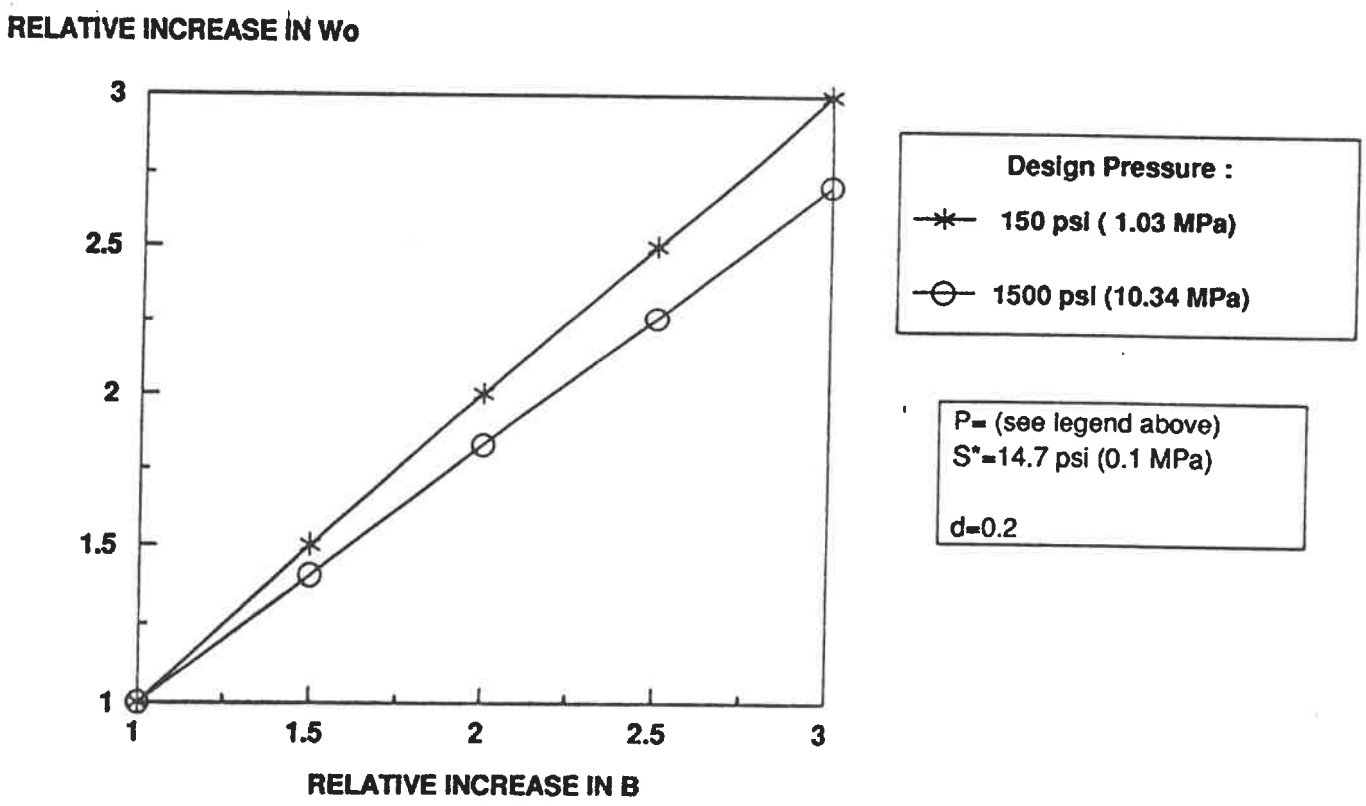

FIGURE 67 : Effect of Gasket Factor B on the optimal load Wo.
(Relative effect at high and low design pressure).

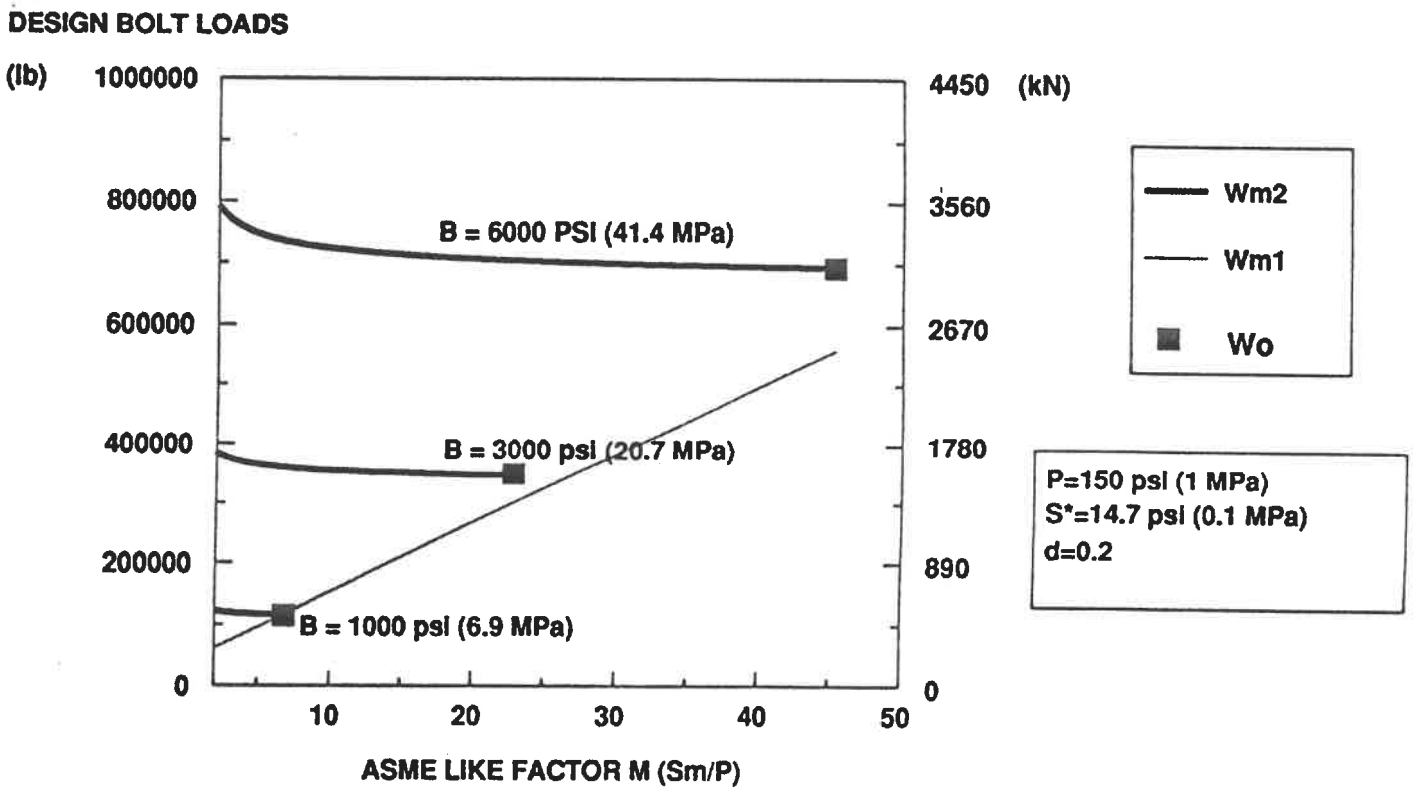

FIGURE 68 : Design Bolt loads Wm1 & Wm2 vs. factor M
(Effect of Gasket Factor B at low pressure)

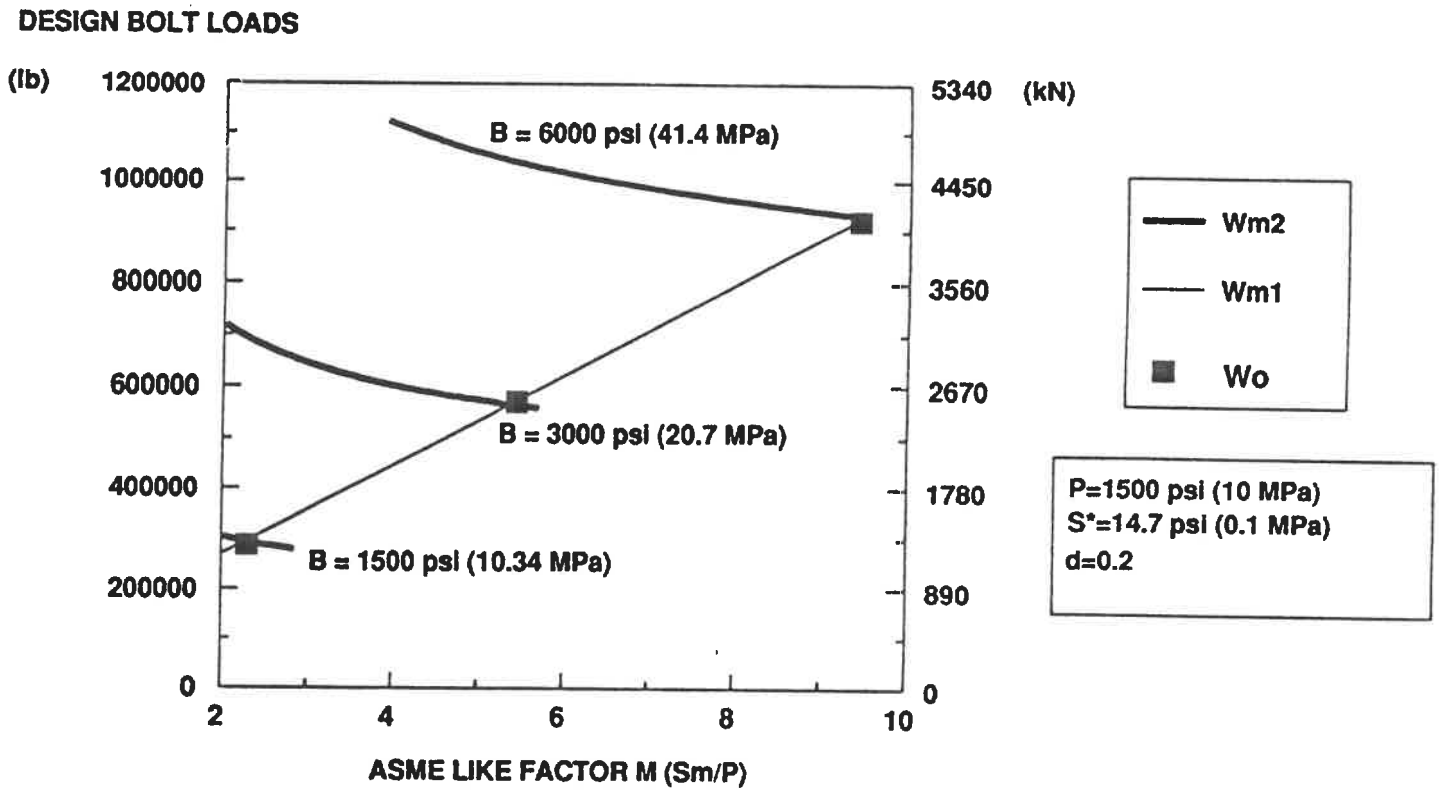

FIGURE 69 : Design Bolt loads Wm1 & Wm2 vs. factor M
(Effect of Gasket Factor B at high pressure)

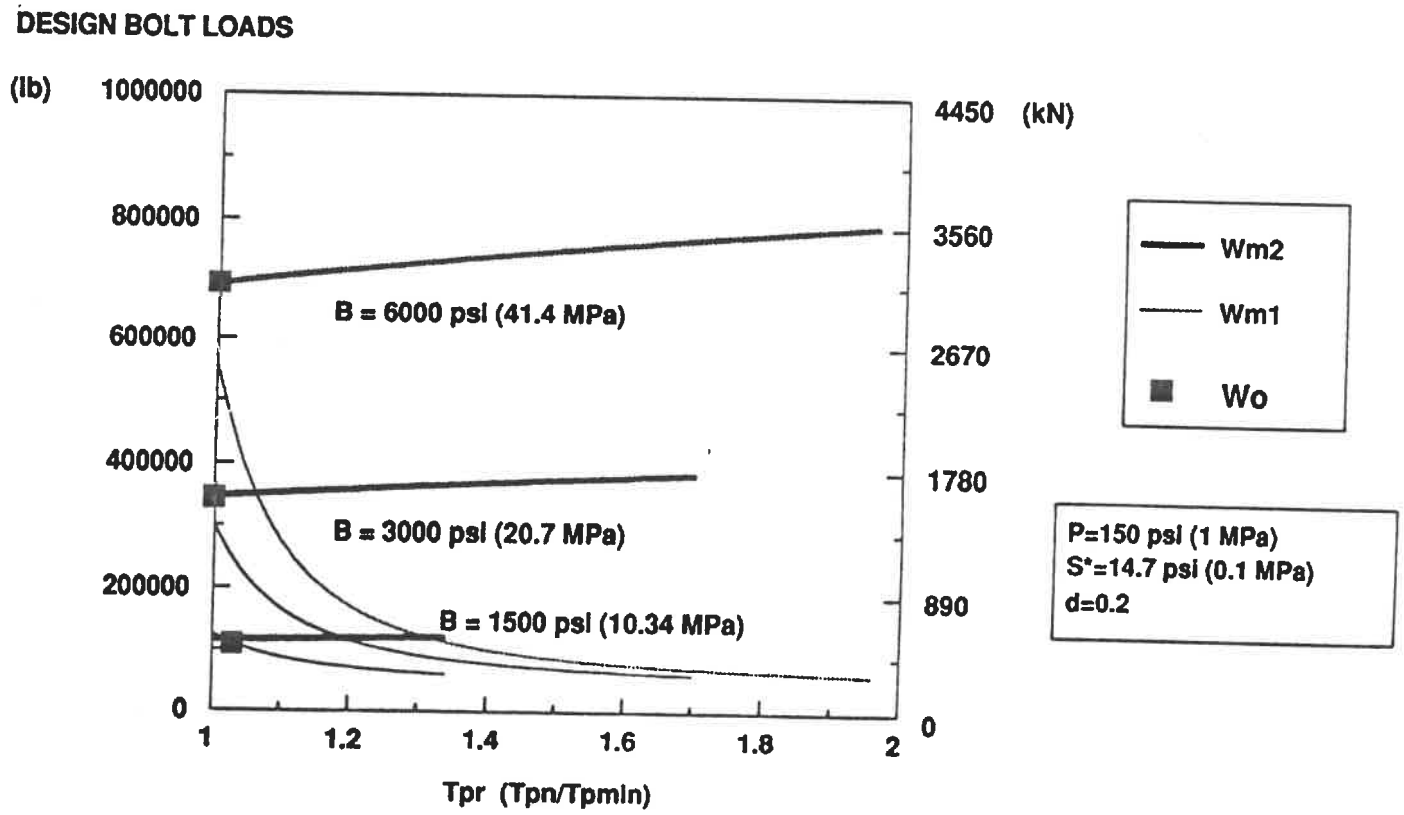

FIGURE 70 : Design Bolt loads Wm1 & Wm2 vs. Tightness Ratio Tpr (Effect of Gasket Factor B at low pressure)

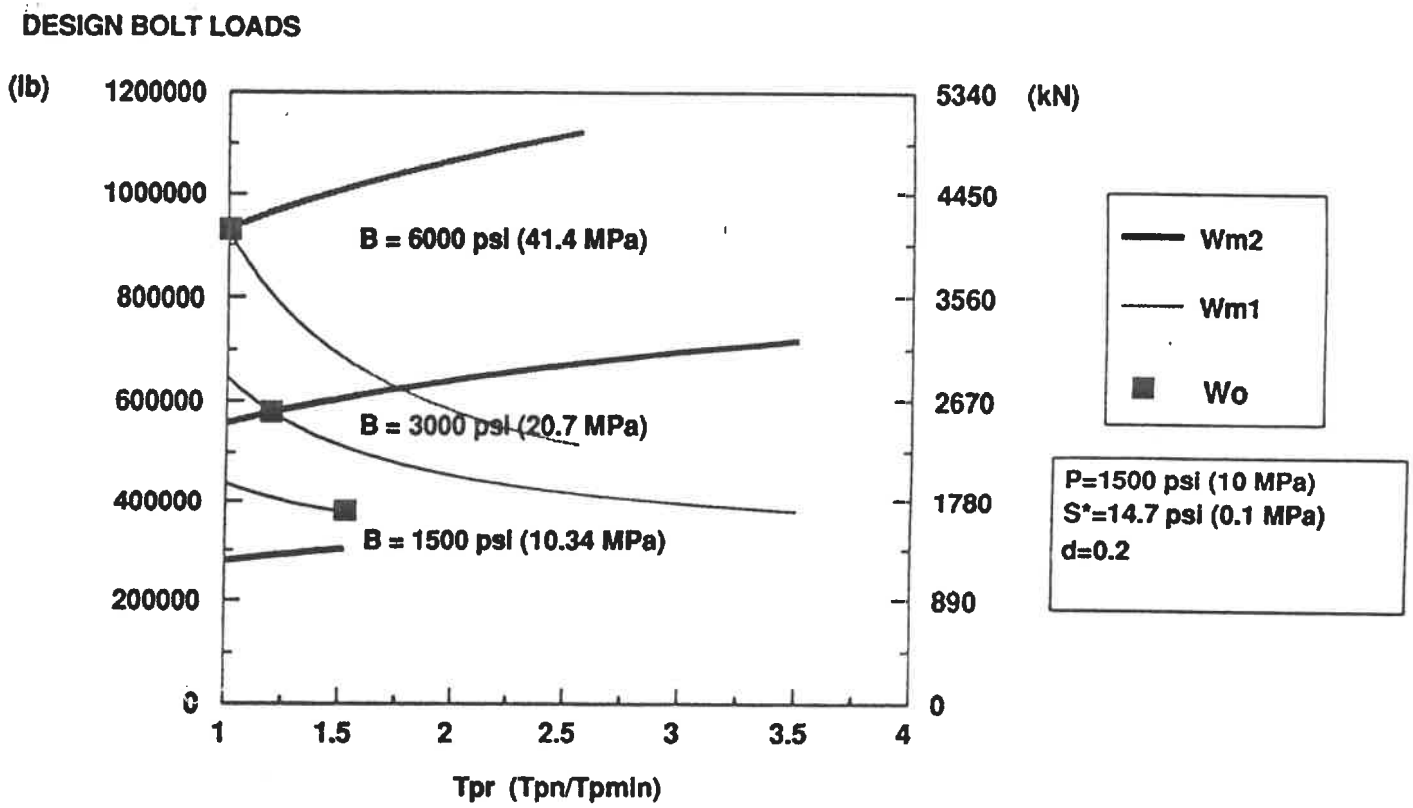

FIGURE 71 : Design Bolt loads Wm1 & Wm2 vs. Tightness Ratio Tpr
(Effect of Gasket Factor B at high pressure)

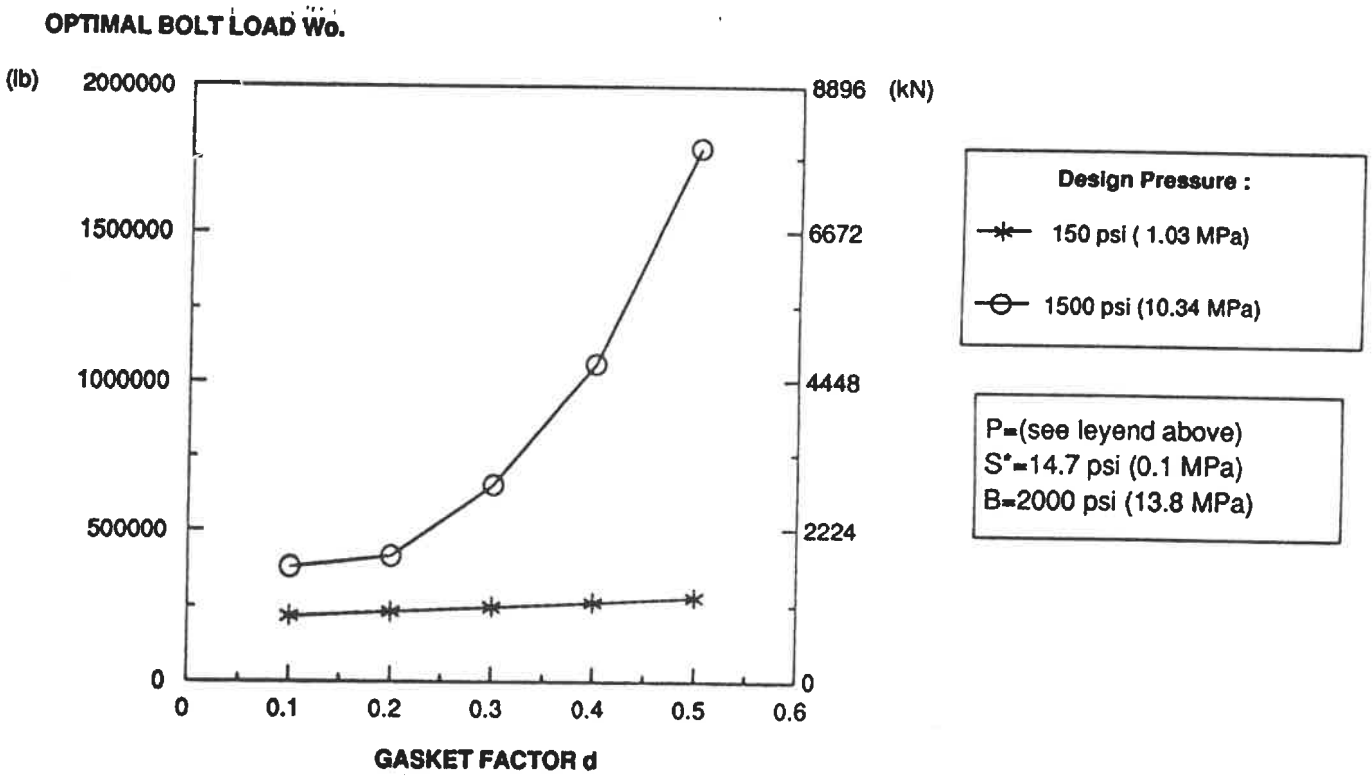

FIGURE 72 : Effect of Gasket Factor d on the optimal load Wo.
(Effect at high and low design pressure).

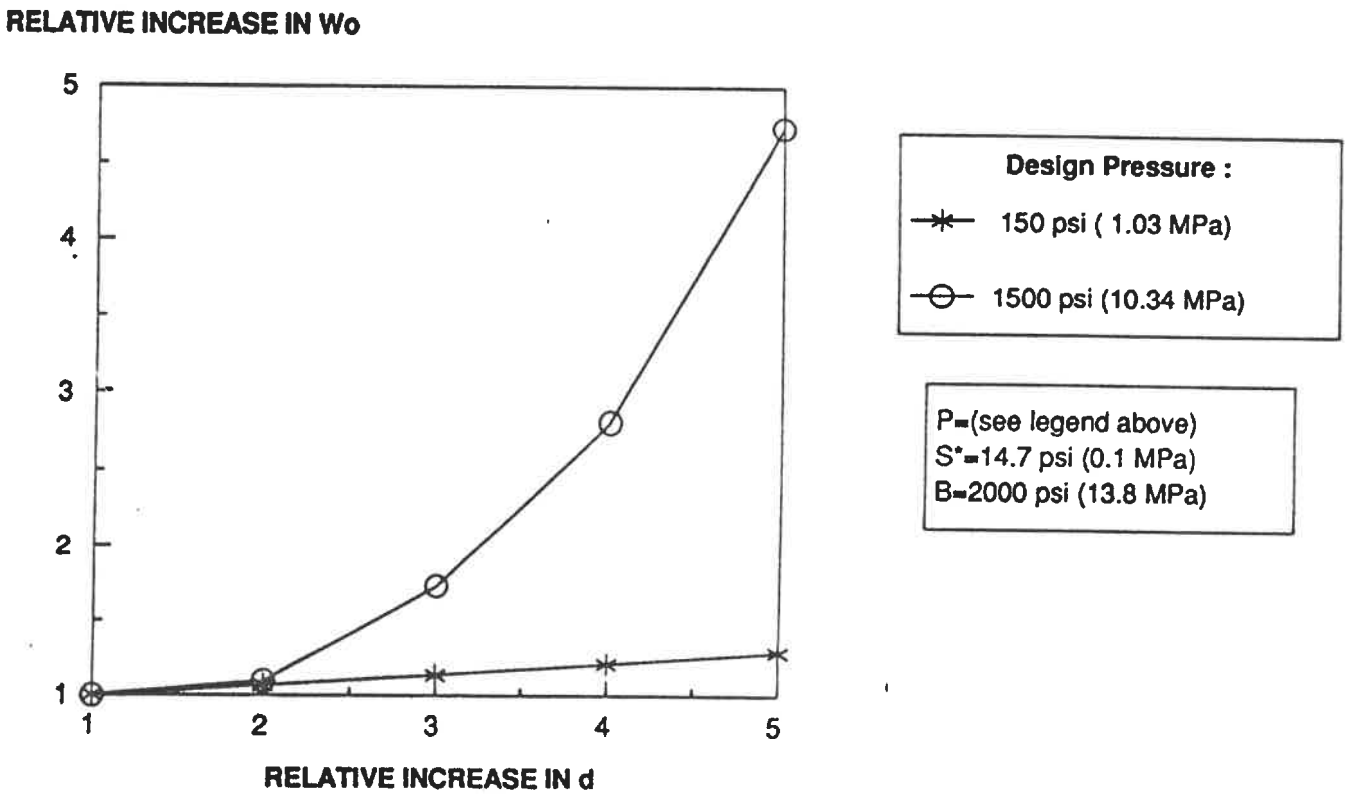

FIGURE 73 : Effect of Gasket Factor d on the optimal load Wo.
(Relative effect at high and low design pressure).

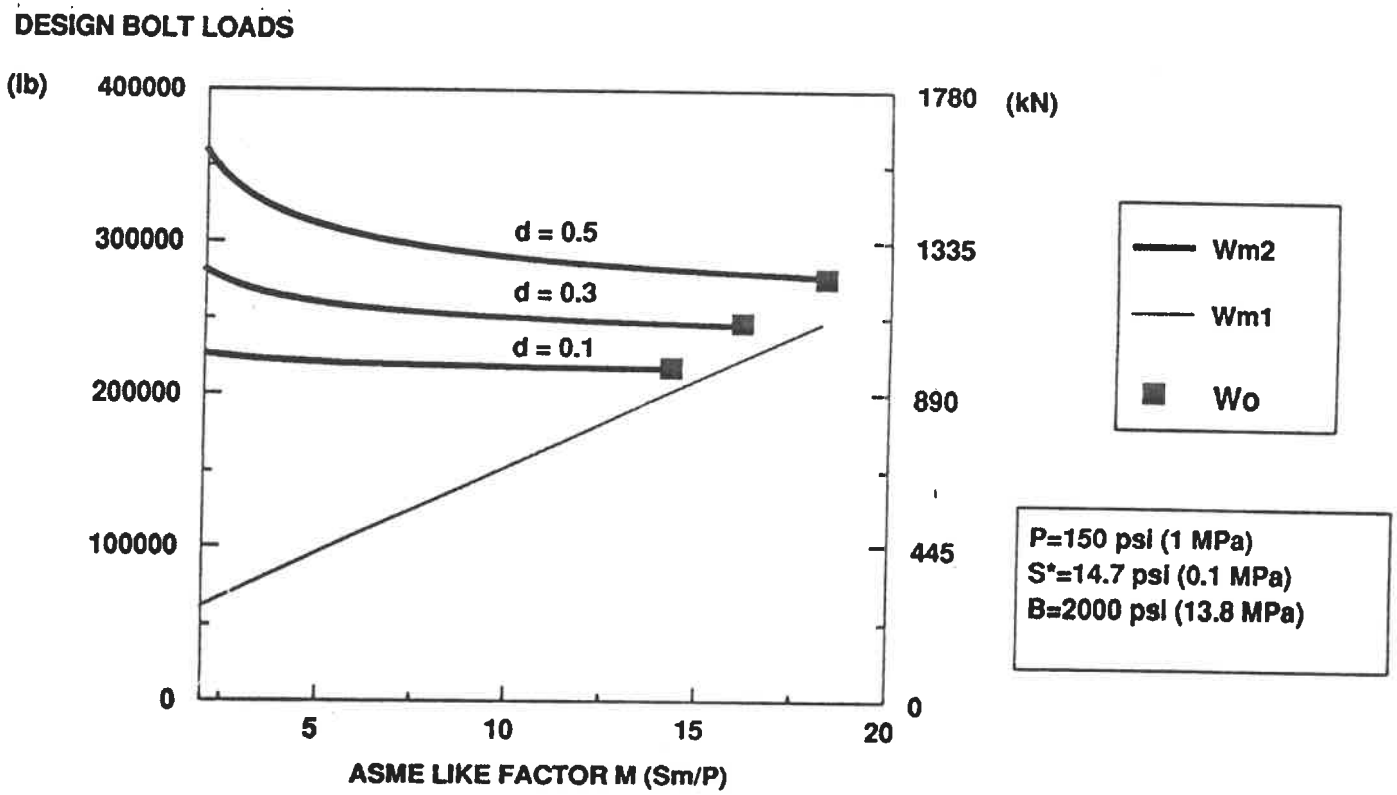

FIGURE 74 : Design Bolt loads Wm1 & Wm2 vs. factor M
(Effect of Gasket Factor d at low pressure)

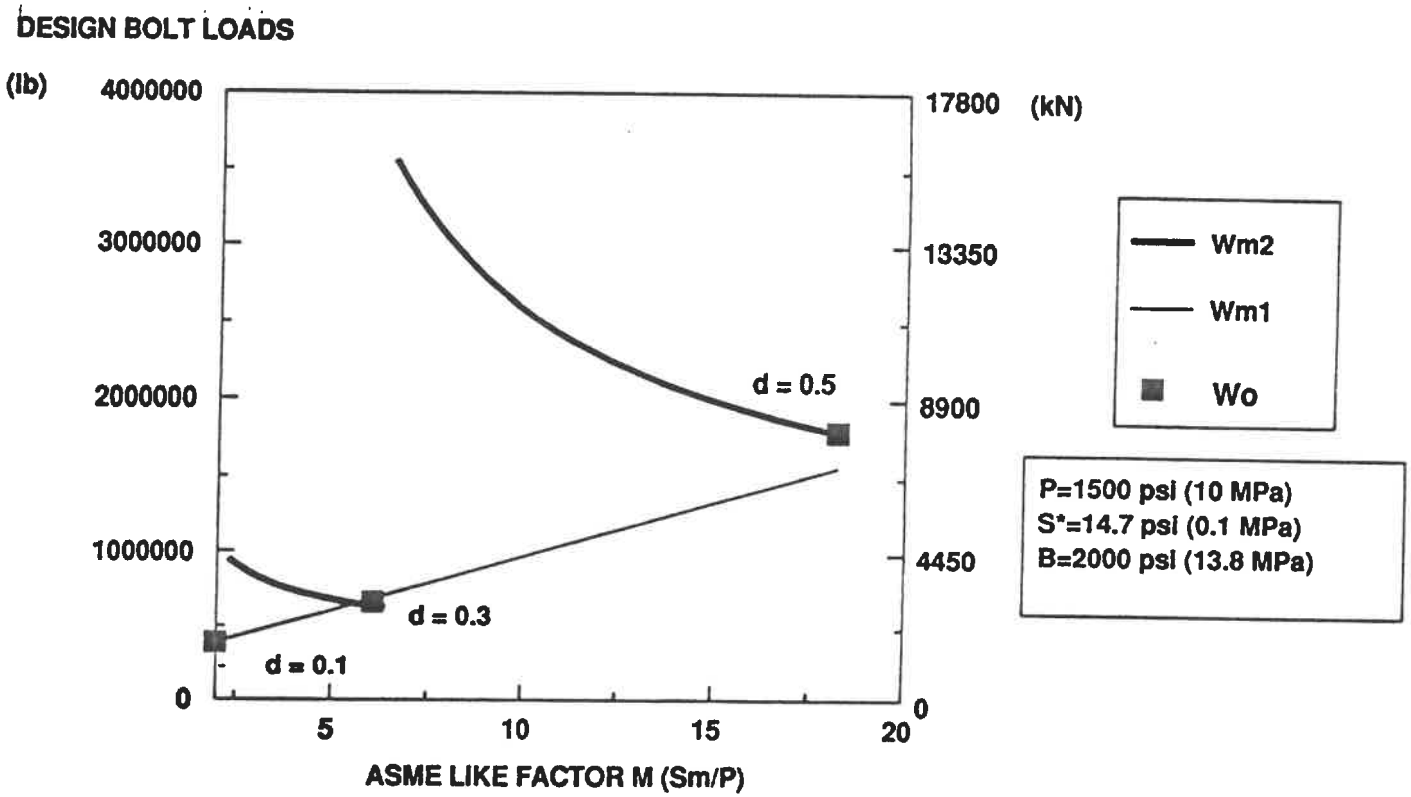

FIGURE 75 : Design Bolt loads Wm1 & Wm2 vs. factor M
(Effect of Gasket Factor d at high pressure)

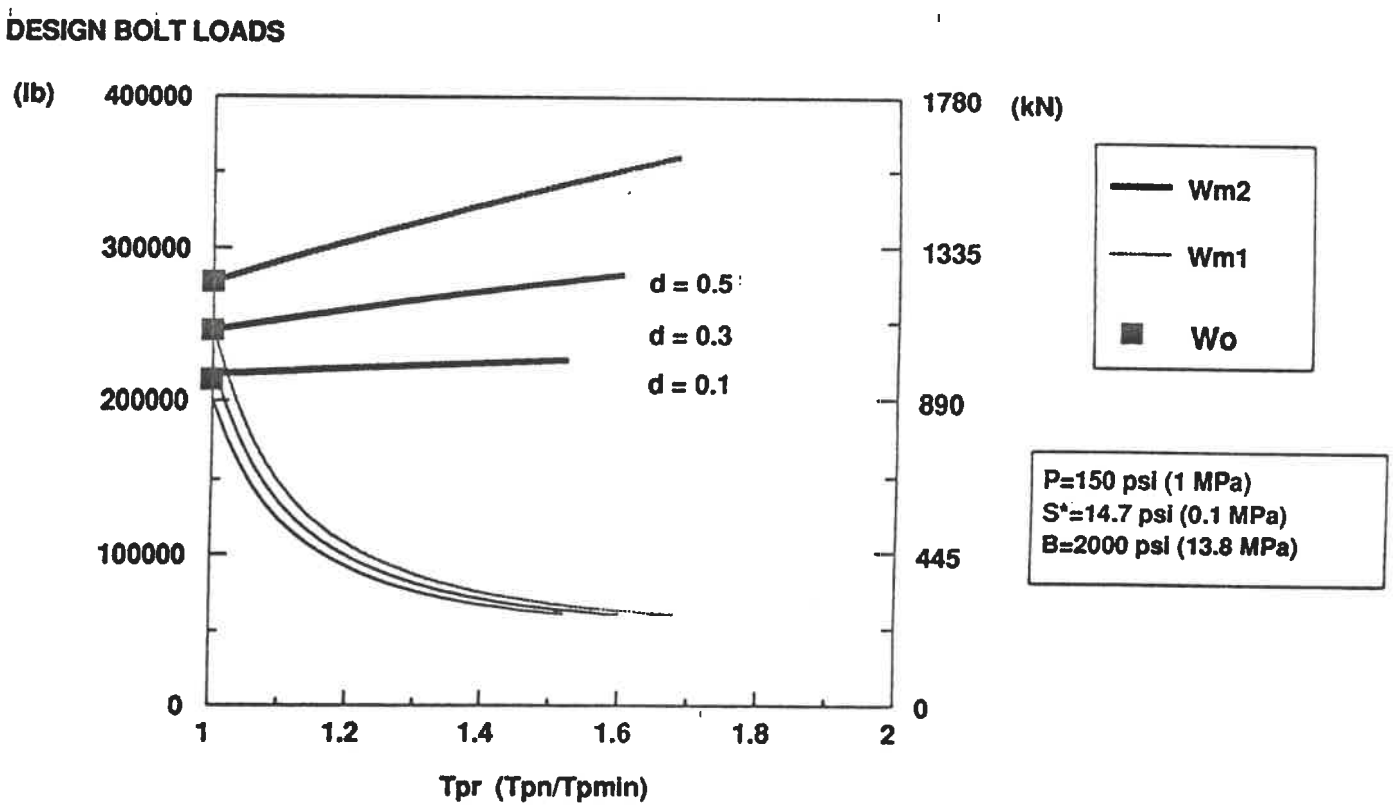

FIGURE 76 : Design Bolt loads Wm1 & Wm2 vs. Tightness Ratio Tpr
(Effect of Gasket Factor d at low pressure)

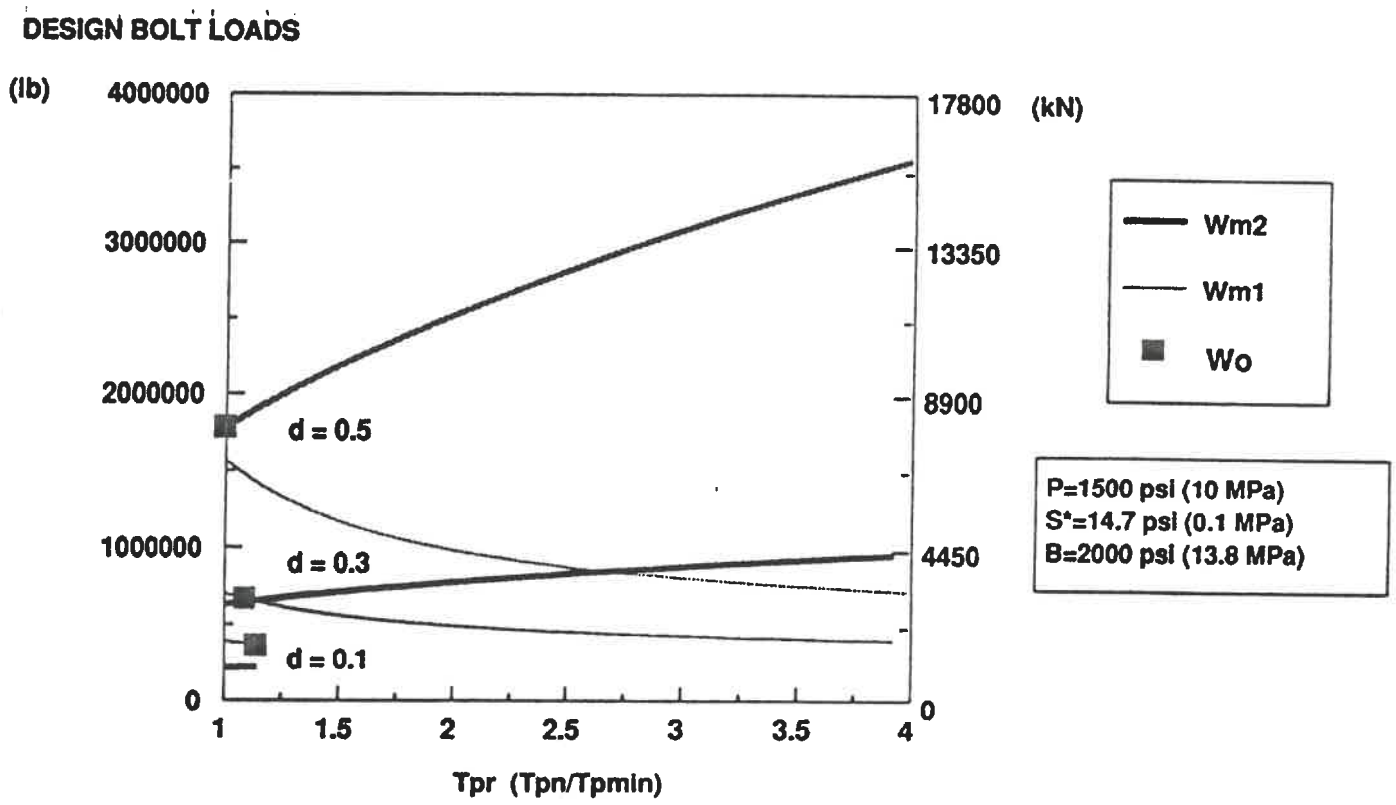

FIGURE 77 : Design Bolt loads Wm1 & Wm2 vs. Tightness Ratio Tpr
(Effect of Gasket Factor d at high pressure)

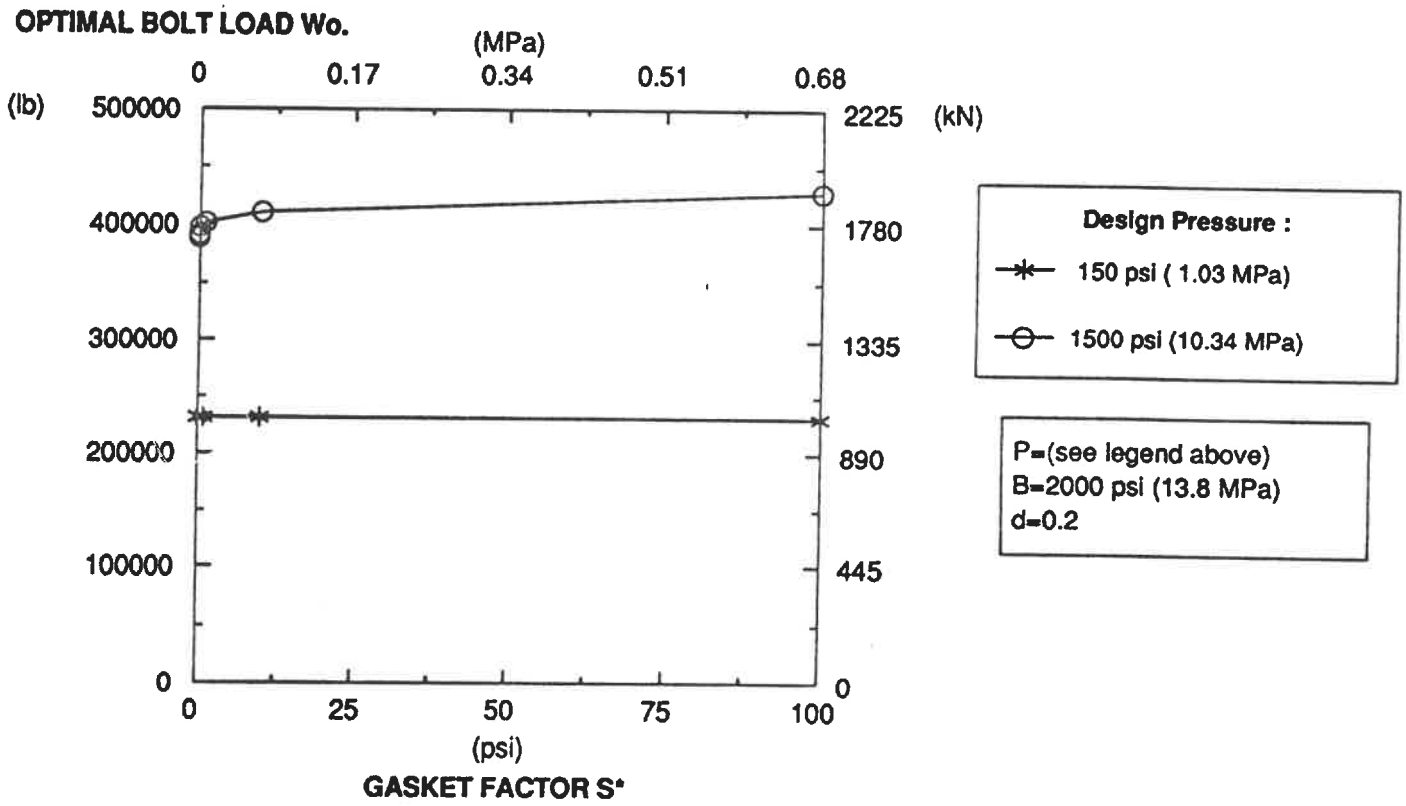

FIGURE 78 : Effect of Gasket Factor S* on the optimal load Wo.

(Effect at high and low design pressure).

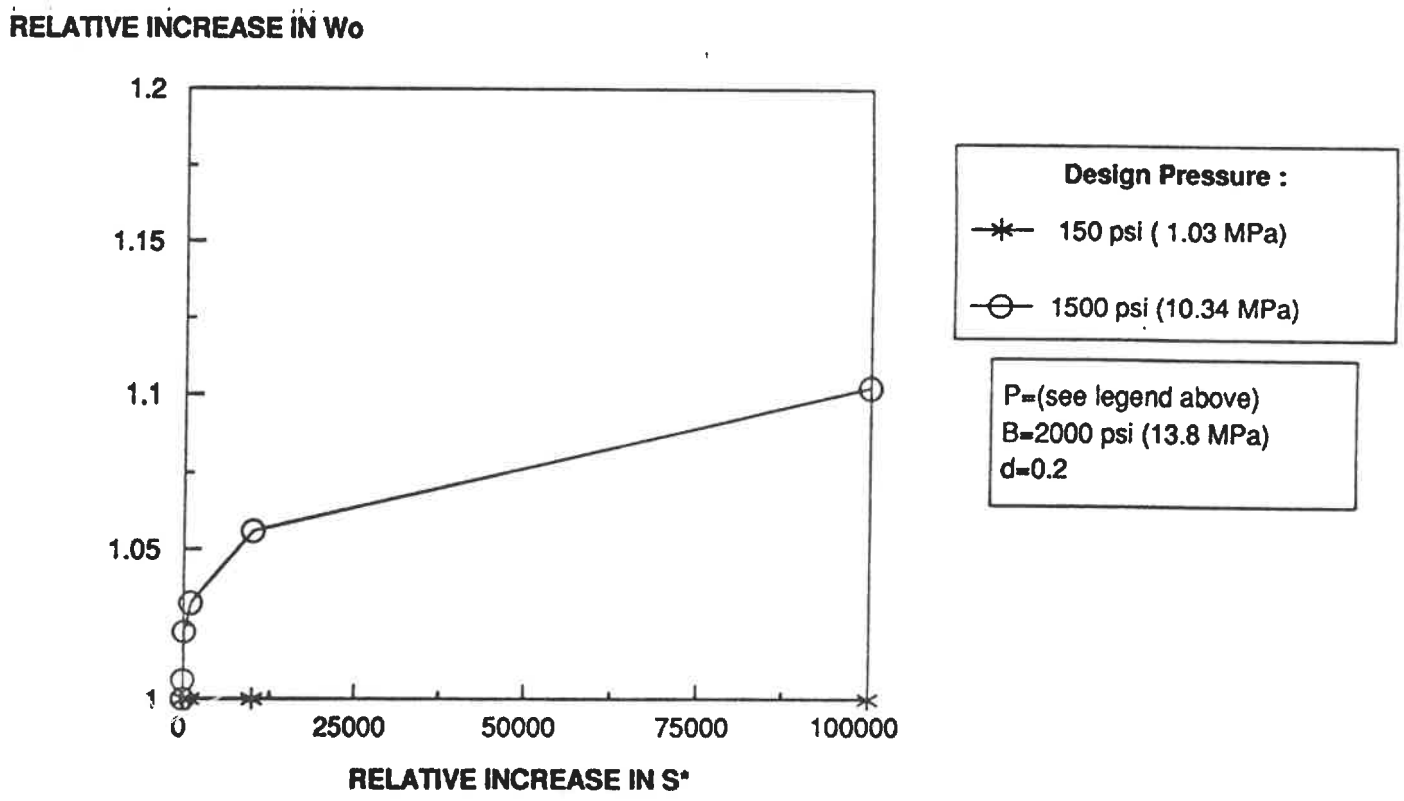

FIGURE 79 : Effect of Gasket Factor S* on the optimal load Wo.
(Relative effect at high and low design pressure).

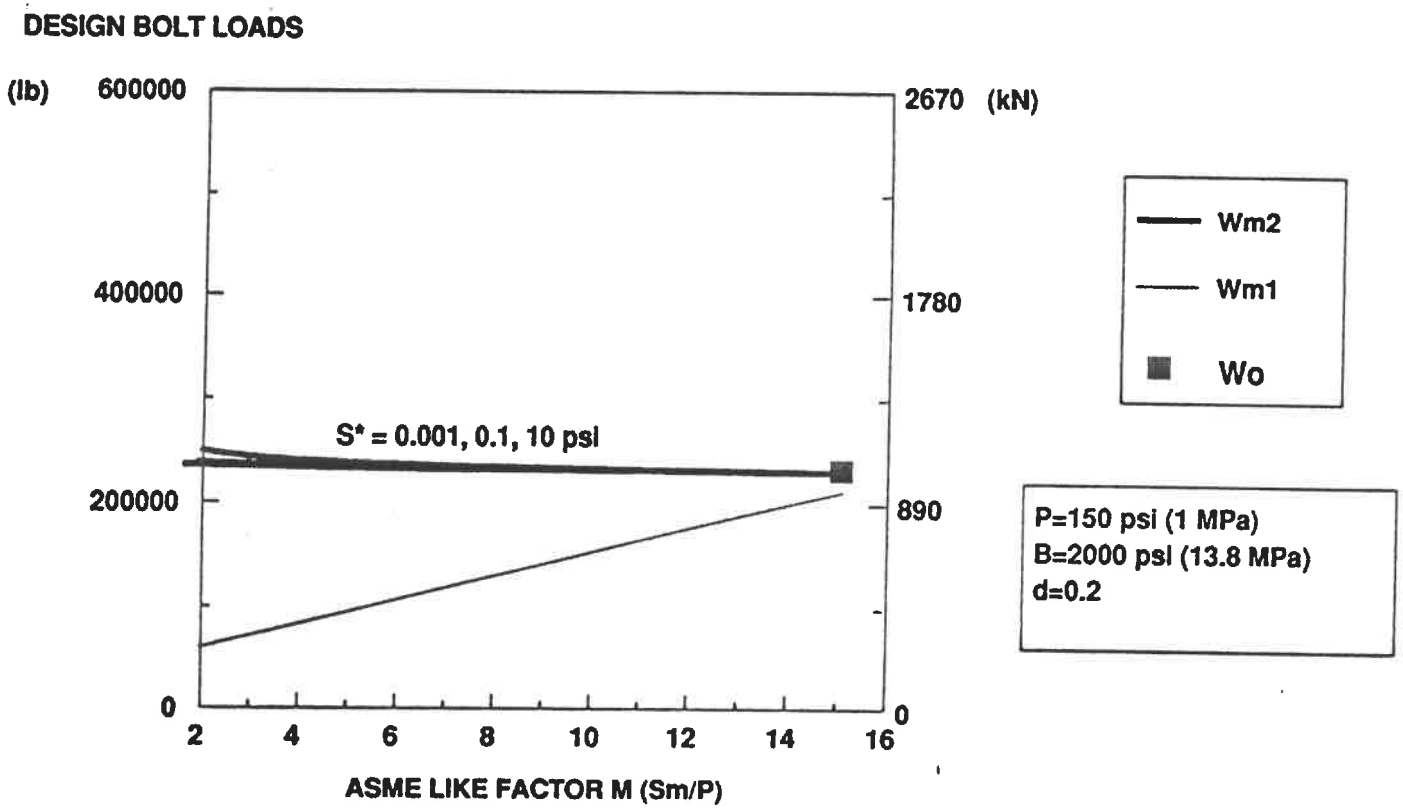

FIGURE 80 : Design Bolt loads Wm1 & Wm2 vs. factor M
(Effect of Gasket Factor S* at low pressure)

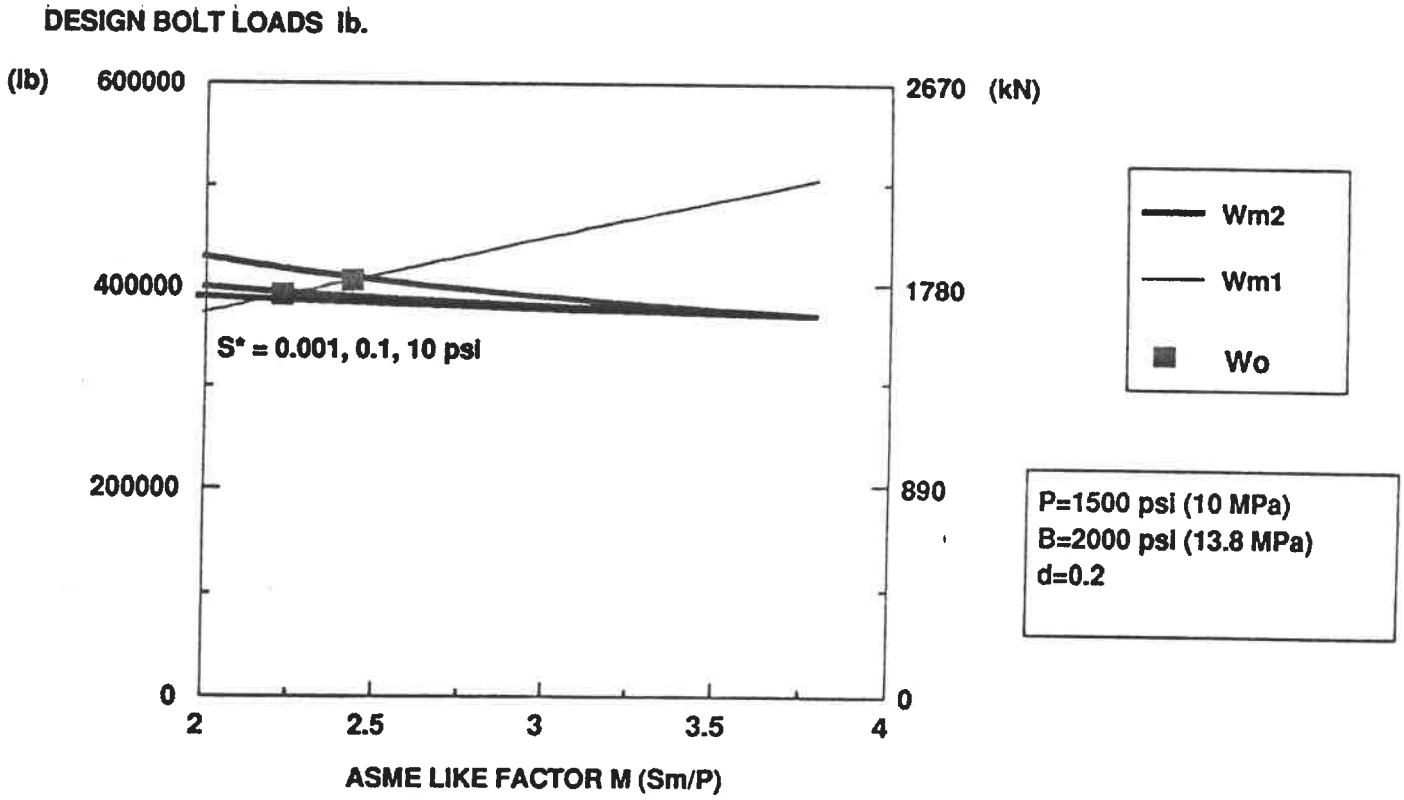

FIGURE 81 : Design Bolt loads Wm1 & Wm2 vs. factor M
(Effect of Gasket Factor S* at high pressure)

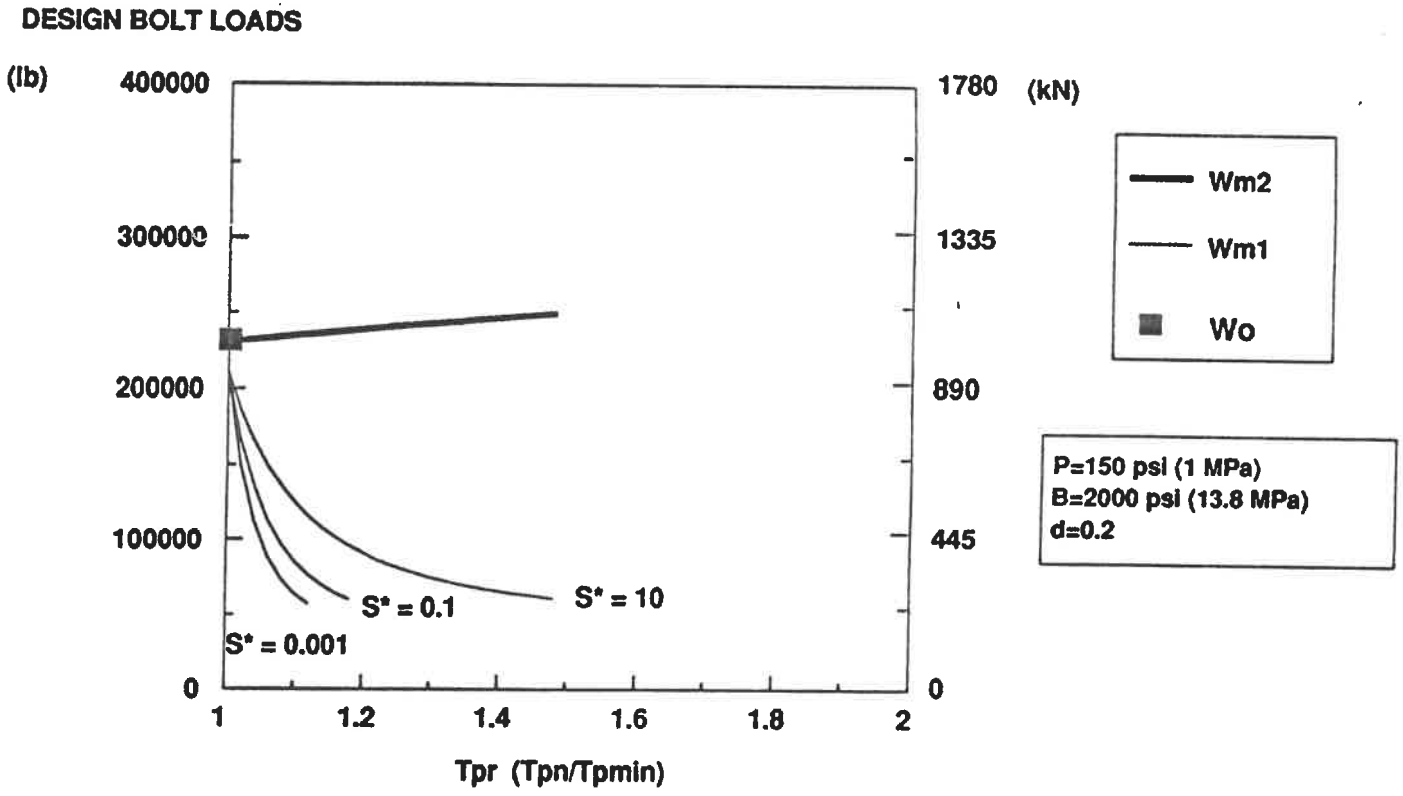

FIGURE 82 : Design Bolt loads Wm1 & Wm2 vs. Tightness Ratio Tpr
(Effect of Gasket Factor S* at low pressure)

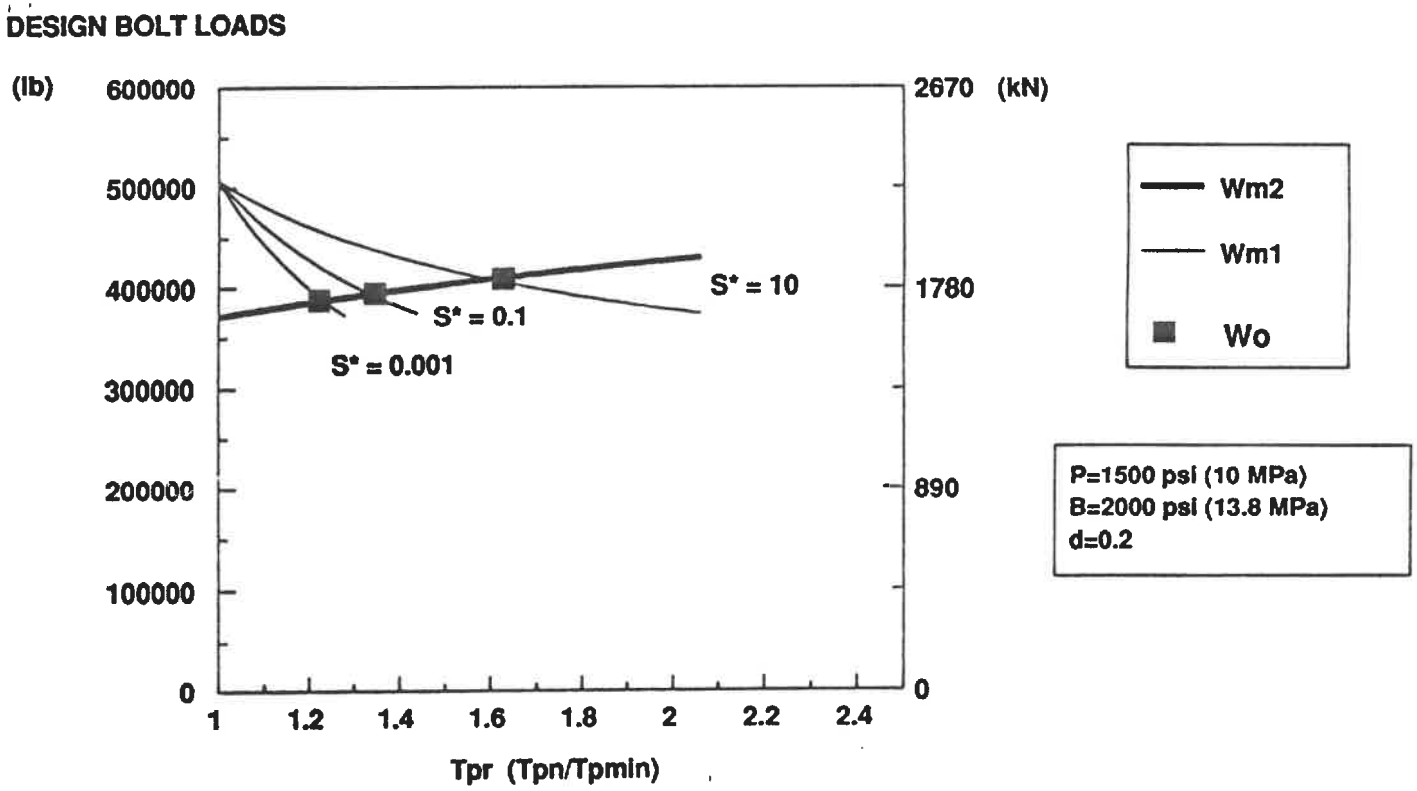

FIGURE 83 : Design Bolt loads Wm1 & Wm2 vs. Tightness Ratio Tpr (Effect of Gasket Factor S* at high pressure)

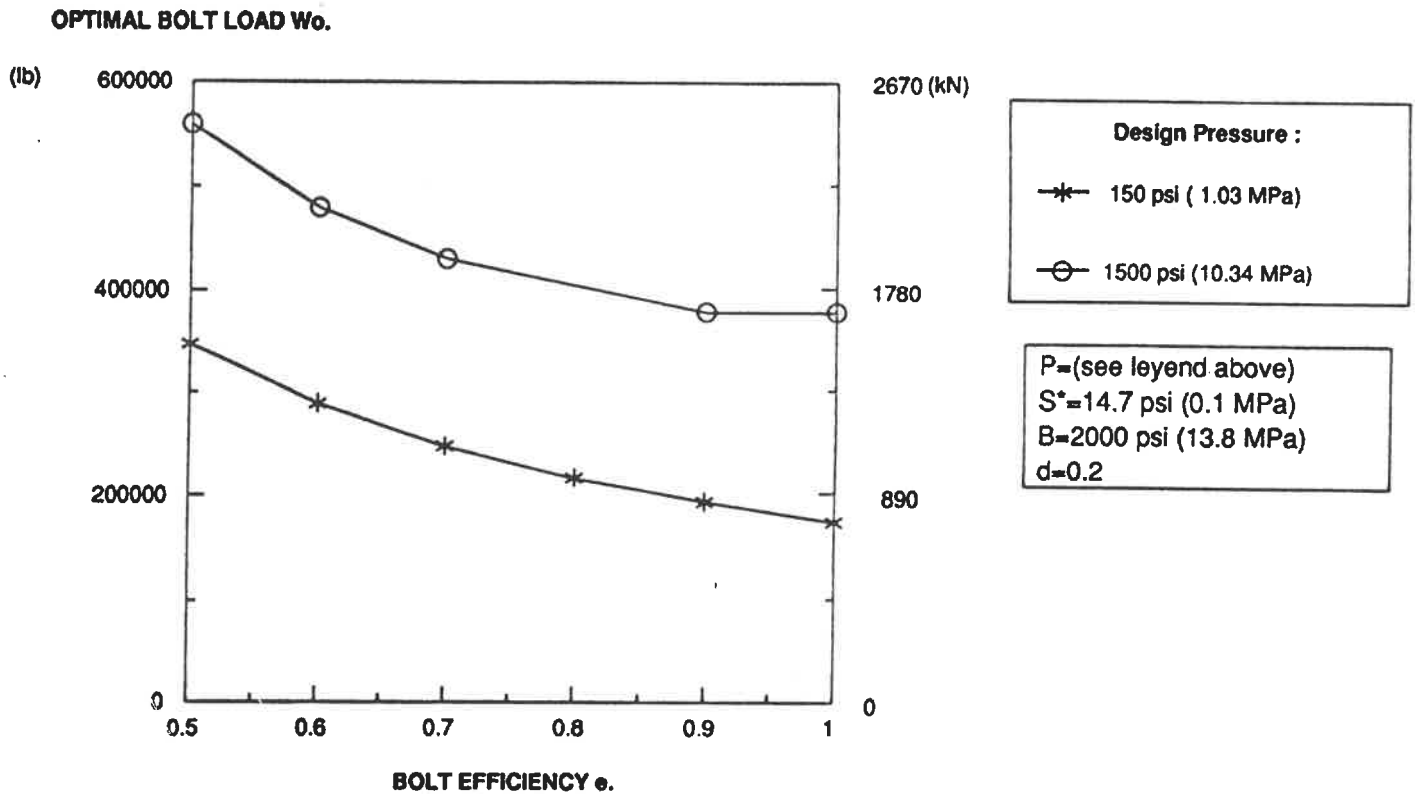

FIGURE 84 : Effect of Bolt Efficiency e on the optimal load Wo.
(Effect at high and low design pressure).

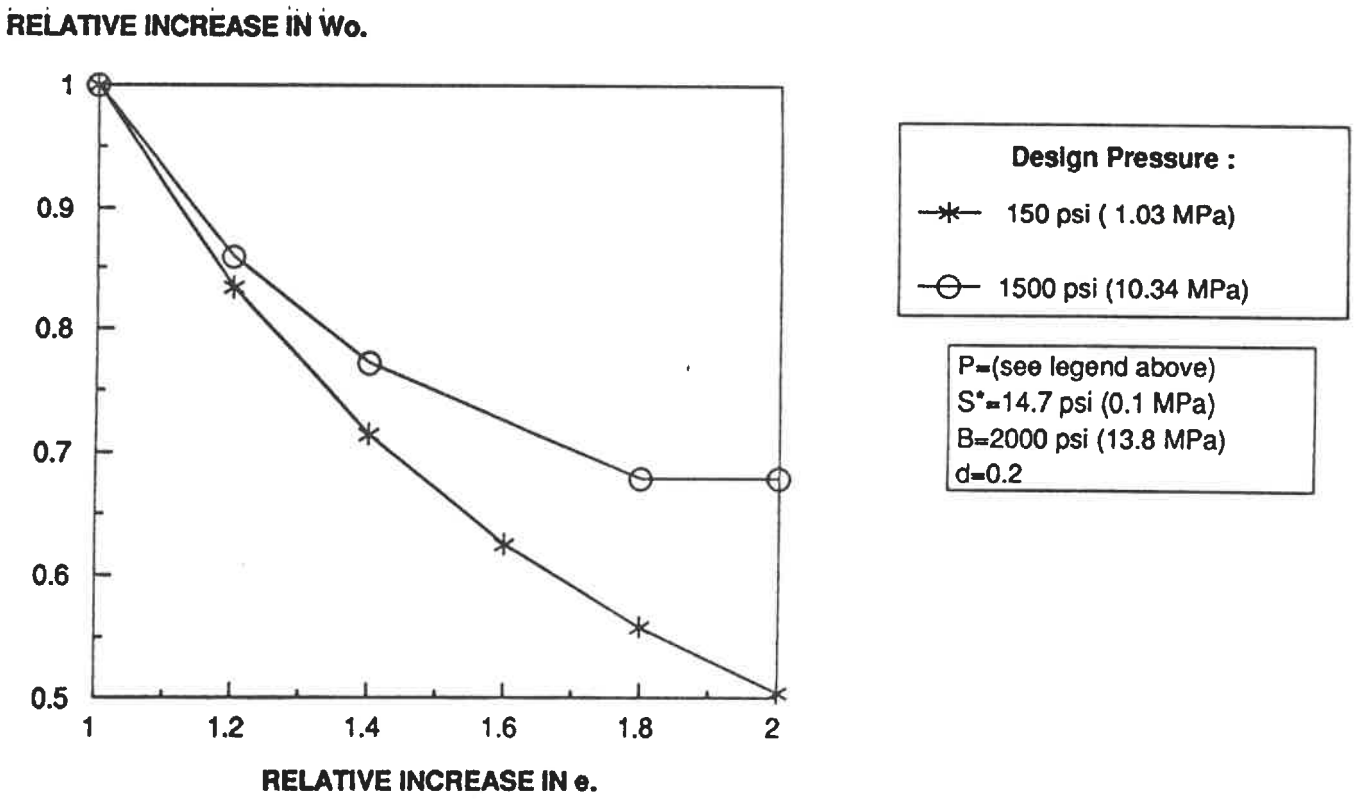

FIGURE 85 : Effect of Bolt Efficiency e on the optimal load Wo.
(Relative effect at high and low design pressure).

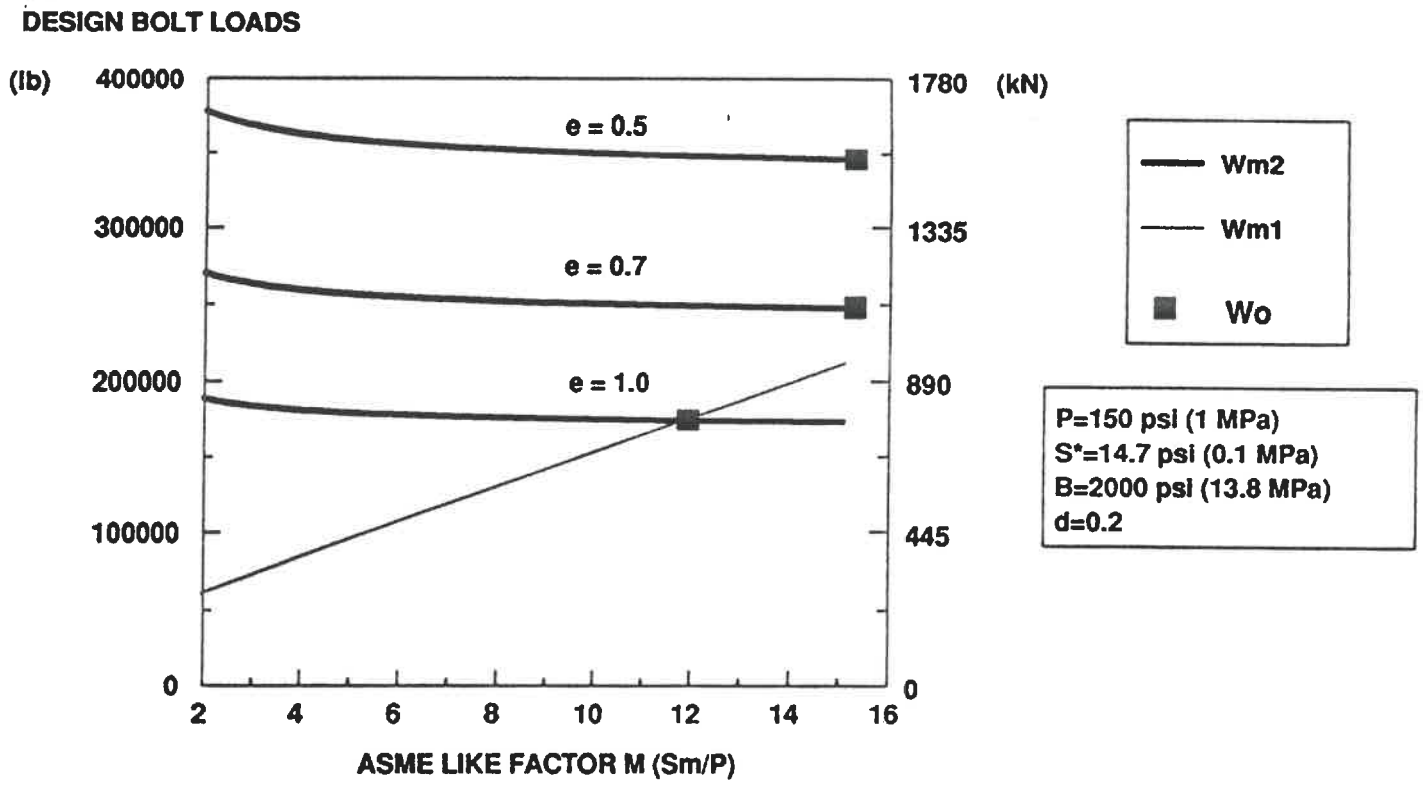

FIGURE 86 : Design Bolt loads Wm1 & Wm2 vs. factor M
(Effect of Bolt efficiency e at low pressure)

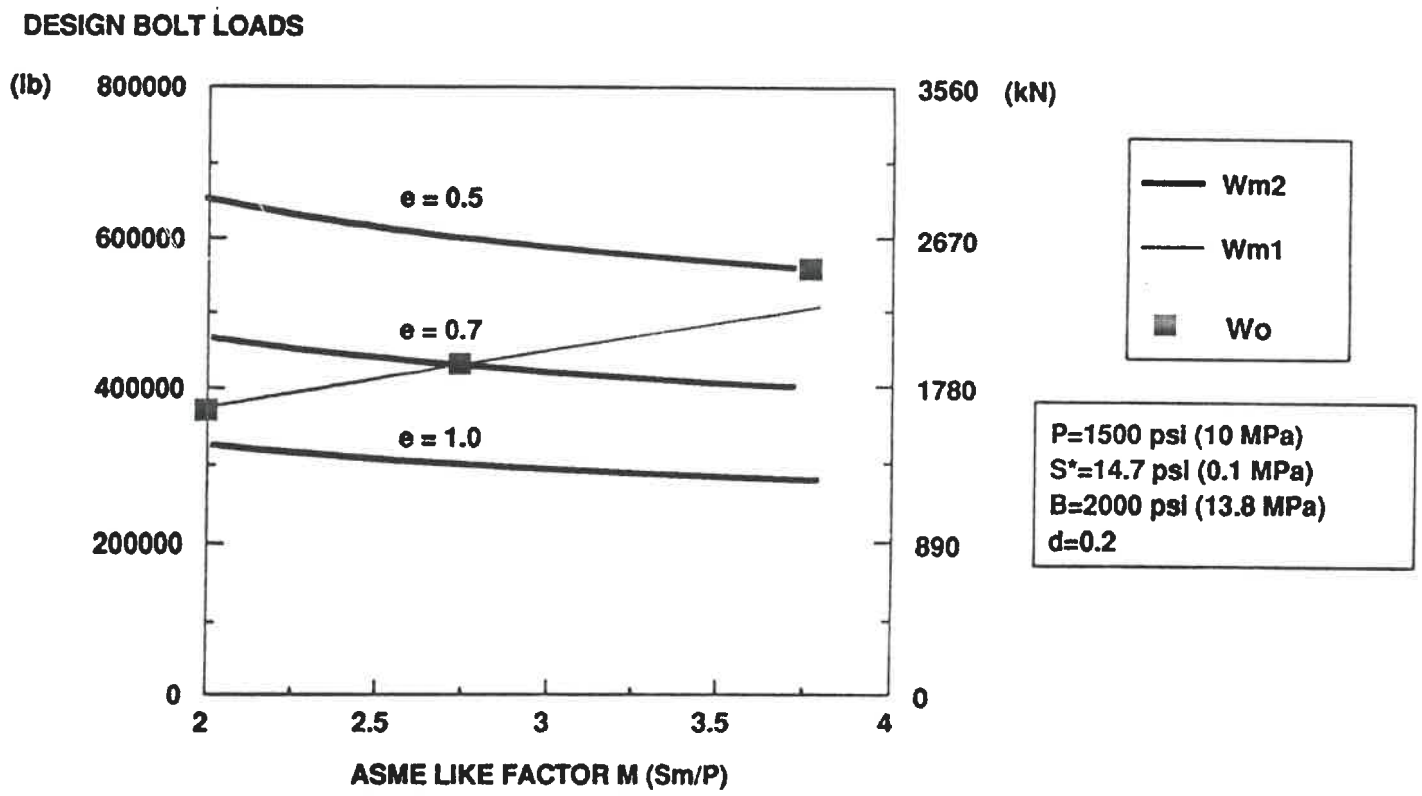

FIGURE 87 : Design Bolt loads Wm1 & Wm2 vs. factor M
(Effect of Bolt efficiency e at high pressure)

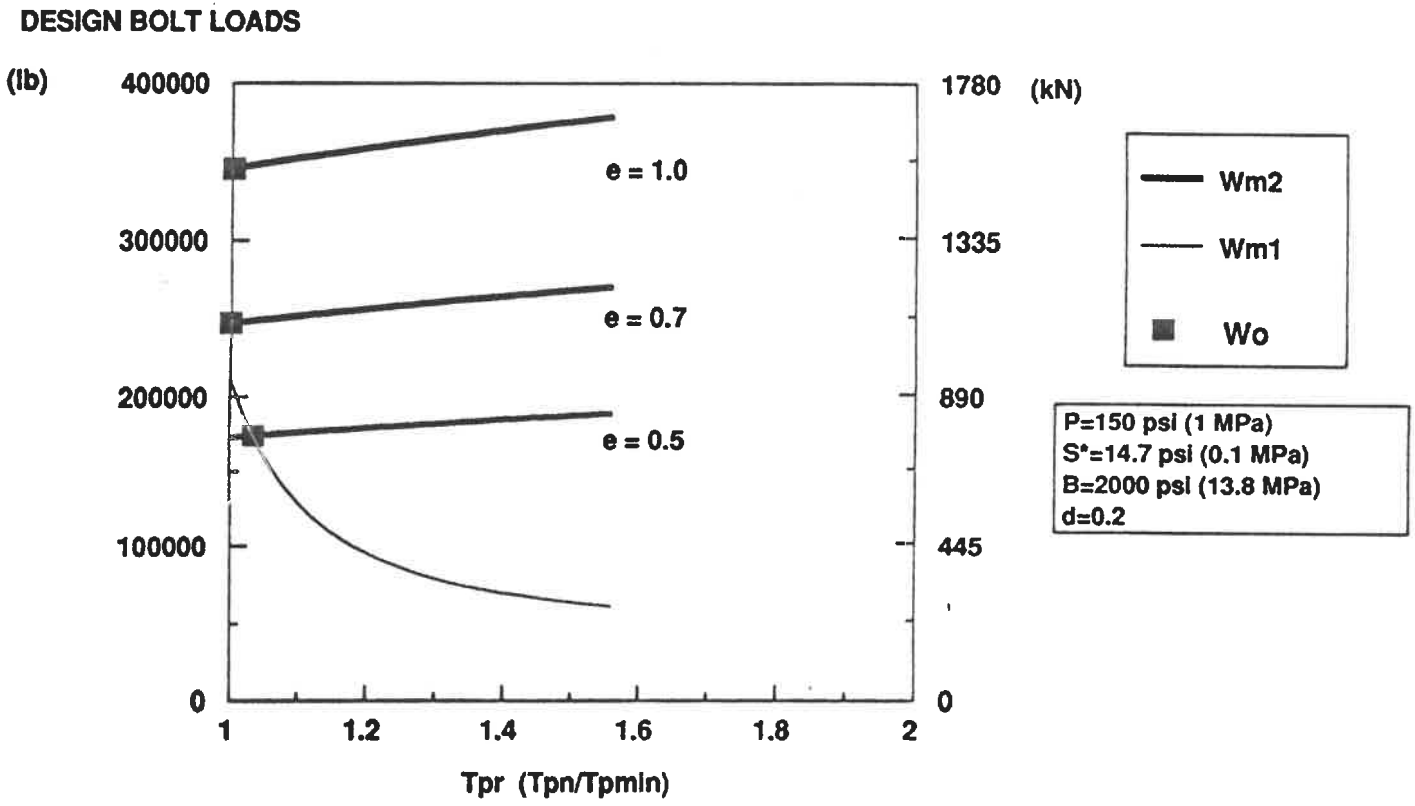

FIGURE 88 : Design Bolt loads Wm1 & Wm2 vs. Tightness Ratio Tpr (Effect of Bolt Efficiency e at low pressure)

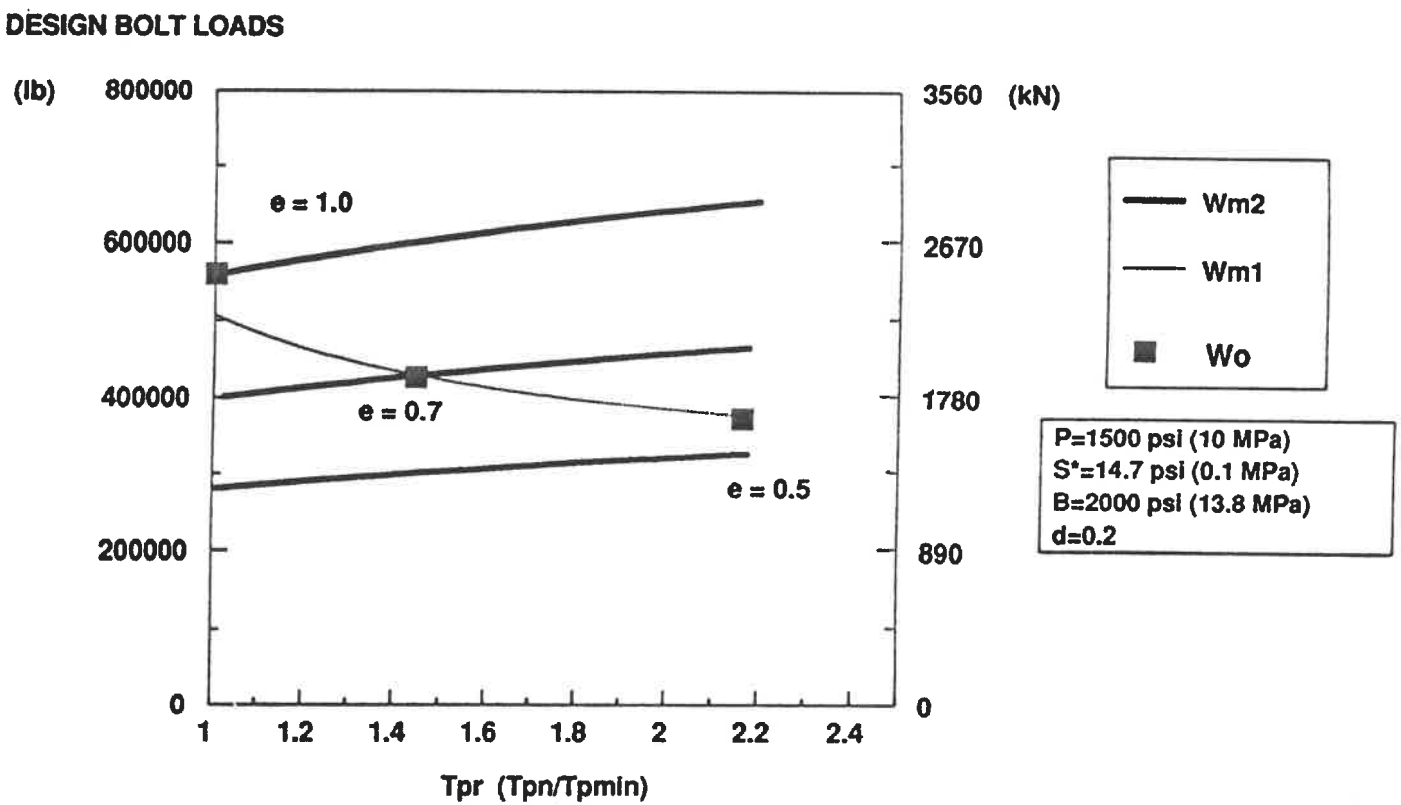

FIGURE 89 : Design Bolt loads Wm1 & Wm2 vs. Tightness Ratio Tpr
(Effect of Bolt Efficiency e at high pressure)

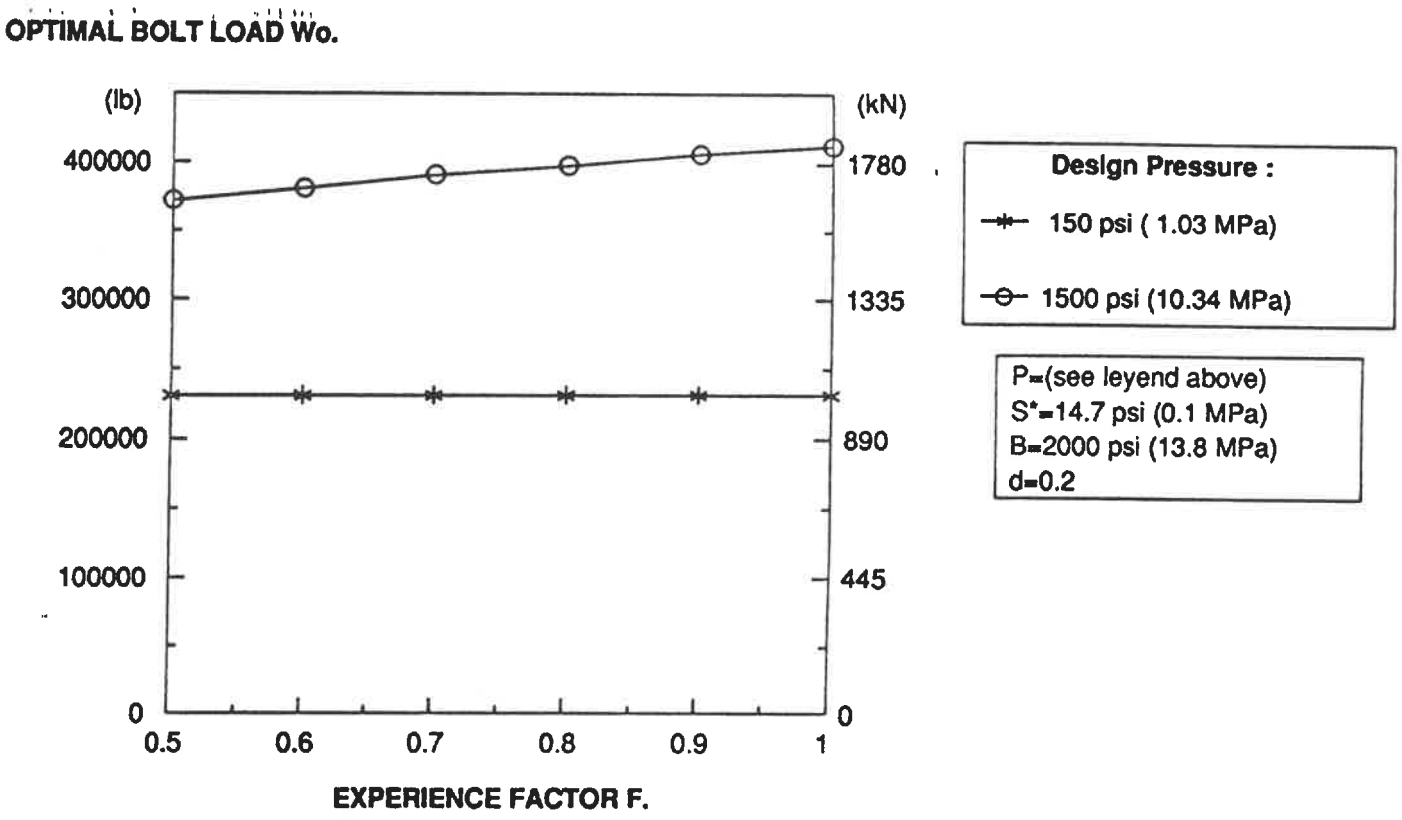

FIGURE 90 : Effect Experience Factor F on the optimal load Wo.

(Effect at high and low design pressure).

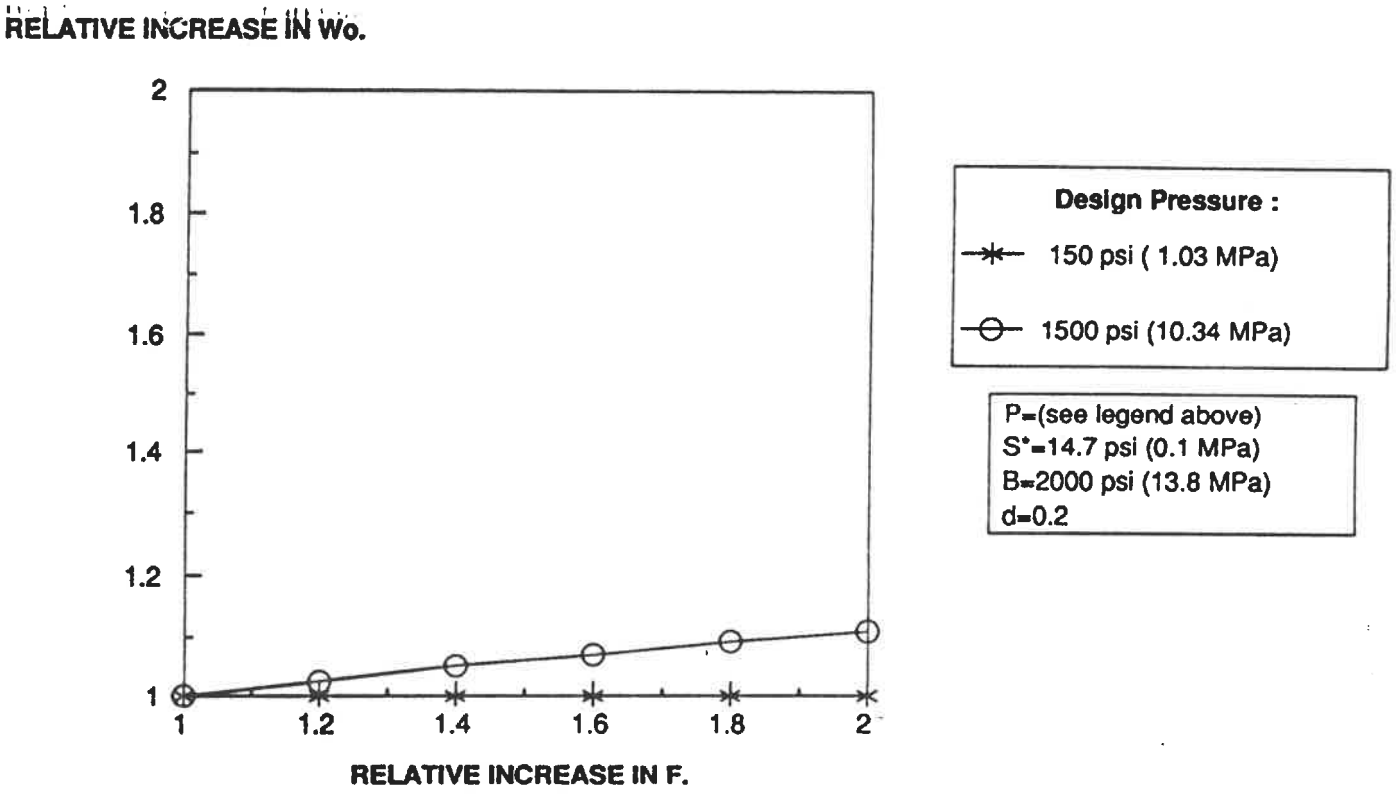

FIGURE 91 : Effect Experience Factor F on the optimal load Wo.
(Relative effect at high and low design pressure).

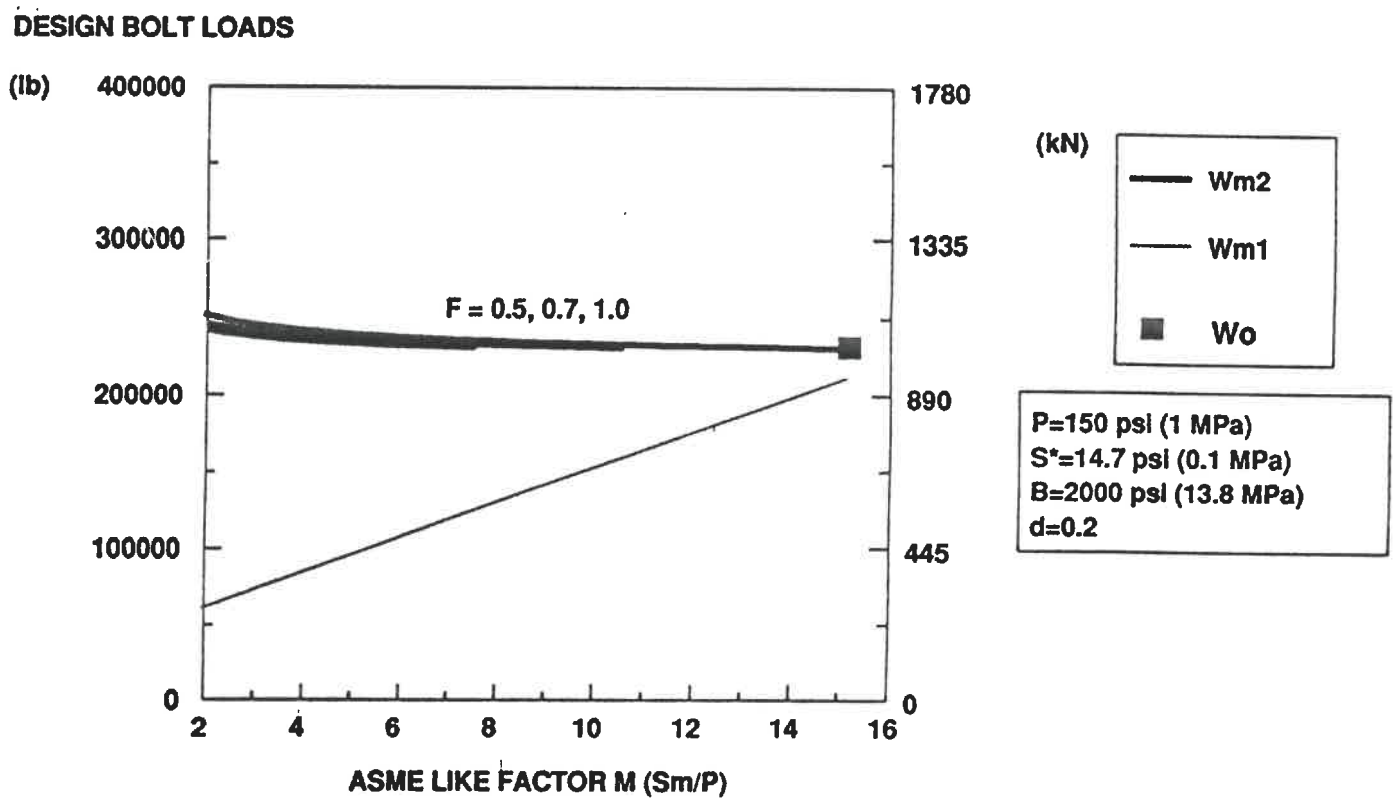

FIGURE 92 : Design Bolt loads Wm1 & Wm2 vs. factor M
(Effect of Experience Factor F at low pressure)

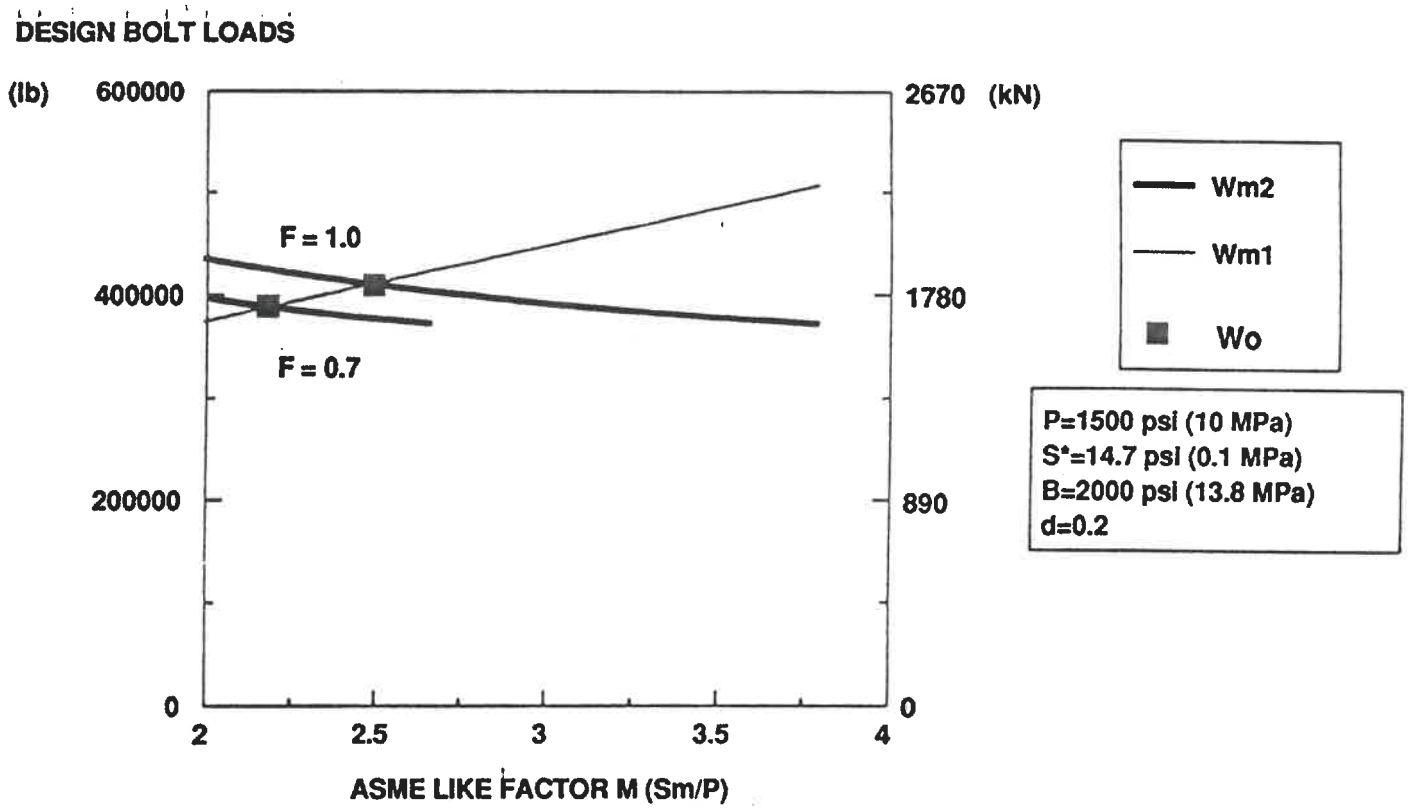

FIGURE 93 : Design Bolt loads Wm1 & Wm2 vs. factor M
(Effect of Experience Factor F at high pressure)

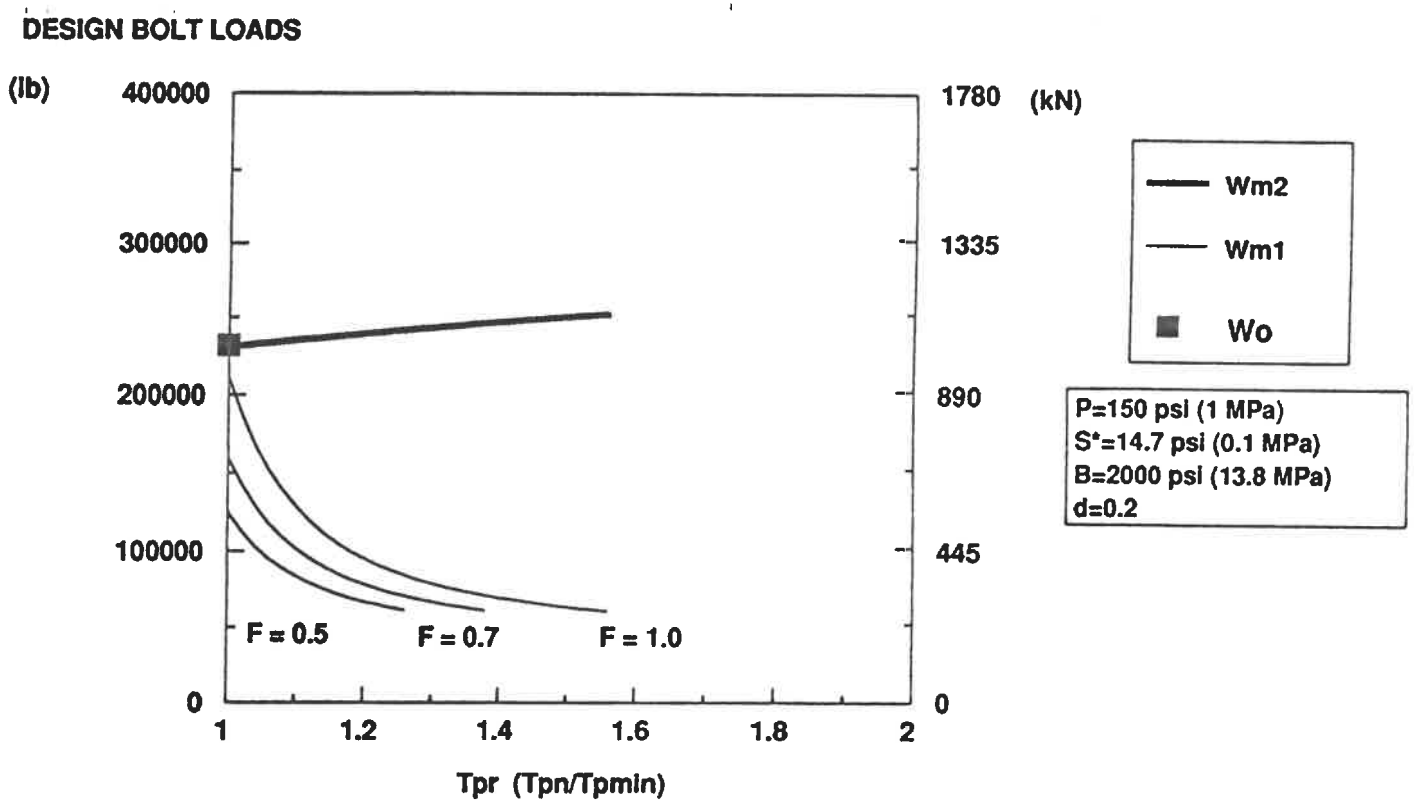

FIGURE 94 : Design Bolt loads Wm1 & Wm2 vs. Tightness Ratio Tpr
(Effect of Experience Factor F at low pressure)

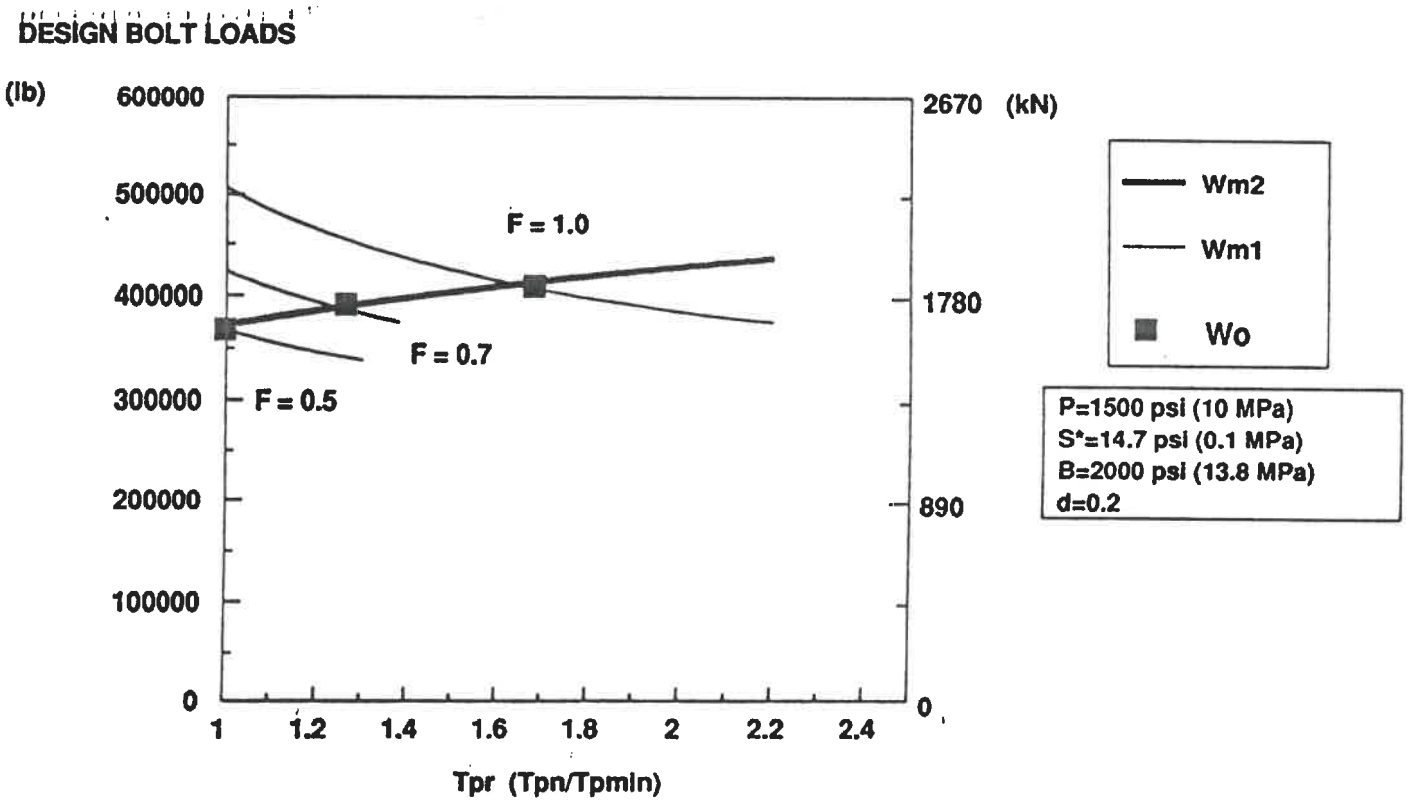

FIGURE 95 : Design Bolt loads Wm1 & Wm2 vs. Tightness Ratio Tpr
(Effect of Experience Factor F at high pressure)

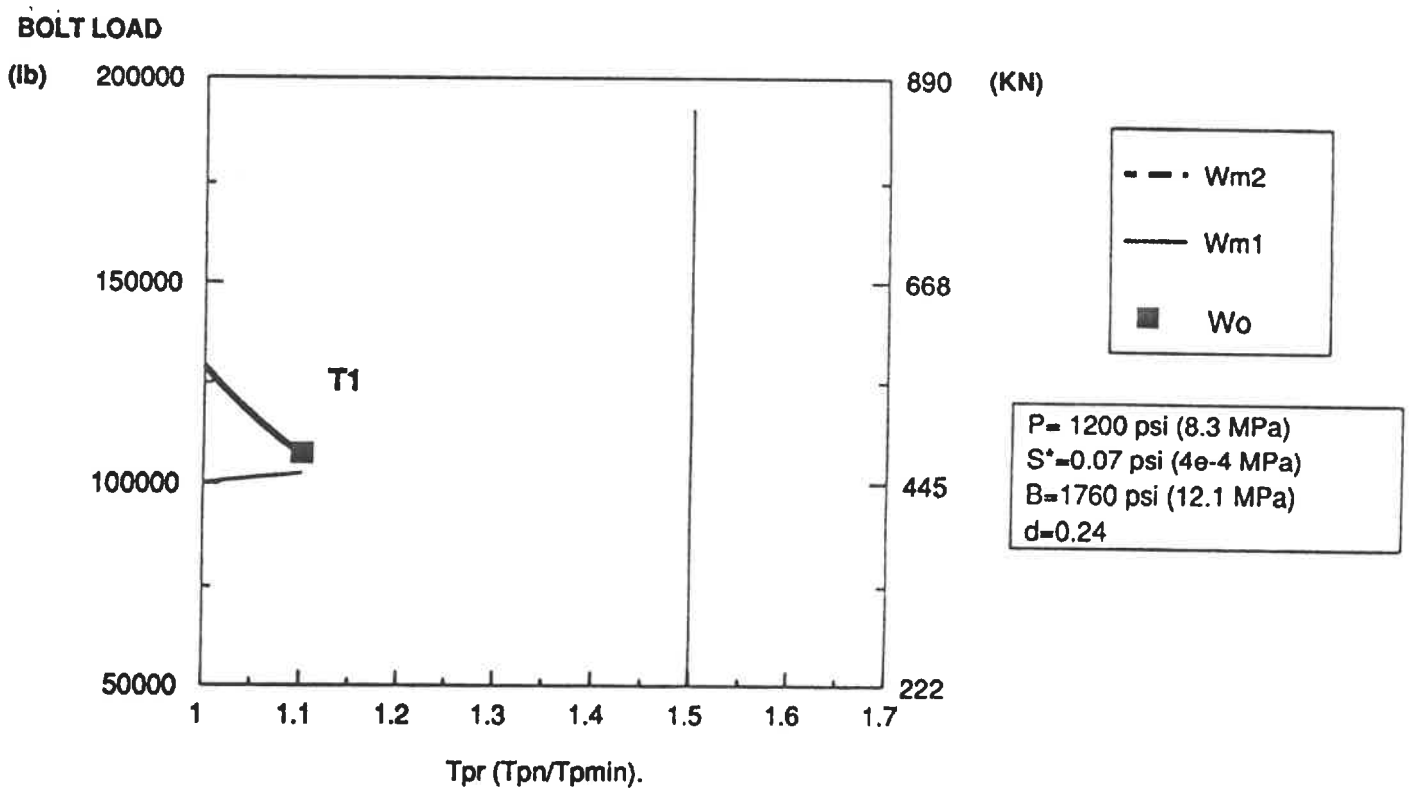

FIGURE 96 : Design bolt loads Wm1 & Wm2 vs tightness ratio Tpr.

(CASE I : Tpr = 1.5 Out of range)

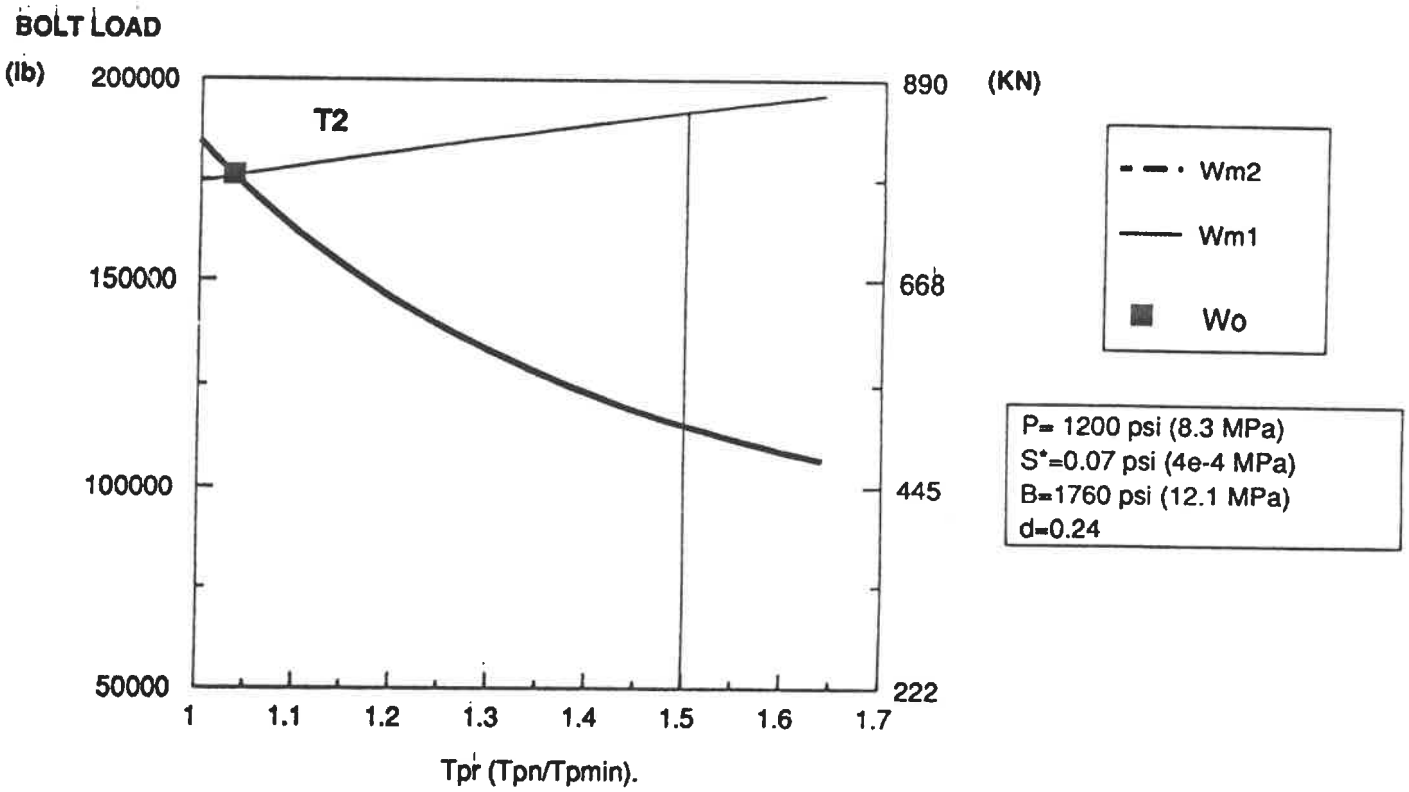

FIGURE 97 : Design bolt loads Wm1 & Wm2 vs tightness ratio Tpr
(CASE II : Tpr = 1.5, Approx. Solution > Optimal Solution)

9 REFFERENCES

1. BAZERGUI, A., MARCHAND, L., RAUT, H.D., "Development of a Production Test Procedure for Gaskets", WRC Bull. No. 309 (Nov. 1985).

2. BAZERGUI, A., MARCHAND, L., "A Test Procedure for Determining Room Temperature Properties of Gaskets", Proc. of the Pressure Vessels and Piping Conf., ASME, PVP-Vol.. 98.2, pp. 95-103.

3. PAYNE, J., BAZERGUI, A., LEON, G., "New Gasket Factors - A Proposed Procedure", Proc. of the 1985 Pressure Vessels and Piping Conf., ASME, PVP-Vol.. 98.2, pp. 85-93.

4. PAYNE, J., BAZERGUI, A., and LEON, G., "Getting New Design Constants from Gasket Tightness data", Experimental Techniques, Nov. 1988.

5. ASME Boiler and Pressure Vessel Code, Sec. VIII Div. 1, Am. Soc. Mech. Engrs.

6. BICKFORD, J.H., "An Introduction to the Design and Behavior of Bolted Joints", Marcel Deckker, Inc., 1981.

7. SOLER, A.I., "Analysis of Bolted Joints with Nonlinear Gasket Behavior",Trans. of the ASME, Vol. 102, pp 249-256 (Aug. 1980).

8. PAYNE, J. R., "Significance of Interim Recommended ASME Gasket Factors on Standard Flange Design", Paper presented at the International Symposium on Fluid Sealing, CETIM (Jun. 1986).

9. J PAYNE ASSOCIATES, "API/PVRC Exchanger Flange Study", Internal Report, (May. 1987).

10. NISHIOKA, K., MORITA, Y., KAWASHIMA, H., "Strength of Integral Pipe Flanges", Bull. of the JSME, Vol. 22, No. 174, pp 1705-1718 (Dec. 1976).

11. THOMPSON, J.C., SZE, Y., STREVEL, D.G., JOFRIET, J.C., "The Interface Boundary Conditions for Bolted Flanged Connections", Journal of Pressure Vessel Technology, Trans. of the ASME, pp 277-282 (Nov. 1976).

12. JOFRIET, J.C., SZE, Y., THOMPSON, J.C., "Further Studies of the interface Boundary Conditions for Bolted Flanged Connections", Journal of Pressure Vessel Technology, Trans. of the ASME, Vol. 103, pp 240-245 (Aug. 1981).

13. HAYASHI, K., CHANG, A.T., "Development of a Simple Finite Element Model for Elevated Temperature Bolted Flange Joint", Report submitted to the PVRC Joint Task Group on Elevated Temperature Behavior of Bolted Flanges (April 1986).

14. PAYNE, J., "Examples of Determination of ASME Code-like Bolt Load using PVRC Gasket Constants (B, d, S*)", S/C on Bolted Flanged Connections Subcommittee on Piping, Pumps and Valves PVRC (Oct. 1987).

15. DERENNE, M., BAZERGUI, A., MARCHAND, L., "Short Term Mechanical Tests at Elevated Temperature", Report submitted to the Joint Task Group on Elevated Temperature Behavior of Bolted Flanges (Oct. 1986).

16. BAZERGUI, A., "Results of Leakage Tests on One Gasket Style", Report submitted to Mr. J.R. Winter, Tenessee Eastman Co. Ref. CDT-7588S, Sec. Applied Mechanics, Dep. Mech. Eng., Ecole Polytechnique (Jul. 1987).

17. BAZERGUI, A., "Elevated Temperature Mechanical Tests on One Gasket Style", Report submitted to Mr. J.R. Winter, Tenessee Eastman Co. Ref. CDT-7588S, Sec. Applied Mechanics, Dep. Mech. Eng., Ecole Polytechnique (Jul. 1987).

18. AMERICAN NATIONAL STANDARD STEEL PIPE FLANGES AND FLANGES FITTINGS, ANSI B16.5-1977.

19. ABAQUS REFERENCE & USER'S MANUAL. Hibbitt, Kalrson and Sorensen, Inc. Finite Element Code. USA.

20. GIFTS CASA REFERENCE & USER'S MANUAL.

21. A. Bazergui, "Short term creep and relaxation behaviour of gaskets", Welding Research Council Bulletin. N.Y. WRC 294, May 1984, pp 9-22.

APPENDIX A

STRESS-DEFLECTION CURVE
GASKET: UCARB GHS

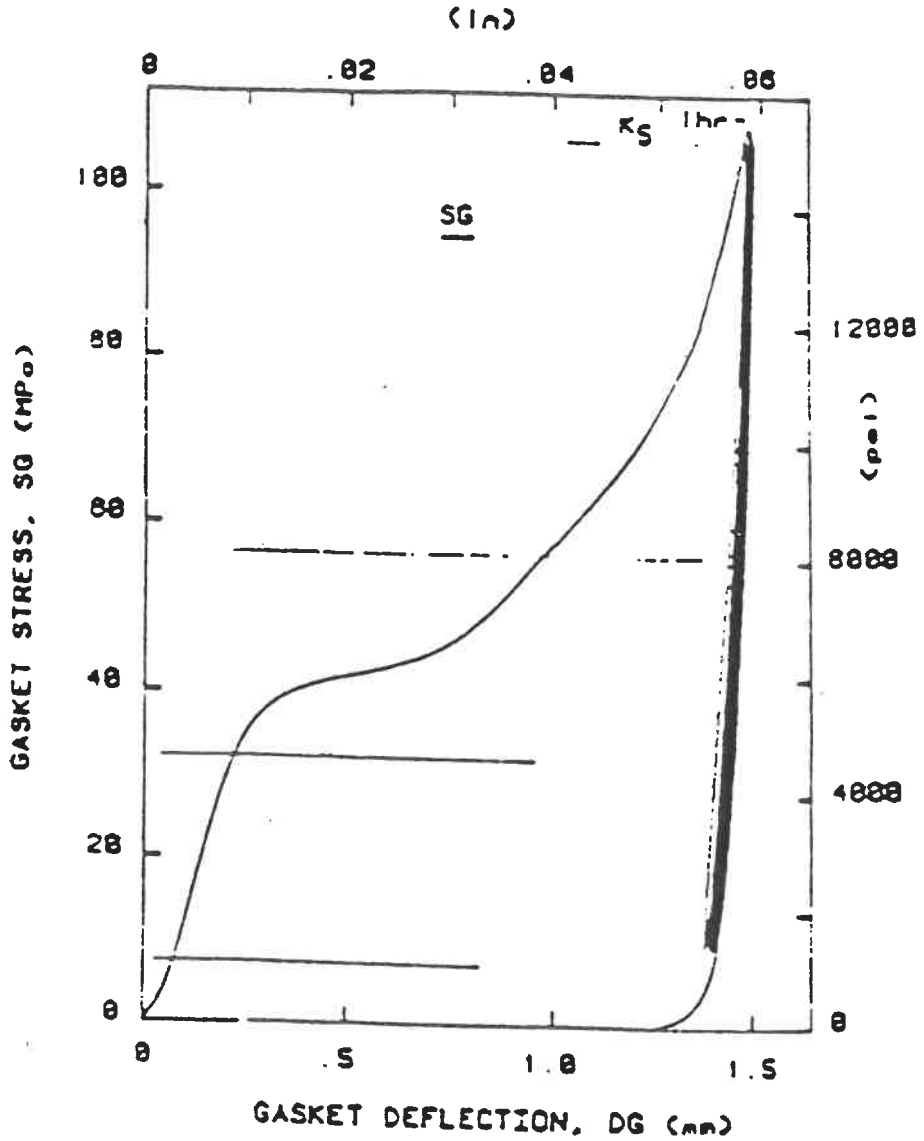

STRESS-DEFLECTION CURVE
GASKET: DJ MICA FILLED

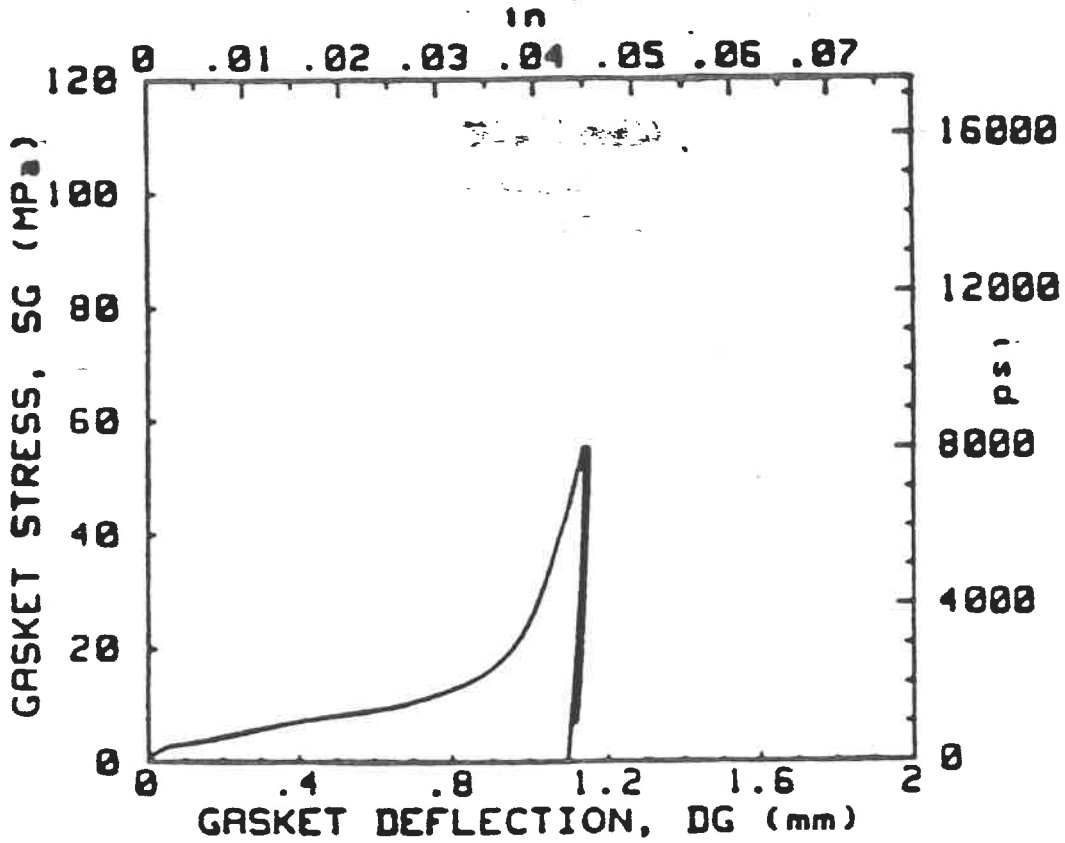

STRESS-DEFLECTION CURVE
GASKET: DJ ASBESTOS FILLED

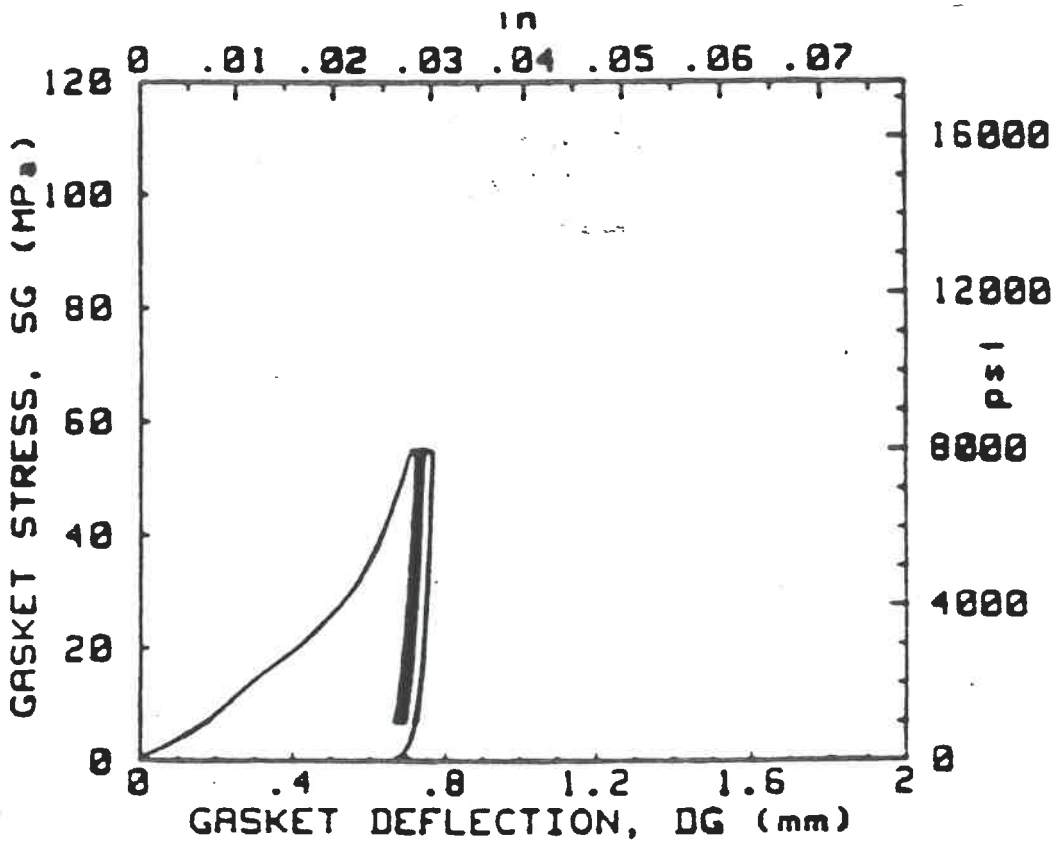

STRESS-DEFLECTION CURVE
GASKET: SELCO

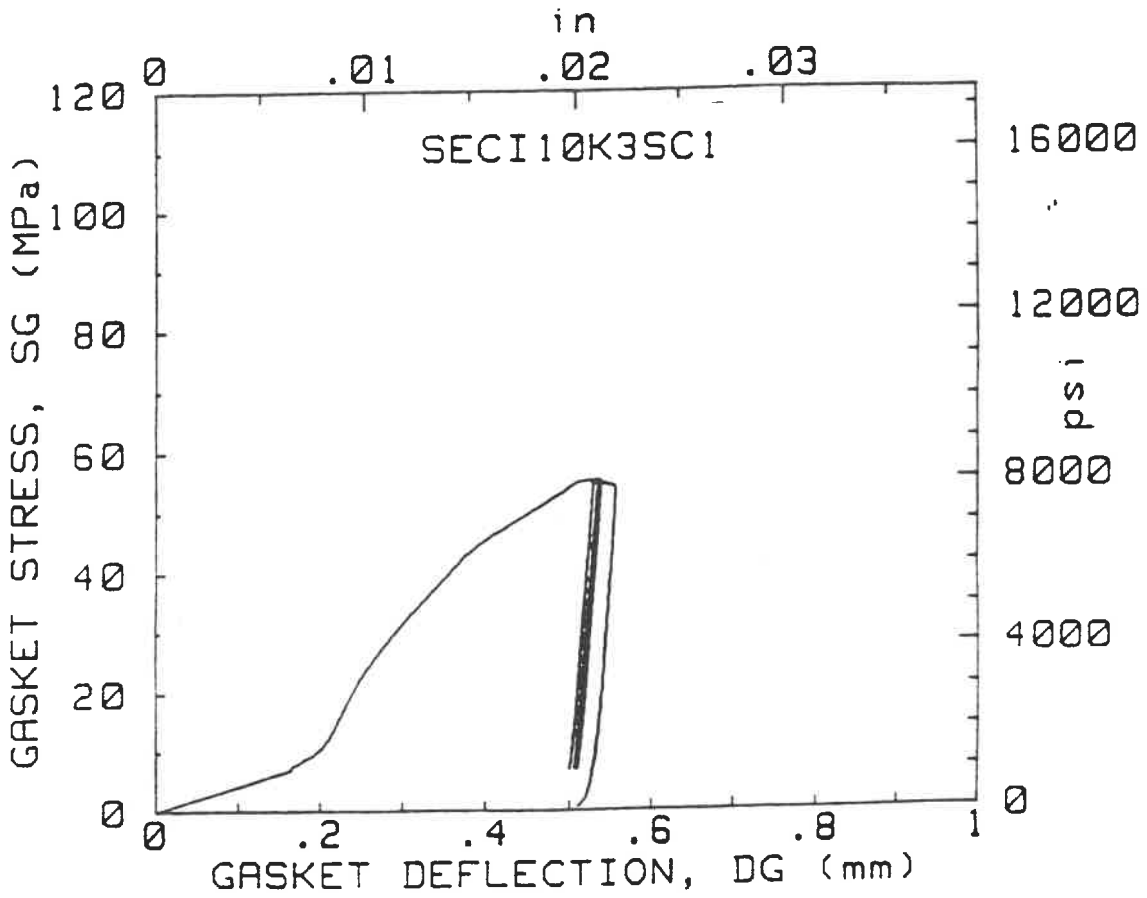

APPENDIX B

INPUT DATA FOR PROGRAM ABAQUS

RUN FILE TO EXECUTE ABAQUS PROGRAM : JOB CONTROL LANGUAGE (JCL).

```
/INC SOUMET.A.OS
//FL00 JOB (T5XBLW,HITSFL),'ALVARO',MSGLEVEL=(1,1),
//    MSGCLASS=A,CLASS=N,TIME=1439,REGION=7500K
/*JOBPARM L=99
/*ROUTE  PRINT MUSIC
//STEP01 EXEC ABQEDIT,TIMP=150
//INPUT.DATA DD *
/INCLUDE FL00:GHS15002.ABA
//*PRE.FT06F001  DD DUMMY
//PRE.FT13F001  DD UNIT=SYSDA,DISP=(NEW,PASS),DSN=&&DUMM2,
//    DCB=(RECFM=VBS,LRECL=16000,BLKSIZE=16004),SPACE=(CYL,(10,10))
//PRE.FT21F001  DD UNIT=&DISK,DCB=(RECFM=VBS,BLKSIZE=&B2,BUFNO=&BNO),
//    SPACE=(CYL,(10,10))
//PRE.FT25F001  DD UNIT=&DISK,DCB=(RECFM=FB,LRECL=8192,BLKSIZE=8192),
//    SPACE=(CYL,(10,10))
//PRE.FT26F001  DD UNIT=&DISK,DCB=*.FT25F001,SPACE=(CYL,(10,10))
//STEP02 EXEC ABAQRUN,TIMM=1400
//GO.FT02F001  DD UNIT=&DISK,SPACE=(CYL,(40,40))
//GO.FT13F001  DD DSN=&&DUMM2,DISP=(MOD,PASS)
//GO.FT19F001  DD DSN=&&T19,UNIT=&DISK,SPACE=(CYL,(10,10))
//GO.FT22F001  DD DSN=&&T22,UNIT=&DISK,SPACE=(CYL,(10,10))
//GO.FT24F001  DD DSN=&&T24,UNIT=&DISK,SPACE=(CYL,(10,10))
//GO.FT25F001  DD DSN=&&T25,UNIT=&DISK,SPACE=(CYL,(10,10))
//GO.FT26F001  DD DSN=&&T26,UNIT=&DISK,SPACE=(CYL,(10,10))
//*STEP03 EXEC ABAPLOT
//*FT13F001  DD DSN=&&DUMM2,DISP=(OLD,PASS)
//*TRACEUR   DD UNIT=INTRDR,SPACE=(TRK,(1)),DSN=&CALC1055
```

DATA FILE FOR ABAQUS : SEATING CONDITION

```
*HEADING
CLASS 1500-24 / GASKET:GHS / BOLT DISPLACEMENT= -13E-3  / POISSON=0.4
**
**
**
**
**        ||||||| GRID1 ||||||||||
**
```

```
*NODE
  1, 11.5 ,  21.0
  3, 11.5 ,  16.0
  7, 11.5 ,  8.0
 11, 11.5 ,  4.0
 13, 11.5 ,  3.0
 17, 11.5 ,  2.0
 25, 11.5 ,  1.0
 41, 11.5 ,  0.0
**
 165, 12.0 , 21.0
 167, 12.0 , 16.0
 171, 12.0 , 8.0
 175, 12.0 , 4.0
 177, 12.0 , 3.0
 181, 12.0 , 2.0
 189, 12.0 , 1.0
 205, 12.0 , 0.0
**
*NGEN
1, 165, 41
3, 167, 41
7, 171, 41
11, 175, 41
13, 177, 41
17, 181, 41
25, 189, 41
41, 205, 41
**
1, 3, 1
3, 7, 1
7, 11, 1
11, 13, 1
13, 17, 1
17, 25, 1
25, 41, 1
**
42, 44, 2
44, 48, 2
48, 52, 2
52, 54, 2
54, 58, 2
58, 66, 2
66, 82, 2
**
83, 85, 1
85, 89, 1
89, 93, 1
93, 95, 1
95, 99, 1
99, 107, 1
107, 123, 1
**
124, 126, 2
126, 130, 2
130, 134, 2
134, 136, 2
136, 140, 2
140, 148, 2
148, 164, 2
**
165, 167, 1
167, 171, 1
171, 175, 1
175, 177, 1
177, 181, 1
181, 189, 1
189, 205, 1
**
*ELEMENT, TYPE=CAX8R
1,1,3,85,83,2,44,84,42
*ELGEN, ELSET=GRID1
1,20,2,1,2,82,20
**
** ||||||| GRID2 |||||||
**
*NODE
6571,18.96, 8.0
6575,18.96, 4.0
*NGEN
171,6571,800
175,6575,400
6571,6575,1
**
172,6572,1600
173,6573,800
174,6574,1600
**
*ELEMENT, TYPE=CAX8R
44,171,173,1773,1771,172,973,1772,971
*ELGEN, ELSET=GRID2
44,2,2,1,4,1600,2
**
** |||||| GRID3 |||||||
**
*NODE
6577, 18.96, 3.0
**
*NGEN
175,6575,400
6575,6577,1
176,6576,800
177,6577,200
*ELEMENT, TYPE=CAX8R
52,175,177,977,975,176,577,976,575
*ELGEN, ELSET=GRID3
52,8,800,1,1
** |||| GRID4 ||||
*NODE
6581, 18.96, 2.0
*NGEN
6577,6581,1
178,6578,400
179,6579,200
180,6580,400
181,6581,100
```

```
*ELEMENT, TYPE=CAX8R
60,177,179,579,577,178,379,578,377
*ELGEN, ELSET=GRID4
60,2,2,1,16,400,2
**
** |||| GRID5 ||||
*NODE
6589, 18.96, 1.0
*NGEN
6581,6589,1
182,6582,200
183,6583,100
184,6584,200
185,6585,100
186,6586,200
187,6587,100
188,6588,200
189,6589,50
*ELEMENT,TYPE=CAX8R
92,181,183,383,381,182,283,382,281
*ELGEN, ELSET=GRID5
92,4,2,1,32,200,4
**
** |||| GRID 6 ||||
*NODE
6605, 18.96, 0.0
*NGEN
6589,6605,1
**
190,6590,100
191,6591,50
192,6592,100
193,6593,50
194,6594,100
195,6595,50
196,6596,100
197,6597,50
198,6598,100
199,6599,50
200,6600,100
201,6601,50
202,6602,100
203,6603,50
204,6604,100
205,6605,50
*ELEMENT, TYPE=CAX8R
220,189,191,291,289,190,241,290,239
*ELGEN, ELSET=GRID6
220,8,2,1,64,100,8
**
** ||| GRID7 |||
*NODE
7371, 20.04, 8.0
7375, 20.04, 4.0
7377, 20.04, 3.0
7381, 20.04, 2.0
7389, 20.04, 1.0
7405, 20.04, 0.0
*NGEN
7371,7375,1
7375,7377,1
7377,7381,1
7381,7389,1
7389,7405,1
**
6571,7371,100
6572,7372,200
6573,7373,100
6574,7374,200
6575,7375,100
6576,7376,200
6577,7377,100
6578,7378,200
6579,7379,100
6580,7380,200
6581,7381,100
6582,7382,200
6583,7383,100
6584,7384,200
6585,7385,100
6586,7386,200
6587,7387,100
6588,7388,200
6589,7389,100
**
6605,7405,100
**
6689,6705,2
6789,6805,1
6889,6905,2
6989,7005,1
7089,7105,2
7189,7205,1
7289,7305,2
*ELEMENT, TYPE=CAX8R
732,6571,6573,6773,6771,6572,6673,6772,6671
*ELGEN, ELSET=GRID7
732,17,2,1,4,200,17
**
** |||| GRID8 |||||
*NODE
7771, 23.0, 8.0
7775, 23.0, 4.0
7777, 23.0, 3.0
7781, 23.0, 2.0
7789, 23.0, 1.0
7805, 23.0, 0.0
*NGEN
7771,7775,1
7775,7777,1
7777,7781,1
7781,7789,1
7789,7805,1
```

```
**
7371,7771,50
7375,7775,50
7377,7777,50
7381,7781,50
7389,7789,50
7405,7805,50
**
7421,7425,2
7425,7427,2
7427,7431,2
7431,7439,2
7439,7455,2
**
7471,7475,1
7475,7477,1
7477,7481,1
7481,7489,1
7489,7505,1
**
7521,7525,2
7525,7527,2
7527,7531,2
7531,7539,2
7539,7555,2
**
7571,7575,1
7575,7577,1
7577,7581,1
7581,7589,1
7589,7605,1
**
7621,7625,2
7625,7627,2
7627,7631,2
7631,7639,2
7639,7655,2
**
7671,7675,1
7675,7677,1
7677,7681,1
7681,7689,1
7689,7705,1
**
7721,7725,2
7725,7727,2
7727,7731,2
7731,7739,2
7739,7755,2
**
*ELEMENT, TYPE=CAX8R
800,7371,7373,7473,7471,7372,7423,7472,7421
*ELGEN, ELSET=GRID8
800,17,2,1,4,100,17
**
**
** !!! GRID9 !!!
** ||||| BOLT RING |||
**
*NODE
38571,18.96,-17.0E-3
39371,20.04,-17.0E-3
**
*NGEN, NSET=B2
38571,39371,100
*NGEN
6571,38571,2000
7371,39371,2000
**
6671,38671,4000
6771,38771,2000
6871,38871,4000
6971,38971,2000
7071,39071,4000
7171,39171,2000
7271,39271,4000
**
*ELEMENT, TYPE=CAX8R
868,6571,10571,10771,6771,8571,10671,8771,6671
*ELGEN, ELSET=GRID9
868,8,4000,1,4,200,8
**
**
*MPC
**
** || LINE1 (GRID2 & GRID3)||
**
12,575,175,975
12,1375,975,1775
12,2175,1775,2575
12,2975,2575,3375
12,3775,3375,4175
12,4575,4175,4975
12,5375,4975,5775
12,6175,5775,6575
**
** || LINE2 (GRID3 & GRID4) ||
**
12,377,177,577
12,777,577,977
12,1177,977,1377
12,1577,1377,1777
12,1977,1777,2177
12,2377,2177,2577
12,2777,2577,2977
12,3177,2977,3377
12,3577,3377,3777
12,3977,3777,4177
12,4377,4177,4577
12,4777,4577,4977
12,5177,4977,5377
12,5577,5377,5777
12,5977,5777,6177
12,6377,6177,6577
```

```
**
** || LINE3 (GRID4 & GRID5) ||
**
12,281,181,381
12,481,381,581
12,681,581,781
12,881,781,981
12,1081,981,1181
12,1281,1181,1381
12,1481,1381,1581
12,1681,1581,1781
12,1881,1781,1981
12,2081,1981,2181
12,2281,2181,2381
12,2481,2381,2581
12,2681,2581,2781
12,2881,2781,2981
12,3081,2981,3181
12,3281,3181,3381
12,3481,3381,3581
12,3681,3581,3781
12,3881,3781,3981
12,4081,3981,4181
12,4281,4181,4381
12,4481,4381,4581
12,4681,4581,4781
12,4881,4781,4981
12,5081,4981,5181
12,5281,5181,5381
12,5481,5381,5581
12,5681,5581,5781
12,5881,5781,5981
12,6081,5981,6181
12,6281,6181,6381
12,6481,6381,6581
**
** || LINE4 (GRID5 & GRID6)
**
12,239,189,289
12,339,289,389
12,439,389,489
12,539,489,589
12,639,589,689
12,739,689,789
12,839,789,889
12,939,889,989
12,1039,989,1089
12,1139,1089,1189
12,1239,1189,1289
12,1339,1289,1389
12,1439,1389,1489
12,1539,1489,1589
12,1639,1589,1689
12,1739,1689,1789
12,1839,1789,1889
12,1939,1889,1989
12,2039,1989,2089
12,2139,2089,2189
12,2239,2189,2289
12,2339,2289,2389
12,2439,2389,2489
12,2539,2489,2589
12,2639,2589,2689
12,2739,2689,2789
12,2839,2789,2889
12,2939,2889,2989
12,3039,2989,3089
12,3139,3089,3189
12,3239,3189,3289
12,3339,3289,3389
12,3439,3389,3489
12,3539,3489,3589
12,3639,3589,3689
12,3739,3689,3789
12,3839,3789,3889
12,3939,3889,3989
12,4039,3989,4089
12,4139,4090,4189
12,4239,4189,4289
12,4339,4289,4389
12,4439,4389,4489
12,4539,4489,4589
12,4639,4589,4689
12,4739,4689,4789
12,4839,4789,4889
12,4939,4889,4989
12,5039,4989,5089
12,5139,5090,5189
12,5239,5189,5289
12,5339,5289,5389
12,5439,5389,5489
12,5539,5489,5589
12,5639,5589,5689
12,5739,5689,5789
12,5839,5789,5889
12,5939,5889,5989
12,6039,5989,6089
12,6139,6089,6189
12,6239,6189,6289
12,6339,6289,6389
12,6439,6389,6489
12,6539,6489,6589
**
** || TRIANGLE ||
**
*NODE
967,  12.870,  16.0
1767, 13.740,  16.0
1768, 13.740,  14.0
1769, 13.740,  12.0
2569, 14.610,  12.0
3369, 15.48 ,  12.0
3370, 15.48 ,  10.0
**
```

```
*NGEN
169,1769,800
1769,1771,1
**
*ELEMENT, TYPE=CAX8R
41,167,169,1769,1767,168,969,1768,967
42,169,171,1771,1769,170,971,1770,969
43,1769,1771,3371,3369,1770,2571,3370,2569
**
*ELSET, ELSET=TRIANG
41,42,43
**
**
**
*ELSET, ELSET=FLANGE
GRID1,GRID2,GRID3,GRID4,GRID5,GRID6,GRID7,GRI
D8,TRIANG
**
**
**
** || MATERIAL 1 (FLANGE) ||
**
*MATERIAL, ELSET=FLANGE
*ELASTIC
30E6,0.3
** || MATERIAL 2 (BOLT) ||
**
*MATERIAL, ELSET=GRID9
*ELASTIC
28E6,0.3
**
**
** || GRID10 (GASKET) ||
**
*NODE
207,12.0   ,-0.05
1707,13.631,-0.05
*NGEN , NSET=FIXED
207,1707,50
*NGEN
205,207,1
1705,1707,1
206,1706,100
207,1707,50
*ELEMENT, TYPE=CAX8R
900,205,207,307,305,206,257,306,255
*ELGEN, ELSET=GRID10
900,15,100
**
** || MATERIAL 3 (GASKET) ||
*MATERIAL, ELSET=GRID10
*ELASTIC
150E3, 0.4
*PLASTIC
300.0, 0.0
1025.0, 0.177
4560.0, 0.286
30000.0, 0.291
**
*NSET,NSET=CONTACT,GENERATE
205,2405,50
**
** || BOLT NSET & ELSET DEFINITIONS
*NSET,NSET=B1,GENERATE
7371,7771,50
**
*ELSET,ELSET=BOLTEND,GENERATE
875,899,8
**
** || BOUNDARY CONDITIONS ||
**
*BOUNDARY
FIXED,2
** || STEP DEFINITION - FIRST STEP ||
*STEP,CYCLE=20
*STATIC, PTOL=0.1
*BOUNDARY
B2,2,,-2E-3
*NODE PRINT
1,1,1,1,1,1,1,1
*EL PRINT
1,1,1,1,1
1,1,1,1,1,1
*END STEP
** || SECOND STEP ||
*STEP, CYCLE=20
*STATIC, PTOL=0.1
*BOUNDARY
B2,2,,-5E-3
*NODE PRINT
1,1,1,1,1,1,1,1
*EL PRINT
1,1,1,1,1
1,1,1,1,1,1
*END STEP
** || THIRD STEP ||
*STEP, CYCLE=30
*STATIC, PTOL=0.1
*BOUNDARY
B2,2,,-8E-3
*NODE PRINT
1,1,1,1,1,1,1,1
*EL PRINT
1,1,1,1,1
1,1,1,1,1,1
*END STEP
** || FOURTH STEP ||
*STEP, CYCLE=30
*STATIC, PTOL=0.1
*BOUNDARY
B2,2,,-10E-3
*NODE PRINT
1,1,1,1,1,1,1,1
*EL PRINT
1,1,1,1,1
1,1,1,1,1,1
*END STEP
```

```
** || LAST STEP ||
*STEP, CYCLE=30
*STATIC, PTOL=0.1
*BOUNDARY
B2,2,,-13E-3
*NODE PRINT, NSET=CONTACT
*NODE PRINT, NSET=FIXED
*NODE PRINT, NSET=B1
*NODE PRINT, NSET=B2
**
*EL PRINT, ELSET=GRID10,COORDS
*EL PRINT, ELSET=BOLTEND,COORDS
**
**PLOT
**DETAIL, ELSET=GRID10
**DISPLACED
*END STEP
```

```
DATA FILE FOR ABAQUS : OPERATING CONDITION
** || STEP DEFINITION - FIRST STEP ||
*STEP,CYCLE=20
*STATIC, PTOL=0.1
*BOUNDARY
B2,2,,-2E-3
*NODE PRINT
1,1,1,1,1,1,1,1
*EL PRINT
1,1,1,1,1
1,1,1,1,1,1
*END STEP
** || SECOND STEP ||
*STEP, CYCLE=20
*STATIC, PTOL=0.1
*BOUNDARY
B2,2,,-5E-3
*NODE PRINT
1,1,1,1,1,1,1,1
*EL PRINT
1,1,1,1,1
1,1,1,1,1,1
*END STEP
** || THIRD STEP ||
*STEP, CYCLE=30
*STATIC, PTOL=0.1
*BOUNDARY
B2,2,,-8E-3
*NODE PRINT
1,1,1,1,1,1,1,1
*EL PRINT
1,1,1,1,1
1,1,1,1,1,1
*END STEP
** || FOURTH STEP ||
*STEP, CYCLE=30
*STATIC, PTOL=0.1
*BOUNDARY
B2,2,,-10E-3
*NODE PRINT
1,1,1,1,1,1,1,1
*EL PRINT
1,1,1,1,1
1,1,1,1,1,1
*END STEP
** || LAST STEP ||
*STEP, CYCLE=30
*STATIC, PTOL=0.1
*BOUNDARY
B2,2,,-13E-3
*NODE PRINT, NSET=CONTACT
*NODE PRINT, NSET=FIXED
**
*EL PRINT, ELSET=GRID10,COORDS
*EL PRINT, ELSET=BOLTEND,COORDS
**
*END STEP
**
**
** || LOADING DUE TO PRESSURE ||
**
** || FIRST STEP ||
*STEP,CYCLE=30
*STATIC, PTOL=0.1
*DLOAD
SET1,P2,5000
*DLOAD
SET2,P1,500
*DLOAD
SET3,P2,500
*NODE PRINT
1,1,1,1,1,1,1,1
*EL PRINT
1,1,1,1,1
1,1,1,1,1,1
*END STEP
**
** || SECOND STEP ||
**
*STEP,CYCLE=30
*STATIC, PTOL=0.1
*DLOAD
SET1,P2,10000
*DLOAD
SET2,P1,1000
*DLOAD
SET3,P2,1000
*NODE PRINT
1,1,1,1,1,1,1,1
*EL PRINT
1,1,1,1,1
1,1,1,1,1,1
*END STEP
**
** || TRIRD STEP ||
**
*STEP, CYCLE=30
*STATIC, PTOL=0.1
*DLOAD
SET1,P2,16883
*DLOAD
SET2,P1,1500
*DLOAD
SET3,P2,1500
*NODE PRINT, NSET=CONTACT
*NODE PRINT, NSET=B1
*NODE PRINT, NSET=B2
**
*EL PRINT, ELSET=GRID10,COORDS
*EL PRINT, ELSET=BOLTEND,COORDS
**
**
*END STEP
```

INPUT DATA FOR PROGRAM GIFTS

```
1500-24
STDMAT
SSTEEL
1
ELMAT,3
2
15E3, 150E3, 0.4
STDMAT
MSTEEL
3
KPOINT
1/11.5,20.0
2/12.0,20.0
3/11.5,16.0
4/12.0,16.0
5/11.5,8.0
6/12.0,8.0
7/11.5,2.0
8/12.0,2.0
KPOINT
9/11.5,1.5
10/11.5,1.0
11/11.5,0.5
12/11.5,0.25
13/11.5,0.0
14/11.5,-0.0625
16/11.5,-0.125
KPOINT
17/15.0,8.0
KPOINT
19/15.0,2.0
20/15.0,1.5
21/15.0,1.0
22/15.0,0.5
23/15.0,0.25
24/15.0,0.0
25/15.0,-0.0625
27/15.0,-0.125
KPOINT
28/18.96,8.0
29/18.96,2.0
30/18.96,0.0
KPOINT
31/20.04,8.0
32/20.04,0.0
KPOINT
33/23.0,8.0
34/23.0,0.0
KPOINT
35/11.97,-0.125
36/13.615,-0.125
37/11.97,-0.175
38/13.615, -0.175
KPOINT
39/18.96, -0.16
40/20.04, -0.16
41/16.32,2.0
42/16.32,0.0
43/17.64,2.0
44/17.64,0.0
SLINE
L12/1,2,2
L24/2,4,2
L13/1,3,2
L46/4,6,3
L35/3,5,3
L68/6,8,4
L57/5,7,4
L78/7,8,2
SLINE
L79/7,9,2
L910/9,10,2
L1011/10,11,2
L1112/11,12,2
L1213/12,13,2
L1314/13,14,2
L1416/14,16,3
SLINE
L617/6,17,3
L1728/17,28,4
L819/8,19,3
SLINE
L1719/17,19,4
L1920/19,20,2
L2021/20,21,2
L2122/21,22,2
L2223/22,23,2
L2324/23,24,2
L2425/24,25,2
L2527/25,27,3
SLINE
L2829/28,29,4
L2930/29,30,2
L2831/28,31,5
L3032/30,32,5
SLINE
L3132/31,32,5
L3133/31,33,3
L3334/33,34,5
L3234/32,34,3
SLINE
L417/4,17,3
SLINE
L920/9,20,7
L1021/10,21,13
L1122/11,22,25
L1223/12,23,49
L1324/13,24,97
L1425/14,25,193
```

```
SLINE
L1635/16,35,27
L3536/35,36,91
L3638/36,38,3
L3537/35,37,3
L3738/37,38,91
L3627/36,27,77
SLINE
L1941/19,41,2
L4143/41,43,2
L4329/43,29,2
L2442/24,42,2
L4244/42,44,2
L4430/44,30,2
L4142/41,42,5
L4344/43,44,3
L2839/28,39,9
L3140/31,40,9
L3940/39,40,5
COMPLINE
L17/L13,L35,L57
L26/L24,L46
L28/L24,L46,L68
L628/L617,L1728
L829/L819,L1941,L4143,L4329
L719/L78,L819

L716/L79,L910,L1011,L1112,L1213,L1314,L1415,L1516
L1927/L1920,L2021,L2122,L2223,L2324,L2425,L2526,
L2627
L1627/L1635,L3536,L3627
L2830/L2829,L2930
L1929/L1941,L4143,L4329
L1924/L1920,L2021,L2122,L2223,L2324
CLASS
AXIS
GETY/QA4/1,1/GRID4
R1/L12,L28,L78,L17
R2/L628,L2829,L829,L68
R3/L2831,L3132,L3032,L2830
R4/L3133,L3334,L3234,L3132
R5/L1425,L2527,L1627,L1416
GETY/TA3/1,1/GRID3
TRIANG/L46,L617,L417
GETY/TA3/1,1/GRIDT
TRAN1/L719,L1920,L920,L79
TRAN2/L920,L2021,L1021,L910
TRAN3/L1021,L2122,L1122,L1011
TRAN4/L1122,L2223,L1223,L1112
TRAN5/L1223,L2324,L1324,L1213
TRAN6/L1324,L2425,L1425,L1314
TRAN7/L1941,L4142,L2442,L1924
TRAN8/L4143,L4344,L4244,L4142
TRAN9/L4329,L2930,L4430,L4344
GETY/QA4/3,1/GRID4
R6/L2831,L3140,L3940,L2839
GETY/QA4/2,1/GRID4
R7/L3536,L3638,L3738,L3537
KN
GNAM/PLOT
quit
```

APPENDIX C

CASE I : RESULTS FROM *CURRENT CODE (Ref. [9])*.

API/PVRC EXCHANGER FLANGE STUDY — J Payne — September 1986

CALCULATIONS BY ASME CODE METHOD

1 DESIGN CONDITIONS		2 GASKET	FACE	3 FROM Fig UA-49
Design Pressure, P	925 PSIG	DJ MICA FILLED	FLAT FACE	h_G = 21/32"
Design Temperature	530 °F	ANALYSIS: 1/8X44 3/4X43 3/8	44 3/4" O.D. X 42" I.D.	b = .2864"
Flange Material	SA-105	PVRC TEST: 1/8X43 3/8X53 3/8	ORIG. W/NUBBIN	G = 44.115"
Bolting Material	A-193-B7			t = 3.2860
Corrosion Allowance	1/8"			g = 2.00

4 LOAD AND BOLT CALCULATIONS

Allowable Stress	Flange	Design Temp. S_{fd}	17500	$W_{m1} = bG\pi S_{fd}$ = 1304300
		Air Temp. S_{fa}	17500	$H_p = 2b\pi G m P$ = 146860
	Bolting	Design Temp. S_{bd}	25000	$H = G^2\pi P/4$ = 1413850
		Air Temp. S_{ba}	25000	$W_{m2} = H_p + H$ = 1560710

$A_m = \frac{\text{greater}}{S_{bd}}$ W_{m1}/S_{bd} or W_{m2}/S_{ba} = 62.43

A_b = 73.92

$W = S_{bd}A_m = A_bS_{ba}$ = 1704370

CONDITION	LOAD		LEVER ARM		MOMENT	
5 Operating	$H_T = H - H_D$ =	1296830	$h_T = R - g_0$ =	2 15/16"	$M_T = H_Th_T$ =	3809440
	$H_G = W_{m1} - H$ =	146860	$h_G = B/2 - G$ =	2 13/16"	$M_G = H_Gh_G$ =	413810
	$H_D = H - H_G$ =	1170200	$h_D = R + g_1 - B/2$ =	3 9/32"	$M_D = H_Dh_D$ =	3842260
					M_o =	4607510
Seating	$H_G = W$ =	1704370	$h_G = B/2 - G$ =	2 13/16"	M_G =	4793540

8 STRESS CALCULATION—Operating

1.5 S_{fd}	Long. Hub. $S_H = f M_o/Lg_1^2$	=	22080
S_{fd}	Radial Flg. $S_R = \beta M_o/Lt^2$	=	2770
S_{fd}	Tang Flg. $S_T = Y M_o/t^2 - ZS_R$	=	10160
S_{fd}	$\frac{S_H+S_R}{2}$ or $\frac{S_H+S_T}{2}$	=	16120

9 STRESS CALCULATION—seating

1.5 S_{fa}	Long. Hub. $S_H = f M_G/Lg_1^2$	=	22970
S_{fa}	Radial Flg. $S_R = \beta M_G/Lt^2$	=	2880
S_{fa}	Tang Flg. $S_T = Y M_G/t^2 - ZS_R$	=	10570
S_{fa}	$\frac{S_H+S_R}{2}$ or $\frac{S_H+S_T}{2}$	=	16770

6 K AND HUB FACTORS

$K = A/B$	= 1.25	h/h_o	= .30
f	= 1.82	f	= .89
Z	= 4.56	V	= .46
Y	= 8.83	f	= 1.00
U	= 9.70	$e = F/h_o$	= .117
g_1/g_0	= 1.18	$d = \frac{U}{V}h_og_0^2$	= 303.8
$h_o = \sqrt{Bg_0}$	= 7.62		

7 STRESS FORMULA FACTORS

T	=	6.15
$Q = Z/T + 1$	=	1.76
$\delta = d^3/(52.14\,V) + 1$	=	2.01
$\gamma = e/T$	=	.97
$\beta = 1/d$	=	.90
$\lambda = \gamma + \beta$	=	1.87
$m_o = M_o/B$ = operating =		109053
$m_G = M_G/B$ = seating =		113456

If bolt spacing exceeds $2a + t$, multiply m_o and m_G in above equations by: $\sqrt{\frac{\text{Bolt spacing}}{2a + t}}$

* CORRODED

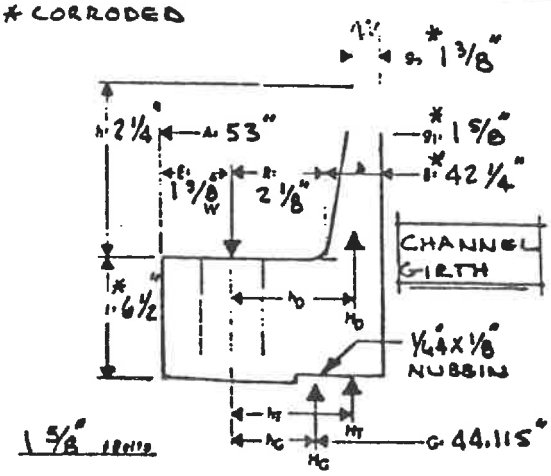

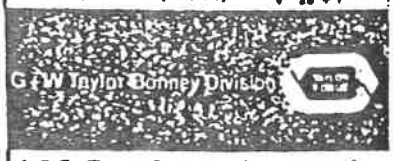

API-PVRC EXCH. CASE:
TIGHTNESS: STD CLASS 150
ASSEMBLY EFF: e = 1.0

CASE II : RESULTS FROM *CURRENT CODE (Ref. [9])*.

API/PVRC EXCHANGER FLANGE STUDY — J Payne — September 1986

CALCULATIONS BY ASME CODE METHOD

1 DESIGN CONDITIONS		2 GASKET	FACE	3 FROM Fig. UA-48
Design Pressure, P	120 PSIG	DJ MICA FILLED	FLAT FACE	h_G = 21/32"
Design Temperature	650°F	ANALYSIS: 1/8 X 44 3/4 X 42 7/8	44 1/4" O.D. X 42" I.D	b = .2864
Flange Material	SA-105	PVRC TEST: 1/8 X 43 3/8 X 5 3/8	ORIG. W/NUBBIN	G = 43.661
Bolting Material	A-193-B7			t_f = 1.3840
Corrosion Allowance	1/16"			t_n = 2.8.15

4 LOAD AND BOLT CALCULATIONS

Flange	Design Temp. S_a	17500	$W_{m1} = bGy$ = 542910	$A_b = \frac{\text{Max}(W_{m1}/S_a, W_m)}{S_a}$ = 21.72
	Atm. Temp. S_a	17500	$H_p = 2b\pi G m P$ = 265110	A_m = 13.29
Bolting	Design Temp. S_a	25000	H = 179270	$W = SA_b - A_m S_a$ = 437550
	Atm. Temp. S_a	25000	$W_{m2} = W_m - H$ = 444380	

CONDITION	LOAD	LEVER ARM	MOMENT
5 Operating	$H_D = \pi B^2 P/4$ = 167240	$h_D = R + g_1/2$ = 1.531	$M_D = H_D h_D$ = 256100
	$H_G = W_{m1} - H$ = 265110	$h_G = \frac{B+G}{4}$ = 1.068	$M_G = H_G h_G$ = 283220
	$H_T = H - H_D$ = 12030	$h_T = \frac{R + g_1 + h_G}{2}$ = 1.440	$M_T = H_T h_T$ = 17320
			M_t = 556650
Seating	$H_G = W$ = 437550	$h_G = \frac{B+G}{4}$ = 1.068	M_s = 467440

8 STRESS CALCULATION—Operating

1.5 S_a	Long. Hub. $S_H = f M_o/\lambda g_1^2$	= 37690
S_a	Radial Flg. $S_R = \beta M_o/t^2$	= 3810
S_a	Tang. Flg. $S_T = M_o Y/t^2 - 2S_R$	= 10560
S_a	$\frac{S_H+S_R}{2}$ or $\frac{S_H+S_T}{2}$ or $\frac{S_R+S_T}{2}$	= 24130

9 STRESS CALCULATION—Seating

1.5 S_a	Long. Hub. $S_H = f M_s/\lambda g_1^2$	= 31650
S_a	Radial Flg. $S_R = \beta M_s/t^2$	= 3200
S_a	Tang. Flg. $S_T = M_s Y/t^2 - 2S_R$	= 8870
S_a	$\frac{S_H+S_R}{2}$ or $\frac{S_H+S_T}{2}$ or $\frac{S_R+S_T}{2}$	= 20260

6 K AND HUB FACTORS

$K = A/B$	= 1.125	h/h_o	= .291
T	= 1.870	f	= .885
Z	= 8.550	e	= .426
Y	= 16.53	f	= 1.000
U	= 18.18	$e = F/h_o$	= .206
F	= 1.286	$d = \frac{U}{V} h_o g_1^2$	= 35.06
$h_o = \sqrt{Bg_1}$	= 4.293		

7 STRESS FORMULA FACTORS

f	= 2.25	
$\alpha = \pi/4 + 1$	= 1.464	
$\beta = 4/3\,\pi + 1$	= 1.618	
$\gamma = \alpha - \beta$	= .783	
$\delta = \beta/\alpha$	= .325	
$\lambda = \gamma + \delta$	= 1.108	L
$M_o = M_t/B$ = operating	= 3210	
$M_s = M_s/B$ = seating	= 11100	

If bolt spacing exceeds $2a + t$, multiply M_o and M_s in above equations by $\sqrt{\frac{\text{Bolt spacing}}{2a+t}}$

* CORRODED

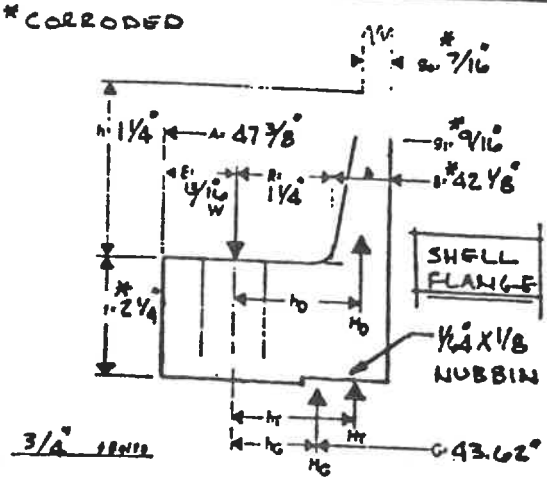

G&W Taylor Bonney Division

API-PVRC EXCH. CASE:
TIGHTNESS: STD (CLASS T2)
ASSEMBLY EFF: e = 1.0

CASE I : RESULTS FROM *TurboFlange.*

Calculations using ***TurboFlange*** with equivalent data as CASE I above.

TurboFlange V:1.0 INFORMATION SHEET.
IMPERIAL UNITS : IN-PSI-LB

DATA PAGE-1

- MODEL DATA -

MODEL NAME	PAYNE1	COMMENTS	TF vs CURRENT CODE 1.
FLANGE MAT.		GASKET MAT.	
OP. PRESSURE	925.00	OP. TEMPERATURE	530.00
CORROSION ALLOW.	0.13		

- FLANGE AND BOLT DATA -

FLANGE OUTSIDE DIA., A	53.00	FLANGE INSIDE DIA., B	42.25
SMALL HUB THICKNESS, go	1.38	LARGE HUB THICKNESS, gi	1.63
HUB LENGTH, h	2.25	FLANGE THICKNESS, t	6.63
BOLT CIRCLE DIA., C	49.75	DIA. OF BOLTS, Bd	3.00
NUMBER OF BOLTS, NB	24.00	ROOT AREA OF BOLTS, RA	3.00
ATM. FLANGE STRESS, Sf	17500.00	DESIGN FLANGE STRESS, Sn	17500.00
ATM. BOLT STRESS, Sa	25000.00	DESIGN BOLT STRESS, Sb	25000.00

- GASKET DATA -

GASKET MATERIAL	SS/MICA DJ	COMMENTS	DJ SS/MICA IIa ANSIB16.5
NOMINAL SIZE	44		

GASKET INSIDE DIA., Gi	43.38	GASKET OUTSIDE DIA., Go	44.70
GASKET WIDTH, N	0.66	ATM. PRESSURE, Po	14.70
GASKET CONSTANT, So	14.69	GASKET CONSTANT, d	0.23
GASKET CONSTANT, B	2900.00	MIN. ASME FACTOR M, Mmin	2.00
JOINT ASSEMBLY EFF., e	0.75	LEAKAGE FACTOR, F	1.00
MAX. ALLOW. STRESS, Sg	20000.00	TIGHTNESS CLASS, TC	T2

TurboFlange V:1.0

INFORMATION SHEET.
IMPERIAL UNITS : IN-PSI-LB

RESULTS PAGE-1

-GASKET STRESS AND BOLT LOAD-

TIGHTNESS PARAMETERS	Tpmin	=	114.88	Tpn	=	670.91
OPERATING STRESS	Sa	=	12957.80	Sya	=	17277.07
SEATING STRESS	Sgmin	=	2060.14	Sm	=	2060.14
GASKET AREAS	Ag	=	91.66	Ai	=	1538.45
BOLT LOADS	Wm1	=	1611886.01	Wm2	=	1583541.66
OPTIMAL VALUES	Mo	=	2.23	Wo	=	1611886.01

-BOLT STRESS AND BOLT AREA-

DESIGN STRESSES Sa = 25000.00 Sb = 25000.00
DESIGN BOLT AREA (Num. of Bolts * Root Area) Ab = 72.00
COMPUTED BOLT AREA (Greater of Wo/Sa and Wo/Sb) Am = 64.48
COMPUTED BOLT STRESS So = Wo/Ab = 22387.31
DESIGN vs COMPUTED VALUES Ab/Am = 1.12 Sa/So = 1.12

-FLANGE LOADS, LEVER ARMS, AND MOMENTS-

	LOAD		LEVER ARM		MOMENT
	Hd =	1296178.51	hd =	2.94	Md = 3807524.37
OPERATING	Hg =	197962.73	hg =	2.81	Mg = 556543.78
	Ht =	117744.78	ht =	3.28	Mt = 386282.73
				Md+Mg+Mt =	4750350.88
SEATING	Wo =	1611886.01	hg =	2.81	Ms = 4531586.09
MAXIMUM MOMENT ACTING ON FLANGE					Mo = 4750350.88

- STRESS FACTORS -

K	=	1.25	T	=	1.82
Y	=	8.70	Z	=	4.49
U	=	9.56	gi/go	=	1.18
ho	=	7.62	h/ho	=	0.30
F	=	0.89	V	=	0.46
f	=	0.71	e	=	0.12
d	=	298.98	t	=	6.63
L	=	1.95	mo	=	112434.34
mg	=	107256.48			

- CALCULATED HUB AND FLANGE STRESSES -

	LONGITUDINAL	RADIAL	TANGENTIAL
OPERATING	Sh = 15554.84	Sr = 2673.58	St = 10279.73
SEATING	Sh = 14838.50	Sr = 2550.46	St = 9806.32

GREATER OF (Sh+Sr)/2 AND (Sh+St)/2 = 12917.28
MAX. ALLOW. STRESS = 17500.00 MAX. COMPUTED STRESS = 12917.28
ALLOWABLE vs COMPUTED STRESS S(allow.)/S(comp.) = 1.35

TurboFlange V:1.0

INFORMATION SHEET.
IMPERIAL UNITS : IN-PSI-LB

RESULTS PAGE-2

- PLOT RESULTS -

M	Tpr	Wm1	Wm2	Sya	Sm
9.34	1.00	2214498.86	1055248.00	11513.18	8634.88
9.13	1.02	2197299.97	1060065.20	11565.73	8447.23
8.94	1.04	2180931.91	1064810.21	11617.50	8268.65
8.76	1.06	2165336.52	1069485.47	11668.51	8098.50
8.58	1.08	2150460.85	1074093.29	11718.78	7936.20
8.41	1.10	2136256.63	1078635.86	11768.35	7781.23
8.25	1.12	2122679.73	1083115.28	11817.22	7633.10
8.10	1.14	2109689.78	1087533.53	11865.42	7491.37
7.95	1.16	2097249.77	1091892.48	11912.98	7355.65
7.81	1.18	2085325.67	1096193.95	11959.91	7225.55
7.68	1.20	2073886.20	1100439.64	12006.23	7100.74
7.55	1.22	2062902.50	1104631.19	12051.97	6980.90
7.42	1.24	2052347.96	1108770.15	12097.12	6865.75
7.30	1.26	2042197.97	1112858.03	12141.72	6755.01
7.19	1.28	2032429.75	1116896.25	12185.78	6648.44
7.08	1.30	2023022.18	1120886.17	12229.31	6545.79
6.97	1.32	2013955.66	1124829.10	12272.33	6446.88
6.87	1.34	2005211.96	1128726.29	12314.85	6351.48
6.77	1.36	1996774.12	1132578.96	12356.89	6259.42
6.67	1.38	1988626.36	1136388.23	12398.45	6170.52
6.58	1.40	1980753.93	1140155.24	12439.55	6084.63
6.49	1.42	1973143.07	1143881.03	12480.20	6001.59
6.40	1.44	1965780.91	1147566.63	12520.41	5921.27
6.32	1.46	1958655.41	1151213.03	12560.19	5843.53
6.24	1.48	1951755.28	1154821.16	12599.56	5768.24
6.16	1.50	1945069.94	1158391.94	12638.52	5695.30
6.08	1.52	1938589.45	1161926.25	12677.08	5624.60
6.01	1.54	1932304.50	1165424.93	12715.25	5556.03
5.93	1.56	1926206.29	1168888.80	12753.04	5489.49
5.86	1.58	1920286.55	1172318.64	12790.46	5424.91
5.80	1.60	1914537.52	1175715.20	12827.52	5362.18
5.73	1.62	1908951.84	1179079.24	12864.22	5301.24
5.67	1.64	1903522.59	1182411.44	12900.58	5242.01
5.60	1.66	1898243.22	1185712.50	12936.59	5184.41
5.54	1.68	1893107.55	1188983.08	12972.28	5128.37
5.49	1.70	1888109.72	1192223.81	13007.64	5073.85
5.43	1.72	1883244.21	1195435.32	13042.67	5020.76
5.37	1.74	1878505.75	1198618.19	13077.40	4969.06
5.32	1.76	1873889.39	1201773.03	13111.82	4918.70
5.26	1.78	1869390.39	1204900.37	13145.94	4869.61
5.21	1.80	1865004.29	1208000.78	13179.77	4821.76
5.16	1.82	1860726.83	1211074.77	13213.31	4775.09
5.11	1.84	1856553.96	1214122.86	13246.56	4729.56
5.07	1.86	1852481.84	1217145.55	13279.54	4685.13
5.02	1.88	1848506.81	1220143.31	13312.25	4641.76
4.97	1.90	1844625.38	1223116.62	13344.69	4599.41
4.93	1.92	1840834.24	1226065.92	13376.87	4558.05

4.88	1.94	1837130.21	1228991.66	13408.79	4517.64
4.84	1.96	1833510.28	1231894.27	13440.46	4478.14
4.80	1.98	1829971.58	1234774.16	13471.88	4439.54
4.76	2.00	1826511.34	1237631.74	13503.05	4401.78
4.72	2.02	1823126.94	1240467.40	13533.99	4364.86
4.68	2.04	1819815.86	1243281.52	13564.70	4328.73
4.64	2.06	1816575.71	1246074.47	13595.17	4293.38
4.60	2.08	1813404.19	1248846.63	13625.41	4258.78
4.57	2.10	1810299.09	1251598.33	13655.44	4224.90
4.53	2.12	1807258.31	1254329.93	13685.24	4191.73
4.50	2.14	1804279.83	1257041.76	13714.83	4159.23
4.46	2.16	1801361.72	1259734.15	13744.20	4127.39
4.43	2.18	1798502.12	1262407.40	13773.37	4096.19
4.40	2.20	1795699.24	1265061.84	13802.33	4065.61
4.36	2.22	1792951.38	1267697.76	13831.09	4035.63
4.33	2.24	1790256.91	1270315.46	13859.65	4006.23
4.30	2.26	1787614.24	1272915.22	13888.01	3977.40
4.27	2.28	1785021.86	1275497.33	13916.18	3949.12
4.24	2.30	1782478.31	1278062.05	13944.17	3921.37
4.21	2.32	1779982.20	1280609.67	13971.96	3894.13
4.18	2.34	1777532.17	1283140.42	13999.57	3867.40
4.15	2.36	1775126.94	1285654.57	14027.00	3841.16
4.12	2.38	1772765.25	1288152.38	14054.25	3815.39
4.10	2.40	1770445.90	1290634.07	14081.33	3790.09
4.07	2.42	1768167.74	1293099.88	14108.23	3765.23
4.04	2.44	1765929.65	1295550.06	14134.97	3740.81
4.02	2.46	1763730.55	1297984.82	14161.53	3716.82
3.99	2.48	1761569.40	1300404.38	14187.93	3693.24
3.97	2.50	1759445.22	1302808.97	14214.16	3670.07
3.94	2.52	1757357.02	1305198.79	14240.24	3647.28
3.92	2.54	1755303.88	1307574.05	14266.15	3624.88
3.89	2.56	1753284.89	1309934.95	14291.91	3602.85
3.87	2.58	1751299.20	1312281.70	14317.51	3581.19
3.85	2.60	1749345.95	1314614.47	14342.97	3559.88
3.83	2.62	1747424.34	1316933.47	14368.27	3538.91
3.80	2.64	1745533.59	1319238.88	14393.42	3518.28
3.78	2.66	1743672.92	1321530.88	14418.43	3497.98
3.76	2.68	1741841.62	1323809.65	14443.29	3478.00
3.74	2.70	1740038.96	1326075.36	14468.01	3458.34
3.72	2.72	1738264.26	1328328.18	14492.59	3438.97
3.70	2.74	1736516.86	1330568.29	14517.03	3419.91
3.68	2.76	1734796.11	1332795.84	14541.33	3401.13
3.66	2.78	1733101.39	1335010.99	14565.50	3382.64
3.64	2.80	1731432.09	1337213.91	14589.54	3364.43
3.62	2.82	1729787.63	1339404.75	14613.44	3346.49
3.60	2.84	1728167.43	1341583.65	14637.21	3328.81
3.58	2.86	1726570.95	1343750.77	14660.86	3311.39
3.56	2.88	1724997.66	1345906.25	14684.37	3294.23
3.54	2.90	1723447.04	1348050.24	14707.76	3277.31
3.53	2.92	1721918.57	1350182.87	14731.03	3260.63
3.51	2.94	1720411.79	1352304.29	14754.18	3244.20
3.49	2.96	1718926.20	1354414.62	14777.20	3227.99
3.47	2.98	1717461.36	1356514.00	14800.11	3212.00
3.46	3.00	1716016.81	1358602.56	14822.89	3196.24
3.44	3.02	1714592.13	1360680.42	14845.56	3180.70

3.42	3.04	1713186.89	1362747.72	14868.12	3165.37
3.41	3.06	1711800.68	1364804.57	14890.56	3150.24
3.39	3.08	1710433.11	1366851.09	14912.89	3135.32
3.37	3.10	1709083.79	1368887.41	14935.11	3120.60
3.36	3.12	1707752.34	1370913.63	14957.21	3106.08
3.34	3.14	1706438.39	1372929.88	14979.21	3091.74
3.33	3.16	1705141.60	1374936.27	15001.10	3077.59
3.31	3.18	1703861.62	1376932.90	15022.89	3063.63
3.30	3.20	1702598.10	1378919.88	15044.56	3049.84
3.28	3.22	1701350.72	1380897.33	15066.14	3036.23
3.27	3.24	1700119.17	1382865.34	15087.61	3022.79
3.25	3.26	1698903.13	1384824.02	15108.98	3009.53
3.24	3.28	1697702.30	1386773.46	15130.25	2996.43
3.23	3.30	1696516.38	1388713.78	15151.42	2983.49
3.21	3.32	1695345.09	1390645.06	15172.49	2970.71
3.20	3.34	1694188.15	1392567.41	15193.46	2958.08
3.18	3.36	1693045.29	1394480.91	15214.34	2945.62
3.17	3.38	1691916.24	1396385.66	15235.12	2933.30
3.16	3.40	1690800.75	1398281.75	15255.81	2921.13
3.14	3.42	1689698.55	1400169.27	15276.40	2909.10
3.13	3.44	1688609.41	1402048.32	15296.90	2897.22
3.12	3.46	1687533.08	1403918.97	15317.31	2885.48
3.11	3.48	1686469.34	1405781.31	15337.63	2873.87
3.09	3.50	1685417.95	1407635.43	15357.86	2862.40
3.08	3.52	1684378.69	1409481.41	15378.00	2851.06
3.07	3.54	1683351.34	1411319.33	15398.05	2839.85
3.06	3.56	1682335.69	1413149.27	15418.02	2828.77
3.05	3.58	1681331.54	1414971.31	15437.90	2817.81
3.03	3.60	1680338.68	1416785.53	15457.69	2806.98
3.02	3.62	1679356.91	1418592.01	15477.40	2796.27
3.01	3.64	1678386.04	1420390.82	15497.03	2785.68
3.00	3.66	1677425.89	1422182.03	15516.57	2775.20
2.99	3.68	1676476.27	1423965.73	15536.03	2764.84
2.98	3.70	1675537.00	1425741.97	15555.41	2754.59
2.97	3.72	1674607.91	1427510.84	15574.71	2744.46
2.96	3.74	1673688.82	1429272.40	15593.93	2734.43
2.95	3.76	1672779.56	1431026.72	15613.07	2724.51
2.93	3.78	1671879.97	1432773.87	15632.13	2714.69
2.92	3.80	1670989.90	1434513.92	15651.12	2704.98
2.91	3.82	1670109.18	1436246.93	15670.02	2695.37
2.90	3.84	1669237.67	1437972.96	15688.86	2685.87
2.89	3.86	1668375.20	1439692.09	15707.61	2676.46
2.88	3.88	1667521.64	1441404.37	15726.29	2667.14
2.87	3.90	1666676.85	1443109.87	15744.90	2657.93
2.86	3.92	1665840.67	1444808.65	15763.44	2648.80
2.85	3.94	1665012.98	1446500.77	15781.90	2639.77
2.84	3.96	1664193.64	1448186.29	15800.29	2630.83
2.83	3.98	1663382.52	1449865.26	15818.61	2621.98

CASE II : RESULTS FROM *TurboFlange.*

Calculations using ***TurboFlange*** with equivalent data as CASE II above.

TurboFlange V:1.0 INFORMATION SHEET.
IMPERIAL UNITS : IN-PSI-LB

DATA PAGE-1

- MODEL DATA -

MODEL NAME	PAYNE2	COMMENTS	TF vs CURRENT ASME CODE 2
FLANGE MAT.		GASKET MAT.	
OP. PRESSURE	120.00	OP. TEMPERATURE	650.00
CORROSION ALLOW.	0.13		

- FLANGE AND BOLT DATA -

FLANGE OUTSIDE DIA., A	47.38	FLANGE INSIDE DIA., B	42.13
SMALL HUB THICKNESS, go	0.44	LARGE HUB THICKNESS, gi	0.56
HUB LENGTH, h	1.25	FLANGE THICKNESS, t	2.25
BOLT CIRCLE DIA., C	45.75	DIA. OF BOLTS, Bd	0.75
NUMBER OF BOLTS, NB	24.00	ROOT AREA OF BOLTS, RA	0.55
ATM. FLANGE STRESS, Sf	17500.00	DESIGN FLANGE STRESS, Sn	17500.00
ATM. BOLT STRESS, Sa	25000.00	DESIGN BOLT STRESS, Sb	25000.00

- GASKET DATA -

GASKET MATERIAL	SS/MICA DJ	COMMENTS	DJ SS/MICA IIa ANSIB16.5
NOMINAL SIZE	24		

GASKET INSIDE DIA., Gi	42.88	GASKET OUTSIDE DIA., Go	44.19
GASKET WIDTH, N	0.66	ATM. PRESSURE, Po	14.70
GASKET CONSTANT, So	14.69	GASKET CONSTANT, d	0.23
GASKET CONSTANT, B	2900.00	MIN. ASME FACTOR M, Mmin	2.00
JOINT ASSEMBLY EFF., e	0.75	LEAKAGE FACTOR, F	1.00
MAX. ALLOW. STRESS, Sg	20000.00	TIGHTNESS CLASS, TC	T1

TurboFlange V:1.0 INFORMATION SHEET.
IMPERIAL UNITS : IN-PSI-LB

RESULTS PAGE-1

-GASKET STRESS AND BOLT LOAD-

TIGHTNESS PARAMETERS	Tpmin	=	1.49	Tpn	=	1.55
OPERATING STRESS	Sa	=	3207.55	Sya	=	4276.73
SEATING STRESS	Sgmin	=	1980.75	Sm	=	1980.75
GASKET AREAS	Ag	=	89.78	Ai	=	1487.18
BOLT LOADS	Wm1	=	356297.06	Wm2	=	383973.38
OPTIMAL VALUES	Mo	=	16.51	Wo	=	383973.38

-BOLT STRESS AND BOLT AREA-

DESIGN STRESSES Sa = 25000.00 Sb = 25000.00
DESIGN BOLT AREA (Num. of Bolts * Root Area) Ab = 13.20
COMPUTED BOLT AREA (Greater of Wo/Sa and Wo/Sb) Am = 15.36
COMPUTED BOLT STRESS So = Wo/Ab = 29088.89
DESIGN vs COMPUTED VALUES Ab/Am = 0.86 Sa/So = 0.86

-FLANGE LOADS, LEVER ARMS, AND MOMENTS-

	LOAD		LEVER ARM		MOMENT
	Hd =	167159.37	hd =	1.53	Md = 255921.00
OPERATING	Hg =	204780.94	hg =	1.07	Mg = 218618.93
	Ht =	12033.07	ht =	1.44	Mt = 17328.07
				Md+Mg+Mt =	491868.00
SEATING	Wo =	383973.38	hg =	1.07	Ms = 409920.23
MAXIMUM MOMENT ACTING ON FLANGE					Mo = 491868.00

- STRESS FACTORS -

K	=	1.12	T	=	1.87
Y	=	16.54	Z	=	8.55
U	=	18.18	gi/go	=	1.29
ho	=	4.30	h/ho	=	0.29
F	=	0.89	V	=	0.43
f	=	0.86	e	=	0.21
d	=	35.15	t	=	2.25
L	=	1.11	mo	=	11676.39
mg	=	9731.04			

- CALCULATED HUB AND FLANGE STRESSES -

	LONGITUDINAL		RADIAL		TANGENTIAL	
OPERATING	Sh =	28517.92	Sr =	3371.97	St =	9307.81
SEATING	Sh =	23766.68	Sr =	2810.18	St =	7757.08

GREATER OF (Sh+Sr)/2 AND (Sh+St)/2 = 18912.86
MAX. ALLOW. STRESS = 17500.00 MAX. COMPUTED STRESS = 18912.86
ALLOWABLE vs COMPUTED STRESS S(allow.)/S(comp.) = 0.93

TurboFlange V:1.0

INFORMATION SHEET.
IMPERIAL UNITS : IN-PSI-LB

RESULTS PAGE-2

- PLOT RESULTS -

M	Tpr	Wm1	Wm2	Sya	Sm
26.49	1.00	463855.11	380525.22	4238.32	3178.74
20.63	1.02	400749.29	382262.32	4257.67	2475.86
16.51	1.04	356297.06	383973.38	4276.73	1980.75
13.51	1.06	323994.95	385659.29	4295.51	1620.97
11.27	1.08	299886.44	387320.88	4314.02	1352.45
9.56	1.10	281472.07	388958.95	4332.26	1147.34
8.23	1.12	267120.19	390574.24	4350.25	987.49
7.17	1.14	255734.42	392167.47	4368.00	860.68
6.32	1.16	246559.04	393739.32	4385.50	758.48
5.62	1.18	239061.14	395290.44	4402.78	674.97
5.05	1.20	232857.23	396821.45	4419.83	605.87
4.57	1.22	227666.25	398332.93	4436.67	548.05
4.16	1.24	223278.76	399825.45	4453.29	499.18
3.81	1.26	219536.35	401299.55	4469.71	457.50
3.51	1.28	216317.54	402755.74	4485.93	421.65
3.25	1.30	213528.01	404194.52	4501.96	390.58
3.03	1.32	211093.69	405616.35	4517.79	363.46
2.83	1.34	208955.76	407021.69	4533.44	339.65
2.66	1.36	207067.09	408410.97	4548.92	318.62
2.50	1.38	205389.57	409784.61	4564.22	299.93
2.36	1.40	203892.11	411143.00	4579.35	283.25
2.24	1.42	202549.15	412486.53	4594.31	268.29
2.12	1.44	201339.53	413815.57	4609.12	254.82
2.02	1.46	200245.61	415130.47	4623.76	242.64
1.93	1.48	199252.60	416431.57	4638.25	231.58

ÉCOLE POLYTECHNIQUE DE MONTRÉAL
3 9334 00290772 1